Control and function of two ferrochelatase isoforms in *Arabidopsis thaliana*

DISSERTATION

zur Erlangung des akademischen Grades
Doctor rerum naturalium
(Dr. rer. nat.)
im Fach Biologie

eingereicht an der
Lebenswissenschaftlichen Fakultät
der Humboldt-Universität zu Berlin

von
M.Sc. Tingting Fan

Präsidentin der Humboldt-Universität zu Berlin
Prof. Dr.-Ing. Dr. Sabine Kunst

Dekan der Lebenswissenschaftlichen Fakultät
Prof. Dr. Bernhard Grimm

Gutachter/innen: 1. Prof. Dr. Bernhard Grimm
2. Prof. Dr. Christian Schmitz-Linneweber
3. Prof. Dr. Mats Hansson

Tag der mündlichen Prüfung: 01.03.2019

Table of contents

Zusammenfassung

Die Tetrapyrrol-Biosynthese der Pflanzen ist ein hoch konservierter Prozess, indem sich die Häm- und Chlorophyllsynthese gemeinsame Syntheseschritte von der 5-Aminolävulinsäure (ALA)- bis hin zur Protoporphyrin IX (Proto)-Bildung teilen. Zur Hämsynthese sind in Pflanzenzellen zwei Isoformen der Ferrochelatase (FC) vorhanden, welche die Insertion von Eisenionen in Proto katalysieren. Die beiden Isoformen der FC unterscheiden sich in Arabidopsis thaliana in ihrem Expressionsmuster und der subzellulären Lokalisation. Vorhergehende Untersuchungen der FC in Arabidopsis zeigen, dass FC2 hauptsächlich der Bereitstellung von Häm im Blattgewebe dient, während FC1 hauptsächlich in Wurzeln aktiv ist, sowie an der Bereitstellung von Häm für Signaltransduktionswege und Stressvorgänge beteiligt ist.

In dieser Arbeit wurden *fc1* und *fc2* Mutanten analysiert und für Komplementationsversuche mit nativen und modifizierten *FC1/FC2*-Sequenzen genutzt. Es konnte gezeigt werden, dass die *fc1-2*-Mutante embryolethal ist. Die in der *fc1-2* Mutante gestörte Embryonalentwicklung infolge des *FC1* Mangels konnte durch Expression eines pFC1::FC2 Genkonstruktes komplementiert werden. Die Expression von *FC2* unter dem *FC1* Promoter (*pFC1::FC2*) konnte die *fc1-2* Mutante unter Standard-Wachstumsbedingungen vollständig komplementieren, jedoch nicht unter Salzstress. Stressversuche mit abgetrennten Blättern der Linien pFC1FC2 (*fc1/fc1*), 35SFC1 und dem Wildtyp zeigten, dass FC1 die Expression von Genen des Chlorophyll-Katabolismus unter Salzstressbedingungen negativ reguliert. Der Umstand der mangelnden Komplementation durch die pFC1FC2 (*fc1/fc1*) Mutante unter Stressbedingungen kann mit einem im Vergleich zur *FC1* Expression erhöhten, Stress induzierten Umsatz von *FC2* mRNA erklärt werden. Sowohl die Komplementationsversuche, als auch der Promotor-Aktivitätsassay ließen auf eine signifikante Rolle des *FC1* Gens während der Embryogenese und der Pflanzenabwehr schließen.

Zusätzlich zu den Komplementationsversuchen der *fc1* Mutanten wurde auch eine *fc2* Null-Mutante zur Expression der beiden genomischen *FC* Sequenzen herangezogen, um die spezifischen Funktionen der FC2-Varianten zu untersuchen. Die Expression von *FC2* unter dem endogenen Promotor konnte die nekrotischen Blätter und das eingeschränkte Wachstum der *fc2-2* Mutanten sowohl im Kurztag, als auch im Dauerlicht verhindern. Während die pFC1FC2 (*fc2/fc2*) Pflanzen unter Dauerlicht eine vollständige Komplementation zeigten, konnte unter Kurztagbedingungen nur eine partielle Komplementation beobachtet werden. Die nekrotischen Blätter der unter Kurztag angezogenen pFC2FC1 (*fc2/fc2*) Pflanzen wiesen eine verminderte PORB Stabilität auf. Der Protochlorophyllid (Pchlide)-Gehalt nach Dunkelinkubation entsprach der Pchlide Akkumulation der *fc2-2* Mutanten. Über BiFC, Hefe-Zwei-Hybrid und Pulldown-Versuche konnte die Interaktion zwischen PORB und FC2 gezeigt werden, wohingegen FC1 nicht mit PORB interagiert. Außerdem lassen Interaktions- und Co-Lokalisationsstudien vermuten, dass FC2 gemeinsam mit dem POR-FLU-GluTR-Komplexes assoziiert ist, welcher für die

Inhibierung der ALA-Synthese im Dunkeln verantwortlich ist. Anhand der Charakterisierung von verschiedenen *fc2, porb* und *flu* Mutanten, 35SFC2 Überexpressoren, sowie dem Wildtyp lässt sich schließen, dass die Hämsynthese von Wildtyp-Arabidopsis im Dunkeln inhibiert wird. Eine fehlerhafte Expression von *FC2*, *PORB* oder *FLU* führt zum Ausbleiben der Dunkelinhibition der ALA-Synthese. Versuche geben erste wichtige Hinweise, dass auch FC2 an der Regulation der ALA-Synthese infolge ihrer Interaktion mit PORB beteiligt ist. Dies deutet darauf hin, dass der Häm- und der Chlorophyllzweig eine gemeinsame Regulation der ALA-Synthese teilen, um das Gleichgewicht der TBS zu wahren.

Neben der Funktion der FC2 in der Regulation der TBS konnte die vorliegende Arbeit ebenfalls die Rolle der FC2 in der Assemblierung der PSII-LHCII Superkomplexe offenlegen. Sowohl die Deletion, als auch eine Störung der Chlorophyll A/B Bindedomäne (CAB) der FC2 führten zu einer Beeinträchtigung in der Assemblierung der PSII-Superkomplexe. Da die *in vitro* Aktivität der FC2 durch die Deletion der CAB-Domäne nicht beeinträchtigt wird, ist dieser Defekt wahrscheinlich unabhängig von der katalytischen Aktivität.

Basierend auf den Ergebnissen, dieser Studie können Modelle für die funktionale Verteilung der beiden FC-Isoformen in unterschiedlichen Geweben und Entwicklungsstadien, sowie die Funktionen in verschiedenen biologischen Prozessen postuliert werden. Zusätzlich wird diskutiert, inwiefern FC1 und FC2 in der Lage sind die Funktionen der jeweils anderen Isoform zu kompensieren.

Schlagworte: Ferrochelatase; Embryo-Entwicklung; Salzstress; Tetrapyrrol-Biosynthese; ALA-synthese; Chlorophyll-katabolische Enzyme; PSII-LHCII Superkomplexe.

Abstract

In plants, heme and chlorophyll synthesis share the common synthetic steps from 5-aminolevulinic acid (ALA) formation to Protoporphyrin IX (Proto) production in the conserved Tetrapyrrole biosynthesis (TBS) pathway. Plant cells utilize two ferrochelatses (FC) to catalyse the insertion of ferrous iron into Proto to yield heme. In *Arabidopsis thaliana*, the two FC isoforms are distinguished by their diverse expression profiles and subcellular allocations. Previous characterization of Arabidopsis FC has indicated that FC2 serves the predominant heme pools in leaf tissues, while FC1 mainly produces heme in roots and serves heme pools in signaling transduction and stress response.

In this study, the *fc1* and *fc2* defective mutants have been re-analysed and used for complementation tests with expression of a native or modified *FC1*/*FC2* sequence. The *fc1-2* mutant has been proven to be embryo lethal. The pFC1FC1 (*fc1*/*fc1*) complementation plants confirmed that the defective embryo maturation in homozygous *fc1-2* seeds is attributed to a lack of FC1. Expression of *FC2* under the *FC1* promoter (*pFC1::FC2*) also contributed to a full complementation of *fc1-2* under standard growth conditions, but not under salt stress. The stress treatment with detached leaves of pFC1FC2 (*fc1/fc1*), 35SFC1 and wild-type plants indicated that FC1 negatively regulates the expression of chlorophyll catabolic genes under salt stress. The incomplete complementation of pFC1FC2 (*fc1*/*fc1*) under stress conditions can be explained by a faster turnover of *FC2* mRNA in comparison to *FC1* mRNA during stress. The complementation tests and the promoter activity assay both argue for a significant role of *FC1* in embryogenesis and plant defense.

In addition to the complementation tests of *fc1* mutants, a *fc2* null mutant has been used to express the two FC genomic sequences to substantiate the specific functions of FC2. Expression of *FC2* under its own promoter was able to rescue the necrotic leaves and defective growth of *fc2-2* mutants under both SD and CL conditions. However, pFC2FC1 (*fc2/fc2*) plants showed a full complementation under CL but only a partial complementation under SD condition. The necrotic leaves of SD-grown pFC2FC1 (*fc2/fc2*) seedlings correlated with a reduced PORB stability as well as *fc2-2* mutant-level of Pchlide accumulation after dark incubation. The analyses of BiFC, yeast two hybrids as well as pull down assays confirmed the interaction between PORB and FC2, whereas FC1 did not interact with PORB. Moreover, interaction and co-localization studies suggest that FC2 is associated with the POR-FLU-GluTR complex, which represses ALA synthesis in darkness. By characterizing multiple *fc2*, *porb*, *flu* defective mutants and 35SFC2 overexpressing plants, as well as wild type, it can be concluded that wild-type Arabidopsis undergoes repressed heme synthesis in the dark compared to light-exposure. Defective expression of *FC2*, *PORB* or *FLU* interfered always with an appropriate inhibition of ALA formation and resulted in non-modified heme production at night, in comparison to daytime. This thesis uncovered a mechanism of FC2 action on ALA synthesis regulation via interaction of FC2 and PORB. This indicates that both branches of heme and chlorophyll synthesis share a common regulation to balance the TBS pathway.

Apart from a role of FC2 involved in the regulation of TBS pathway, the presented study also revealed FC2 function in the assembly of the PSII-LHCII supercomplexes. Either a deletion or disruption of the chlorophyll A/B-binding (CAB) domain of FC2 resulted in a compromised assembly of PSII supercomplexes. This defect was probably independent of heme synthesis, as the *in vitro* activity of FC2 was not affected due to a lack of CAB domain.

Based on all the results obtained in this study, the functional distribution models of the two FC in different tissues and development stages, as well as diverse biological processes, have been proposed. In addition, to which extent that FC1/FC2 could compensate the function of the other isoform has been discussed.

Key words: ferrochelatase; embryo development; salt stress; tetrapyrrole synthesis; ALA synthesis; chlorophyll catabolic enzymes; PSII-LHCII supercomplexes.

Abbreviation

ALA	5-aminolevulinic acid
APX1	Ascorbate Peroxidase 1
3AT	3-amino-1,2,4-triazole
BAP1	BON association protein 1
BiFC	bimolecular fluorescence complementation
BN PAGE	blue native polyacrylamide gel electrophoresis
CAB	chlorophyll A/B binding
CCEs	Chlorophyll Catabolic Enzymes
CFP	Cyan Fluorescence Protein
Chl	chlorophyll
Chlide	chlorophyllide
CHLM	MgProto IX methyltransferase
CL	continuous light (24h light)
Col-0	Columbia
CPO	Coproporphyrinogen III Oxidase
cpSRP	chloroplast signal recognition particle
Cytb559	Cytochrome b559
Cytb6f	Cytochrome b6f
Cytf	Cytochrome f
2D	two-dimension
DAP	days after pollination
ddH_2O	double distilled water
DDM	dodecyl maltoside
DIC	differential interference contrast
FC	ferrochelatase
FLU	Fluorescent
GBP	GluTR binding protein
GFP	Green Fluorescence Protein
GluTR	glutamyl-tRNA Reductase
GSAAT	glutamate-1-Semialdehyde Aminotransferase
GUN4	GENOMES UNCOUPLED 4
GUS	β-glucuronidase
H_2O_2	hydrogen peroxide

HCAR	7-Hydroxymethyl-Chlorophyll A Reductase
HO	Heme Oxygenase
HPLC	high performance liquid chromatography
HRP	Horseradish Peroxidase
LD	long day (16h light/8h dark cycles)
Ler	Landsberg erecta
MgCH	Magnesium chelatase
MgProto	magnesium protoporphyrin IX
MS	Murashige and Skoog
NBT	Nitro blue tetrazolium
NF	Norflurazon
NOL	NYC1-like
NYC1	Non-Yellow Coloring 1
PAM	Pulse Amplitude Modulation
PAO	Pheophorbide A Oxygenase
Pchlide	protochlorophyllide
PhANGs	photosynthesis-associated nuclear genes
PIF	phytochrome-interacting factor
POR	Protochlorophyllide Reductase
PPH	Pheophytin Pheophorbide Hydrolase
PPO	Protoporphyrinogen IX Oxidase
Proto	protoporphyrin IX
PSI	photosystem I
PSII	photosystem II
ROS	reactive oxygen species
RT	room temperature
SAG	senescence-associated gene
SD	short day (8h light/16h dark cycles),
SD medium	Synthetic Dropout
SDS-PAGE	sodium dodecyl sulfate polyacrylamide gel electrophoresis
SGR1	Stay-Green1
TBS	Tetrapyrrole synthesis
UTR	untranslated region
Y2H	yeast two-hybrid
YFP	Yellow Fluorescence Protein

1. Introduction

1.1 Heme derivatives and function

Heme, as an essential biomolecule involved in a large number of cellular processes, is widely distributed in almost all living organisms. There are a few exceptions, such as the plant parasitic flagellate *Phytomonas serpens*, which however is heme auxotrophs and does not possess well-known hemoproteins involved in electron transfer chain, oxidative stress defending or desaturation of fatty acids (Koreny et al., 2012). Heme mainly serves as a prosthetic group of hemoproteins in numerous fundamental biological processes, such as oxygen-mediated metabolism as well as oxygen storage and transfer, respiration, catalysis and photosynthetic electron transport (Layer et al., 2010). Heme also plays a regulatory role in gene expression control and signal transduction in yeast and mammalian cells, as well as in higher plants (Moulin and Smith, 2005; Mense and Zhang, 2006; Tsiftsoglou et al., 2006; Woodson et al., 2011).

Living organisms ranging from bacteria to plants and mammalian cells, synthesize heme de novo, except for *Caenorhabditis elegans* parasitic helminths which require heme but are natural heme auxotrophs (Rao et al., 2005; Anzaldi and Skaar, 2010; Sinclair and Hamza, 2015). In addition, there also exist certain microorganisms, such as *Haemophilus influenzae*, requires exogenous synthetic precursors, maintains only late steps of heme synthesis (Panek and O'Brian, 2002; Sah et al., 2002; Koreny et al., 2013).

1.1.1 Important heme derivatives

According to the types of functional groups attached to the periphery of the tetrapyrrole macrocycles, heme species are classified mainly into four derivates, namely heme a, heme b, heme c and o (Figure 1.1). Among all the heme variants, heme b is the most abundant heme as well as the basic synthetic precursor for other derivatives (Hansson and von Wachenfeldt, 1993; Hederstedt, 2012). Heme b contains a methyl group at position C8 and a vinyl group at position C2, is referred to an iron protoporphyrin IX (protoheme). Heme b acts as the prosthetic group of most hemoproteins, for instance, hemoglobins involved in oxygen metabolism and cytochrome b of electron transfer chains. In contrast to heme b, the type-a heme has a C2 hydroxyethylfarnesyl group and a C8 formyl group. Heme a is an essential cofactor for cytochrome a, functioning in aerobic respiration distributed in numerous organisms. Heme c, in comparison to heme a and b, harbors two thioether side chains, which enable the heme molecule to covalently attach to the cysteine residues of its apoprotein cytochrome c. In contrast to heme a and b, this covalent association, however, does not allow heme c molecules to be easily disassociated from its apoproteins (Hou et al., 2006; Bowman and Bren, 2008). Heme o, as an intermediate product in heme a synthesis from heme b, has a heme a-like isoprenoid chain at position C2. Instead of a C8 formyl group in the a-type heme, heme o displays a methyl group at the C8 position. Similar to heme a, heme o serves in the reduction of oxygen to H_2O in bacteria but not mammalian cells (Puustinen and Wikstrom, 1991; Saiki et al., 1992).

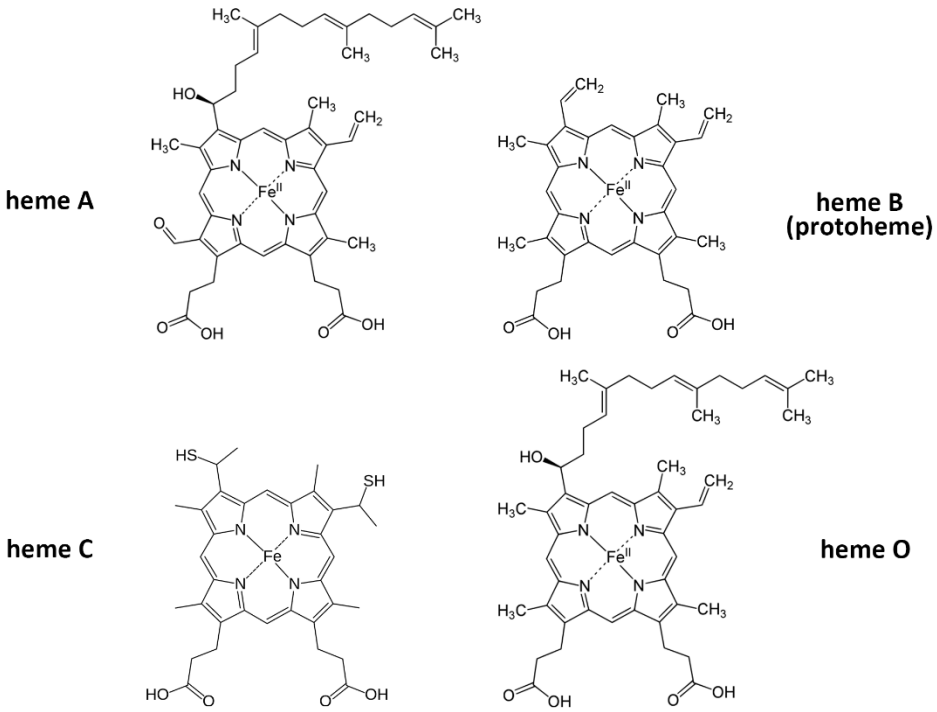

Figure 1. 1 Structures of important heme derivates.

1.1.2 Function of heme

1.1.2.1 Heme acts as a prosthetic group for various gas sensors.

Heme is an indispensable cofactor for multiple fundamental biological processes, widely distributed in numerous living organisms. The most important function of heme in eukaryotic cells is oxygen sensing and utilization (Rodgers and Lukat-Rodgers, 2005). Globin is a superfamily of globular proteins binding and transporting oxygen and always requires heme as a cofactor. Hemoglobin is the most abundant globin, carries 97% of oxygen in mammalian blood cells. In vertebrates, hemoglobin carries oxygen in lungs or gills (in fishes) and distributes it into different tissues (Hardison, 2012; Burmester and Hankeln, 2014). Besides oxygen, hemoglobin also binds other gas molecules such as CO_2, CO and NO in a similar manner (Li et al., 2004; Stuehr et al., 2004; Shimizu et al., 2015). However, the binding of CO to hemoglobin is irreversible as the affinity is more than 200-fold higher than oxygen. In addition to globin, there also exists a large group of hemoproteins sensing O_2 and other gases, for example, cytochrome c mediating electron transfer, cytochrome P450, the monooxygenase etc.

1.1.2.2 Heme is a cofactor involved in oxygen catabolism and electron transfer

Besides the function as a gas sensor, heme also acts as the prosthetic group for plenty enzymes, such as catalases/peroxidases for oxygen catabolism and cytochrome P450s for

electron transfer. Catalases and peroxidases are widely distributed antioxidant enzymes, which contain heme as a cofactor (Kirkman and Gaetani, 1984; Jones, 2001). In aerobic organisms ranging from bacteria to mammals, catalases catalyze the reduction of hydrogen peroxide to yield water and oxygen. The catalysis process can be generally divided into two steps: in the first step, one molecule of hydrogen peroxide oxidizes the Fe^{3+} from the pyrrole ring center of heme to form water and Fe^{4+}; in the second step, a second hydrogen peroxide functions as a reductant to regenerate the enzyme in a Fe^{3+} form and release water as well as oxygen (Jones, 2001; Alfonso-Prieto et al., 2009; Alfonso-Prieto et al., 2012).

Compared to catalases, peroxidases can also utilize organic hydroperoxides as substrates in addition to hydrogen peroxide. Peroxidases catalyze the reduction of organic and inorganic compounds in a similar manner as catalases (Rodriguez-Lopez et al., 2001; Vlasits et al., 2007). Because of its broader substrate specificity, peroxidases are widely applied in industry and pollution control as it has the potential to degrade hazardous compounds in water waste, such as phenols and cresols (Bansal and Kanwar, 2013).

In contrast to both catalases and peroxidases, cytochrome P450 proteins, although also require heme as a cofactor, conduct the oxidation of organic substrates and consume bimolecular oxygen to yield water.

In cyanobacteria, green algae and plants, heme contributes to photosynthesis process not only by acting as a prosthetic group in complexes mediating electron transfer (for instance, cytochrome b6f complex), but also by directly composing the photosystem II (PSII) core. A PSII core complex consists of D1, D2, cytochrome b559 (Cytb559) as well as chlorophyll binding proteins CP43 and CP47 (Nixon et al., 2010; Komenda et al., 2012; Nickelsen and Rengstl, 2013; Nelson and Junge, 2015). Among them, Cytb559 is a heterodimeric protein containing α and β subunits as well as heme as a cofactor. Each subunit of Cytb559 provides a His-ligand to coordinate heme. A mutation of either heme axial ligand severely abolishes the stability of PSII (Pakrasi et al., 1991; Morais et al., 2001; Hung et al., 2007; Hung et al., 2010; Chu and Chiu, 2015).

1.1.2.3 Heme regulates gene expression in yeast, mammals as well as plants.

In addition to playing a prosthetic role for heme-dependent enzymes, heme also regulates gene expression by activating or inhibiting transcription factors. In yeast *Saccharomyces cerevisiae*, the *Hap1* (*Heme Activator Protein*) gene encodes a transcription factor which consists of a N-terminal DNA binding domain, a heme binding motif and a C-terminal transcriptional activation domain (Hon et al., 2000). Without the presence of heme, the Hap1 protein forms a high molecular weight multichaperone-Hap1 complex (Lan et al., 2004). Once heme is attached to the binding domain of Hap1, the protein is released from the big complex in a dimeric form. Therefore, the transcription regulator is available for DNA binding, which activates transcription of respiration responsive genes and oxidative damage regulators (Hon et al., 1999; Zhang and Hach, 1999; Hou et al., 2006). In contrast

to its activation role for the transcription regulator in yeast, however, heme inhibits the activity of transcription repressor Bach1 (BTB and CNC Homology 1) in mammalian cells (Ogawa et al., 2001; Warnatz et al., 2011). Under normal conditions, Bach1 is localized in nucleus and mainly forms heterodimers with the Maf-related oncoproteins. The heterodimer directly binds and regulates its target genes, such as *Heme Oxygenase1* (*HO1*), in heme degradation, oxidative stress response and for globins (Sun et al., 2002; Kitamuro et al., 2003). However, in the presence of increased heme content, Bach1 is exported from the nucleus to the location of cytoplasm. As a consequence, the remaining nucleus-located Bach1-Maf complex could neither perform its regulatory function, as the DNA-binding ability would be diminished by binding heme (Ogawa et al., 2001; Yamasaki et al., 2005). Although no heme-dependent transcription factors in plants has been identified so far, Woodson et al. (2011) were able to prove that an overproduction of FC1-catalysed heme in Arabidopsis could restore Photosynthesis Associated Nuclear Genes (PhANGs) expression, which genes expression are normally drastically repressed in the presence of Norflurazon (NF) in wild type seedlings.

Despite of the indispensable role of heme in the important biology processes, a free heme amount above 1μM in cells triggers drastic accumulation of reactive oxygen species (ROS), which is cytotoxic (Girvan and Munro, 2013; Ponka et al., 2017). Thus, a tight regulation of heme synthesis and consumption is required to maintain an adequate heme homeostasis *in vivo*.

1.2 Tetrapyrrole biosynthesis pathway (TBS)

Heme is a critical cofactor for diverse biological processes. In human, deficiency of heme biosynthesis causes severe metabolic disorders, termed kinds of porphyrias and X-linked side-roblastic anemia (Layer et al., 2010). In bacteria, such as *E. coli*, inadequate heme synthesis perturbs the growth on oxidizable substrates (Rao et al., 2005). In photosynthetic organisms, such as cyanobacteria and higher plants, deficient heme supply causes severe retarded growth, affected photosynthetic machinery and even lethality (Papenbrock et al., 2001; Woodson et al., 2011; Scharfenberg et al., 2015; Espinas et al., 2016). Except few free-living worms including *Caenorhaditis elegans* and parasitic helminths, most eukaryotes characterized so far are able to synthesize heme on their own (Rao et al., 2005). In all eukaryotes and most prokaryotes, except Archaea and some eubacteria, heme is synthesized through a widely distributed biosynthetic pathway — the Tetrapyrrole synthesis (TBS) pathway. In oxygenic photosynthetic organisms, such as cyanobacteria, algae and plants, heme and chlorophyll synthesis share the synthetic steps from ALA formation to the synthesis of the common precursor protoporphyrin IX (Proto). Generally, TBS pathway is divided into 4 parts: (1) ALA synthesis; (2) the formation of Proto; (3) heme branch; (4) chlorophyll branch (Fig 1.2).

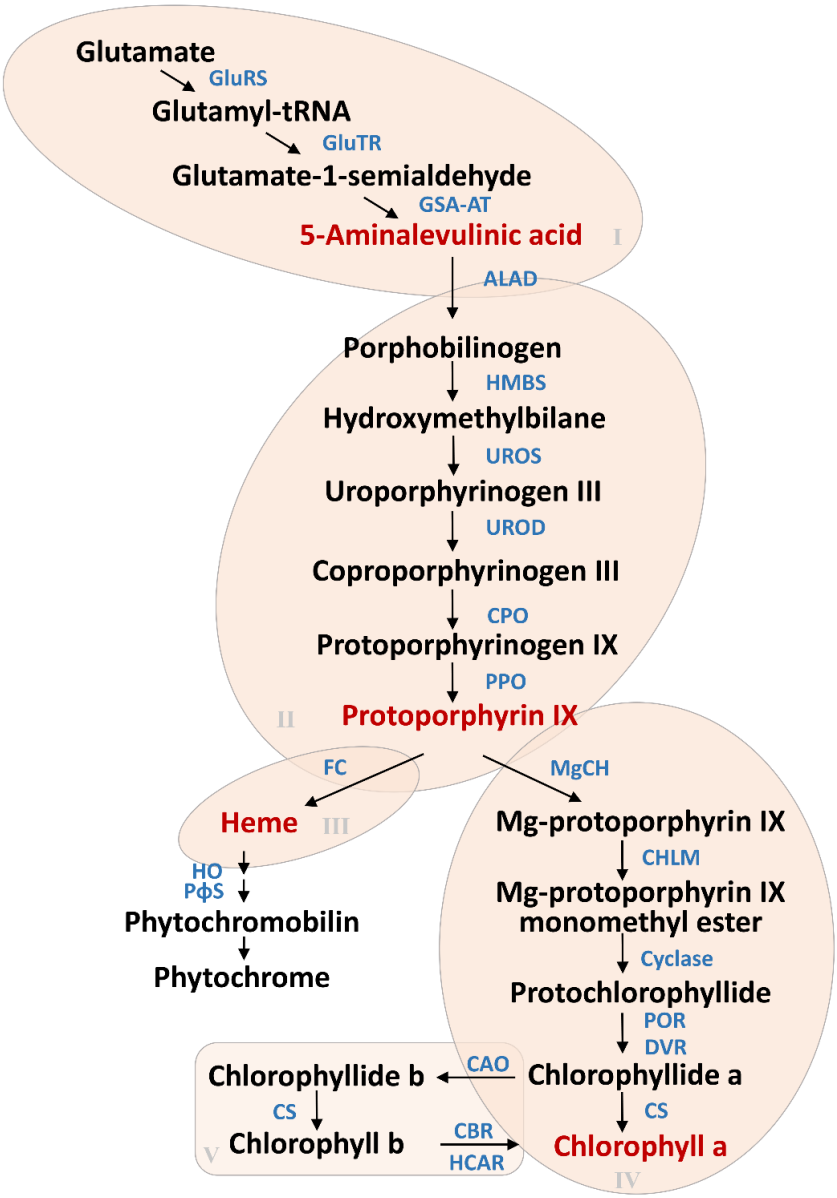

Figure 1. 2 Overview of TBS pathway in higher plants.

In plants, chlorophyll and heme biosynthesis share the common TBS pathway starting with the formation of ALA. This highly conserved synthetic pathway is generally divided into four parts: (I) ALA formation; (II) ALA to Proto production; (III) heme branch and (IV) chlorophyll branch. GluRS: glutamyl-tRNA synthetase; GluTR: glutamyl-tRNA reductase; GSA-AT: glutamate-1-semialdehyde aminotransferase; ALAD: 5-aminolevulinic acid dehydratase; HMBS:PBG deaminase; UROS: uroporphyrinogen III synthase; UROD: uroporphyrinogen III decarboxylase; CPO: coproporphyrinogen III oxidase; PPO: protoporphyrinogen IX oxidase; HO: heme oxygenase; PΦS: MgCH: Mg chelatase; CHLM: Mg-Proto IX methyltransferase; POR: Protochlorophyllide reductase; DVR: 3,8-divinyl chlorophyllide reductase; CS: chlorophyll synthase; CAO: chlorophyllide a oxidase; CBR: chlorophyll b reductase; HCAR: 7-hydroxymethyl chlorophyll a reductase.

1.2.1 ALA synthesis

In plants, the TBS pathway always starts with the formation of 5-aminolevulinic acid (ALA), which carries the basic source of carbon and nitrogen atoms for all the pyrrole variants. To accomplish the synthesis of ALA, glutamate (Glu) is ligated to $tRNA^{Glu}$ by glutamyl-tRNA synthetase (GluRS). The activated tRNA-bound glutamate is then reduced by glutamyl-tRNA reductase (GluTR) in a NADPH-dependent manner, to yield glutamate-1-semialdehyde (GSA). Subsequently, GSA aminotransferase (GSAAT) catalyzes the conversion of GSA into ALA through an intermolecular amino-exchange.

1.2.2 ALA to Proto formation

To yield a cyclic pyrrole ring from the linear ALA, two ALA molecules are condensed into one porphobilinogen (PBG) by ALA dehydratase (ALAD). Then the first formed pyrrole molecule is polymerized into an open pyrrole macrocycle, hydroxymethylbilane, which is catalyzed by PBG deaminase (HMBS). The ring closure reaction is subsequently driven by uroporphyrinogen III synthase (UROS), resulting in the formation of uroporphyrinogen III. Uroporphyrinogen III is the first cyclic tetrapyrrole intermediate, ready for a series of side chain modifications to achieve various tetrapyrrole variants. Firstly, a decarboxylation reaction driven by uroporphyrinogen III decarboxylase (UROD) converts uroporphyrinogen III into coproporphyrinogen III. Afterwards, an additional decarboxylation catalyzed by coproporphyrinogen III oxidase (CPO) contributes to the production of protoporphyrinogen IX. Finally, protoporphyrinogen IX oxidase (PPO) extracts six electrons from protoporphyrinogen IX to produce protoporphyrin IX (Proto), the most critical tetrapyrrole intermediate branching the syntheses of heme and chlorophyll.

1.2.3 Chlorophyll branch

1.2.3.1 Magnesium chelatase

Chlorophyll biosynthesis which is divided from Proto formation by the insertion of Mg^{2+} into the tetrapyrrole ring, is also named Mg branch. Enzymes involved in Mg branch was firstly characterized by genetic analyses of the photosynthetic gene cluster in purple bacteria, *Rhodobacter sphaeroides* (Pierce and Rey, 2013) and *Rhodobacter capsulatus* (Wang et al., 2008; Kurihara et al., 2009; Zeller et al., 2009). By further mutagenesis studies and heterozygous expression in *E. coli*, more genes responsible for bacteriochlorophyll (Bchl) synthesis were identified. Subsequently, enzymes contributing to plant chlorophyll biosynthesis have been characterized, which are encoded in bacteria.

In planta, Magnesium chelatase (MgCH) consists of three main subunits CHLI, CHLD and CHLH, catalyzes the insertion of Mg^{2+} into ProtoIX for chlorophyll synthesis. In addition to the three subunits, the activity of MgCH requires ATP as well as Mg^{2+}. The Mg chelation mechanism was proposed to be very complex. The process contains two parts: An ATP

dependent enzyme-activation step and the Mg^{2+} chelation step (Walker and Weinstein, 1994). To start the activation step, six subunits of the I and D subunits form two hexameric rings, respectively. The oligomerization proceeds in an ATP dependent manner, as both subunits belong to AAA+ proteins (ATPase associated with various cellular activities) family. However, the ATPase activity was reported for CHLI only (Hansson and Kannangara, 1997; Jensen et al., 1999; Petersen et al., 1999). With Mg^{2+}, the two hexameric rings form the Mg-ATP-I-D complex (Willows et al., 1996; Gibson et al., 1999). Meanwhile, the H subunit binds the substrate Proto as well as Mg^{2+} forming the Mg-Proto-H complex. To continue with the chelation step, the two complexes are combined through the interaction between D and H subunit, which triggers ATP hydrolysis and the insertion of Mg^{2+} into Proto (Fodje et al., 2001). It has been suggested that binding of the D subunit may block ATPase activity of CHLI, and this interaction will be released when CHLH interacts with CHLD at its integrin I domain. Meanwhile the ATP binding site of CHLI is exposed, which triggers ATP hydrolysis.

In Arabidopsis, the genes encoding the three subunits of MgCH have been well characterized. In contrast to the subunits D and H, CHLI in Arabidopsis is encoded by the two genes *CHLI1* (At4g18480) and *CHLI2* ((At5g45930) (Koncz et al., 1990; Rissler et al., 2002). Previous studies from the Rissler and Apchelimov group suggested that the two isoforms of CHLI show similar mRNA accumulation in wild-type and *ch42-3* (*chli1* mutation) plants, however at protein level CHLI2 is almost undetectable in both plants (Rissler et al., 2002). Characterization of *ch42-2* and *ch42-3* mutants revealed that CHLI1 plays the predominant role in MgCH activity. Deletion or point mutation of *CHLI1* resulted in inactivation of MgCH activity in the pale green seedlings (Soldatova et al., 2005), while CHLI2 contributes to MgCH activity to a minor extent, since it cannot compensate for the *chli1* albino phenotype (Apchelimov et al., 2007). Further study from Huang et al. (2009) showed that *CHLI2* expression driven by the *CHLI1* promoter could rescue CHLI1 deficiency in a new *chli* mutant (*cs215*) (Huang and Li, 2009).

Besides the three main subunits, MgCH activity also requires the accessory regulator GENOMES UNCOUPLED 4 (GUN4) (Larkin et al., 2003). GUN4 binds the substrate Proto as well as the product MgProto, and interacts with CHLH. By binding Proto, the interaction between GUN4 and H subunit promotes the chloroplast membrane association of CHLH, and contributes to the active MgCH complex (Adhikari et al., 2011). Additionally, the concentration of free Mg^{2+} in stroma alters from 0.5mM to 2mM during a day-night shift, which affects MgCH activity (Ishijima et al., 2003). With the presence of GUN4, the concentration of Mg^{2+} required for full activation of MgCH activity could be lowered from 6mM to 2mM (Davison et al., 2005).

1.2.3.2 S-adenosyl-L-methionine: Mg-Proto IX methyltransferase and Mg-Proto IX monomethyl ester cyclase

To continue the chlorophyll biosynthesis with MgProto, an enzyme named Mg-Proto IX methyltransferase (CHLM) transfers the methyl group from the general methyl donor S-

adenosyl-L-methionine (SAM) to the C13 propionate side chain of MgProto, leading to the formation of Mg protoporphyrin IX monomethyl ester (MgPME) (Gibson et al., 1963). The CHLM enzyme activity was first identified and analyzed in *Rhodobacter sphaeroides* (Gibson et al., 1963; Bollivar et al., 1994; Gibson and Hunter, 1994). Subsequently, *CHLM* cDNA sequences were characterized also from higher plants, such as Arabidopsis, Zea mays, rice and tobacco (Radmer and Bogorad, 1967; Kruse et al., 1997; Block et al., 2002; Wang et al., 2017). Interestingly, studies from algae and tobacco demonstrated that CHLM enzymatic activity is directly coupled with the activity of MgCH through the interaction between CHLM and CHLH (Gorchein, 1972; Alawady et al., 2005; Sawicki and Willows, 2010). The H subunit from *Rhodobacter sphaeroides* increased the activity of recombinant CHLM protein up to seven folds (Hinchigeri et al., 1997). Additionally, CHLM is also redox-regulated by the NADPH-dependent thioredoxin reductase C (NTRC) (Richter et al., 2013; Richter et al., 2016).

MgProto IX monomethyl ester cyclase catalyzes the conversion of MgProtoME to divinyl protochlorophyllide (Pchlide) through an oxidative cyclase reaction resulting in the formation of the fifth ring characteristic for all Chls (Tottey et al., 2003). Depending on the resources of the oxidation donor, MgProto IX monomethyl ester cyclases in photosynthetic organisms are classified into two groups: anaerobic and aerobic cyclase. MgProto IX monomethyl ester cyclase in *Rba. capsulatus* is encoded by the *bchE* gene and belongs to anaerobic cyclases. The anaerobic cyclase incorporates the atomic oxygen into MgProtoME from water. In contrast, the aerobic type of cyclases take O_2 as the atomic oxygen resource. In *Chlamydomonas reinhardtii*, two genes encode MgProto IX monomethyl ester cyclase, named *CRD1* and *CTH1*. However, the two isoforms show different expression patterns based on copper nutrition status. The *crd1* mutant exhibits a chlorotic phenotype, which could not be compensated by *CTH1* expression (Moseley et al., 2000; Moseley et al., 2002). In Arabidopsis, *CHL27* encodes MgProto IX monomethyl ester cyclase. The mutant with reduced CHL27 protein amount results in chlorotic leaves and retarded growth. Localization study of CHL27 suggested the protein is equally distributed on envelope and thylakoid membranes, which may indicate specific sites of chlorophyll synthesis due to different chloroplast developmental stages or environmental factors (Tottey et al., 2003).

1.2.3.3 Protochlorophyllide oxidoreductase

Protochlorophyllide reductase (POR) catalyzes the reduction of the double bond in the D ring of Pchlide (Fujita, 1996; Masuda and Takamiya, 2004). In angiosperm, POR enzymes are found to be light dependent, and regulated by NADPH. Due to these properties, POR proteins accumulate to high levels in the etiolated seedlings under dark conditions, but show enzymatic activity only during light exposure (Apel, 1981; Mosinger et al., 1985; Benli et al., 1991; Forreiter et al., 1991). In darkness, POR in etioplasts binds to its substrate, Pchlide, as well as NADPH and forms a ternary complex in prolamellar bodies (PLBs). Upon light irradiation , the highly structured PLBs immediately dissolve and the primary thylakoids membranes are formed. The light triggered activity of POR results in a

rapid chlorophyll synthesis as the formation of stroma lamellae and grana stacks are built up (or during transition from etioplasts to chloroplasts). However, although the activity of POR is strictly induced by light exposure, the bulk of POR accumulated in etioplasts degraded upon illumination (Hauser et al., 1984; Forreiter et al., 1991). In contrast to angiosperm species, the reduction of Pchlide in other photosynthetic organisms like algae, cyanobacteria, gymnosperms and bacteria, is however performed by a light-independent protochlorophyllide reductase, also designated as DPOR (dark-dependent protochlorophyllide reductase) (Zsebo and Hearst, 1984; Yang and Bauer, 1990; Choquet et al., 1992; Burke et al., 1993; Fujita et al., 1993; Bollivar et al., 1994; Wu and Vermaas, 1995; Fujita et al., 1996, 1998). In contrast to POR, DPOR consists of three subunits which resemble structurally to nitrogenase. Moreover, the catalytic mechanism differs in respect to use of ATP and thiol reductants and molecular oxygen sensitivity (Fujita and Bauer, 2000). Thus, DPOR may contribute to chlorophyll synthesis in light grown cells of these species . And its activity decreases due to an increase of light intensity (Fujita et al., 1998).

In continuation to initial studies on gymnosperms and bacteria, genes encoding POR variants were subsequently identified in higher plants, such as Arabidopsis, barley, cucumber, pea, wheat and tobacco (Armstrong et al., 1995; Dahlin et al., 1995; Holtorf et al., 1995; Fusada et al., 2000; Oosawa et al., 2000; Masuda et al., 2002). In Arabidopsis chloroplasts, three isoforms of PORs contribute to the photoreduction from Pchlide to Chlide, they are PORA, PORB and PORC. PORA and PORB were first found in 1995 by Armstrong et al. Although the two isoforms are highly identical at the amino acids level, they exhibit quite varied expression profiles. Both *PORA* and *PORB* mRNA accumulate in the etiolated seedlings in darkness. *PORA* transcript rapidly becomes undetectable during de-etiolation, whereas *PORB* expression persists throughout the greening and in mature plants (Armstrong et al., 1995). The third POR isoform, PORC, was first described in 2000. Like the *PORB*-encoding isoform, *PORC* transcript accumulates throughout the plant development, its mRNA level can also be induced by illumination in etiolated seedlings (Oosawa et al., 2000; Su et al., 2001). Consistent with its expression profile, PORA plays a vital role in etiolated seedlings. A *pora* knockdown mutant showed smaller prolamellar bodies and a late greening phenotype. Additionally, dark-grown *pora* mutant accumulated reduced chlorophyll content after illumination compared to wild type (Runge et al., 1996; Masuda et al., 2009). Primary characterization of *porb* and *porc* null mutants revealed no visible phenotypes, while a double mutation of both genes led to severe chlorophyll deficiency and developmental arrestment (Frick et al., 2003; Masuda et al., 2003). This indicated PORB and PORC proteins share common control of expression in Arabidopsis. However, *PORA* expression under the constitutively operating cauliflower mosaic virus (CaMV) 35S promoter was able to rescue the severe phenotype of *the porb-1 porc-1* double mutant (Paddock et al., 2010). This successful complementation verified that the three structurally related POR isoforms in Arabidopsis possess similar enzymatic features. The diverse functional occurrence of the three proteins is explained by their distinct expression patterns.

1.2.4 Heme branch / Ferrochelatase

In contrast to the complex chlorophyll biosynthesis pathway, the heme biosynthetic branch consists only of one enzymatic step catalyzed by the ferrochelatase (FC). FC catalyzes the insertion of ferrous iron into Proto IX, forming protoheme (heme b). Subsequently, protoheme is cleaved by heme oxygenase (HO) into the linear tetrapyrrole biliverdin IXα prior to further heme break down products (Muramoto et al., 1999; Kikuchi et al., 2005).

In contrast to MgCH, FC, is a single-subunit enzyme requiring no cofactors or external energy resource for catalysis. Besides the primary characterization of *FC* cDNA in yeast, mice and human in 1990, multiple coding sequences of bacterial *FC*s were identified in 1991 and 1992 (Labbe-Bois, 1990; Nakahashi et al., 1990; Taketani et al., 1990; Miyamoto et al., 1991; Frustaci and O'Brian, 1992; Hansson and Hederstedt, 1992; Miyamoto et al., 1994). Meanwhile FC homologues from higher plants were obtained. For instance, the first Arabidopsis FC isoform was isolated by functional complementation of a yeast mutant *hem15* (Smith et al., 1994). At the same time, genetic sequences encoding cucumber and barley FC were obtained by screening a cDNA library (Miyamoto et al., 1994). Subsequently more FC enzymes have been identified from other higher plants like tobacco, soybean and rice (Kanjo et al., 2001; Papenbrock et al., 2001; Kang et al., 2010).

1.2.4.1 Localization study of FC

In higher plants two genes encode FC, *FC1* (AT5G26030) and *FC2* (AT2G30390). The two Arabidopsis isoforms share 69% identical and 83% similar amino acid residues (Chow et al., 1998). Although these two types of FC share high structural similarities, they are distinguished by diverse expression patterns and subcellular allocations.

In photosynthetic organisms, the type-II FC has been found to be located in chloroplasts, while FC1 was presumed to be dual-targeted to both plastids and mitochondria, as it was shown by *in vitro* uptake experiments with pea mitochondria and chloroplast extracts (Chow et al., 1997; Chow et al., 1998). However, this assumption was subsequently challenged by the studies from Lister et al. in 2001. The authors performed similar import experiment of both Arabidopsis FCs using mitochondria and plastids from Arabidopsis instead of those from pea. In contrast to Chow et al.'s results, their outcome revealed a failed (mistargeted) import of both FC precursors into mitochondria. To compare the experimental systems, they tested import of multiple proteins to Arabidopsis and pea mitochondria and concluded that pea mitochondria were not a suitable system for dual-targeting studies (Lister et al., 2001).

In *Chlamydomonas reinhardtii* and red algae, there exists only a single FC variant. In Chlamydomonas, the FC isoform shares similarity with the type-II FC in plants localized exclusively in chloroplasts (van Lis et al., 2005). In contrast, FC in red alga *Cyanidius chyzonmerolae* is only localized in mitochondria, which makes the subcellular localization of FC in photosynthetic organisms a more elusive question (Watanabe et al., 2013). In

plants, heme is required in mitochondria for multiple fundamental biological processes. Regardless, whether the synthesis of heme originates in chloroplasts or heme is independently synthesized in mitochondria remains a big controversy. As FC is the sole enzyme catalyzing heme production after Proto formation, the clarification of this localization issue might be one of the key questions for source of mitochondrial heme. Recently according to the work from our group, overexpressed tobacco FC1 could be detected in mitochondria by immunoblot analysis. Relatively increased FC activity was determined in the mitochondria of 35SFC1 overexpressing plants in comparison with the wild-type mitochondria extracts (Hey et al., 2016). These results provide additional evidence for mitochondria-localized FC in tobacco.

In addition to direct studies on FC subcellular localization, research on the interacting partners of FC can also provide a clue to this debate. In both mouse and cyanobacteria, FC was found to form a membrane-associated complex with PPO, which catalyzes the upper synthetic step to generate Proto (Ferreira et al., 1988; Masoumi et al., 2008). Crystal structure from PPO was modeled with FC for a complex consisting of two dimers each for the two enzymes (Koch et al., 2004). As the tobacco PPO isoforms are localized in both chloroplasts (PPO1) and mitochondria (PPO2) (Lermontova et al., 1997), it indirectly favors the existence of a mitochondria-localized pathway, at least in certain higher plants. Recently, a new CPO isoform was identified in Arabidopsis, which activity contributes to heme supply during embryogenesis. Interestingly, the CPO protein was only located in mitochondria instead of plastids. These results furthermore implied a mitochondria-localized FC protein and heme synthesis pathway.

1.2.4.2 Current functional characterization of FC in higher plants

Although the two types of FC share high protein sequence similarity, FC2 harbors a unique putative chlorophyll a/b binding domain (CAB domain, also designated LHC (light-harvesting complex) domain) at the C-terminus (Suzuki et al., 2002). Using the FC2 homolog from cyanobacterium *Synechocystis sp. PCC 6803*, Sobotka et al. suggested that synFC lacking the CAB domain can fully restore FC activity, but protein dimerization would be disrupted. The absence of the CAB domain also led to a drastic accumulation of multiple chlorophyll-binding protein complexes and chlorophyll precursors under high light condition, suggesting a regulatory role of the CAB domain in chlorophyll biosynthesis and catabolism. Besides the catalytic domain in the synFC protein sequence, the proline-rich linker region (region II) between the core domain and CAB motif is also required for its catalytic activity (Sobotka et al., 2008; Sobotka et al., 2011).

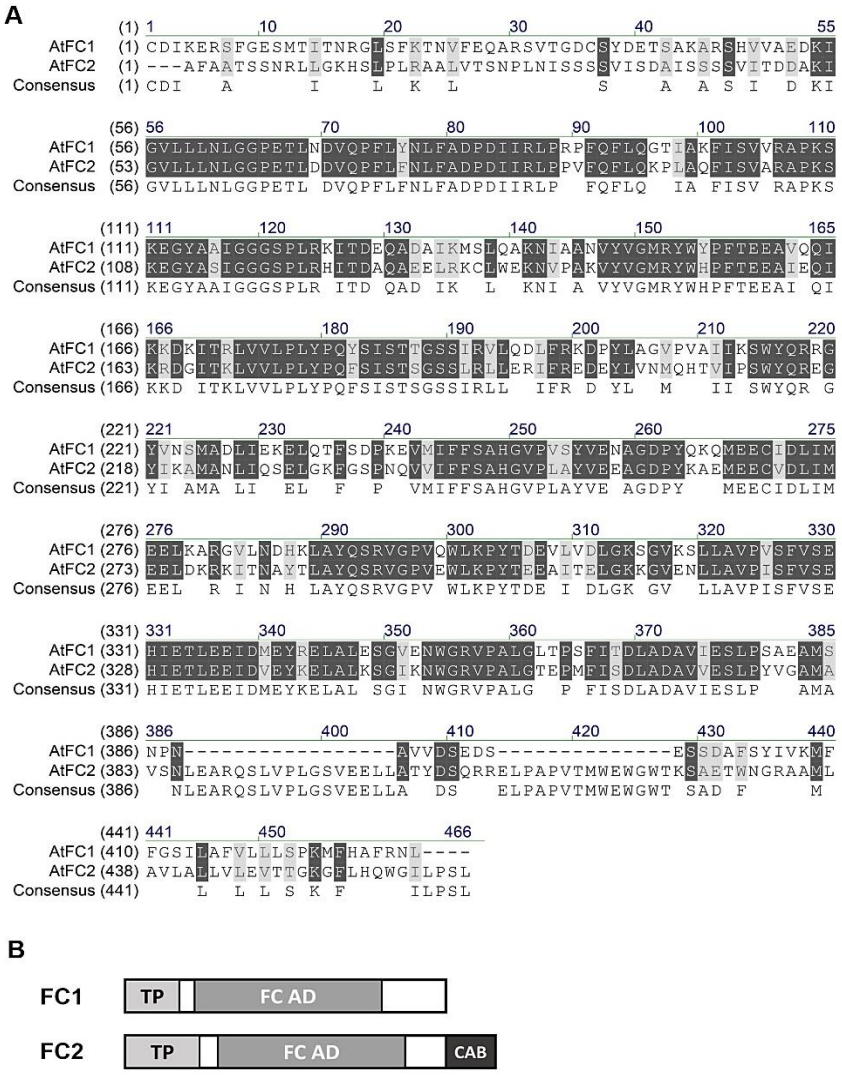

Figure 1. 3 Alignment of Arabidopsis FC1 and FC2 amino acid sequences.

(A) Alignment of amino acid sequences of mature FC1 and FC2 proteins. (B) Scheme of the conserved domains in Arabidopsis FC1 and FC2 proteins. TP: transit peptide; FC AD: ferrochelatase activity domain; CAB: chlorophyll A/B binding motif.

Although both FC isoforms share high structural similarities in Arabidopsis, they are distinguished by diverse expression patterns in various tissues and at different developmental stages. *FC1* is ubiquitously expressed in all tissues with comparable expression levels, whereas *FC2* mRNA mainly accumulates in photosynthetic tissues, such as leaves. Both *FC* transcripts are light-induced. *FC1* expression can be induced by sucrose, wounding, viral infection and oxidative stress, whereas transcription of *FC2* is not altered under those conditions (Smith et al., 1994; Chow et al., 1998; Singh et al., 2002; Nagai et al., 2007). Upregulation of *FC1* transcript upon stress treatment was then confirmed by co-expression analysis of both genes. The distinct expression profiles of the two *FC* genes

argue for their contribution to different heme pools (Woodson et al., 2011; Espinas et al., 2016; Hey et al., 2016).

Analysis of the T-DNA insertion mutants of the two *FC* genes revealed initial insights in the physiological function of the both FC isoforms. The *fc2* knockdown (*fc2-1*) and knockout (*fc2-2*) mutants are characterized by a gradually increasing phenotype of abnormally small and necrotic leaves with reduced chlorophyll content. In addition, *fc2-2* does not grow under short day condition (8h light / 16h dark) (Scharfenberg et al., 2015). The necrotic phenotype of *fc2* mutants was explained with enhanced photosensitization by accumulating tetrapyrrole intermediates, which was initially observed in transgenic tobacco expressing antisense *FC2* mRNA (Papenbrock et al., 2001).

In contrast to *fc2* mutants, a *fc1* knockdown mutant (*fc1-1*) showed no visible phenotype, while a *fc1-2* null mutant was proposed to be most likely embryo lethal, as homozygous *fc1-2* progenies could not be identified from the heterozygous parents (Woodson et al., 2011). More recently, an additional T-DNA insertion was proposed to be responsible for *fc1-2* embryo lethality (Scharfenberg et al., 2015), whereas Espinas et al. (2016) observed a few *fc1-2* homozygous seedlings on MS medium containing sugar. The *fc1-2* mutants were severely growth retarded and the seedlings died after occasional germination. Thus, the authors suggested FC1 may play an important role in newly emerging tissues rather than affecting embryogenesis (Espinas et al., 2016). However, the controversy regarding the embryo or seedling lethality of *fc1-2* mutant needs to be ultimately elucidated. Further, the cause of the phenotype should be also explored to characterize the real function of FC1 in plants.

The *fc2* mutants grown under light-dark conditions were reported to exhibit a *flu*-like phenotype due to the accumulation of the photoreactive chlorophyll precursor Pchlide in darkness and subsequent light exposure (Scharfenberg et al., 2015). Furthermore, Woodson et al. detected highly accumulated Proto in the *fc2* mutants during day time. In addition, the authors' approach to complement *fc2* by expressing *FC1* under its own and the 35S promoter revealed rescue of the necrotic phenotype under constant light, but not under day-night shift conditions confirming an important FC2 function for light-dark growth (Woodson et al., 2015). Comparative Blue-Native (BN) gel analysis of photosynthetic complexes of *fc2-2*, *fc1-1* and wild-type seedlings revealed an impaired assembly of photosystem II in *fc2-2* as well as modified photosynthetic parameters of *fc2* mutants, but not in *fc1-1* or the control seedlings (Scharfenberg et al., 2015; Espinas et al., 2016).

Interestingly, Arabidopsis FC1 overexpression provokes a *gun* (genomes uncoupled) mutant phenotype, which defines mutants under Norflurazon treatment with modified plastid-mediated retrograde signaling. Upon FC1 overexpression, the young seedlings (also designated as *gun6*) partially restore expression of photosynthesis-associated nuclear genes (PhANGs) when chloroplast development is blocked by Norflurazon treatment (Woodson et al., 2011). However, FC2 overexpression failed to demonstrate the

gun mutant effect, suggesting a unique role FC1 plays in signaling pathway compared to FC2. Recently, more evidences have been given regarding FC1 function in signaling. Based on the study from Zhao et al. (2017), FC1-synthesized heme regulates genes involved in sodium uptake under salinity stress. FC1 overexpression plants showed lower Na^+ uptake, exhibited more tolerance to the stress in comparison with wild-type seedlings. However, a *fc1* knockdown mutant displayed high sensitivity towards salt stress by accumulating more Na^+ in both roots and shoots (Zhao et al., 2017). Consistent with the salinity stress condition, FC1 overexpressing seedlings also exhibited more tolerance when high amounts of Cd were present, while *fc1* knockdown mutant displayed a reverse phenotype. The phenotypes were explained by an activation of genes involved in the GSH-dependent phytochelatin synthetic pathway by FC1-generated heme (Song et al., 2017).

The previous data presented arises the conclusion that the two FC isoforms serve for different heme pools in Arabidopsis. FC2 is proposed to be the predominant heme-synthesizing enzyme in leaves of green plants, supplying heme for photosynthetic activities, while FC1 is mainly distributed in roots and its expression and activity affects biogenic retrograde signaling during early chloroplast development and stress defense. However, the functional differences of both isoforms in the supply of heme in other tissues and their diverse functions referring to the distinct structures still await further elucidation.

1.3 TBS pathway regulation in higher plants

In vivo, tetrapyrroles are assembled in specific tetrapyrrole-apoproteins, and it is likely that the amount of "free" tetrapyrroles within the cell is extremely low (Moulin and Smith, 2005). In higher plants, many tetrapyrrole intermediates and end-products are readily excited by light. Accumulation of tetrapyrrole molecules *in vivo* leads to the formation of toxic radicals and reactive oxygen species (ROS), which cause damage during plant growth. Thus, a complex regulation of the TBS pathway is required, including an internal pathway regulation by regulatory factors, such as GUN4 (regulating MgCH activity) and FLU (inhibiting GluTR activity), intermediates (for instance, heme) as well as transcriptional regulation of key genes in response to environmental changes.

1.3.1 Regulation of ALA synthesis

Among all consequences of the TBS pathway control, the regulation of ALA synthesis is most demanding and complex, which determines the flux through the entire pathway. As a rate limiting synthetic step, the reduction of glutamyl-tRNA by GluTR is a highly regulated enzymatic reaction. Recent findings revealed that the control of GluTR activity is mainly achieved by feedback regulation through TBS end-product (heme) and regulatory proteins (FLU and GBP) which establish the crosstalk between other synthetic branches and ALA formation. In addition, GluTR stability is also regulated by Clp protease system and

chaperone factor cpSRP43. Last but not least, GluTR expression is also coordinated by phytochrome from transcript level.

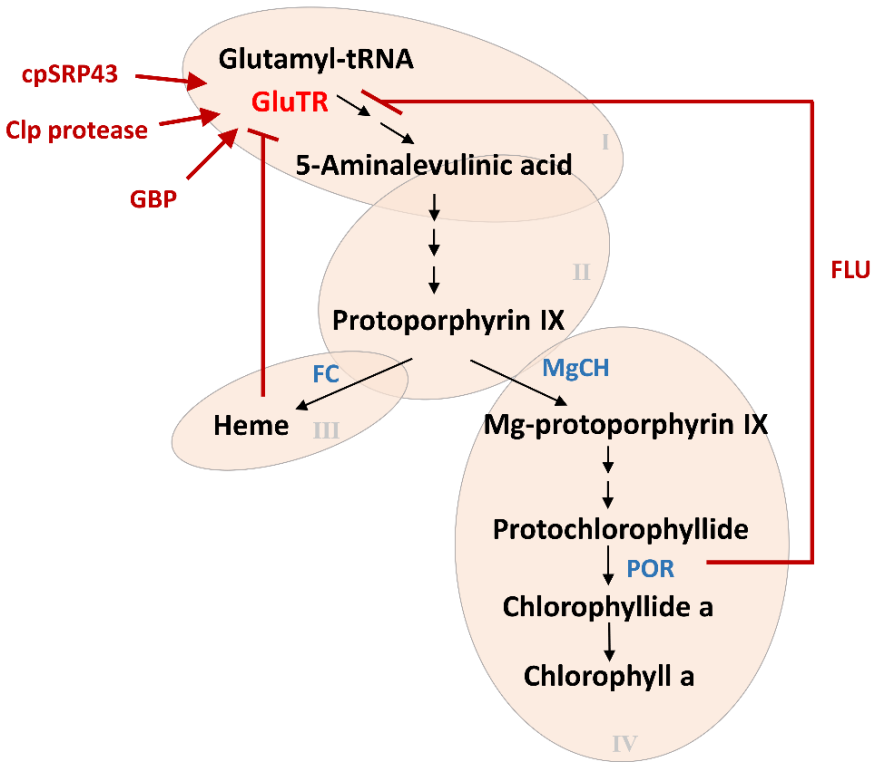

Figure 1. 4 Scheme describing regulation of GluTR activity by various posttranslational regulation factors.

Possible regulations are indicated in red lines. Arrow heads symbolize positive regulation or direct targeting. Flat ends indicate negative effects on GluTR activity. Current research reveals five posttranslational regulation mechanisms on GluTR protein: (i) heme directly inhibits GluTR activity as a feedback control from Fe branch; (ii) FLU links chlorophyll synthesis and ALA formation by binding and repressing GluTR activity; (iii) GBP interacts with GluTR and stabilizes the protein in darkness; (iv) GluTR is a substrate of Clp protease machinery; (v) cpSRP43 acts as a chaperone protein for the prevention of GluTR aggregation.

1.3.1.1 Regulation of ALA formation by heme

In angiosperms, GluTR is encoded by *hemA* gene family, and more than two *hemA* genes were found in each plant species. In 1985, Weinstein et al. obtained cell-free fractions from the unicellular green alga, *Chlorella vulgaris*. The activity assays suggested that the soluble fraction contains major ALA synthesis activity, but application of protoheme inhibits the initial activity by 50% (Weinstein and Beale, 1985). Subsequently, chloroplast extracts from cucumber were used for ALA formation analysis. Heme was proved to perturb ALA synthesizing capacity instead of other tetrapyrrole intermediates such as MgProto and Pchlide (Huang and Castelfranco, 1989; Castelfranco and Zeng, 1991). Catalytic assay of

recombinant protein of barley GluTR further demonstrated *in vitro* GluTR activity is suppressed in the presence of heme (Vothknecht et al., 1996). In bacteria, both *Salmonella enterica* and *Acidithiobacillus ferrooxidans* GluTR proteins were purified from cell extracts, which contain type b heme (Jones and Elliott, 2010; de Armas-Ricard et al., 2011). Additionally, heme preferentially bound dimeric GluTR. A Cys_{170}-Ala mutation of *Salmonella enteric* HemA protein sequence resulted in a non-heme-bound enzyme fraction under the same purification condition (Jones and Elliott, 2010; de Armas-Ricard et al., 2011).

Besides *in vitro* analyses of heme impact on ALA synthesis, more investigation regarding GluTR regulation by heme was conducted in mutants. Two phytochrome chromophore-deficient tomato mutants, *aurea* (*au*) and *yellow-green-2* (*yg-2*) displayed pale green leaves. In darkness, both etiolated mutants showed reduction of Pchlide content compared to wild-type plants. Feeding experiments revealed that the reduced level of Pchlide in the mutants was not due to a block in chlorophyll synthesis. Instead, supply of exogenous ALA was able to rescue the reduced Pchlide production in both mutant lines. Thus the pale green phenotype might be a consequence of decreased ALA synthesizing capacity, which was explained by feedback inhibition of accumulated heme (Terry and Kendrick, 1999). In barley, a 30-amino-acid-long N-terminal extension of GluTR protein is responsible for the perception from heme-dependent inhibition (Vothknecht et al., 1998; Czarnecki and Grimm, 2012). Similar conclusion has also been drawn in Arabidopsis, based on characterization of a *heme oxygenase* (*hy1*) mutant, which has a defect in heme degradation. The mutant which was supposed to accumulate more heme compared to wild-type seedlings, exhibited pale green leaves (Parks and Quail, 1991; Muramoto et al., 1999). Null mutation of *hy1* in a *fluorescent (flu)* knockout mutant background in which GluTR activity was not properly suppressed, significantly alleviated the uncontrolled-upregulated ALA synthesis activity in etiolated seedlings. The double mutant *flu/hy1* accumulated less Pchlide compared to *flu,* however still higher content than wild-type seedlings. These results implicated heme inhibits GluTR activity independently from the regulation by FLU (Goslings et al., 2004). In all the heme catabolic deficient mutants, however over-accumulated heme could never be shown by spectrophotometric assay or HPLC analyses. One can only argue this with the poor heme measurement technique which currently only allows the detection of non-covalently bound heme, the existences of other heme portions, for instance, “free heme” and covalently bound heme could not be determined (Sinclair et al., 2001).

1.3.1.2 FLU, a negative regulator of GluTR activity from Chl branch

Fluorescent (FLU), is a nuclear-encoded plastid protein, which locates exclusively in thylakoid membranes. FLU is characterized as a negative regulator of GluTR activity, which selectively affects only the Mg branch of TBS pathway. Arabidopsis and barley seedlings lacking FLU protein accumulate high amounts of Pchlide in darkness (Nielsen, 1974; Wettstein et al., 1974; Meskauskiene et al., 2001; Lee et al., 2003). The over-accumulated Pchlide then causes irreversible photooxidative damages after a subsequent

illumination (Fluhr et al., 1975; Ford and Kasemir, 1980; Stobart and Ameen-Bukhari, 1986; Richter et al., 2010). The etiolated Arabidopsis *flu* mutant shows elevated ALA synthesis capacity and a 9-fold increased Pchlide content compared to wild type. The heme content, however, is not altered in this mutant, which leads to a hypothesis of chlorophyll-dependent regulation on ALA formation (Meskauskiene et al., 2001). The interaction between FLU and GluTR was first confirmed by a yeast-two-hybrid approach (Meskauskiene and Apel, 2002). Although the Arabidopsis genome contains at least two *hemA* genes encoding GluTR, FLU specifically binds only GluTR1, but not GluTR2 (Goslings et al., 2004). This definitive interaction was further verified *in vivo* via a characterization of *pHEMA1::HEMA2* (*hema1/hema1*) (designated as A2) complementation plants. The *hema1* null mutant was severely growth retarded and could only survive heterotrophically on MS (Murashige and Skoog) plates, while the complemented A2 lines restored wild-type levels of heme and chlorophyll contents under standard growth condition suggesting a full complementation. However, when these transgenic A2 lines were exposed to extended darkness, the seedlings exhibited necrotic leaves which was explained with an over-accumulation of Pchlide. This was attributed to a lack of FLU inhibition to GluTR2 activity, which lacks the FLU binding motif (also designated as FBD) in comparison with GluTR1. Thus, it could be concluded that FLU specifically regulates GluTR1 and fails to suppress GluTR2 activity in darkness (Apitz et al., 2014).

Responsible domains of GluTR1 and FLU contributing to their interaction were identified by the yeast-two-hybrid assay and the crystal structure of the two proteins (Meskauskiene and Apel, 2002; Zhang et al., 2015; Fang et al., 2016). The Tetratricopeptide Repeat (TPR) domain, located at the C-terminus of Arabidopsis FLU protein forms a concave surface which binds to the helix bundle at the C-terminus of the dimeric GluTR. The i*n vitro* enzymatic assay also indicated that the TPR domain (of FLU) is able to independently inhibit GluTR activity (Zhang et al., 2015).

In Angiosperms, the rate of ALA synthesis has been found to be inversely proportional to the accumulation of photoactive Pchlide. Multiple hypotheses were raised regarding the regulation mechanism of Pchlide accumulation upon ALA formation (Fluhr et al., 1975; Ford and Kasemir, 1980; Stobart and Ameen-Bukhari, 1986; Richter et al., 2010). In 2012, Kauss et al. revealed a chloroplast membrane complex containing FLU as well as several proteins involved in late steps of chlorophyll biosynthesis. Those FLU interacting candidates were PORB, PORC, CHL27 and DVR, which interactions were confirmed by co-immunoprecipitation. Based on these interactions of FLU and chlorophyll synthetic enzymes, the authors proposed a possible regulation model of Pchlide upon GluTR activity (Figure 1.5). During daylight, in planta, there exists only a “Pchlide-free” POR-Cyclase-FLU complex. However, in darkness, Pchlide could accumulate and bind to this membrane protein complex and activates the interaction between FLU and GluTR. Therefore, FLU could only negatively regulate ALA formation when a “Pchlide-bound” POR-Cyclase-FLU complex is present. Additionally, it was assumed that a lack of either POR or cyclase protein *in vivo* could also result in a failure of FLU inhibition on ALA synthesis attributing

to the previous characterization of *por* and *chl27* mutants (Franck et al., 2000; Lee et al., 2003; Tottey et al., 2003; Rzeznicka et al., 2005; Pontier et al., 2007).

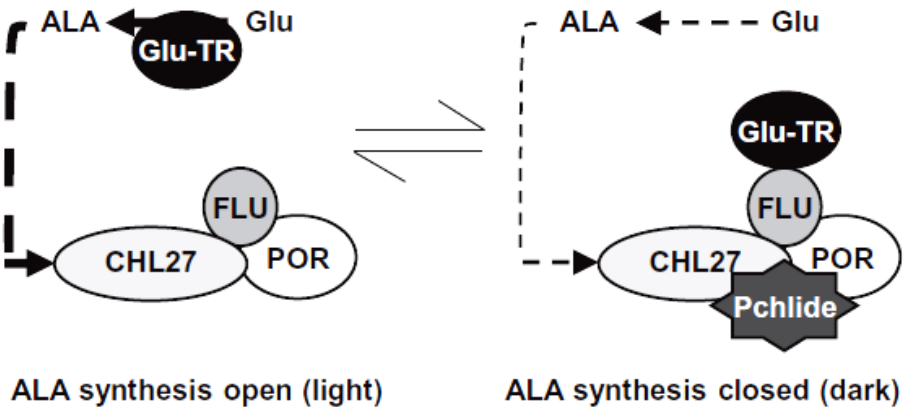

Figure 1. 5 Hypothetical model of "Pchlide-bound" POR- Cyclase-FLU complex regulating ALA formation under both light and dark conditions.

(Figures cited from Kauss et al., 2012)

1.3.1.3 GluTR binding protein (GBP) stabilizes GluTR protein, positively regulates its activity.

In 2010, a *PROTON GRADIENT REGULATION 7 (pgr7)* mutant was characterized as a growth retarded mutant with compromised photosynthesis. Positional cloning located the mutation site in *At3g21200* locus (Jung et al., 2010). Further studies from our group revealed the genuine function role of PGR7 protein, which turned out to be a stimulator of ALA formation. The protein interacts with GluTR in yeast cells as well as in chloroplasts. Therefore, it is also named as GluTR-binding protein (GBP) (Czarnecki et al., 2011). GBP is localized in both stroma and membrane fractions of chloroplasts. An antisense mutant of *gbp* exhibits reduction of heme content and slightly affected chlorophyll synthesis. Thus, a positive impact of GBP on ALA formation was assigned to heme synthesis, but less to chlorophyll production during early developmental stages. It is proposed that there may exist different ALA synthesizing pools towards heme and chlorophyll synthesis (Czarnecki and Grimm, 2012, 2013). Crystal structure of GluTR revealed that the dimeric GBP binds to the V-shaped GluTR dimer *in vitro*. By adding GBP, the GluTR catalytic efficiency is stimulated up to three-fold compared to the control. In addition, GBP belongs to a heme-binding protein family, nevertheless heme inhibits GluTR activity regardless of the presence of GBP *in vitro* (Zhao et al., 2014). Although both FLU and GBP regulate GluTR activity through physical interactions, they are assigned with different binding motifs. FLU interacts with the N-terminus of GluTR, i.e. FBD, while GBP binds to the heme-binding (HBD) motif at C-terminal GluTR (Apitz et al., 2016; Fang et al., 2016). In addition to its stimulatory role, GBP also protects GluTR from degradation in darkness. As GluTR has been proved to be a target protein for the Clp protease complex, Apitz et al. (2016) could show that both Clp protease components and GBP interact with the GluTR HBD domain in

a competitive manner. In darkness, Clp protease machinery on one hand attenuates GluTR activity to prevent excessive accumulation of TBS intermediates which were mostly phototoxic. On the other hand, GBP contributes to maintenance of the essential ALA formation for heme production during night. The two mutual dependent control mechanisms balance ALA homeostasis in darkness.

1.3.1.4 Turnover of GluTR protein

The Clp protease machinery in planta consists of multiple components including five proteolytically active subunits (ClpP), four proteolytically inactive subunits (ClpC/D), activating factor ClpT, chaperone proteins and adaptor ClpS (Nakabayashi et al., 1999; Sjogren et al., 2006; Zheng et al., 2006; Wu et al., 2010; Nishimura et al., 2013; Kim et al., 2015; Nishimura and van Wijk, 2015; Welsch et al., 2018). In a screen for Clp protease substrates, GluTR was found to be one protein candidate which can be degraded by the Clp protease (Nishimura et al., 2013; Nishimura et al., 2015). Further *in vivo* evidence was provided by *clp* mutants characterization. In both *clpc1-1* and *clpr2-1* mutants, GluTR protein was retained after three days dark incubation while its amount was drastically reduced in wild-type leaves. However, degradation of GluTR could be still observed in *clps1* mutant, which can be explained by the compensatory function of the newly identified ClpF subunits, which acts as a selector protein in the Clp system (Apitz et al., 2016). Besides GBP which binds to the GluTR HBD domain to prevent its proteolytic degradation by the Clp protease, the chloroplast signal recognition particle 43 (cpSRP43) also positively regulates GluTR stability. cpSRP43 stabilizes GluTR by preventing its self-aggregation which structure form is likely to be degraded. Due to a lack of cpSRP43, the destabilized GluTR led to an attenuated chlorophyll production without any effect on heme synthesis. Interestingly, cpSRP43 also interacts with GluTR at its N-terminal HBD domain. A double mutation of *cpSRP43*and *gbp* causes more severe reduction of the GluTR amount compared to the single mutations. This leads to the conclusion that cpSRP43 and GBP compete for the overlapping binding site of GluTR and cooperatively stabilize GluTR from degradation for the sake of chlorophyll and heme synthesis, respectively (Wang et al., 2018).

1.3.2 Transcription regulation of TBS pathway

Both chlorophyll and heme are the most critical tetrapyrrole products for massive fundamental biological processes in plants. An excess of most TBS intermediates stimulates accumulation of reactive oxygen species and toxic radicals under light exposure which consequently cause cell damages. Thus, multiple regulations must be utilized by plants to achieve efficient photosynthesis as well as avoiding potential photodamage. Despite of posttranscriptional regulation of ALA formation and enzymatic regulators, such as GUN4 contributing to fine-tune the synthetic flow of chlorophyll, diverse transcriptional regulations are also devoted to a strictly balanced TBS pathway.

1.3.2.1 Key genes involved in TBS pathway are regulated by light

To coordinate the synthesis of heme and chlorophyll to different developmental stages and changing environmental conditions (for example, light intensity, temperature and humidity), expression of key genes of TBS pathway is regulated rhythmically to maintain adequate production of end products. Via a transcriptome analysis of Arabidopsis seedlings, Matsumoto et al. was able to classify TBS genes into four groups based on their expression patterns in response to light and the circadian clock (Matsumoto et al., 2004). The cluster 1 represents four genes which are rapidly induced by light exposure showing a *LHC* gene-like expression, including *HemA1*, *CHLH*, *CRD1* (encoding a putative Mg-protoporphyrin IX monomethyl ester cyclase) and *CAO*. Sixteen genes comprise cluster 2, exhibit a gradual stimulated expression by light instead of a rapid increase compared to cluster 1 genes. This group contains mainly genes involved in the earlier synthetic steps in TBS pathway and *PORC*, *CHLG* (encoding chlorophyll synthase) as well as *HO2*. The cluster 3 consists of thirteen genes including majority of genes in heme metabolism, showing a constitutive expression pattern. Only two genes belong to the cluster 4. They are both isoforms of POR, *PORA* and *PORB*, which are negatively regulated by light.

1.3.2.2 Transcription factors regulate genes involved in TBS pathway.

To conduct the required expression profile of TBS key genes, several transcription factors have been revealed to target certain genes involved in TBS pathway and regulate the latter expression. Among them, typical well-characterized TBS transcription factors include Long Hypocotyl 5 (HY5) and phytochrome-interacting factors (PIFs). HY5 is an important transcription factor regulating general light responsive genes. The transcription factor is able to conduct the regulation due to its degradation by ubiquitin protease machinery during night phase but not day time (Ang et al., 1998; Delker et al., 2014). In 2007, via a chromatin immunoprecipitation-chip assay, HY5 was proved to target all TBS genes from cluster 1 in addition to various PhANGs (Lee et al., 2007). Particularly, HY5 directly binds to G-box *cis*-element-containing promoter of *CHLH* and *PORC*. A *hy5* knockout mutant exhibits reduction of chlorophyll content as well as a partially inhibited *CHLH* transcript (Holm et al., 2002; Kobayashi et al., 2012). However, in comparison to chloroplast biogenesis of leaf tissues, HY5 plays a more critical regulatory role for TBS genes expression in roots, as *hy5* mutation causes severe reduction of TBS genes expression, results in albino roots (Toledo-Ortiz et al., 2014).

In addition to a stimulation of TBS genes expression by HY5 upon light exposure, a series of inhibition of the pathway genes under darkness are conducted by multiple phytochrome interacting factors (PIFs) in order to avoid accumulation of phototoxic TBS intermediates (Kobayashi and Masuda, 2016). PIFs consist of a group of basic helix-loop-helix transcription factors which binds to the photoactivated phytochromes during night phase (Quail, 2000; Castillon et al., 2007). Both PIF1 and PIF3 bind to the G-box containing promoter of *CHLH* (Monte et al., 2004; Liu et al., 2013). Additionally, PIF1 also interacts with *PORC* and *CAO* promoter. A lack of both *PIF1* and *PIF3* results in elevated expression

of cluster 1 genes in TBS pathway, for instance, *HemA1* and *CHLH*, which leads to accumulation of chlorophyll intermediates (Huq et al., 2004). In addition to that, functional loss of *PIF5* also triggers an increase of *CHLH* transcript, results in bleached leaves upon light illumination. Moreover, a quadruple mutation of *PIF1*, *PIF3*, *PIF4* and *PIF5* leads to global upregulation of TBS genes as well as PhANGs, indicating that all the four PIFs play essential functions in repressing tetrapyrrole synthesis in darkness (Leivar et al., 2009; Shin et al., 2009).

2. Materials and methods

2.1 Plant materials and growth conditions

The Arabidopsis T-DNA insertional mutants of *fc1-1* (SALK_150001), *fc1-2* (GK_110D_02), *fc2-1* (GK_766_H08), *fc2-2* (SAIL_20_C06) were obtained from Nottingham Arabidopsis Stock Centre. Comparable wild-type Arabidopsis used was Columbia (Col-0) or Landsbergerecta (Ler). All the Arabidopsis seedlings were grown on soil or MS plates under short day (8h light/16h dark cycles), long day (16h light/8h dark cycles) or continuous light (24h light) conditions with 100μE light intensity, at 22°C. The information of the transgenic Arabidopsis plants and mutant lines used in this study was listed in Table 2.1.

In this study, wild-type *Nicotiana benthamiana* was used for transient transformation of tobacco. Seedlings were grown under long day (16h light/8h dark cycles) condition at 22°C.

Mutants / Transgenic plants	Transformation background	Construct	Source
fc1-1 *(fc1 knockdown)*	-	T-DNA insertion site: 5'UTR	Nottingham Arabidopsis Stock Centre (Scharfenberg et al., 2015)
fc1-2 (*fc1* knockout) (only heterozygotes available, F47)	-	T-DNA insertion site: the 3rd exon	
fc2-1 (*fc2* knockdown)	-	T-DNA insertion site: 5'UTR	
fc2-2 (*fc2* knockout)	-	T-DNA insertion site: the 6th intron	
heterozygous *fc2-2*, F2-14	-	T-DNA insertion site: the 6th intron	
porb	-	T-DNA insertion	Hey et al., 2017
flu	-	point mutation	Nottingham Arabidopsis Stock Centre
hy1	-	T-DNA insertion	
pFC1FC1	heterozygous *fc1-2*	*pFC1::FC1*	this study
pFC1FC2	heterozygous *fc1-2*	*pFC1::FC2*	this study
pFC2FC1	heterozygous *fc1-2*	*pFC2::FC1*	this study
	heterozygous *fc2-2*		this study
pFC2FC2	heterozygous *fc1-2*	*pFC2::FC2*	this study
	heterozygous *fc2-2*		this study
FusA	heterozygous *fc1-2* (plants analyzed are in Col-0 background)	*pFC1::FC2*(1-240)_*FC1*(230-466)	this study
FusB	heterozygous *fc1-2* (plants analyzed are in Col-0 background)	*pFC1::FC2*(1-425)_*FC1*(415-466)	this study
35SFC1	Col-0	*p35S::FC1*	this study
35SFC2	Col-0	*p35S::FC2*	this study
35SFC1-YFP	Col-0	*p35S::FC1_YFP*	Woodson et al., 2011
35SFC2-CFP	Col-0	*p35S::FC2_YFP*	Woodson et al., 2011

Table 2. 1Information of transgenic plants and mutants used in this study

2.2 Bacteria and growth conditions

In this study, *E.coli* bacteria (DH5α, BL21 and Rosetta) and Agrobacterium GV2260 were used, and they were cultured with LB and YEB medium respectively (Table 2.2). The growth temperature was 37°C for *E.coli* and 28°C for Agrobacterium.

LB medium (1L)
10g tryptone
5g yeast extract
10g NaCl
adjust pH to 7.0

YEB medium (1L)
5g beef extract
1g yeast extract
5g peptone
5g sucrose
2mM $MgSO_4$
adjust pH to 7.0

Table 2. 2 Ingredients for LB/YEB medium

2.3 Transformation of bacteria/ agrobacteria and plants

2.3.1 *E.coli* transformation

Designated vectors in this study were transformed into *E.coli* cells by a chemical transformation method. The *E.coli* competent cells were firstly thawed on ice for 2min. 40µl cells suspension were mixed with 10-100ng plasmids, followed by 25-30min incubation on ice. The cells were then shortly heat shocked at 42°C for 30s. Afterwards, the reaction was incubated again on ice for another 1min before adding SOC medium (2% (w/v) tryptone, 0.5% (w/v) yeast extract, 10mM NaCl, 2.5mM KCl, 10mM $MgCl_2$, 20mM glucose). The cell culture was placed on a 37°C shaking incubator for 1h. *E.coli* colonies were grown overnight on LB medium plates at 37°C. Positive transformants were selected by the application of certain amount of specific antibiotics.

2.3.2 *Agrobacterium tumefaciens* transformation

An aliquot of Agrobacteria competent cells was thawed on ice before adding 2-20ng purified plasmids. The mixture was shortly suspended by pipetting, and then transferred into a pre-cooled electroporation cuvette (slit 1mm). The suspension was pulsed by an electroporator with a setting listed in Table 2.3. The cells were immediately resuspended with 500µl YEB medium at room temperature, and cultured on a 28°C shaker for 2-3h. Afterwards, the transformants were plated on YEB agar medium supplied with specific antibiotics for selection. The growing condition for Agrobacterium is 28°C for 2 days on plates and overnight growth for liquid culture.

Electroporator setting
Voltage: 1800V
Capacitance: 50μF
Resistance: 129Ω

Table 2. 3 Electroporator settings for Agrobacteria transformation

2.3.3 Transient transformation of *Nicotiana benthamiana* leaves by Agrobacterium infiltration

An overnight culture of Agrobacterium was prepared with fresh colonies from selective YEB medium plates. The cells were harvested by 20min centrifugation at 5,000g at room temperature. The pellet was then diluted to a cell intensity of OD_{600}=0.6 with infiltration buffer (Table 2.4). The suspension was afterwards incubated at room temperature for 2-3h, followed by the final infiltration which was performed on the underside of the leaves with a syringe. The transformed tobacco was placed into a standard phyto-chamber for 72h dark growth before fluorescence detection.

Infiltration medium
10mM $MgCl_2$
10mM MES, pH 5.7
100μM Acetosyringone

Table 2. 4 Constituents of infiltration medium

2.3.4 Stable transformation of *Arabidopsis thaliana*

Healthy *Arabidopsis thaliana* plants with newly emerged inflorescences were chosen for transformation. An overnight culture of Agrobacterium GV2260 was prepared with fresh colonies carrying the designated expression vector. Agrobacteria cells were harvested at room temperature by centrifugation, and then diluted with Inoculation medium (Table 2.5) to a cell intensity of OD_{600}=0.8. The suspension was directly dropped onto the top of newly emerged inflorescences with pipet. Transformed plants should be incubated under dim light for 1-2 days before transferring to standard growth conditions.

Inoculation medium (100ml)
0,5 x MS salts
0,05% MES buffer,
5% sucrose
0.05% Silwet L-77
adjust to pH 5.7

Table 2. 5 Ingredients for inoculation medium

2.4 Nucleic acid extraction and analyses

2.4.1 DNA extraction

Genomic DNA extraction was performed using a "quick and dirty" method. Arabidopsis leaves were homogenized in 100µl extraction buffer (200mM Tris pH 8.0, 150mM NaCl, 25mM EDTA and 0.5% SDS), followed by 2min centrifugation at 16,000g, 4°C. The supernatant was transferred to a new Eppendorf tube, DNA was precipitated with an equal amount of isopropanol by 10min centrifugation at 16,000g, 4°C. DNA pellet was then washed twice with 75% ethanol and dissolved in 25µl ddH_2O.

2.4.2 Polymerase chain reaction (PCR)

PCR is a common laboratory technique to obtain specific DNA fragments from genomic DNA or cDNA. PCR system used in the study was listed in Table 2.6, which reaction was proceeded in Thermal cycler (Biometra) according to the procedure in Table 2.7.

PCR reaction	
Dream Taq polymerase	0.1µl
10x Buffer	2µl
10mM dNTPs	0.5µl
10µM forward primer	1µl
10µM reverse primer	1µl
DNA template	0.5µl
ddH_2O	14.9µl
total volume	20µl

Table 2. 6 PCR reaction system applied in this study.

Standard PCR program		
Step No.	Temprature (℃)	Time
1	95	2min
2	95	10s
3	56-60	10s
4	72	1-2min
step 2-4, x 35 cycles		
5	72	4min
6	4	pause

Table 2. 7 Standard PCR process applied in this study

2.4.3 RNA extraction

RNA from Arabidopsis leaf tissues was extracted with TriSure reagent (Bioline) according to the manufacturer's instruction. More than 30mg leaf material was homogenized in liquid Nitrogen, the fine powder was then suspended with 1ml TriSure solution, followed by 5min incubation at room temperature. 200µl chloroform was added to each reaction

with vigorous vortex. An additional 5min incubation was necessary before the 15min centrifugation at 12,000g, 4°C. The upper aliquot phase was transferred to new Eppendorf tubes for RNA isolation. Subsequently, the RNA was precipitated with 500µl isopropanol, followed by 10min centrifugation at 12,000g, 4°C. The pellet was then washed twice with 75% ethanol. Finally, the pellet was air-dried and dissolved with RNase free ddH_2O. RNA concentration was determined with the NanoDrop 2000 Spectrophotometer (Thermo Scientific), and integrity of RNA was checked by gel electrophoresis.

2.4.4 Reverse transcription and quantitative real-time polymerase chain reaction (qRT-PCR) analyses

To synthesize cDNA, 1µg RNA was treated with 0.5µl DNaseI (Thermo Scientific) at 37°C for 30min. The reaction was terminated by adding 1µl EDTA with 10min incubation at 65°C.

The pre-treated RNA was then reverse transcribed with Oligo(dT) using RevertAid reverse transcriptase (Thermo Scientific) according to the reaction system in Table 2.8.

Reverse transcription	
RNA samples	6µl
oligo-T primer (100µM)	0.5µl
5x RT buffer	2µl
10mM dNTPs	1µl
Ribo Lock Rnase-Inhibitor	0.25µl
Reverse Transcriptase RevertAid	0.5µl

Table 2. 8

qRT-PCR in this study was performed by using SYBR green PCR master mix (Biotool) according to the reaction system in Table 2.9. Reactions were taken place on a BioRad C1000™ Thermal Cycler (CFX96 real-time system). Expression levels were calculated by the $2^{-\triangle\triangle Ct}$ method and normalized to the reference gene *ACTIN2* or *GADPH*.

qRT-PCR reaction	
2x Syber MIX	3µl
forward primer	0.15µl
reverse primer	0.15µl
cDNA	1µl
ddH_2O	1.7µl
total volume	6µl

Table 2. 9 Components of qRT-PCR reactions

2.4.5 Plasmid isolation

To isolate plasmids from *E.coli*, buffers listed in Table 2.10 were used. The bacteria cells were harvested by 2min centrifugation at maximum speed after overnight cultivation. 300µl Solution P1 was used to resuspend the *E.coli* cells. Then the cells were lysed by adding 300µl Solution P2 with 5min incubation at room temperature. After adding 300µl pre-cold Solution P3, the lysate became viscous with white fluffy pellet. The supernatant was transferred to new reaction tubes after 10min centrifugation at 16,000g, 4°C. Plasmids were precipitated with 800µl isopropanol followed by 15min centrifugation at 16,000g, 4°C. The final pellet was then washed twice with 75% ethanol and dissolved with 30µl ddH_2O.

Plasmid isolation	
Buffer	**Ingredients**
P1	50mM Tris/HCl, pH 8.0
	10mM EDTA
	100µg/ml RNase A
P2	200mM NaOH
	1% SDS(w/v)
P3	3M potassium acetate pH 5.5

Table 2. 10 Buffers used for plasmid isolation.

2.5 Protein isolation and analyses

2.5.1 Isolation of protein samples and electrophoresis

For protein extraction from Arabidopsis leaf tissues, samples were weighed and frozen in liquid nitrogen followed by homogenizatio. Then the fine powders were dissolved in 2-fold SDS-PAGE (polyacrylamide gel electrophoresis) sample buffer (100mM Tris/HCl, pH 6.8, 4% SDS, 20% glycerol, 2mM dithiothreitol) at 95°C for 10min. Equal amount of protein samples were applied to a SDS-PAGE or Tricine-PAGE for subsequent immunoblot analysis or Coomassie staining. The preparation of SDS-PAGE gels was done according to Table 2.11.

SDS PAGE gel			
Solution	**separation gel (ml)**		**stacking gel (ml)**
	10%	12%	4%
ddH_2O	1.9	1.6	1.4
30% Acrylamide (29:1)	1.7	2	0.33
1.5M Tris/HCl pH 8.8	1.3	1.3	-
0.5M Tris/HCl pH 6.8	-	-	0.25
10% SDS	0.05	0.05	0.02
10% APS	0.05	0.05	0.02
TEMED	0.002	0.002	0.002
total volume	5	5	2

Table 2. 11 Ingredients for SDS-PAGE gels.

SDS-PAGE electrophoresis was performed with 1x SDS-PAGE buffer (25mM Tris, 192mM Glycine, 0.1% SDS (w/v), pH 8.3), started with 80V voltage for stacking gel and increased to 120V for separation gel.

2.5.2 Coomassie staining and western blot analyses

The SDS-PAGE gels used for staining were incubated in Coomassie solution (0.1 % (w/v) Coomassie brilliant blue R-250, 40% methanol, 10% acetic acid) at room temperature for 1h. Then the gels were washed several times with de-staining buffer (45 % methanol, 10% acetic acid), and detected with a CanoScan 5600F scanner.

For immunoblotting analysis, protein samples were transferred to a Nitrocellulose membrane (GE health) through a sandwich-layer described in Figure 2.1 via a Semi-Dry Blotter (Bio-Rad). All the membranes and Whatman papers were soaked in transfer buffer (25mM Tris, 192mM Glycine, 20% methanol) before the construction.

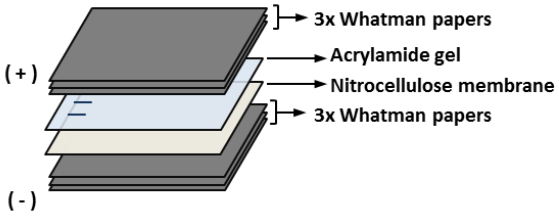

Figure 2. 1Scheme of the sandwich-layer structure for transfer.

For a 0.75mm and 1.5mm Acrylamide gel, 40mA and 60mA constant current was applied for 1h transfer, respectively. Afterwards, membranes were pre-checked with Ponseau solution (0.1% (w/v) Ponceau S, 5% acetic acid) before immunoblotting analyses.

2.5.3 Immunoblotting assay

To detect the protein amount from loaded samples, the transferred Nitrocellulose membrane was firstly blocked with TBST (1xTBS, 0.1% Tween-20) buffer containing 2% milk for 1h at room temperature. This step is critical to avoid the antibodies from unspecific binding to the membrane. The blocked membrane was then washed once with TBST and two times with TBS buffer (150mM NaCl; 50mM Tris-HCl, pH7.5), and incubated overnight with primary antibodies in TBS containing 1% milk at 4°C. Afterwards, the antibody solution was discarded and membranes were washed once again with TBST and three times with TBS. Information of the primary antibodies used in this study was listed in Table 2.12.

Afterwards, membranes were incubated in a secondary antibody (in TBS+1% milk) labelled with horseradish peroxidase (HRP) for 1h at room temperature. The unbound antibody was removed through once wash with TBST and three times with TBS buffer.

Finally, the luminescence in proportion to the protein amount was determined with Clarity Max™ ECL Substrate (Bio-Rad) by an ECL Chemostar Imager (INSTAS).

Name	Antibodies raised against	Dilution	source
α-AtpB	ATP synthase β subunit	1:10,000	Agrisera
α-CHL27	Cyclase in Arabidopsis	1:5,000	Agrisera
α-CHLD	MgCH D subunit (pea)	1:2,000	From Meizhong Luo's lab (Luo et al., 2012)
α-CHLH	MgCH H subunit (pea)	1:1,000	
α-CHLI	MgCH I subunit (pea)	1:2,000	
α-CHLM	CHLM in Arabidopsis	1:200	Richter et al., 2016
α-FC1	FC1 in Arabidopsis	1:100	this study
α-FC2	FC2 in Arabidopsis	1:100	this study
α-FLU	FLU in Arabidopsis	1:100	this lab
α-GBP	GBP in Arabidopsis	1:2,000	Czarnecki et al., 2016
α-GluTR	GluTR in Arabidopsis	1:2,000	Agrisera
α-GSAAT	GSAAT in Arabidopsis	1:5,000	Grimm et al., 1990
α-GUN4	GUN4 in Arabidopsis	1:2,000	Peter et al., 2009
α-LHCA1	Chlorophyll a binding protein	1:5,000	Agrisera
α-LHCB1	Chlorophyll b binding protein	1:5,000	Agrisera
α-LHCB5	Chlorophyll b binding protein	1:5,000	Agrisera
α-LHCB6	Chlorophyll b binding protein	1:5,000	Agrisera
α-POR	recognizes both Arabidopsis PORA and PORB	1:5,000	Agrisera
α-PORC	PORC in Arabidopsis	1:5,000	Agrisera
α-PsaA	core subunit of photosystem I	1:5,000	Agrisera
α-PsbA	D1, core sununit of photosystem II	1:5,000	Agrisera
α-PsbB	CP43 in photosystem II	1:5,000	Agrisera
α-PsbC	CP47 in photosystem II	1:5,000	Agrisera
α-PsbE	Cytochrome 559 α subunit	1:5,000	Agrisera
α-PsbF	Cytochrome 559 β subunit	1:5,000	Agrisera
Tag Antibodies			
α-GFP	Green Fluorescence Protein	1:2,000	Sigma
α-His	polyHistidine	1:2,000	Sigma
Secondary Antibodies			
α- mouse	-	1:5,000	Agrisera
α- rabbit	-	1:5,000	Agrisera

Table 2. 12 Antibodies applied in this study.

2.6 Overexpression and purification of recombinant proteins

2.6.1 Overexpression of proteins in *E.coli*

In this study, three recombinant proteins were overexpressed and purified from *E.coli*: Arabidopsis FC1 (pET-22b_FC1), FC2 (pET-22b_FC2) and PORB (pET-15b_PORB).

The expression vectors were transformed into *E.coli* (BL21 for pET-22b_FC1/FC2, Rosetta for pET-15b_PORB) competent cells. Single colony from the positive transformants was selected to make an overnight culture at 37°C, as a starter culture. The culture was then expanded into 1L system with a dilution of 1:100. 0.5mM IPTG was applied to induce the cells when an OD_{600}=0.5 was reached, and the induction was performed at 30°C for 3 hours. The *E.coli* cells were eventually harvested by centrifugation and stored at -20°C for further protein purification.

2.6.2 Protein purification

Proteins used in this study were purified according to manual introduction of Qiagen expression handbook with modifications.

To obtain specific and pure protein aliquots, the induced *E.coli* cells were harvested by centrifugation at room temperature. The pellet was firstly suspended in Lysis buffer with 1% Triton X-100 (for PORB, under native condition) or 8M urea (for FC1 and FC2, under denaturing condition). Then the cells were lysed with sonication at 4°C. Afterwards, supernatant was obtained after 10min centrifugation at 16,000g, 4°C, and loaded on a column filled with Ni-NTA resin beads (Qiagen). The mixture of lysate and Ni-NTA beads was incubated for 10min at 4°C. Most of the proteins from the lysate flew through the column after the incubation, while the target proteins were coupled to the column. The column was washed at least twice with wash buffer to furthermore get rid of the unspecific bindings. Finally, the target protein was eluted with elution buffer. For further use of the protein fractions, the elution aliquots can be dialyzed and concentrated with Amicon® Ultra Centrifugal Filters.

Protein purification		
Buffer	**Native condition**	**Denaturing condition**
Lysis buffer	50mM NaH_2PO_4 300mM NaCl, pH 8.0 10mM imidazole	100mM NaH_2PO_4 10mM Tris·HCl, pH 8.0 8M urea
Wash buffer	50mM NaH_2PO_4 300mM NaCl, pH 8.0 20mM imidazole	100mM NaH_2PO_4 10mM Tris·HCl, pH 6.3 8M urea
Elution buffer	50mM NaH_2PO_4 300mM NaCl, pH 8.0 250mM imidazole	100mM NaH_2PO_4 10mM Tris·HCl, pH 4.5 8M urea

Table 2. 13 Buffers for protein purification under native conditions.

To produce efficient antibodies for both Arabidopsis FC proteins, purified protein aliquots were dialyzed with PBS buffer to remove extra ingredients according to the buffer requirements listed in Table 2.14. The final fractions from Figure 2.2 were used as antigens. The immunization has been performed against rabbits for 3 times by BioGenes company.

Ingredients	Maximum conc.
urea	1M
imidazole	200mM
EDTA	1mM
DTT	2mM
NaCl	200mM
maltose, manitol	0.1%
SDS	0.1%
Glycerol	10%

Table 2. 14 Requirement of ingredients in antigen solutions.

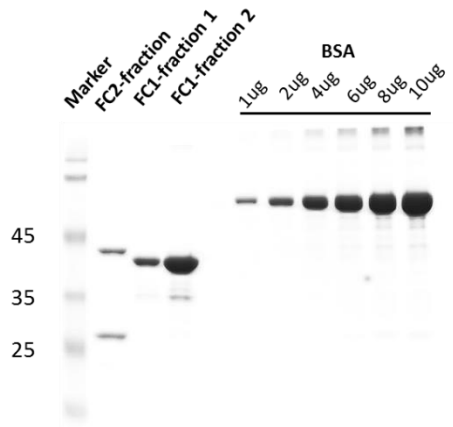

Figure 2. 2 Concentration evaluation of FCs antigen fractions on SDS-PAGE gel.

After immunization, anti-sera were obtained and purified according to a "homemade" method. Antigen aliquots were loaded on a SDS-PAGE gel, and then transferred onto a Nitrocellulose membrane. The membrane was shortly stained with Ponceau S solution.

Specific strips containing antigen proteins can be cut out. The strips were firstly blocked with TBST containing 5% milk for 1h at room temperature, followed by 3 times wash with TBS. Then the membranes were incubated overnight at 4°C, with antiserum diluted in TBS buffer containing 5% milk. The membranes were eventually eluted with 1ml Glycine buffer (0.2M Glycine/HCl, 0.5M NaCl, 1mg/ml BSA, 0.02% NaN_3, pH2.5-3) for 1min after 3 times wash with TBS. The final elution was neutralized with 200µl Tris/HCl (pH8.0) before storage.

2.7 Measurements of intermediates and end products of TBS pathway

Intermediates and end products of TBS pathway were measured as described by Czarnecki et al.(2011) (Czarnecki et al., 2011). More than 30mg Arabidopsis leaves were weighed and ground with liquid nitrogen. The fine powder was then resuspended with 250µl alkaline acetone (acetone:0.2N NH_4OH, 9:1) at 4°C. The suspension was incubated at -20°C for 20min followed by 10min centrifugation at maximum speed at 4°C. The first supernatant was transferred to a new reaction tube followed by 30min centrifugation at maximum speed at 4°C. After that, 50µl supernatant was used for porphyrins (Proto IX, MgProto IX and MME) measurements. Meanwhile, additional 1ml alkaline acetone was added to resuspend the pellet which remained pale green. Another 20min incubation and 10min centrifugation was then performed to obtain the second supernatant. The two supernatant fractions were combined and centrifuged for 30min at maximum speed. 50µl aliquot of the final supernatant was taken for Pchlide/Chlide and pigments measurements. The extraction procedures above were performed at 4°C.

For the extraction of non-covalently bound heme, the final white pellet obtained after the second suspension was resuspended with 200µl AHD buffer (acetone:dimethylsulfoxide:37% HCl, 100:20:5) at room temperature. The suspension was incubated at room temperature for 20min, and then centrifuged for 30min at maximum speed. The supernatant was applied for measurement.

All the different extracts were separated and determined by high performance liquid chromatography (HPLC).

2.8 Enzymatic assays

2.8.1 ALA synthesis capacity assessment

To assess ALA synthesis rates in the mutant and wild-type leaf tissues, a method from Mauzerall and Granick (1956) was applied with modifications.

More than 30mg 3 to 4-week-old Arabidopsis leaves were harvested and weighed. Then leaf discs were incubated in 5ml Solution 3 under applied growth conditions for 2-4h. Afterwards, leaves were finely dried with tissue papers and homogenized with liquid Nitrogen. 500µl Solution 4 was added to resuspend the powders followed by 5min centrifugation at 16,000g, 4°C. Subsequently 400µl

supernatant was transferred to a new reaction tube and mixed with 100µl EAA at 100°C for 10min. After that, the reaction was cooled down on ice, and 500µl freshly prepared Solution (1+2) was added. A 5min centrifugation at 16,000g was necessary before the absorption was measured at 553nm, 525nm und 600nm.

ALA synthesis capacity	
Solution No.	**Ingradients**
1	Ehrlich-Reagenz
	373ml acetic acid 90ml 70% perchloric acid 1.55g $HgCl_2$ add H_20 to 500ml
2	Dimethylaminobenzaldehyd (DMABA) (2g for 110ml Ehrlich-Reagenz)
3	40mM levulinic acid
	24.23g Tris 2.1ml 98% levulinic acid add H_20 to 500ml pH7.2
4	20 mM Tripotassium phosphate buffer
	0.497ml 1M K_2HPO_4 0.503ml 1M KH_2PO_4 add H_20 to 50ml pH6.8
5	Acetoacetic acid ethyl ester (EAA, Roth)

Table 2.15 Solutions prepared for ALA synthesis assay.

2.8.2 FC activity assay

FC activity was determined as described by Papenbrock et al. with modifications (Papenbrock et al., 2001). Crude chloroplasts were isolated in extraction buffer (0.45M Sorbitol, 20mM Tricine/KOH pH 8.4, 10mM $NaHCO_3$, 0.1% BSA), the suspension was filtered through one layer of Miracloth (EMD Millipore Corporation), followed by centrifugation at 6,500 g, 4°C. The pellet was dissolved in FC assay buffer (100mM Tris/HCl pH7.6, 1mM DTT, 0.25% Triton X-100, 1.75mM palmitic acid), protein concentration was determined with Bradford reagent (Bio-Rad). Then 400µg protein was applied for each reaction at 30°C by adding 10µM Proto and 100µM $ZnSO_4$. Samples were taken at designated time points and immediately frozen in liquid nitrogen. ZnProto was extracted with PEX solution (acetone:methanol:0.1 N NH_4OH=50:49:1) and detected by HPLC.

2.9 Bimolecular fluorescence complementation (BiFC) analyses

BiFC is a widely used technique to verify protein-protein interaction. The fluorescence complementation method used in this study was according to a Venus YFP fluorescence system supplied with a GATEWAY vector construction system described by Gehl et al (2009).

2.9.1 BiFC vector construction via GATEWAY strategy

Different from traditional BiFC vectors, Venus system vectors (pVENUS^N/ pVENUS^C) are generated via a Gateway cloning method, which is based on site-specific recombination system used by phage λ to integrate its DNA to *E.coli* chromosome. Firstly, a cDNA fragment containing transit peptide was amplified through standard PCR procedure with primers containing attB sequences. The fragment was purified using a DNA purification kit(STRATEC) according to the instruction before it was applied for the second amplification. The second PCR was performed with attB1/attB2 primer pairs according to a two-step amplification procedure (Table 2.17).

Primer	Sequence
attB(5')	CAAAAAAGCAGGCT
attB (3')	CAAGAAAGCTGGGT
attB1	GGGGACAAGTTTGTACAAAAAAGCAGGCT
attB2	GGGGACCATTTGTACAAGAAAGCTGGGT

Table 2. 16 Primers used for Gateway cloning.

2nd PCR for Gateway Cloning		
Step No.	Temprature (°C)	Time
1	95	2min
2	95	60s
3	54	30s
4	72	30s/1kb
step 2-4, x 14 cycles		
5	72	2min
6	95	60s
7	60	30s
8	72	30s/1kb
step 6-8, x 29 cycles		
9	72	4min
10	4	pause

Table 2.17 Program applied for 2nd PCR.

After 2 steps of PCR, the product was purified and inserted into the entry vector (pDONER207, Invitrogen) via BP reaction according to the manual (Table 2.18). The reaction aliquot was then transformed into *E.coli*, and transformants were selected with 20μg/ml Gentamycin. Positive colonies were verified by sequencing before next step. By LR reaction, the attB products can be inserted into the destination vectors (pVENUS^N/ pVENUS^C) according to the reaction listed in Table 2.18. Positive colonies were selected with 50μg/ml Kanamycin.

BP reaction		
1	attB PCR product (15-150ng)	1-7µl
	pDONR (150ng/µl)	1µl
	add TE buffer (pH8.0) to 8µl	
2	add 2µl BP Clonase™ II enzyme mix	
reaction incubated at 25°C for 1h		
3	add 1µl Proteinase K solution	
reaction incubated at 37°C for 10min		
LR reaction		
1	entry vector (15-150ng)	1-7µl
	pVENUS$^{N/C}$(150ng/µl)	1µl
	add TE buffer (pH8.0) to 8µl	
2	add 2µl LR Clonase™ II enzyme mix	
reaction incubated at 25°C for 1h		
3	add 1µl Proteinase K solution	
reaction incubated at 37°C for 10min		

Table 2. 18 Procedures of Gateway cloning.

2.9.2 Fluorescence detection using confocal microscopy

The designated vectors were transformed into *Agrobacteria* GV2260, and transformant selection was performed on YEB medium plates containing 100 µg/ml Ampicillin, 50µg/ml Kanamycin and 25µg/ml Rifamycin. Transient transformation of the expression vectors was then performed in Nicotiana tabacum leaves.

2.10 Pull down assays

To perform pull down assay, 20µl Ni-NTA agarose beads were equilibrated in PBS buffer at 4°C. More than 40µg purified recombinant protein containing a 6xHis tag, as the bait, was ligated to Ni-NTA agarose (Qiagen) by incubating at 4°C for 1h. Crude chloroplast extracts were obtained by homogenization of wild-type leaves on ice followed by filtering through one-layer miracloth (EMD Millipore Corporation). The extract was dissolved in 25BTH20G solution (details described in chapter 2.12.1), and further solubilized in 1% (w/v) DDM on ice for 10min. The supernatant obtained after the solubilization was incubated with Ni-NTA agarose immobilized with the His-tag protein overnight at 4°C. As a negative control, the empty Ni-NTA agarose beads were reacted with solubilized plastid extracts under same condition. Subsequently, the agarose beads were washed at least three times with PBS buffer. The bound proteins were finally eluted and denatured in 2x SDS-PAGE sample buffer for western blot analysis.

2.11 Split-ubiquitin yeast two-hybrid (Y2H)

Yeast two-hybrid is an extensively utilized molecular biology tool to screen or verify interactions either between protein and protein or protein and DNA molecules. The classic Y2H system using the Gal4 transcription factor activates the reporter gene *Laz* to accomplish selection of positive interactions, however could not be applied in this study, as the method requires both prey and bait proteins to be soluble. Therefore, a split-ubiquitin Y2H system was utilized in the screen for FCs interacting partners. As the prey and bait constructs, pDHB1(MCS2) and met25pXCgate (pNub)(Hey et al., 2017) vectors were applied. The construction of pDHB1 containing target gene was performed via subcloning by restriction digestion. Target sequence was firstly inserted in to intermediate plasmid pJET2.1. The objective fragment was then obtained and inserted into final vector pDHB1 by enzyme restriction digestion and ligation. To obtain a pNub vector carrying aimed gene, a Gateway cloning strategy was applied via pDONR221 (method descried in chapter 2.9.1). The transformation of yeast in this study was performed via a LiAc/SS carrier DNA/PEG method (Gietz and Schiestl, 2007), with modifications.

2.11.1 Preparation of yeast competent cells

To conduct a successful yeast transformation, one yeast colony (L40ccuA for pDHB1/ L40ccuα for pNub) was cultivated in 10ml liquid YPAD medium overnight at 30°C. 40ml fresh YPAD medium was added into the overnight culture followed by another 3h growth. OD_{600} was recorded to estimate the cell density based on the calculation of an OD_{600}=1 equals $3x10^7$ cells per ml. A cell number of $1x10^8$ is a prerequisite for each successful transformation. Needful yeast cells were harvested by centrifugation at 3,000rpm for 10min, at room temperature. One time washing with sterile ddH_2O is necessary to remove the salts from liquid medium. Subsequently, the cells were washed again with 100mM LiAc followed by 1min centrifugation at 13,000rpm. The pellet was finally resuspended in 200µl 100mM LiAc for each transformation.

YPAD medium
1%(w/v) yeast extract
2%(w/v) peptone
2%(w/v) glucose (filter sterilized)
20mg/l Adenine sulfate (filter sterilized)

Table 2. 19 Components of YPAD medium.

2.11.2 Yeast transformation

For further transformation steps, aliquots of 2mg/ml single stranded carrier DNA (ssDNA) were pre-heated at 95°C for 5min before use. To each reaction, more than 5µl plasmid DNA was added into 355µl freshly prepared LiAc-PEG-ssDNA solution (Table 2.20). The reaction was subsequently incubated at 42°C for 30min with gentle inversion every 10min. 1ml sterile ddH_2O was added to the transformed cells before harvesting. Then the cells were plated onto an appropriate Synthetic Dropout (SD) plate, grown at 30°C for 2-4days.

LiAc-PEG-ssDNA solution
36µl 1M LiAc
240µl 50%PEG
10µl ssDNA (10mg/ml)
60µl sterile ddH20

Table 2. 20 Buffer for yeast transformation reaction.

2.11.3 Yeast mating

Positive selected colonies for both L40ccuA and L40ccuα transformants were inoculated in the same YPAD medium overnight at 30°C. The cells were suspended well by vortexing before a cell density of OD_{600}=1.0 was adjusted. Eventually, 10µl mating solution was dropped on SD/-Leu/-Trp (SD/-lt) plate. After 2-4 days cultivation at 30°C, positive colonies were picked for a new overnight culture in YPAD medium. The same adjustment was done to achieve an OD_{600} of 1.0. In addition to the adjusted cells, dilutions of 1:10 and 1:100 were prepared for better quantification. 10µl of each concentrated cell cultures were parallelly dropped on three selective SD plates, including SD/-lt and SD/-His/-Ura/-Leu/-Trp (SD/-hult) with or without 20mM 3-amino-1,2,4-tiazole (3-AT, Sigma). After 3-5 days growth at 30°C, the growth was recorded by CanoScan 5600F scanner.

SD medium		
SD/-Leu	Yeast nitrogen base (-amino acid /+20mg/l adenine sulfate); 2%(w/v) glucose (filter sterilized); 20g/l Agar	Amino acid -Leu
SD/-Trp		Amino acid -Trp
SD/-lt		Amino acid -Leu-Trp
SD/-hult		Amino acid -His-Ura-Leu-Trp
SD/-hult +20mM 3AT		Amino acid -His-Ura-Leu-Trp; 20mM 3AT

Table 2. 21 Ingredients for all selective SD media.

2.12 Analyses of thylakoid membrane complexes

2.12.1 Thylakoids extraction

To analyze the photosynthetic complexes in the mutants and wild-type plants, Arabidopsis thylakoids were extracted according to Jarvi et al. with modifications (Jarvi et al., 2011). Thylakoid fractions isolation was performed under dim light at 4°C. Fresh leaves were ground with ice-cold extraction buffer (50mM Hepes/KOH pH 7.5, 330mM sorbitol, 2mM EDTA, 1mM $MgCl_2$, 5mM ascorbate). The suspension was filtered through two layers of Miracloth, and the supernatant was discarded after 7min centrifugation at 6,000 g, 4°C. The pellet was then washed once with shock buffer (50mM Hepes/KOH pH 7.5, 5mM sorbitol and 5mM $MgCl_2$), followed by a centrifugation at 6,000g for 7min. The final pellet was dissolved in 25BTH20G solution (25mM Bis Tris/HCl pH 7.0, 20% (w/v) glycerol and 0.25 mg/ml Pefabloc). The chlorophyll concentration was determined with alkaline acetone (acetone:0.2N NH_4OH, 9:1).

2.12.2 Blue native polyacrylamide gel electrophoresis (BN PAGE) analysis

To assess the photosynthetic complexes assembly in the thylakoids membranes, a 4.5-12.5% gradient BN PAGE gel was used. The preparation for a mini gel was done with a gradient mixer according to the discription in Table 2.22.

BN PAGE gel			
Solution	**separation gel (ml)**		**stacking gel (ml)**
	4.5%	**12.5%**	**4%**
ddH_2O	1.27	0.312	1.72
40% Acrylamide (32:1)	0.28	0.781	0.3
3x Gel buffer (150mM Bis Tris/HCl, 1.5 M 6-amino-caproic acid, pH 7.0)	0.833	0.833	1
Glycerol	0.11	0.56	-
10% APS	0.0075	0.0075	0.016
TEMED	0.003	0.003	0.006
loading volume	1.75	1.65	-

Table 2. 22 Preparation for BN PAGE gradient gels.

Prior to the loading, the thylakoid fractions were solubilized with 1% (w/v) DDM (dodecyl maltoside) on ice for 5min with a final chlorophyll concentration of 1mg/ml. A 10x Serva Blue G buffer (100mM BisTris/HCl pH 7.0, 30% (w/v) sucrose and 50mg/ml Serva Blue G) was added to introduce a negative charge to increase the mobility of the protein samples. The BN PAGE gel electrophoresis was performed with cathode buffer (50mM Tricine, 15mM BisTris/HCl pH 7.0 and 0.02% (w/v) Coomassie brilliant blue G-250) and anode buffer (50mM BisTris/HCl pH 7.0) with a gradually increased voltage from 50V-200V until the protein samples reach the end of the gel.

2.12.3 Second dimension (2D) PAGE electrophoresis

As certain complexes (such as PSII monomer and Cytb6f, PSII dimer and PSI) cannot be well separated by the applied BN PAGE system, a 2D PAGE electrophoresis is necessary for further analysis. For the 2nd dimensional separation, the stripes from the 1st-dimension BN PAGE gel were excised and denatured with SDS sample buffer at RT for 30 min. Then the stripes were loaded to a thick 12% SDS PAGE gel with 6M urea. Finally, the SDS PAGE gel was used for Coomassie staining or immunoblotting.

2.13 GUS (β-glucuronidase) assay

2.13.1 Vectors construction and transgenic plants generation for GUS assay.

To generate vectors for GUS assay, primers FC1_comp5'- ACACGTGCATGGTGTGGTCCCCTTAAT-3'and pFC1_rev5' ATCACGTGTCAGAACCGATCAGTAATTG-3' were used to amplify FC 1 promoter sequence. For FC2 promoter, pFC2_Fw: 5'-ATGATATCGATACATTTGAAGACAATGC-3' and pFC2_rev: 5'-ATGATATCGTTTAAACGAAACTTGAAGAAACCTTAAC-3' primers were applied. Both promoter fragments were then inserted into vector pCAMBIA1302, the final vectors were used for transformation of wild-type Arabidopsis.

To obtain the transgenic plants carrying the designed GUS vector, the transformants were grown and selected on plates with 40μg/ml hygromycin.

2.13.2 Histochemical Detection of GUS Activity

For GUS activity detection, Arabidopsis material was incubated in GUS assay buffer (2mM 5-bromo-4-chloro-3-indolyl-D-glucuronide, 10mM potassium ferrocyanide, 10mM potassium ferricyanide, 0.2 % (w/v) Triton X-100) overnight at 37°C. The plant materials were washed with water and suspended in 5% glycerol before microscopy check. Images were acquired with an Olympus CX21LED microscope equipped with an Olympus DP26 digital camera.

2.14 Determination of ROS accumulation

2.14.1 Nitro blue tetrazolium (NBT) staining

ROS accumulation was estimated by staining determination of superoxide. NBT was used for the visual detection. Detached leaves from the mutants or control plants were mounted in NBT staining solution (0.2% NBT; 50mM Na_3PO_4, pH7.5) overnight in darkness. Afterwards, pigments from the green leaves were removed through incubation with pure ethanol.

2.14.2 3,3′-Diaminobenzidine(DAB) staining

Visual quantification of hydrogen peroxide (H_2O_2) accumulation in leaves were determined with DAB. DAB is an organic compound which is water soluble in its unoxidized form, however forms a water-insoluble brown precipitate when oxidized by H_2O_2in the presence of hemoproteins, such as peroxidases(Daudi and O'Brien, 2012). Detached leaves from 3-week old Arabidopsis seedlings were incubated at least 8h in DAB staining solution (0.05% DAB; 0.015% H_2O_2; 10mM PBS, pH 7.2)in darkness. The stained leaves were afterwards de-stained either in pure ethanol or by 10min boiling in Bleach solution (ethanol: acetic acid: glycerol=3:1:1).

2.15 Ion leakage measurement

Electrolyte leakage from plant tissues defines the loss of cell membrane integrity, is a common evaluation of cell viability. To assess the ion leakage rates in wild type and mutant leaves, at least 8 rosette leaves (both control and stress-treated leaves) were incubated in 6ml 0.4mM mannitol solution. The solutions were placed at room temperature for 3h. Leakage conductance (C_0) was immediately recorded with WTW LF318 conductivity meter after the incubation. 10min boiling of the leaves was necessary before the full conductivity (C_t) was measured. Finally, ion leakage rates were calculated by C_0/C_t.

2.16 Microscopy examination of developing Arabidopsis seeds

For seeds examination, siliques from wild-type and mutant plants were dissected using light microscopy on an Olympus SZX7. For DIC microscopy, seeds from different developmental stages were dissected and mounted in Hoyer's medium (15g Gum Arabic, 75g Chloral Hydrate, 5ml Glycerol, 25ml ddH_20). The seeds were incubated in the buffer for at least 3 days. Afterwards, they were directly used for examination. The DIC microscopy was performed with a Zeiss microscope equipped with Nomarski differential interference contrast optics.

3. Results

Two isoforms of ferrochelatase contribute to the conversion of Proto to protoheme in Arabidopsis. Although both FC proteins share a high similarity of amino acid sequences, they display distinguished expression profiles. *FC1* is ubiquitously expressed in all tissues with comparable expression levels, while *FC2* transcript plays predominant functions in photosynthetic tissues. Preliminary characterization of *fc* mutants suggested that a defect of FC1 function leads to either slightly reduction of heme content (*fc1-1*) without any effect on pigment accumulation or a lethal phenotype (*fc1-2*). Both *fc2* knockdown (*fc2-1*) and knockout (*fc2-2*) mutants exhibit necrotic leaves and reduced chlorophyll accumulation as well as affected photosynthesis machineries. These fundamental analyses of various *fc* mutants offer a hint that certain cellular processes differentially utilize the two FC isoforms. While FC2 produces heme for photosynthetic activities in leaves, FC1, however, may serve essential heme pools for embryo biogenesis or seedling development. To reveal the distinct functions of each FC isoform, complementation tests of the *fc2* (or *fc1*) knockout mutant have been conducted via expressing either genomic *FC* sequence with or without modifications.

3.1 FC2 contribution to the GluTR inactivation complex to control appropriate heme and chlorophyll synthesis.

Due to the difficulties in production of FC antibodies as well as protein overexpression *in vitro*, so far functional characterization of both FC isoforms remains in a lag phase after the first analysis of *fc* mutants. In 2011, by overexpressing the two FC proteins in Arabidopsis seedlings, Woodson et al. were able to reveal FC1 function in retrograde signal transduction (Woodson et al., 2011). In 2017, Yang et al. implied FC1 function in regulating responsive genes expression to salt and cadmium stress, as FC1 overexpressing Arabidopsis showed more tolerance to both stress conditions (Song et al., 2017; Zhao et al., 2017). However, besides the hypothesis that FC2 may provide heme for photosynthesis machineries, its genuine function in photosynthetic tissues, particularly in chlorophyll metabolism, remains unknown. A defective expression of FC2 always leads to a distinct reduction of chlorophyll content, in comparison to *fc1* mutation, suggests that FC2 may play a role in the regulation chlorophyll biosynthesis. But in which manner, and why FC1 could not conduct this function role, remain intriguing open questions.

To address those questions and obtain more insights into FC2 physiological function, additional FC2 transgenic plants should be generated for investigation. In this part of the study, a *fc2* knockout (*fc2-2*) mutant was used for multiple complementation attempts. In addition, various FC2 overexpressing transgenic plants have been generated and analyzed to examine the effect of FC2-overproduction in wild-type Arabidopsis seedlings.

3.1.1 Phenotypical characterization of *fc2* mutants.

The Arabidopsis T-DNA insertional mutants of *fc2-1* (GK_766_H08) and *fc2-2* (SAIL_20_C06) were obtained from Nottingham Arabidopsis Stock Centre. The *fc2-1* mutant possesses a T-DNA copy inserted in the 5'-untranslated region (UTR), while a T-DNA disrupts *FC2* genomic sequence in the 6th exon in a *fc2-2* mutant (Figure 3.1A). To confirm phenotypes of the mutant seedlings, both mutation lines and comparable wild type Col-0 were germinated and grown under short day (SD) and constant light (CL) conditions at 22°C. Under CL, 2-week-old *fc2-2* and *fc2-1* seedlings both exhibited necrotic leaves and *fc2-2* showed severely retarded growth compared to wild type. When all the seedlings were grown under an 8h light/16h dark cycle, only very few *fc2-2* seeds could germinate and died fast. The SD-grown *fc2-1* mutants displayed necrotic leaves similar to the CL-grown seedlings, and its growth was more retarded compared to a CL growth (Figure 3.1B).

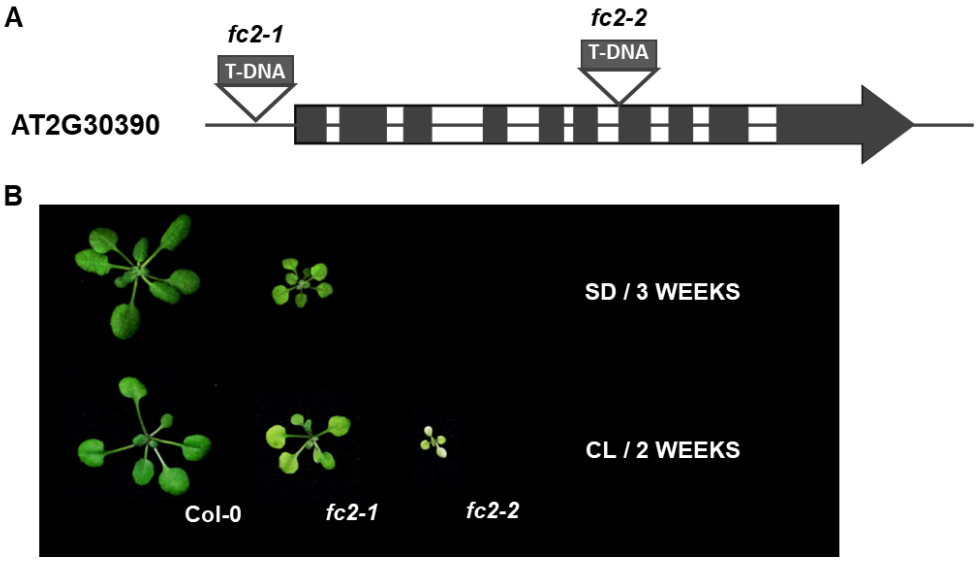

Figure 3. 1 Phenotypes of *fc2* knockout and knockdown mutants.
(A) The scheme of T-DNA insertion of the *FC2* (AT2G30390) loci. Introns (white boxes), exons (black boxes) are indicated. (B) Growth of homozygous *fc2-1, fc2-2* mutants and wild-type seedlings under short day (SD) and continuous light (CL) conditions. *fc2-2* mutants could not survive under SD condition.

3.1.2 FC1 expression could only partially rescue *fc2-2* phenotype under SD condition, while pFC2FC2 (*fc2/fc2*) displayed wild type-like phenotype.

After the phenotypes of *fc2* mutants were confirmed, two complementation attempts have been made in a heterozygous *fc2-2* mutant background. The two complementation constructs contain a *FC1* and *FC2* genomic sequence, respectively, under the control of a *FC2* promoter. As *fc2-2* seedlings were not able to survive under SD condition, selection of the complemented transformants was performed under a day-night growth condition

instead of constant light. As a result, twenty two transformants containing a *pFC2FC2* (*pFC2::FC2*) fragment were obtained. Among them, four seedlings were in wild-type background. Eighteen pFC2FC2 transformants carried the T-DNA insertion for *fc2* knockout, while six lines were proved to be homozygous *fc2-2* mutants. All the six pFC2FC2 (*fc2/fc2*) T1 seedlings exhibited wild-type-like phenotype, and two lines (#3 and #16) were selected as representatives for further analysis. Fifteen transgenic plants were obtained for pFC2FC1 transformation in T1 generation. Eleven out of fifteen seedlings contain T-DNA insertion for *fc2* knockout. And three individuals were identified as pFC2FC1 (*fc2/fc2*) mutants according to genotyping analysis. The three pFC2FC1 (*fc2/fc2*) plants displayed necrotic leaves and slightly retarded growth under the selective growth condition. Progenies of two lines (#2 and #12) were used for further physiological characterization.

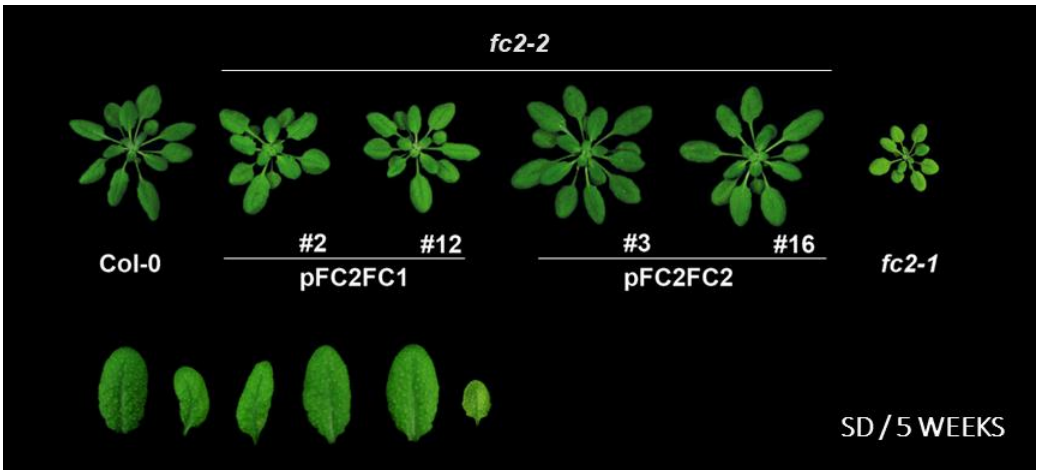

Figure 3. 2 Phenotypic characterization of *fc2-2* complemented plants with a *FC1* or *FC2* expression under *FC2* promoter.

Pictures of pFC2FC1 (*fc2/fc2)*, pFC2FC2 (*fc2/fc2*) complementation seedlings as well as comparable wild type and *fc2-1* mutants. Plants were grown under SD condition for 5 weeks. Under SD condition, *fc2-2* mutants could not survive, while both complementation constructs contributed to growth of *fc2-2* seedlings. Moreover, pFC2FC1 (*fc2/fc2*) seedlings exhibited necrotic leaves and slightly retarded growth, while pFC2FC2 (*fc2/fc2*) seedlings were wild-type-like.

Before biochemical analyses were performed on the complemented *fc2-2* seedlings, complementation of *fc2* via the expression of both transgenic constructs was confirmed by genotyping and western blot analyses. For that, progenies from pFC2FC2 (*fc2/fc2*), pFC2FC1 (*fc2/fc2*) mutants and Col-0 were grown on soil under SD condition. As *fc2-2* was not viable, *fc2-1* was grown as a phenotypical control (Figure 3.2). The T2 complementation seedlings displayed similar phenotypical patterns compared to the T1 transformants, i.e. both pFC2FC1 (*fc2/fc2*) lines showed necrotic leaves and slightly retarded growth compared to Col-0, while the two pFC2FC1 (*fc2/fc2*) individual lines displayed wild-type-like phenotype (Figure 3.2).

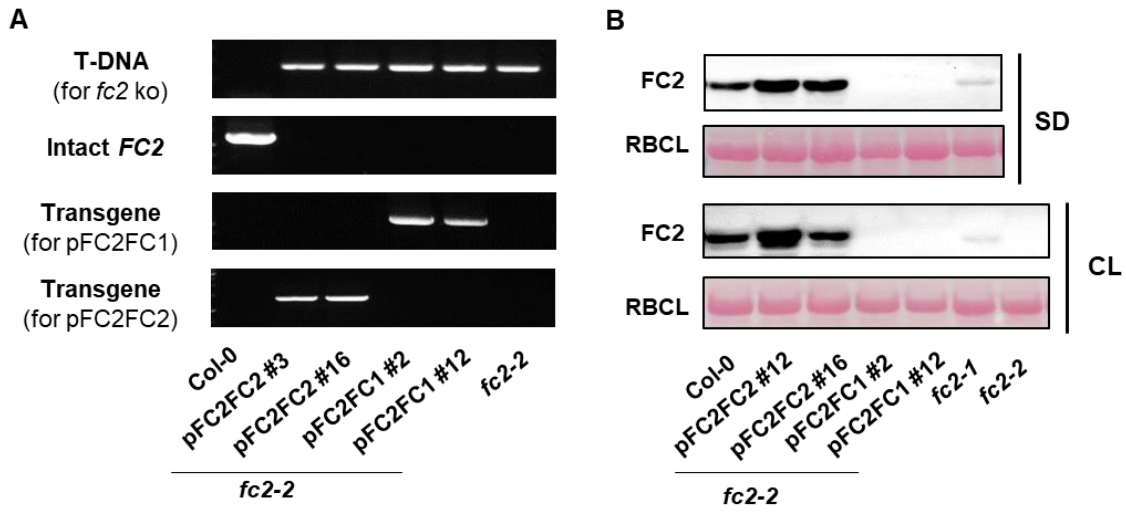

Figure 3. 3 Both genotyping and western blot analyses confirmed the complementation of *fc2-2* by pFC2FC1 and pFC2FC2 constructs.
(A)Genotyping analyses of pFC2FC1 (*fc2/fc2*), pFC2FC2 (*fc2/fc2*) and *fc2-2* mutants as well as wild-type seedlings. (B) Examination of FC2 protein contents in pFC2FC1 (*fc2/fc2*), pFC2FC2 (*fc2/fc2*), *fc2-2*, *fc2-1* and wild-type leaves.

Different primer pairs were applied to verify the genotypes of all mutants (Figure 3.3A). First of all, the T-DNA insertion of *fc2* knockout was confirmed with primers Garlic-LB and FC2_sail_FW. Except wild type, all *fc2-2* and its complemented lines contained this T-DNA insertion copy. Both *pFC2FC1* and *pFC2FC2* transgenes were amplified with forward primers containing *FC1* or *FC2* sequence in combination with a reverse primer binding to the transformation vector. A *FC2* primer pair overlapping its 3' UTR was applied to testify homozygosity of *fc2* knockout. An intact *FC2* sequence can only be detected in wild-type seedlings but not in *fc2-2* or its complementation plants. The homozygosity of *fc2* knockout in *fc2-2* and pFC2FC1 (*fc2/fc2*) seedlings was also confirmed by western blot analyses with the newly generated α-FC2 antibody. Due to the expression of *pFC2FC2* transgene, wild-type-level or accumulated FC2 protein could be detected in the two pFC2FC2 (*fc2/fc2*) lines. Under both SD and CL growth conditions, *fc2-1* were viable and displayed strongly reduced FC2 protein amount while no bands representing FC2 could be detected in the CL-grown *fc2-2* mutants (Figure 3.3B).

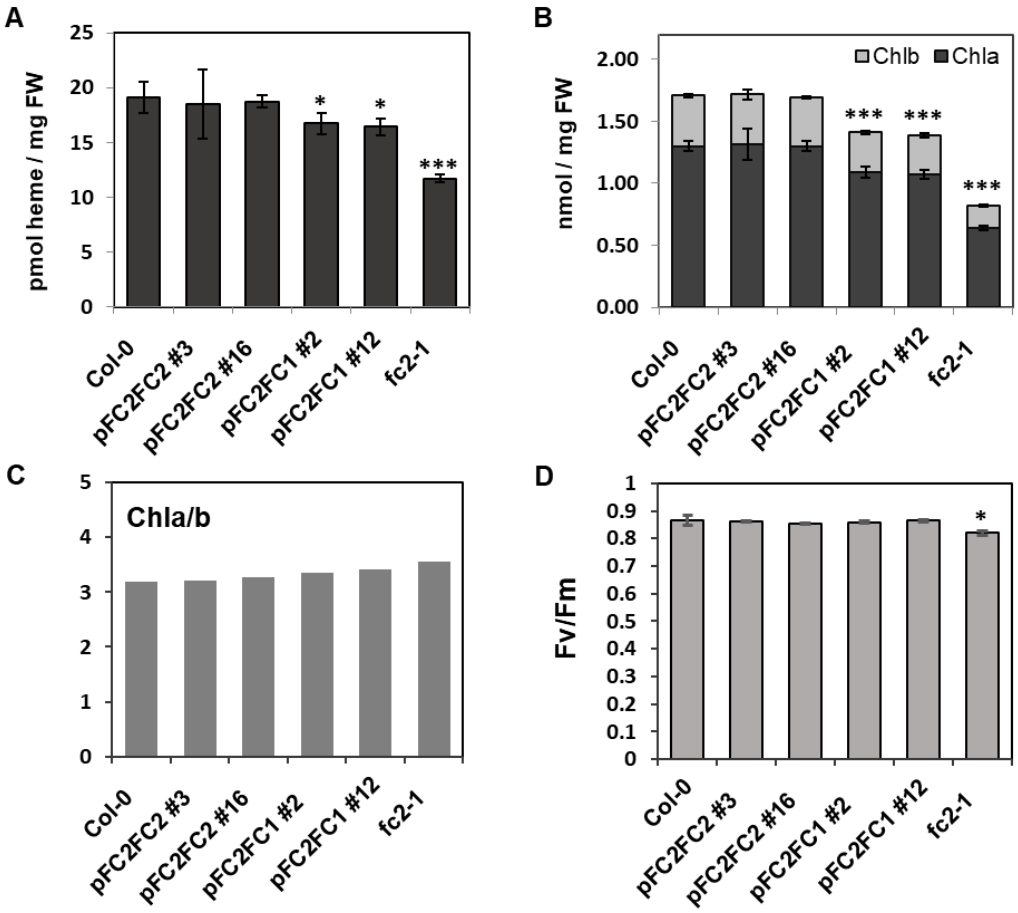

Figure 3. 4 Determination of end products of TBS pathway and photosynthesis efficiency in pFC2FC1 (*fc2/fc2*) and pFC2FC2 (*fc2/fc2*) complemented plants.
Heme (A), chlorophyll (B) contents and chla/chlb ratios of pFC2FC1 (*fc2/fc2*), pFC2FC2 (*fc2/fc2*), *fc2-1* mutants and comparable wild-type seedlings. Leaf samples were harvested from 3-week-old SD-grown plants. (D) Photosynthesis efficiency was measured in 5-week-old rosette leaves of the complemented plants, *fc2-1* mutants as well comparable wild type. Error bars indicate standard deviations. Asterisks represent significant differences, which were calculated by Student's t-test; * P value < 0.05, ** P value < 0.01, *** P value < 0.001.

As the two different *fc2-2* complementation approaches with *pFC2::FC1* and *pFC2::FC2* resulted in different phenotypes, heme and chlorophyll contents were determined to estimate the impact of the transgenic FC1 and FC2 expression on tetrapyrrole synthesis (Figure 3.4A/B). As a result, in consistence with previous studies, *fc2-1* mutants displayed decreased heme and chlorophyll contents when grown under SD condition. FC2 expression under its native promoter was able to restore wild-type levels of heme and chlorophyll in the *fc2-2* background. Whereas FC1 expression driven by a *FC2* promoter failed to fully rescue the necrotic phenotype of *fc2-2*, as the pFC2FC1 (*fc2/fc2*) lines showed significantly reduced heme and chlorophyll contents without an alteration in Chla/Chlb ratio (Figure 3.4A-C). Photosynthesis efficiency was also measured in the complemented plants and *fc2* mutants. 5-week-old *fc2-1* leaves exhibited compromised

photosynthesis. The complemented plants pFC2FC2 (*fc2/fc2*) and pFC2FC1 (*fc2/fc2*) showed unaltered Fv/Fm ratios compared to wild type, although the latter complementation plants displayed reduced heme and chlorophyll contents (Figure 3.4D).

3.1.3 pFC2FC1 fully complemented *fc2-2* under CL condition but showed only partial compensation in light-dark condition.

According to Scharfenberg et al. (2015), *fc2-2* mutants were only viable under long day and CL conditions with severely retarded growth (Scharfenberg et al., 2015). Compared to long day condition, the knockout mutant displays relatively better growth under CL with larger leaf areas. *fc2-2* could tolerate more constant light rather than light/dark incubation, which might attribute to the accumulation of photosensitizer Pchlide during night phase. Etiolated *fc2-2* seedlings accumulated 2-fold Pchlide contents compared to wild type. Once exposed to light, the phototoxic chlorophyll intermediate causes photobleaching, results in necrotic leaves exhibiting a *flu*-like phenotype (chapter 1.3.1.2).

To better characterize pFC2FC1 (*fc2*/*fc2*) complemented lines in comparison to *fc2-2* mutants, the mutant plants and wild type were grown under both SD and CL conditions with 100µE light intensity.

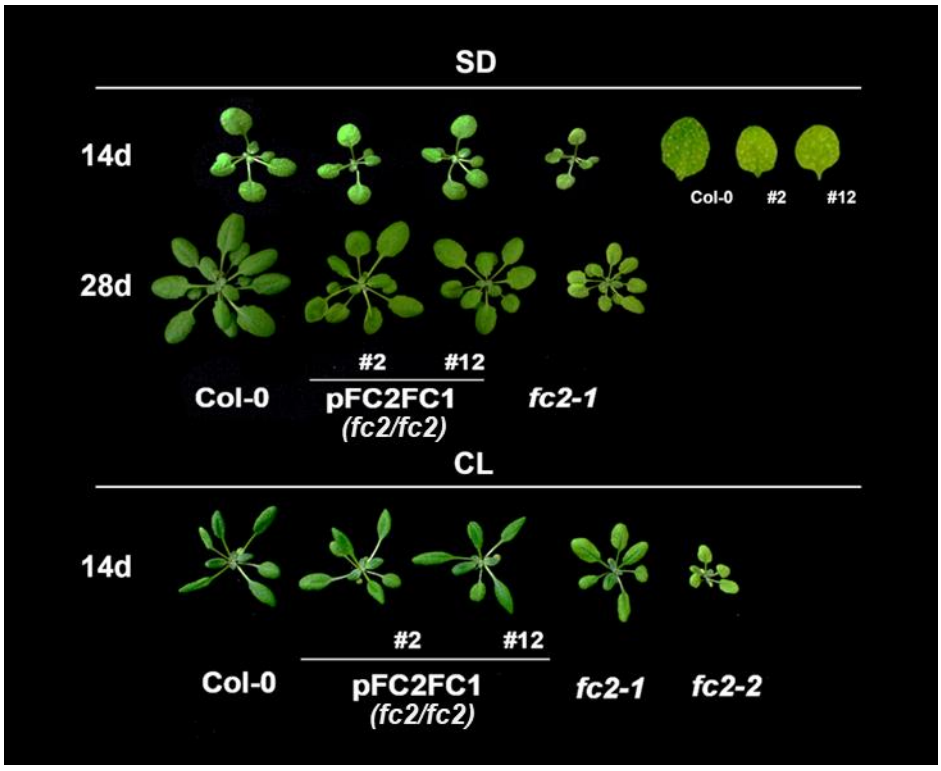

Figure 3. 5 Phenotypes of pFC2FC1 (*fc2/fc2*) plants under SD and CL conditions.
Growth of pFC2FC1 (*fc2/fc2*) complementation seedlings as well as comparable Col-0 and *fc2* mutants.

Consistent with previous observations, the pFC2FC1 (*fc2/fc2*) complemented lines displayed necrotic leaves in a smaller size compared to Col-0. Interestingly, this necrotic phenotype could not be observed when the seedlings were grown under CL. Under CL condition, 14-day-old pFC2FC1 (*fc2/fc2*) line #2 and #12 displayed wild-type-like growth rate without leaf necrosis, while both *fc2-1* and *fc2-2* showed necrotic leaves (Figure 3.5). To verify the necrosis phenotype, end products accumulation of TBS pathway was determined via HPLC analysis. 4-week-old pFC2FC1 (*fc2/fc2*) #2 and #12 plants revealed a significant reduction of heme and chlorophyll contents under SD condition. However, the two complemented individuals restored wild-type-level tetrapyrroles production when grown under CL condition (Figure 3.6), implying a full complementation.

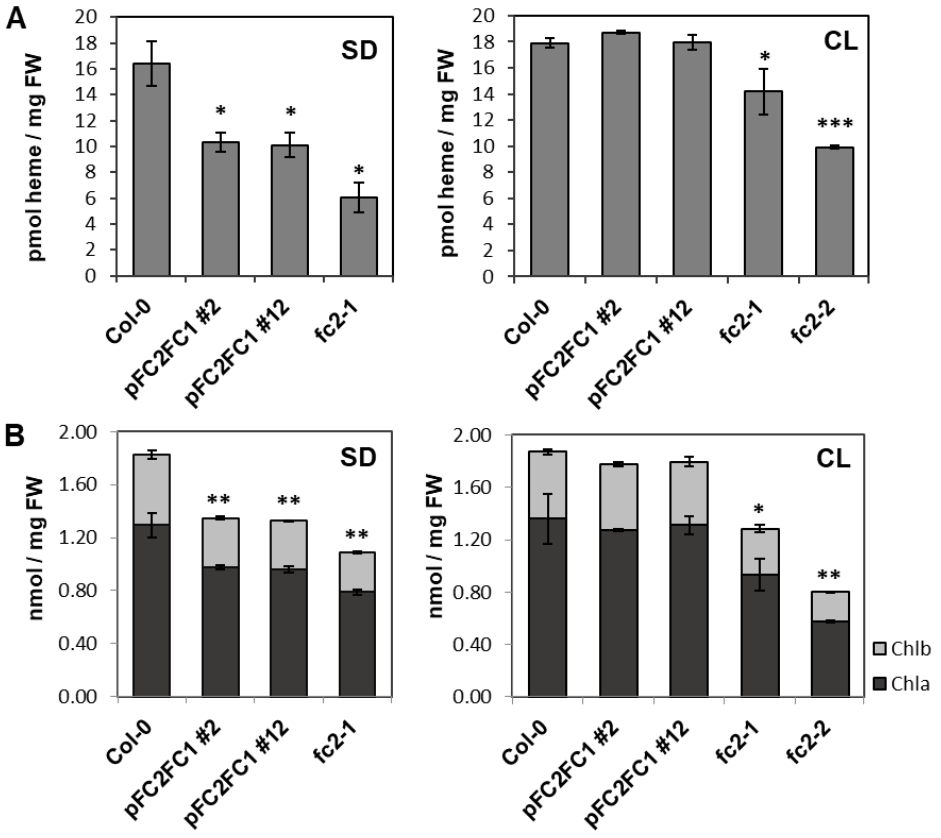

Figure 3. 6 Heme and chlorophyll contents in SD and CL-grown pFC2FC1 (*fc2/fc2*) plants.

Heme (A) and chlorophyll (B) were extracted from pFC2FC1 (*fc2/fc2*), *fc2* mutants and comparable wild-type plants. Leaf samples were harvested from 4-week-old SD-grown and 2-week-old CL-grown seedlings. Error bars indicate standard deviations (n≥3). Asterisks represent significant differences, which were calculated by Student's t-test; * P value < 0.05, ** P value < 0.01, *** P value < 0.001.

It has been reported from Scharfenberg et al. (2015) that the *fc2-2* mutants accumulate Pchlide during night phase, exhibiting a *flu*-like phenotype. The pFC2FC1 (*fc2/fc2*) plants grown under both SD and CL conditions were incubated in darkness for 12h. HPLC measurements revealed that, when transferred to darkness, both SD and CL-grown pFC2FC1 (*fc2/fc2*) plants (#2 and #12) accumulated 2-fold higher of Pchlide amount in comparison to wild type, showed a *fc2-2*-like phenotype (Figure 3.7). This observation suggested that in contrast to heme and chlorophyll production, Pchlide accumulation of *fc2-2* in darkness could not be complemented by FC1 expression. The phenotypes (Figure 3.5) and accumulation of TBS intermediates (Figure 3.6 and Figure 3.7) suggested that the partial complementation of pFC2FC1 (*fc2/fc2*) under SD could be related to the *fc2-2* levels of Pchlide accumulation in dark incubation. Why does Pchlide accumulate when FC2 is lacking, and in which manner does Pchlide accumulation affect heme and chlorophyll synthesis. These questions await elucidation.

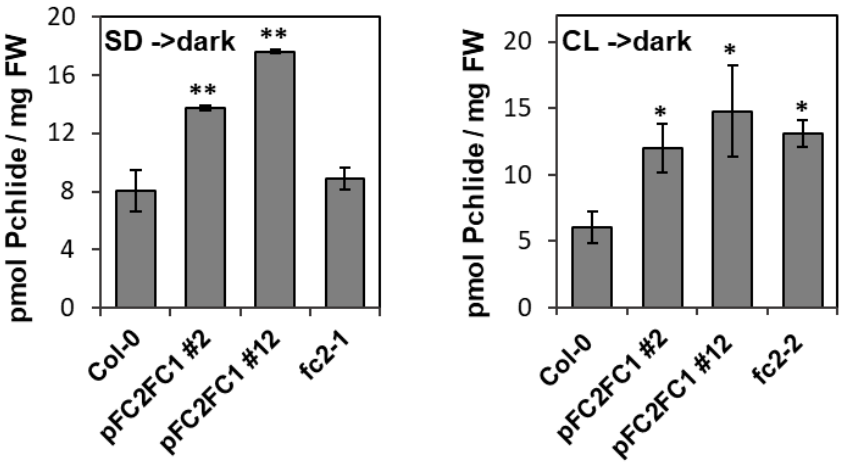

Figure 3. 7 Both SD and CL-grown pFC2FC1 (*fc2/fc2*) plants accumulated *fc2-2* mutant-level Pchlide in darkness.

pFC2FC1 (*fc2/fc2*) and *fc2* mutants, as well as wild-type seedlings, were grown under SD and CL conditions. Pchlide contents were determined after 12h darkness treatment. Error bars represent standard deviations (n≥3). Asterisks indicate significant differences calculated by Student's t-test; * P value < 0.05, ** P value < 0.01.

Subsequently, enzymes involved in the TBS pathway and photosynthesis processes were analyzed at transcript and protein levels in the SD and CL-grown plants (Figure 3.8 and Figure 3.9). As a result, the CL-grown *fc2-2* mutants showed 2-3 folds increase of the expression of most TBS genes, such as genes involved in ALA synthesis: *HemA1*, *FLU* and *GBP*; chlorophyll synthesis genes *CHLD*, *GUN4*, *CHLM* and *PORB*, as well as genes encoding both heme oxygenases: *HO1* and *HO2*. However, except *CHLM*, *GUN4, HO2* and *PORB*, mRNA accumulation of other genes was restored to wild-type levels in the pFC2FC1 (*fc2/fc2*) lines. Nevertheless, under SD condition, the pFC2FC1 (*fc2/fc2*) seedlings exhibited more than 10-fold accumulation of *PORB* transcript in comparison to Col-0. This

could also be observed in the *fc2* knockdown mutant. Besides *PORB*, transcript levels of *GUN4* in pFC2FC1 (*fc2/fc2*) lines accumulated two-fold compared to wild-type level, in accordance with its expression under CL condition. Other TBS genes examined in both *fc2-1* and pFC2FC1 (*fc2/fc2*) lines showed wild-type transcript levels, despite the slightly increased *HemA1* mRNA in *fc2-1* mutants.

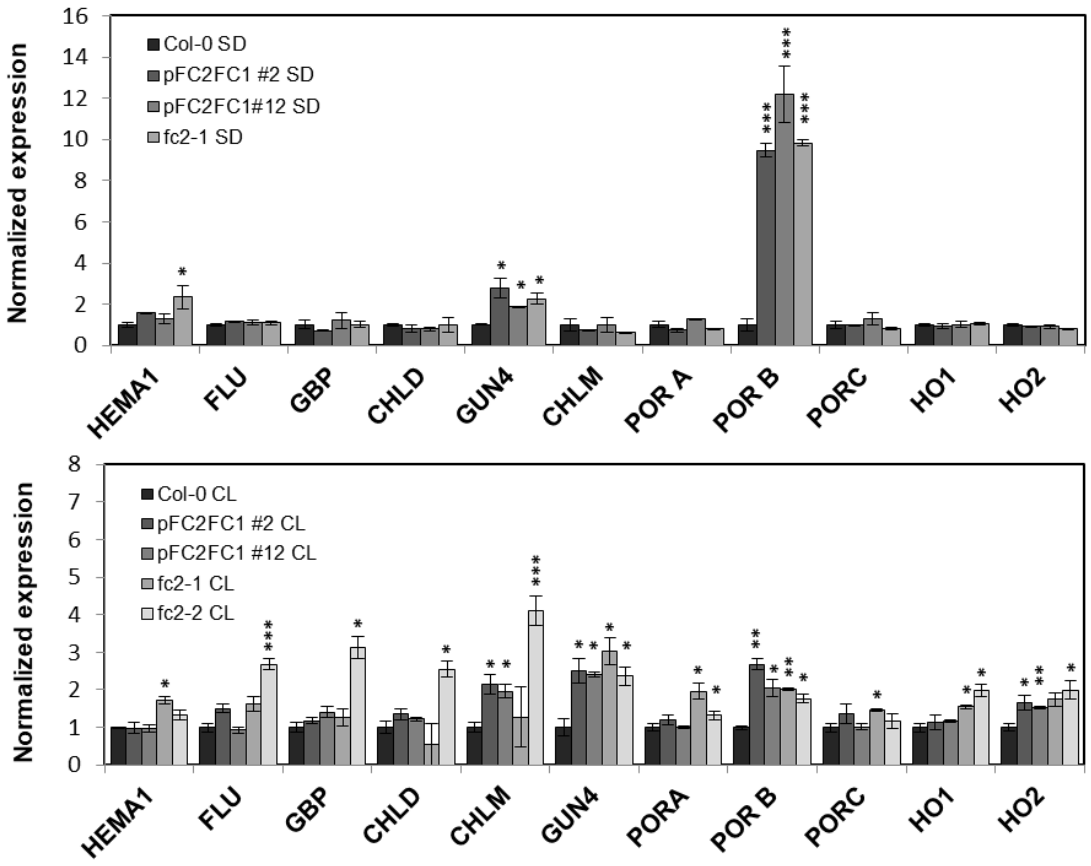

Figure 3. 8 Transcription analysis of TBS genes in SD and CL-grown pFC2FC1 (*fc2/fc2*) plants.

qRT-PCR analysis of genes encoding enzymes involved in tetrapyrrole biosynthesis. 3-week-old pFC2FC1 (*fc2/fc2*) and *fc2* mutants, as well as wild-type leaves were harvested for RNA extraction. Seedlings were grown under short day (SD) and continuous light (CL) conditions. *HEMA1*: encoding glutamyl-tRNA reductase 1; *FLU*: *fluorescent; GBP: GluTR binding protein*; *CHLD*: encoding Mg chelatase subunit D; *GUN4*: *genomes uncoupled 4*; *CHLM*: encoding Mg-protoporphyrin IX methyltransferase; *POR A/B/C*: *protochlorophyllide oxidoreductases A/B/C*; *HO1/HO2: heme oxygenases 1 and 2.* Error bars represent standard deviations. Asterisks indicate significant differences calculated by Student's t-test; * P value < 0.05, ** P value < 0.01, *** P value < 0.005.

In contrast to the drastic accumulation of *PORB* transcript, PORB protein amount was reduced by 50% in SD-grown pFC2FC1 (*fc2/fc2*) plants compared to wild-type control, while LHC proteins and other TBS enzymes examined showed wild-type accumulation (Figure 3.9). The *fc2-1* mutant displayed a general reduction of most TBS enzymes as well

as both LHC proteins under SD. When grown under CL, all the examined TBS proteins and LHC proteins in pFC2FC1 (*fc2/fc2*) lines accumulated to wild-type levels, while in both *fc2* mutants, a significant reduction could be observed for the two LHC proteins and most TBS proteins, except for GluTR, GSAAT and CHL27. Interestingly, the dramatic reduction of PORB protein in the SD-grown pFC2FC1 (*fc2/fc2*) lines could not be observed under CL. Thus, the distinctive reduction of PORB protein in pFC2FC1 (*fc2/fc2*) seedlings under SD growth condition indicated that FC2 presence may contribute to PORB protein stability under a day-night growth.

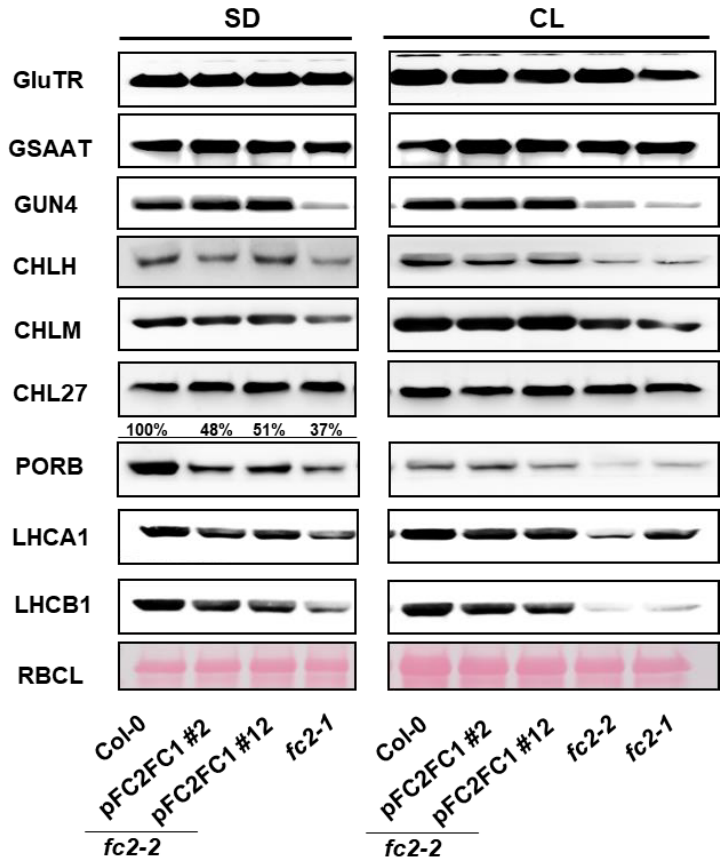

Figure 3. 9 Protein analysis of SD and CL-grown pFC2FC1 (*fc2/fc2*) plants.
2-week-old pFC2FC1 (*fc2/fc2*) and *fc2* mutants, as well as wild-type leaves, were harvested for protein extraction. Seedlings were grown under SD and CL conditions. GluTR: Glutamyl-tRNA reductase; GSAAT*:* Glutamate-1-semialdehyde aminotransferase; CHLH: Mg chelatase subunit H; GUN4: genomes uncoupled 4; CHLM: Mg-protoporphyrin IX methyltransferase; PORB: protochlorophyllide oxidoreductases B; LHCA1/LHCB1: Light-harvesting chlorophyll-binding proteins a1 and b1; RBCL: ribulose 1,5-bisphosphate carboxylase oxygenase, large subunit.

3.1.4 FC2 stabilizes PORB throughout seedling development.

To verify the altered stability of PORB in pFC2FC1 (*fc2/fc2*) lines, protein levels of GluTR, PORB and both FC isoforms were evaluated at different developmental stages in pFC2FC1 (*fc2/fc2*) and wild-type plants (Figure 3.10). Both FC2 and PORB showed a constant and stable accumulation in young and old leaves in Col-0, while GluTR protein exhibited slightly reduced accumulation in old leaves. In pFC2FC1 (*fc2/fc2*) leaf tissues, a similar reduction of GluTR could be observed in an age-dependent manner. However, the accumulation of PORB in pFC2FC1 (*fc2/fc2*) was severely reduced in the old leaves compared to the young leaves. Due to a lack of FC2, the presence of FC1 failed to maintain the accumulation of PORB throughout the seedling development, indicating FC2 essential function for PORB stability.

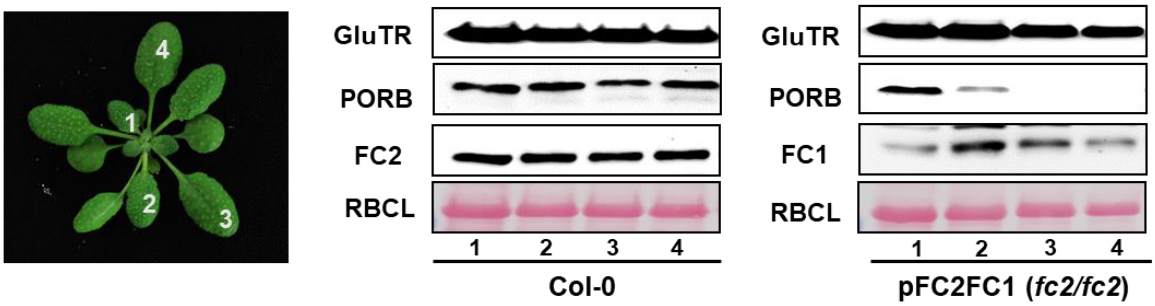

Figure 3. 10 FC2 is required for proper accumulation of PORB.

Leaves from position #1-#4 (indicated in left panel) were harvested from 4-week-old wild-type and pFC2FC1 (*fc2/fc2*) plants for western blot analysis. Seedlings were grown under SD condition with 100μE light intensity.

3.1.5 FC2 but not FC1 interacts with PORB *in vivo* and *in vitro*.

3.1.5.1 Pull-down assays suggested interaction between Arabidopsis FC2 and PORB.

To determine whether FC2 affects PORB stability via direct interactions or not, pull-down analysis was conducted with a recombinant 6xHis-tagged PORB protein. Purified His-PORB proteins were incubated with 1% DDM-solubilized chloroplast extracts from wild-type Arabidopsis, and then ligated to Ni-NTA resins. After three times washing with PBS buffer, proteins bound to the Ni-NTA beads were eluted and separated by SDS-PAGE followed by immunoblotting analysis. As a result, a thick immune reaction band representing FC2 was observed in the elution in the presence of both chloroplasts and recombinant PORB protein, whereas no signal could be detected when only chloroplast extracts were applied (Figure 3.10B). Although FC1 and GBP are also present in chloroplasts, no immune reacting band representing either FC1 or GBP (as a negative control) could be identified in the eluted fractions with or without the presence of His-PORB protein. These results verified a direct interaction between FC2 and PORB protein *in vitro*.

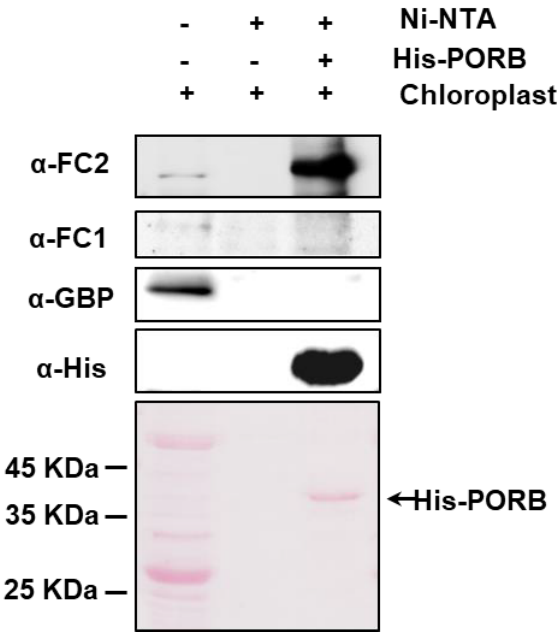

Figure 3. 11 Pull-down assay of the interaction between PORB and FC2.
Recombinant His-PORB-bound Ni-NTA resin was incubated with solubilized crude plastid extracts. Empty Ni-NTA resins were incubated with solubilized plastids as a negative control. The elution of Ni-NTA-bound proteins was analyzed immune-biochemically by employing the α-FC2, α-FC1, α-GBP and α-His antibodies.

3.1.5.2 FC2 but not FC1 interacts with PORB in yeast.

To further validate the interaction between PORB and FC2, a split-ubiquitin yeast two hybrid (Y2H) system was applied in addition to pull-down assay. Full-length cDNA sequences of *FC1* and *FC2* without transit peptides were fused to a pNub vector and transformed into L40ccuα yeast cells as preys. cDNA fragments of *PORB*, *FC2* and *CHL27* were used to generate the bait vectors (pCub). Then each bait construct was transformed into L40ccuA cells and subsequently mated with ccuα cells expressing FC1 or FC2 protein. L40ccuA cells carrying an empty pCub plasmid were used as a negative control. Aliquots of mated cells were grown on selective SD plates (SD/-lt and SD/-hult/20mM 3AT) for 3-5 days. Yeast cells co-expressing CHL27 and FC1 or FC2, like the negative control, grew only on SD/-lt plates but not on SD/-hult plates containing 20mM 3AT, indicating no interactions of CHL27 and either FC isoform. By co-expressing FC1 and FC2 or FC2 and FC2, the mated cells could grow on both selective plates, suggesting that FC2 form homodimers and may also generate heterodimers with FC1 in yeast. However, yeast cells expressing PORB protein could only survive on both selective conditions when FC2 but not FC1 was co-expressed. These results revealed that PORB interacts with FC2 but not FC1 in yeast.

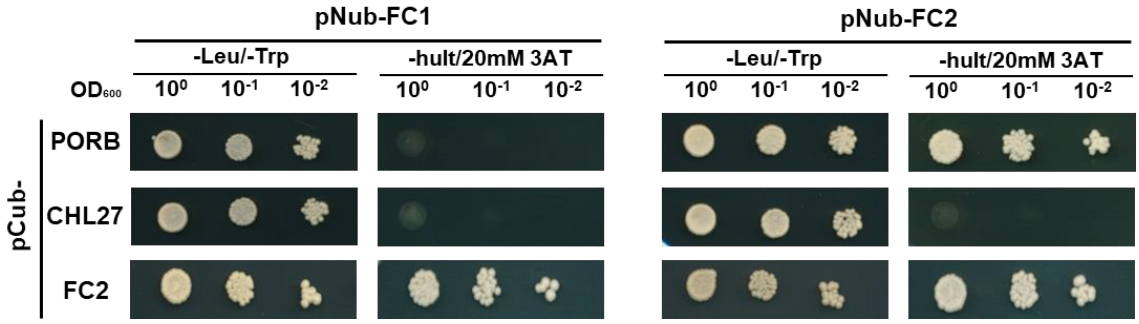

Figure 3. 12 Yeast two hybrid assays suggested CAB domain of FC2 is essential for its interaction with POR proteins.

Y2H assays were performed between FC isoforms and CHL27 as well as PORB protein. As a bait, either a full-length of FC1 or FC2 was fused to the C-terminal half of Ubiquitin. *FC2*, *CHL27* and *PORB* fragments were fused to the N-terminal of Ubiquitin respectively, as pray vectors. The prey and bait proteins were co-expressed by mating at 30°C. Transformants were primarily selected on SD/-Leu/-Trp plates. Then for the interaction screening, yeast cells expressing the corresponding serial vectors were plated on SD/-Leu/-Trp /-His/-Urea (-hult) media containing 20mM 3-amino-1,2,4-triazole (3AT), a competitive inhibitor of the His3p enzyme.

3.1.5.3 Bimolecular fluorescence complementation (BiFC) analysis suggested FC2 physically interacts with PORB.

Besides pull-down assay and Y2H analysis, to further confirm the interaction between FC2 and PORB, bimolecular fluorescence complementation (BiFC) analysis was performed by transiently expressing both proteins in epidermal cells of *Nicotiana benthamiana* leaves. No fluorescence could be detected when nYFP-FC2 with cYFP or cYFP-FC2 with nYFP constructs were co-transformed. However, co-expression of nYFP-tagged FC2/cYFP-tagged PORB and nYFP-tagged PORB/cYFP-tagged FC2 resulted in significant fluorescence in chloroplasts (Figure 3.10A). These observations suggested an interaction of FC2 and PORB *in vivo*.

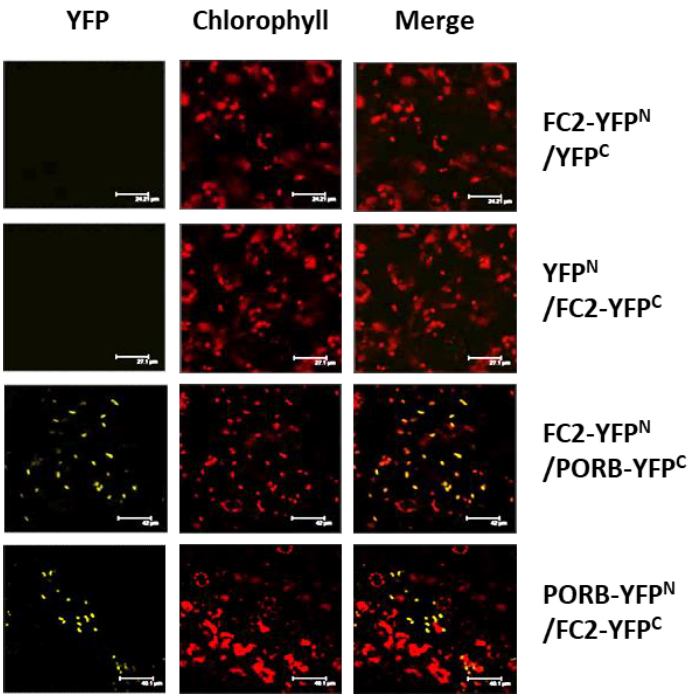

Figure 3. 13 : BiFC analysis revealed an interaction between FC2 and PORB protein in chloroplasts.

BiFC analysis of interaction between FC2 and PORB was performed by transiently expressing both proteins in leaf epidermal cells of *Nicotiana benthamiana* plants. Yellow fluorescence indicates YFP, red fluorescence displays chloroplast autofluorescence, and an overlay image shows merged signal from both types of fluorescence. Either a combination of nYFP-tagged FC2 and cYFP-tagged PORB or nYFP-tagged PORB and cYFP-tagged FC2 showed interaction in chloroplasts. Two negative controls expressing nYFP-tagged FC2 with cYFP protein and cYFP-tagged FC2 with nYFP protein displayed no fluorescent signal.

3.1.6 FC2 is in association with POR-FLU-GluTR complex

When a BiFC analysis was conducted to screen for interaction partners of FC2, FLU and GluTR also showed physical interactions with the type-II FC in addition to PORB protein (Figure 3.14A). A POR-cyclase-FLU complex has been proposed to regulate GluTR activity via pull-down and co-immunoprecipitation assays (Kauss et al., 2012). In this study, to verify the proposed complex and elucidate FC2 association with the complex, physical interactions of PORB, FLU, GluTR and FC2 were investigated by BiFC assays. As a result, FC2, PORB, FLU and GluTR interacted with each other in chloroplast, while CHL27 physically interacted with FLU and GluTR but not FC2.

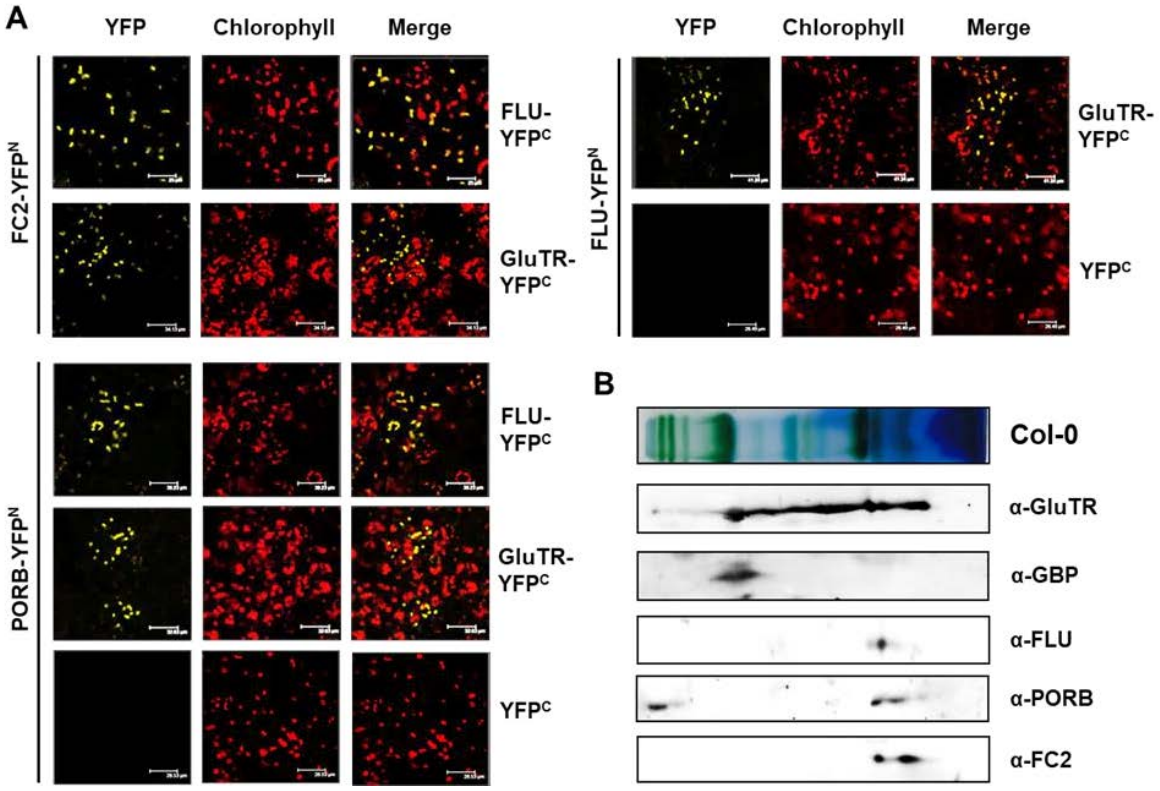

Figure 3. 14 Association of FC2 with a POR-FLU-GluTR complex.

(A) BiFC analyses of physical interactions of FC2, PORB, FLU and GluTR proteins. BiFC analyses were conducted by transiently expressing FC2, PORB, FLU and GluTR proteins in tobacco leaves. Yellow fluorescence indicates YFP, red fluorescence displays chloroplast autofluorescence, and an overlay image shows merged signal from both types of fluorescence. Leaf tissues expressing nYFP-tagged PORB or nYFP-tagged FLU with cYFP protein were used as negative controls. (B) Allocations of ALA synthesis-associated proteins on thylakoid membranes. Solubilized wild-type thylakoids (equivalent to 10µg chlorophyll) were separated in the first dimension by a BN-PAGE gel, followed by SDS-PAGE analysis in the second dimension. The resolved proteins were immunodetected with α-GluTR, α-GBP, α-FLU, α-PORB and α-FC2 antibodies.

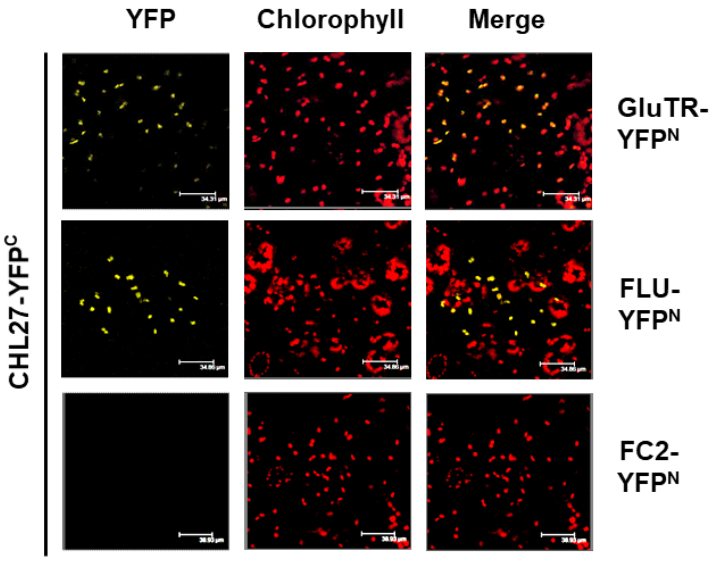

Figure 3. 15 Interaction analyses of CHL27 and GluTR, FLU as well as FC2 by BiFC.
cYFP-tagged CHL27 was co-expressed with nYFP-tagged GluTR, FLU and FC2 respectively in tobacco leaf cells. Merge indicates an overlay of the YFP and chlorophyll autofluorescence images. Sale bars were indicated.

To validate whether FC2 is in association with the POR-FLU-GluTR complex or not, distributions of the relevant proteins in thylakoid complexes were determined via a two-dimension (2D) PAGE assay. Freshly extracted thylakoids were solubilized with 1% DDM and subjected firstly to a BN-PAGE gel followed by SDS-PAGE analysis in the second dimension. Immunoblot analysis of the second dimension gels revealed that GluTR was widely distributed in the thylakoid complexes in multiple low and high molecular weight complexes. As a positive regulator of GluTR protein, GBP was solely localized in a high molecular weight complex with also the presence of GluTR. However, different from GBP, FLU, PORB and FC2 migrated mainly in the lower molecular weight complexes. Moreover, FC2 co-migrated with PORB in two different complexes, while one of the complexes was also co-localized with FLU and GluTR. These migration patterns indicated FLU and GBP may interact with GluTR in separated complexes, while FC2 and PORB are involved in the GluTR-FLU-containing complex. Overall, both protein-protein interactions and subcellular localization studies suggest that FC2 is in associated with a POR-FLU-GluTR complex.

3.1.7 FC2 is critical for the stabilization of PORB-FLU-GluTR complex and ALA synthesis regulation.

Interaction and localization studies indicated that FC2 may contribute to the assembly of the proposed POR-FLU-GluTR complex which suppresses ALA synthesis in the dark. Therefore, in this study, a series of ALA synthesis-associated mutants were characterized to validate FC2 genuine function in ALA synthesis regulation.

3.1.7.1 A lack of FC2 or PORB perturbs ALA synthesis inhibition.

The pFC2FC1 (*fc2*/*fc2*) complemented plants exhibited different phenotypes under CL and day-night conditions. As both *fc2* and *flu* knockout mutants could not survive SD growth, pFC2FC1 (*fc2/fc2*), *fc2* knockdown (*fc2-1*), *porb* knockout mutants and FC2 overexpression (35SFC2) plants were grown with comparable wild type under SD condition with 100μE light intensity. Besides the necrotic phenotypes of the pFC2FC1 (*fc2/fc2*) lines and *fc2-1* mutants which has been shown in previous chapters, a lack of PORB resulted in slightly growth-retarded seedlings with chlorotic leaves (Figure 3.16). Interestingly, overexpression of FC2 in wild-type background also resulted in pale-green leaves of reduced size compared to Col-0. These phenotypes could be further confirmed by the measurement of chlorophyll contents. All the mutant lines, as well as the 2 representative FC2 overexpressing plants, displayed significant reduced chlorophyll compared to wild-type seedlings (Figure 3.17).

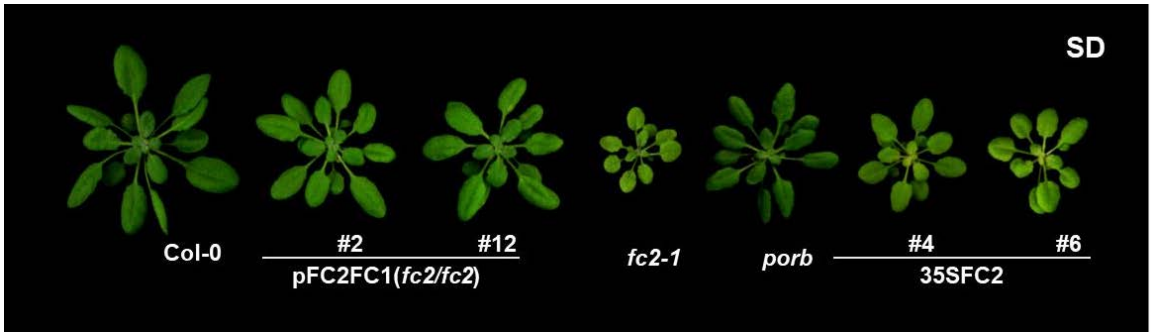

Figure 3. 16 Phenotypes of mutants grown under SD condition.

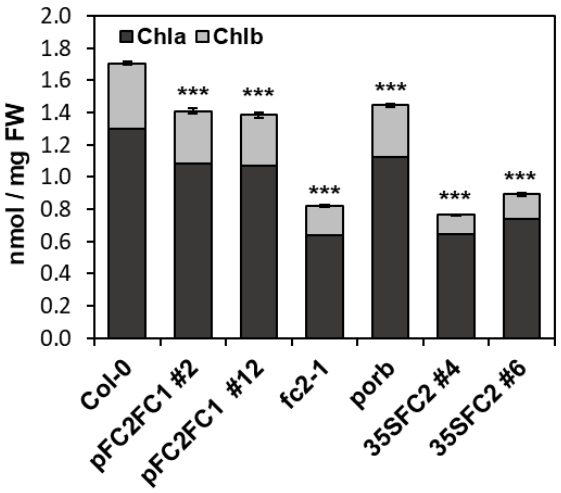

Figure 3. 17 Chlorophyll contents of mutants and wild-type seedlings.
Chlorophyll contents were determined for pFC2FC1 (*fc2/fc2*), *fc2-1*, *porb* mutants as well as wild-type seedlings. Leaf samples were harvested from 3-week-old SD-grown plants. Error bars indicate standard deviations (n≥3). Asterisks represent significant differences, which were calculated by Student's t-test; *** P value < 0.001.

In addition to pigmentation analysis, ALA synthesis rates were determined in the 3-week-old mutants and wild-type seedlings to investigate the impact of *FC2* and *PORB* expression on ALA synthesis regulation. Under SD condition (100μE light intensity, 22°C), both *fc2-1* and pFC2FC1 (*fc2/fc2*) lines showed around 50% elevated ALA synthesis rates compared to wild type. Additionally, a lack of PORB also led to a similar increase of ALA synthesis capacity. However, overexpression of FC2 resulted in at least 40% reduction of ALA synthesis ability. Based on these results, it could be concluded that although either a defect or over-accumulation of FC2 led to reduced chlorophyll production (Figure 3.17), their regulations of ALA synthesis and the TBS pathway were quite different. A defective *FC2* or *PORB* expression promoted ALA synthesis *in vivo*.

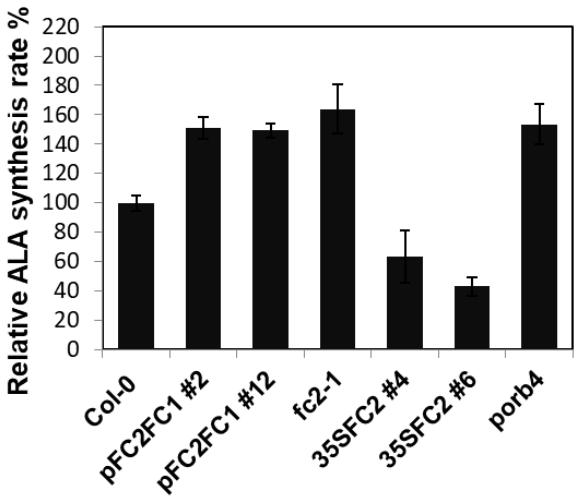

Figure 3. 18 ALA synthesis rates of wild-type and mutant plants.
ALA synthesis rates were determined in Arabidopsis leaf discs after a 4h incubation in 40mM levulinic acid solutions under growth light (100µE, 22°C). ALA was then extracted and determined with Ehrlich-Reagenz reagent. Relative ALA synthesis rates in the *fc2* and *porb* defective mutants, as well as 35SFC2 plants, were calculated by normalizing to the level of Col-0. Error bars represent standard deviations (n≥3).

To investigate the reason for the diverse ALA synthesis rates in all the mutant lines, protein contents of ALA synthesis-associated enzymes, as well as LHCPs, were determined by immunoblot analysis. The absence of PORB protein could be confirmed in the *porb* knockout mutant. By employing an α-FC2 antibody, the drastic accumulation of FC2 protein in both 35SFC2 transgenic lines could be detected, while an immune reacting band representing FC2 could not be observed in pFC2FC1 (*fc2*/*fc2*) plants. Although a reduced PORB content could always be observed in the FC2 deficient mutants, a lack of PORB did not affect FC2 accumulation. Both LHCA1 and LHCB1 were reduced to different extents in the mutant lines, in correlation with the alleviated chlorophyll contents (Figure 3.17). Except for the alteration in PORB contents in *fc2* deficient mutants, accumulation of ALA synthesis-associated enzymes, such as GSAAT, GluTR and the two regulators GBP and FLU, showed no notable changes in all the analyzed mutants. These results suggested that the changes of ALA synthesis rates in all of the mutants and the FC2 overexpression lines were not attributed to a modified accumulation of ALA synthesis enzymes.

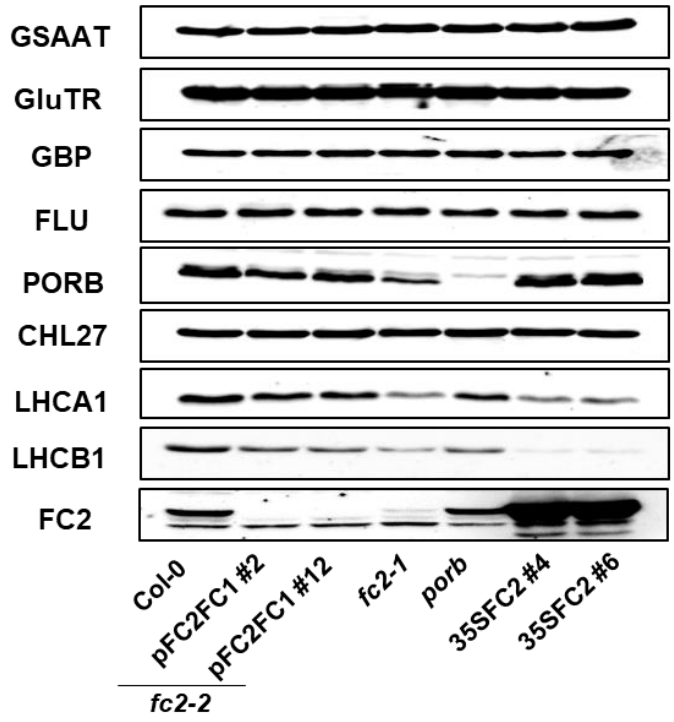

Figure 3. 19 Immunoblot analysis of TBS enzymes and LHCPs.
Total proteins were extracted from 3-week-old SD-grown seedlings and separated by a 12% SDS PAGE gel. The resolved proteins were determined via immunoblot analysis by employing antibodies raised against TBS enzymes and LHCPs.

As the protein levels of ALA synthesis enzymes stayed unchanged compared to wild type, in order to explain the altered ALA synthesis rates in all the mutant lines, the distributions of GluTR-containing complexes were examined. Thylakoid membranes were isolated from 4-week-old mutants and wild-type seedlings followed by solubilization with 1% DDM for 10min on ice. The resolved thylakoid complexes were subjected firstly to a 4.5-12.5% BN-PAGE gel and subsequently separated by a 12% SDS-PAGE gel in the second dimension. Finally, allocations of relevant proteins were analyzed immunochemically by employing antibodies indicated in Figure 3.20.

As a result, under the harvest condition, wild-type GluTR was widely distributed in multiple thylakoid complexes with the presence of three major GluTR-containing complexes. They were designated as complex 1, 2 and 3 (Figure 3.20A). The migration of FLU and FC2 proteins in thylakoid complexes indicated a FLU-bound GluTR complex migrated in the low molecular weight part, which complex was designated as complex 3. Besides wild type, mutant lines pFC2FC1 (*fc2*/*fc2*), *porb* as well as the 35SFC2 overexpression plants were also used for thylakoids extraction. By applying the same gradient BN-PAGE/SDS-PAGE analysis, allocations of GluTR-containing complexes were examined. Compared to wild type, 35SFC2 thylakoids accumulated generally more GluTR protein. Nevertheless, the relative distribution of GluTR in complexes 1-3 did not display significant changes in 35SFC2 thylakoids in comparison to the wild-type control. However,

the three major GluTR-containing complexes showed varying distributions in both pFC2FC1 (*fc2*/*fc2*) and *porb* mutants. GluTR contents in complex 1 and complex 2 in the two lines displayed wild-type-level accumulation, whereas the amount of GluTR in complex 3 was significantly decreased. To determine to which extent the complex 3 was affected, relative accumulation of the three complexes was analyzed by an ImageJ program (National Institutes of Health, NIH) via normalizing to the complex 2 amount. As a result, relative accumulation of GluTR-containing complex 1 and complex 2 showed no difference in pFC2FC1 (*fc2*/*fc2*) and *porb* mutants, whereas the complex 3 GluTR contents dropped by 47% and 75% respectively, compared to wild type (Figure 3.20B and C).

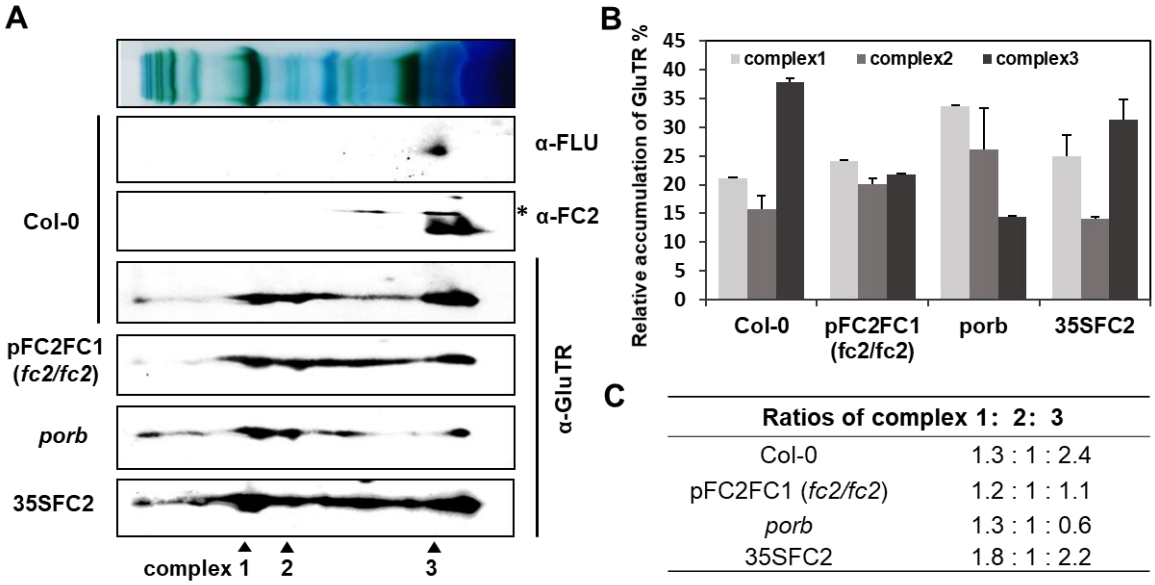

C

Ratios of complex 1: 2: 3	
Col-0	1.3 : 1 : 2.4
pFC2FC1 (*fc2/fc2*)	1.2 : 1 : 1.1
porb	1.3 : 1 : 0.6
35SFC2	1.8 : 1 : 2.2

Figure 3. 20 Lack of FC2 or PORB affects the allocation of GluTR on thylakoid membranes.

(A-C) Distribution of GluTR in thylakoid complexes. (A) Solubilized wild-type and mutant thylakoids (equivalent to 10μg chlorophyll) were separated in the first dimension by a 4.5-12.5% BN-PAGE gel, followed by SDS-PAGE analysis in the second dimension. The resolved proteins were immunodetected with α-GluTR, α-FLU and α-FC2 antibodies. Experiments were performed more than two times, similar results could be obtained. Main complexes containing GluTR protein were indicated with black triangles. Asterisks indicate non-specific immune-reacting bands. (B) Relative contents of GluTR-containing complexes in wild-type and mutant plants. Percentages were calculated by ImageJ via normalizing to the total amount of GluTR. (C) Ratios of GluTR containing complexes contents were calculated. The content of complex 2 was set to 1.

These results suggest that a defective *FC2* or *PORB* expression affects exclusively the stability of GluTR-containing complex 3 on thylakoid membranes. This complex refers to a FLU-bound GluTR complex. In other words, a lack of either FC2 or PORB perturbs the assembly of a FLU-GluTR complex and this maybe the explanation for the elevated ALA synthesis rates in the *fc2* and *porb* defective mutants (Figure 3.18).

In wild-type plants, Pchlide accumulation in darkness always correlates with the down-regulated ALA synthesis. And it has been shown that a reduced Pchlide content reflects a defective ALA synthesis (Richter et al., 2010). Thus, to assess the consequences of these modified GluTR allocations and ALA synthesis capacities, Pchlide contents in all the mutant lines and wild type were determined in light and dark phases (Figure 3.21). During daytime, Pchlide contents retain at a very low level, as this chlorophyll intermediate is phototoxic and its accumulation easily triggers oxidative stress. Due to a defect in protochlorophyllide reductase activity, Pchlide was more accumulated in *porb* mutant compared to Col-0. Interestingly, an overexpression of FC2 led to a significant decrease of Pchlide accumulation during daytime, which may be explained by the decelerated ALA synthesis (Figure 3.18). However, during night, Pchlide content accumulated several-fold higher in wild-type seedlings compared to light-exposed plants. In the dark, the two pFC2FC1 (*fc2*/*fc2*) plants, as well as *porb* mutants, showed more than 170%-wild-type level Pchlide accumulation, while the FC2 overexpression lines still displayed a defective Pchlide formation in consistence with the light-exposed seedlings.

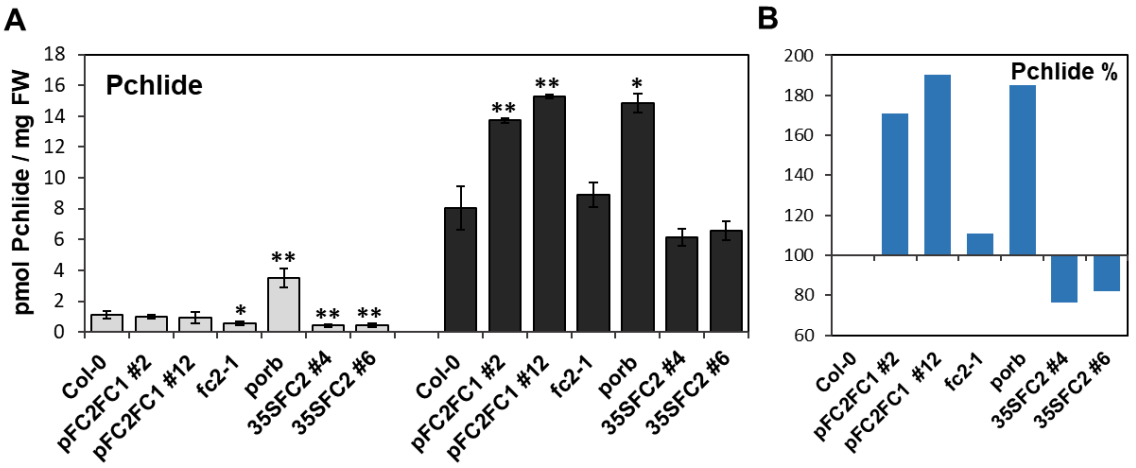

Figure 3. 21 A defect in FC2 or PORB expression affected Pchlide accumulation in darkness.

(A) Accumulation of Pchlide in light (white boxes) and dark (black boxes)-incubated plants. Dark samples were harvested after a 12h incubation. Error bars indicate standard deviations, n≥3. Asterisks represent significant differences, which were calculated by referring to light- and dark- incubated Col-O respectively; * P value < 0.05, ** P value < 0.01. (B) Percentages of Pchlide accumulation in darkness. The Pchlide content of dark-incubated Col-0 was set to 1.

To estimate the effect of modified ALA synthesis rates in a combination with altered FC expression, heme contents in *porb* and *fc2* mutant lines were determined during day and night time. As a consequence of down-regulated ALA synthesis, heme content in wild-type seedlings was reduced by 15% after a 12h dark incubation. The two 35SFC2 lines synthesized 7% less heme during night compared to daytime, possessing reduced heme contents in comparison with wild-type control. In contrast, the *fc2-1* mutants, with a compromised FC activity, showed non-modified heme production in comparison to the

light-exposed seedlings when transferred to dark. Additionally, the pFC2FC1 (*fc2*/*fc2*) lines, as well as *porb* mutant seedlings, also showed no alterations in heme production when the plants were transferred from light to darkness. These changes resulted in wild-type levels of heme accumulation in the pFC2FC1 (*fc2*/*fc2*) and *porb* seedlings during night.

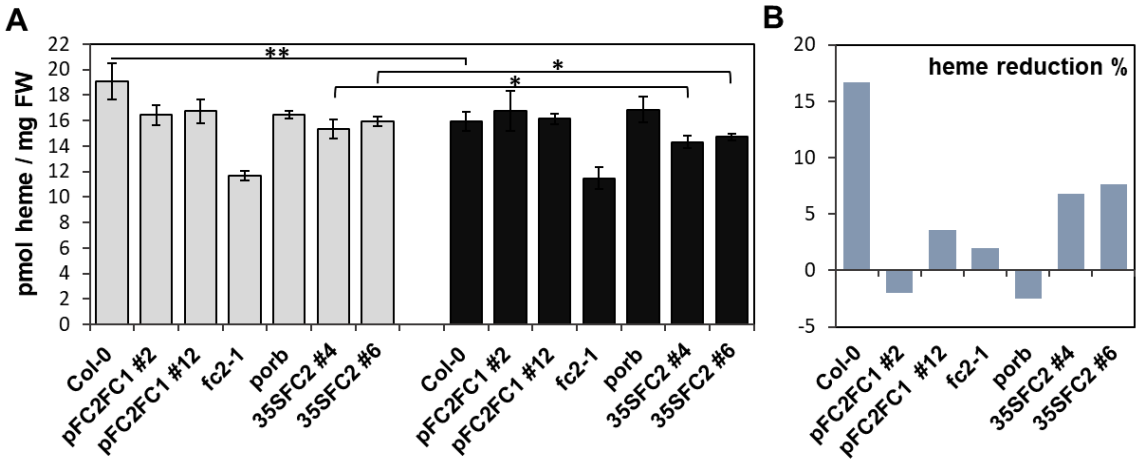

Figure 3. 22 Defective FC2 or PORB expression perturbs repression of heme synthesis in darkness.

(A) Heme contents were determined in the light (white boxes) and dark (black boxes)-incubated plants indicated in Figure 3.21. Error bars indicate standard deviations, n≥3. Asterisks represent significant differences calculated by comparing light- and dark-incubated samples. (B) Ratios of heme reduction were determined by comparing heme contents in the light- and dark-incubated plants, Heme contents of the light-exposed samples were set to 1.

Under the condition applied, the *fc2* knockdown mutants (*fc2-1*) exhibited a decrease of Pchlide accumulation in daytime, but a wild-type-level accumulation during night. Previous characterization of *fc2* mutants revealed an increased Pchlide accumulation in both *fc2* (knockout and knockdown) mutants, which results were contradictory to the data obtained in this study. As the author's measurement was performed based on dry weight instead of fresh weight (Scharfenberg et al., 2015), tetrapyrrole products of the dark-incubated *fc2-1* seedling were also measured based on dry weight. By normalizing to dry weight, the elevated accumulation of Pchlide in *fc2-1* could be confirmed, while the reduction of chlorophyll content was in accord with the results obtained based on fresh weight (Figure 3.17). In addition, when the measurements were conducted based on dry weight, *fc2-1* mutants showed an increased heme accumulation compared to wild type in darkness, which could not be observed based on a fresh- weight-calculation.

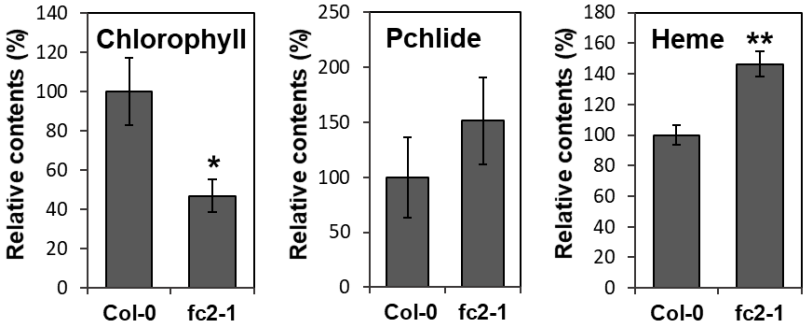

Figure 3. 23 Accumulation of TBS intermediate and end-products in dark-incubated *fc2-1* mutants determined by referring to dry weight.

3-week-old *fc2-1* and comparable wild-type seedlings were harvested after 12h incubation in darkness. The fresh leaves were homogenized and freeze-dried before the extraction was performed. Relative accumulation in *fc2-1* was obtained by normalizing to wild-type-level content. Error bars indicate standard deviations, n≥3. Asterisks represent significant differences. * P value < 0.05, ** P value < 0.01.

Taken all together, the light-dark incubation tests suggest that wild-type Arabidopsis which are transferred to darkness undergoes a repressed heme synthesis due to a down-regulated ALA synthesis. However, mutant lines with defective *FC2* or *PORB* expression, i.e. pFC2FC1 (*fc2*/*fc2*), *fc2-1* and *porb* plants, show perturbed inhibition of heme synthesis and increased Pchlide accumulation in darkness, as a consequence of elevated ALA synthesis rates.

3.1.7.2 Inhibition of ALA synthesis by FLU not only represses chlorophyll synthesis but also lowers heme production in darkness.

As a FC2-PORB-FLU complex has been proposed based on the protein-protein interactions and subcellular localization studies, a *flu* null mutant has been characterized in addition to *porb* and *fc2* mutants. Down-regulation of ALA synthesis by FLU in darkness is indispensable for plant growth (Meskauskiene et al., 2001). A null mutation of *flu* led to a lethal phenotype under light-dark cycles. pFC2FC1 (*fc2*/*fc2*), *fc2-2*, *flu* mutants as well as FC2 overexpression plants were grown under CL condition for 3 weeks. The *fc2* knockout mutants (*fc2-2*) displayed severely retarded growth with necrotic leaves, while *flu* showed a wild-type-like phenotype accumulating identical chlorophyll content compared to Col-0. The pale-green leaves of 35SFC2 plants could be also observed under a CL-growth, while the CL-grown pFC2FC1 (*fc2*/*fc2*) leaves displayed neither necrotic phenotype nor reduced chlorophyll accumulation in comparison to the SD-grown seedlings (Figure 3.24 and 3.25).

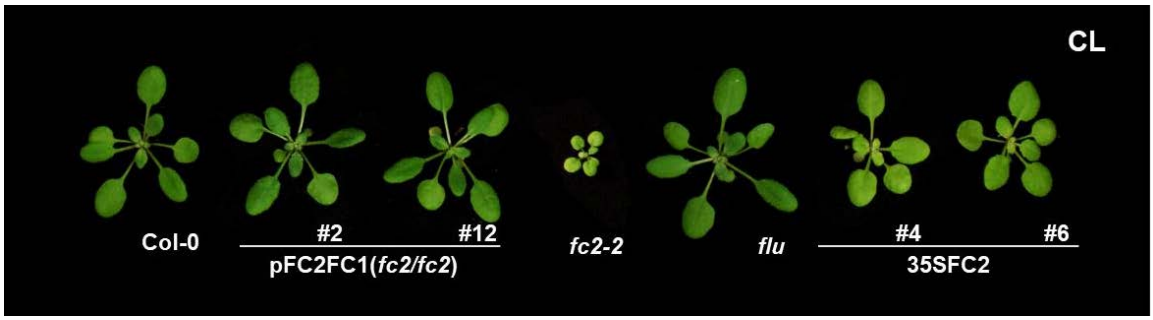

Figure 3. 24 Phenotypes of 2-week-old pFC2FC1 (*fc2/fc2*), *fc2-2*, *flu* mutants and 35SFC2 overexpression plants grown under CL condition.

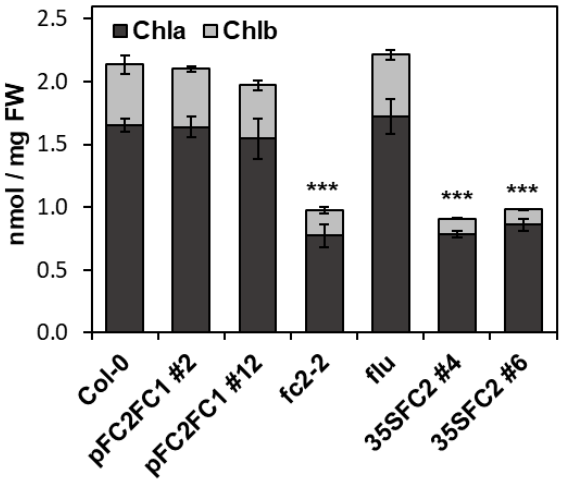

Figure 3. 25 Chlorophyll contents of mutants and wild-type seedlings grown under CL condition.

Chlorophyll contents were determined for pFC2FC1 (*fc2/fc2*), *fc2-2*, *flu* and 35SFC2 mutants as well as wild-type seedlings. Leaf samples were harvested from 3-week-old CL-grown plants. Error bars indicate standard deviations (n≥3). Asterisks represent significant differences, which were calculated by Student's t-test; *** P value < 0.001.

To assess the effect of a defective *FC2* and *FLU* expression in the dark, Pchlide contents were determined after the mutants and wild-type plants were treated with a 12h dark incubation. As a consequence of an inappropriate inhibition of ALA synthesis in *flu* mutants, Pchlide content was drastically elevated in the dark in comparison to Col-0. After dark incubation, CL-grown 35SFC2 plants showed reduced Pchlide accumulation compared to wild type, which also occurred in the SD-grown seedlings. Additionally, the *fc2-2*-level of Pchlide accumulation could also be observed in the CL-grown pFC2FC1 (*fc2/fc2*) seedlings after dark incubation. This indicated that deficiency of *FC2* or *FLU* expression resulted in increased Pchlide accumulation in the dark compared to the wild-type control.

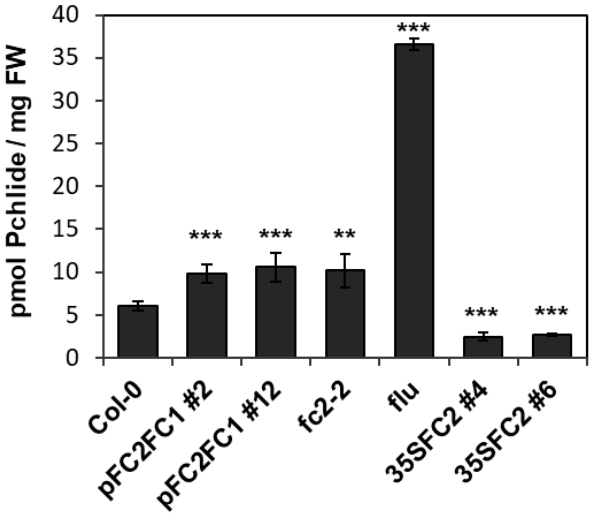

Figure 3. 26 Pchlide accumulation in darkness.
Pchlide contents were measured in leaf samples harvested from plants in Figure 2.24, after 12h dark incubation. Error bars indicate standard deviations, n≥3. Asterisks represent significant differences; ** P value < 0.01, *** P value < 0.001.

Moreover, heme contents were determined in the CL-grown plants before and after dark incubation. In consistence with a SD-growth, CL-grown Col-0 also exhibited a 15% reduction of heme amounts in darkness, in comparison to the light-exposed seedlings (Figure 3.27). However, when transferred to dark, mutants lacking *FC2* (*fc2-2* and pFC2FC1 (*fc2*/*fc2*)) accumulated identical heme contents compared to the light-exposed seedlings. These observations were in consistence with the SD-grown plants. FLU is proposed to be a negative feedback regulator for ALA synthesis, specifically linked to the chlorophyll synthesis branch (Meskauskiene et al., 2001; Kauss et al., 2012). Etiolated *flu* mutants accumulate elevated Pchlide contents, with similar heme levels in comparison to wild-type seedlings (Meskauskiene et al., 2001). In the CL-grown *flu* seedlings, heme content in daytime displayed a wild-type-level accumulation. However, *flu* seedlings showed no changes of heme contents when the mutants were transferred from light to dark, resembled a similar phenotype in comparison to a *fc2* null mutation (*fc2-2* and pFC2FC1 (*fc2*/*fc2*)). The two 35SFC2 overexpression lines displayed different changes of heme accumulation in darkness. 35SFC2 line #6 showed a wild-type level reduction of heme contents when transferred to dark, whereas line #4 displayed a 10% higher accumulation of heme in darkness compared to the light-incubated seedlings. These distinctive changes could be attributed to the different FC2 expression levels (Figure 3.28). The line #4 plants could potentially produce more FC activity in comparison to line #6, as more FC2 proteins were present in comparison to the latter line. In the FC2 overexpressing plants, an overall heme production may depend on the synthesis rates of ALA as well as the elevated FC activity.

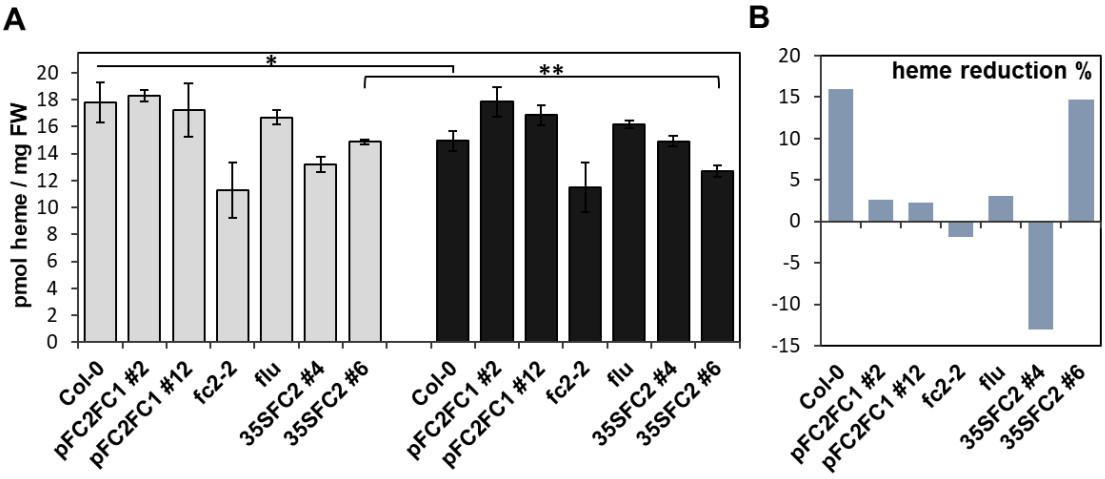

Figure 3. 27 Defective *FLU* expression perturbs inhibition of heme synthesis in darkness.

(A) Heme contents were determined in the light (white boxes) and dark (black boxes)-incubated mutants as well as wild-type plants. Error bars indicate standard deviations, n≥3. P values were calculated by comparing light- and dark-incubated samples; * P value < 0.05, ** P value < 0.01. (B) Changes of heme accumulation were determined by comparing heme contents in light- and dark-incubated plants. Heme contents of light-exposed samples were set to 1.

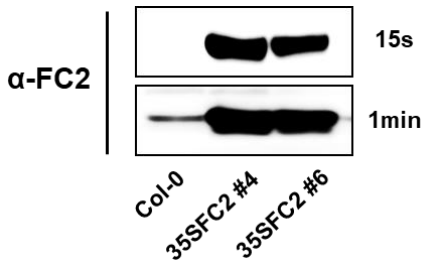

Figure 3. 28 Determination of FC2 contents in the 35SFC2 overexpression plants.

Total proteins were extracted from leaves of 3-week-old CL-grown FC2 overexpression and wild-type plants. The immunoblot analysis was performed by employing a specific FC2 antibody. The exposure time was indicated on the right.

Taken together all the results, the light/dark incubation tests of *fc2*, *porb*, *flu* mutants and FC2 overexpression lines indicates that defective expression of *FC2*, *PORB* or *FLU* results in a perturbed inhibition of ALA synthesis and subsequent heme formation in the dark.

3.2 Chlorophyll A/B binding (CAB) domain of FC2 contributes to its essential role in PSII-LHCII supercomplexes assembly.

Preliminary characterization of *fc* mutants suggested that *FC2*, but not *FC1* mutation alleviates photosynthesis efficiency in addition to the reduction of chlorophyll (Scharfenberg et al., 2015). Subsequent BN gel analysis of photosynthetic complexes in *fc2-2*, *fc1-1* and wild-type seedlings revealed an altered migration pattern of PSII complexes in *fc2-2* compared to wild type, which could not be observed in a *fc1-1* mutant (Espinas et al., 2016). It was proposed that FC2 activity serves for hemoproteins in photosynthetic complexes (Scharfenberg et al., 2015; Espinas et al., 2016). But how does FC2 affect the assembly of PSII complexes? Does this function role depend on the presence of FC2 or the allocations of heme? These questions awaits further elucidation.

3.2.1 Defective *FC2* expression interferes PSII-LHCII supercomplexes assembly.

To gain deeper insights into the functional differences between Arabidopsis FC1 and FC2, the partially complemented SD-grown pFC2FC1 (*fc2*/*fc2*) plants were examined for the assembly of photosynthetic complexes. As a consequence of the decreased heme contents, pFC2FC1 (*fc2*/*fc2*) seedlings showed a slightly reduced accumulation of Cytf protein, which is an essential hemoprotein involved in Cytb6f complex. The content of key subunit PsaA in PSI showed no alterations in comparison to wild type, whereas D1 subunit, a representative component of PSII displayed a slightly decrease in the pFC2FC1 (*fc2*/*fc2*) plants due to the reduced heme content (Figure 3.4).

Figure 3. 29 Phenotypical characterization of pFC2FC1 (*fc2/fc2*) and *fc2-1* mutants.
(A) Phenotypes of 4-week-old pFC2FC1 (*fc2*/*fc2*), *fc2-1* mutants and wild-type plants under SD condition. (B) Western blot analysis of photosynthetic proteins in plants indicated in panel A. Cytf: Cytochrome f, a heme-binding protein from cytochrome b6f complex, D1: an essential subunit of PSII core complex; PsaA; a main subunit of PSI.

BN-PAGE analysis was subsequently applied to assess the assembly of photosynthetic complexes in pFC2FC1 (*fc2*/*fc2*), *fc2-1* and wild-type seedlings. Thylakoids were extracted from both young and old leaf tissues of 4-week-old SD-grown plants. The thylakoid

membrane complexes (equivalent to 10µg chlorophyll) were separated in a 4.5-12.5% gradient BN-PAGE gel after solubilization. The migration patterns of resolved thylakoid complexes revealed an identical assembly of photosynthetic complexes in both young and old leaves of wild-type plants. In early developmental stages, pFC2FC1 (*fc2/fc2*) and *fc2-1* mutants displayed wild-type-like assembly of major photosynthetic complexes. However, the old leaves of pFC2FC1 (*fc2/fc2*) and *fc2-1* mutants revealed an impaired assembly of PSII-LHCII supercomplexes (complexes II) (Figure 3.30). Instead, PSII dimer and monomer (complex V and VI) complexes accumulated in both mutant lines in comparison to wild type. These photosynthetic criteria suggested that FC1 could not compensate FC2 functional loss in the assembly process of photosynthetic complexes, in addition to chlorophyll synthesis.

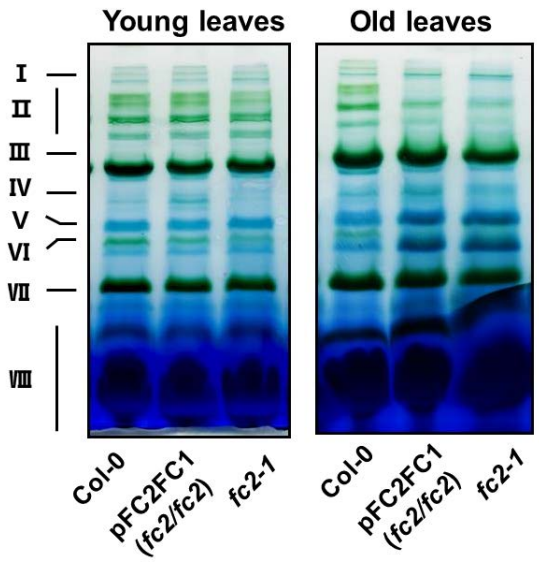

Figure 3. 30 BN-PAGE analysis of photosynthetic complexes in thylakoid membranes isolated from wild-type and pFC2FC1 (*fc2/fc2*), *fc2-1* leaves.
Solubilized thylakoid membranes were separated on a 4.5-12.5% BN-PAGE gel. Predominant photosynthetic complexes were indicated on the left: (I) PSI-NDH megacomplex; (II) PSII-LHCII supercomplexes; (III) PSI and PSII dimer; (IV) ATP synthase; (V) PSII monomer and Cytochrome b6f complex; (VI) CP47 less complex; (VII) LHCII trimer; (VIII) free proteins.

3.2.2 Disruption of CAB domain of FC2 perturbs the assembly of PSII-LHCII supercomplexes.

3.2.2.1 Overexpression of FC2 variants leads to a chlorotic phenotype.

In Arabidopsis, the two isoforms of FC are structurally distinguished by their C-terminus. While FC1 possesses a transmembrane domain after the FC activity motif, FC2 harbours a putative chlorophyll binding domain (also designated as CAB domain) within its C-terminal extension (Chow et al., 1998). Thus, to testify whether the essential function of

FC2 in PSII complex assembly is attributable to its structural differences in comparison to FC1, various FC2 overexpressing plants with c-terminus modifications were generated. A 35SFC2 (*p35S::FC2*) construct contained a full *FC2* genomic sequence driven under a 35S promoter, while the 35SFC2-CFP (*p35S::FC2-CFP*) construct carried a 26.7kDa Cyan Fluorescence Protein tag attached to the CAB domain. In a FusB (*pFC1::FC2(1-425)_FC1(415-466)*) expression vector, the CAB domain of FC2 is substituted by a c-terminal fragment of *FC1* gene which ensures its membrane binding (Figure 3.31).

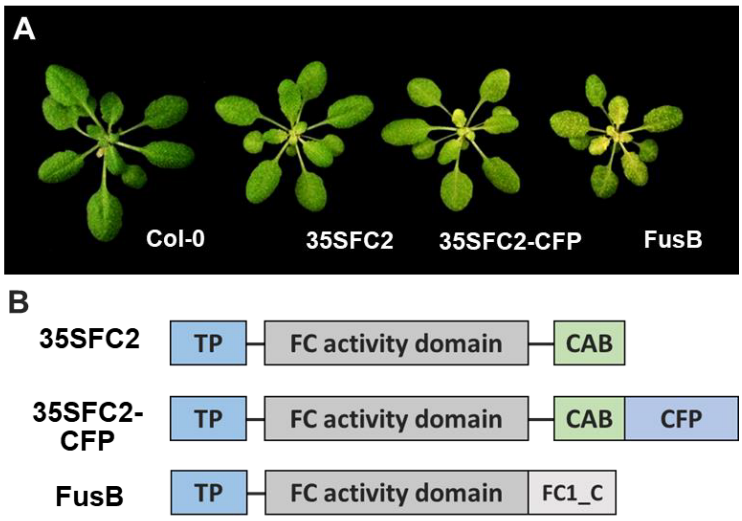

Figure 3. 31 Phenotypes of various FC2 overexpression lines.
(A) 35SFC2, 35SFC2-CFP, FusB and wild-type seedlings were grown under SD condition. Pictures were taken after 4-week growth. (B) Schemes of 35SFC2, 35SFC2-CFP and FusB constructs. TP: transit peptide; FC activity domain indicates amino acid sequeces of FC2 catalytic domain; CAB: chlorophyll A/B binding motif; FC1_C: C-terminus of FC1 protein; CFP: Cyan Fluorescence Protein.

When grown under SD with 100µE light intensity, all the three FC2 overexpression mutants exhibited pale-green leaves. Moreover, the FusB mutant leaves showed necrotic leaves in addition to a chlorotic phenotype in comparison to 35SFC2 and 35SFC2-CFP overexpression plants. Expression of the three FC2 variants were confirmed by western blot analysis (Figure 3.32A). By employing both α-FC1 and α-FC2 antibodies, highly accumulated FC2 and FC2-CFP proteins could be detected in 35SFC2 and 35SFC2-CFP plants respectively. As a FusB sequence was expressed under a *FC1* promoter, the protein was less accumulated in comparison to the other two FC2 variants. Subsequently, to confirm the function of all three FC2 variants, FC activity was determined by an *in vitro* assay (Figure 3.32B). The results revealed that all three FC2 variant proteins were functional and contributed to enhanced FC activity in comparison to endogenous FC in wild-type plants.

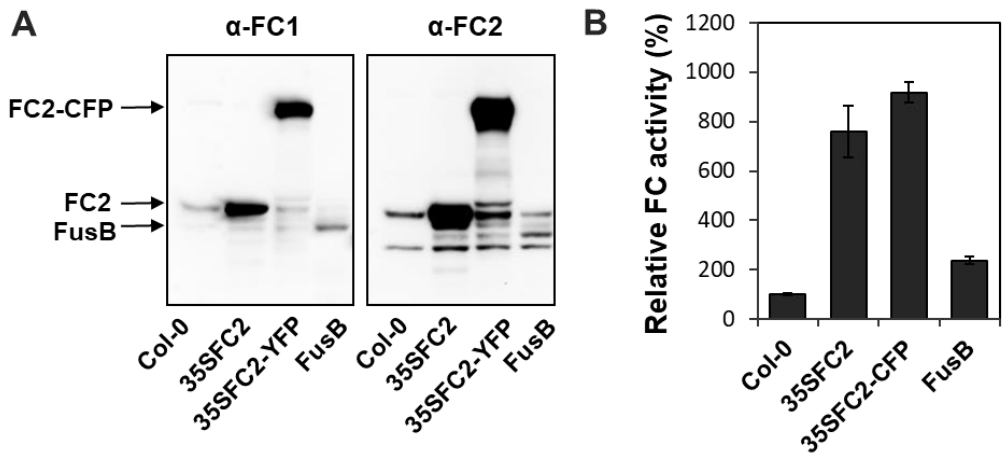

Figure 3. 32 FC contents and activity in the FC2 overexpression plants.
(A) Determination of FC protein contents in 35SFC2, 35SFC2-CFP and FusB mutants. Total proteins were extracted from 4-week-old FC2 overexpression and wild-type plants. Immunoblot analysis was performed by employing α-FC1 and α-FC2 antibodies. An α-FC1 antibody recognizes both FC1 and FC2 isoforms in Arabidopsis. The α-FC2 antibody specifically recognize FC2. (B) *In vitro* FC activity from leaf extracts of the three FC2 overexpression lines compared to wild type. FC activity of Col-0 was set to 1. Error bars indicate standard deviations (n>3).

3.2.2.2 35SFC2, 35SFC2-CFP and FusB expression led to a similar impact on the TBS pathway.

To evaluate the impact of the expression of all three FC2 variants, transcripts and protein levels of enzymes involved in the TBS pathway were investigated. qRT-PCR analysis of numerous TBS genes confirmed the drastically elevated *FC2* transcripts in 35SFC2, 35SFC2-CFP and FusB plants. Additionally, slightly increased *FC1* mRNA could be detected in all three overexpression lines. Despite of a moderately elevated *CHLD* mRNA, other TBS genes examined in the three transgenic lines did not show a significant alteration (Figure 3.33A). Interestingly, expression of 35SFC2, 35SFC2-CFP and FusB resulted in a similar high accumulation of GUN4, as well as slightly increased CHLM, PORB and FLU protein contents (Figure 3.33B). Regardless of these accumulated TBS proteins, the three expression plants showed a reduced chlorophyll accumulation in comparison to Col-0 (Figure 3.33C). It is has been concluded from the previous chapter (chapter 3.1) that *FC2* expression may have a negative impact on ALA synthesis and eventually, result in a moderate synthetic flow of tetrapyrroles. Thus, although with the potentials to produce more heme, expression of the three FC2 variants all resulted in decreased heme accumulation in comparison to wild-type plants (Figure 3.33D).

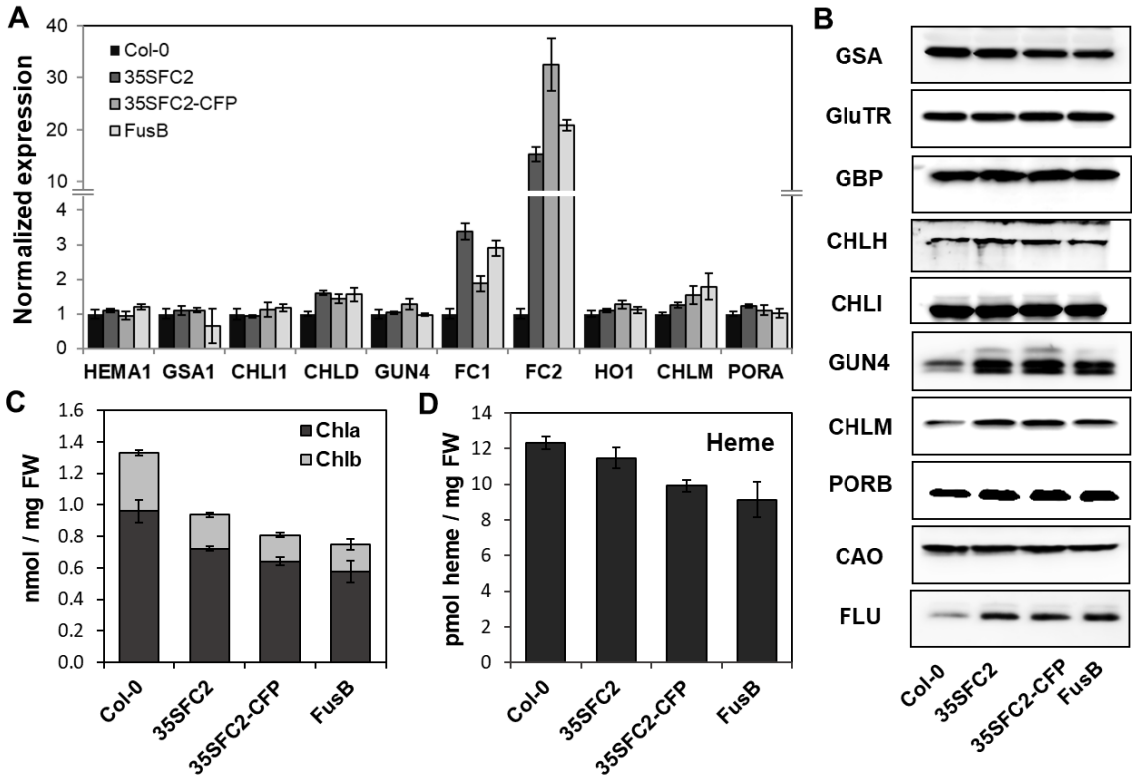

Figure 3. 33 Biochemical analyses of FC2 overexpression plants.

qRT-PCR (A) and western blot (B) analysis of enzymes involved in tetrapyrrole biosynthesis. RNA and protein samples were extracted from leaves of 3-week-old 35SFC2, 35SFC2-CFP, FusB and wild-type plants. *GSA1: Glutamate-1-semialdehyde aminotransferase*; *HEMA1*/*HEMA2*: encoding Glutamyl-tRNA reductase; *CHLI1*: encoding Mg chelatase subunit I; *CHLD*: Mg chelatase subunit D; *GUN4*: *Genomes uncoupled 4*; *CHLM*: Mg-protoporphyrin IX methyltransferase; *PORA*: protochlorophyllide oxidoreductases A and B; *CHLM*: Mg-Proto IX methyltransferase; *HO1*: *Heme oxygenases 1*. (C-D) Chlorophyll and heme contents in 35SFC2, 35SFC2-CFP, FusB as well as wild-type seedlings. Error bars indicate standard deviations (n≥3).

3.2.2.3 35SFC2-CFP and FusB plants exhibited impaired PSII complexes assembly in comparison to 35SFC2 and wild-type seedlings.

It has been demonstrated that a defective *FC2* expression resulted in an impaired assembly of photosynthetic complexes (Scharfenberg et al., 2015; Espinas et al., 2016). The *in vitro* FC activity assay suggested that the three FC2 expression mutants may potentially produce extra heme for photosynthetic activities in chloroplasts. Key proteins involved in photosynthesis were examined in 35SFC2, 35SFC2-CFP, FusB and wild-type plants by western blotting. In accord with the reduced chlorophyll contents, LHC proteins (LHCA1, LHCB1 and LHCB5) showed diminished accumulations in the three FC2 overexpression mutants compared to wild type (Figure 3.34A). Despite of the wild-type-level AtpB protein content, 35SFC2, 35SFC2-CFP and FusB seedlings displayed slightly more D1 and Cytf protein accumulation compared to the wild-type control (Figure 3.34A).

Cytf is a hemoprotein and belongs to the Cytochrome b6f complex (Baniulis et al., 2008). Its accumulation could be attributable to the increased prosthetic group, i.e. FC2-producing heme. D1 is an essential subunit involved in PSII core complex. A PSII core complex consists of D1, D2, CP43, CP47 and a heme-binding enzyme, Cytochrome b559 (Cytb559) (Nixon et al., 2010; Nickelsen and Rengstl, 2013). A mutation of the axial heme ligands of Cytb559 suggested that lack of proper coordination of heme destabilizes the PSII reaction-center proteins D1 and D2 (Pakrasi et al., 1991). In other words, more FC2-producing heme may potentially stabilize the PSII reaction-center in FC2 overexpression plants, leading to an increased accumulation of D1.

Moreover, thylakoid complexes in 35SFC2, 35SFC2-CFP, FusB and wild-type leaves were examined by a BN-PAGE gel. Solubilized thylakoid complexes of 35SFC2 plants revealed a similar migration pattern in comparison to wild type, except for a slightly alleviated accumulation of LHCII trimer. Both 35SFC2-CFP and FusB plants, nevertheless, exhibited severely diminished assembly of PSII-LHCII supercomplexes (complexes II) in comparison to 35SFC2 and wild-type plants. Meanwhile, the migration bands representing complex V (PSI monomer/PSII dimer) and complex VI (PSII monomer /Cytb6f complex) accumulated in both lines, which could be products from dis-assembled PSII-LHCII supercomplexes (Figure 3.34B).

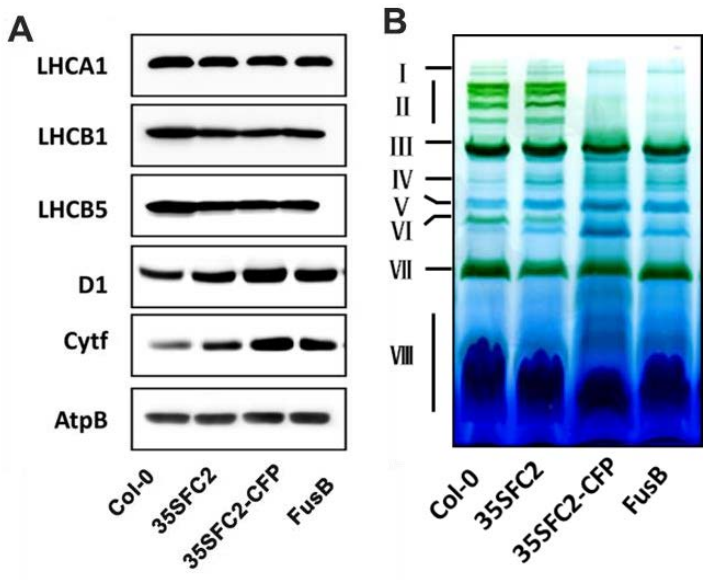

Figure 3. 34 Examination of photosynthetic machineries in the FC2 overexpression lines.

(A) Western blot analysis of photosynthesis proteins from wild-type and 35SFC2, 35SFC2-CFP, FusB plants. LHCA1/ LHCB1/ LHCB5: Light-harvesting proteins; D1: a major subunit of PSII core complex; Cytf: Cytochrome f, heme-binding protein from cytochrome b6f complex, AtpB: β subunit of ATP synthase. (A) BN-PAGE analysis of photosynthetic complexes in thylakoid membranes isolated from 35SFC2, 35SFC2-CFP, FusB and wild-type leaves. Solubilized thylakoid membranes were separated on a BN-PAGE gel. Predominant photosynthetic complexes were indicated on the left: (I) PSI-NDH megacomplex; (II) PSII-LHCII supercomplexes; (III) PSI and PSII dimer; (IV) ATP synthase; (V) PSII monomer and Cytochrome b6f complex; (VI) CP47 less complex; (VII) LHCII trimer; (VIII) free proteins.

As PSI monomer/ PSII dimer and cytochrome b6f/ PSII monomer co-migrate and could not be separated under the BN-PAGE condition applied, the resolved photosynthetic proteins were further separated on a SDS-PAGE gel in a second dimension. The Coomassie-stained gels revealed that main PSII subunits in 35SFC2 leaves displayed wild-type-like distributions, while in the PAGE gels, 35SFC2-CFP and FusB thylakoids did not show accumulation of PSII-LHCII supercomplexes (Figure 3.35). Instead, protein contents of PSII main subunits, i.e. D1, D2, CP43 and CP47 were increased in 35SFC2-CFP and FusB plants in other PSII-containing complexes (PSII dimer, PSII monomer and CP43 less complex) compared to 35SFC2 and wild-type plants.

Furthermore, immunoblot analysis of the second dimension gels with an α-D1 antibody confirmed the visualized distributions of D1 in all FC2 expressing mutants as well as wild-type seedlings. D1 protein in Col-0 and 35SFC2 thylakoid extracs accumulated mainly in complex II, III, V and VI. However, the protein could be only detected in complex III, V and VI in both 35SFC2-CFP and FusB thylakoids, lines with expression of modified FC2 proteins. Taken all together, examination of photosynthetic complexes in the three FC2 expressing plants and wild-type seedlings revealed that disruptions in FC2 C-terminus,

particularly CAB domain, mainly affected the assembly and connection of LHC antenna to reaction center complexes rather than the assembly of PSI and PSII core complexes. These results were in consistence with the characterization of *fc2-2* mutant, which accumulated relatively higher amounts of LHC proteins to reaction center subunits (Espinas et al., 2016).

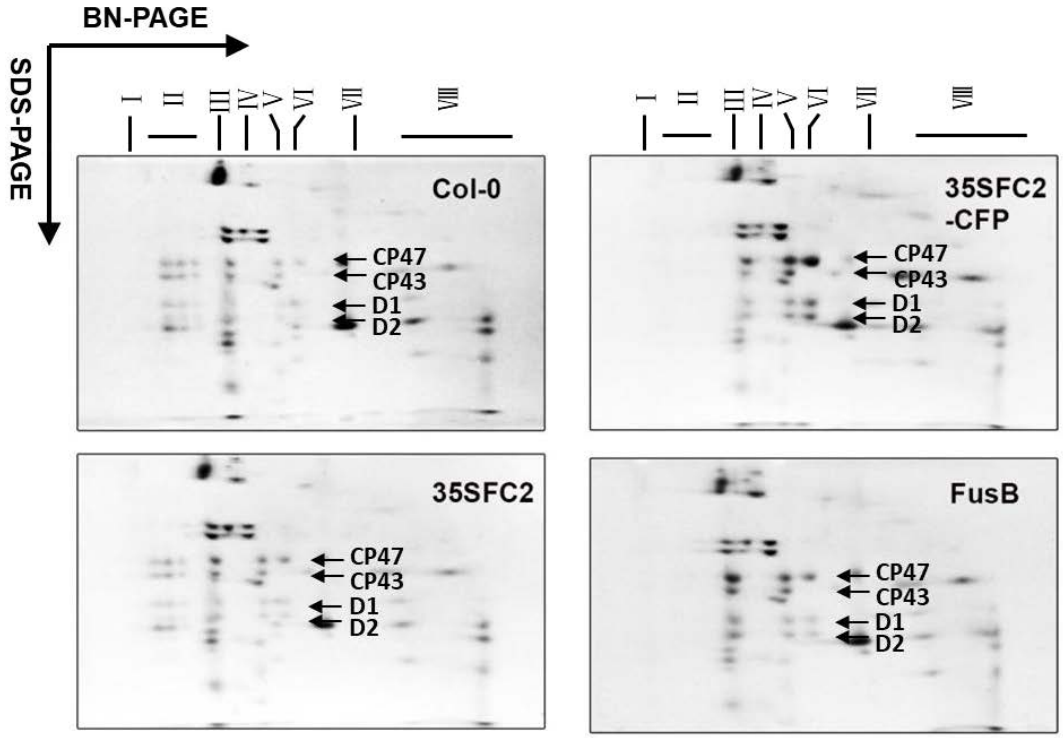

Figure 3. 35 Second dimension analysis of thylakoid complexes.
Solubilized 35SFC2, 35SFC2-CFP, FusB and wild-type thylakoids were firstly separated by a gradient BN-PAGE gel. Multiple photosynthetic proteins were then uncoupled by SDS-PAGE analysis. The protein spots were eventually detected by Coomassie staining. (I) PSI-NDH megacomplex; (II) PSII-LHCII supercomplexes; (III) PSI and PSII dimer; (IV) ATP synthase; (V) PSII monomer and Cytochrome b6f complex; (VI) CP43 less complex; (VII) LHCII trimer; (VIII) free proteins. Subunits of PSII core complex (D1, D2, CP43 and CP47) were indicated with arrows.

Figure 3. 36 Distributions of D1 protein in 35SFC2, 35SFC2-CFP, FusB thylakoid membranes.

Thylakoid proteins of 35SFC2, 35SFC2-CFP, FusB and wild-type plants were separated by a two-dimension analysis. The resolved proteins were immunochemically analyzed by employing an α-D1 antibody. Predominant photosynthetic complexes were indicated: (I) PSI-NDH megacomplex; (II) PSII-LHCII supercomplexes; (III) PSI and PSII dimer; (IV) ATP synthase; (V) PSII monomer and Cytochrome b6f complex; (VI) CP47 less complex; (VII) LHCII trimer; (VIII) free proteins.

3.3 Complementation studies of the Arabidopsis *fc1* mutant substantiate essential functions of FC1 during embryogenesis and salt stress

3.3.1 Deficiency of *FC1* in Arabidopsis perturbs embryo development.

For Arabidopsis *fc1* mutants, both knockdown and knockout mutants are available. A *fc1* knockdown mutant (*fc1-1*) has a T-DNA insertion located in 5'-untranslated region (UTR), which showed no visible phenotype under different growth conditions (Scharfenberg et al., 2015). In the *fc1* null mutant (*fc1-2*), the T-DNA copy is located in the 3rd exon of *FC1* genomic sequence (Fig. 3.37A). Woodson et al. (2011) suggested that the *fc1* null mutant is likely to be embryo lethal as a homozygous *fc1-2*mutant could not be recovered from the heterozygous parents (Woodson et al., 2011). However, no experimental evidence for embryo lethality or experimental analysis data of a *fc1* knockout mutant could be provided. Subsequently, Scharfenberg et al. (2015) suggested a different reason for embryo lethality of the *fc1-2* phenotype. By backcrossing *fc1-2* heterozygous plants to wild type, the authors found a sulfonamide resistance ratio of 94% among the resulted progenies. This led to the assumption that an additional T-DNA insertion might cause the embryo lethality (Scharfenberg et al., 2015). A third explanation was given by Espinas et al. (2016) who observed that few *fc1-2* homozygotes could indeed germinate on MS medium with sugar. Anyhow, the growth of the *fc1-2* mutants was severely retarded and the seedlings died occasionally after germination. Thus, the authors suggested that *FC1* may play an important role in newly emerging tissues rather than affecting embryogenesis (Espinas et al., 2016).

To characterize the physiological functions of FC1 during embryogenesis, heterozygous seedlings of the *fc1* null mutant, designated *fc1-2* (GK_110D_02), were genetically reanalyzed. The T-DNA insertion was confirmed by genotyping (Figure 3.37). When seeds were grown on soil, only wild-type (*FC1/FC1*) and heterozygous (*FC1/fc1*) individuals were identified. The segregation of 88 *fc1-2* progenies revealed 59 heterozygous and 23 wild-type progenies, suggesting a 2:1 ratio of *FC1/FC1:FC1/fc1* seedlings. None of the analyzed seedlings carried the homozygous mutant allele indicating that loss of *FC1* triggers embryo-lethality.

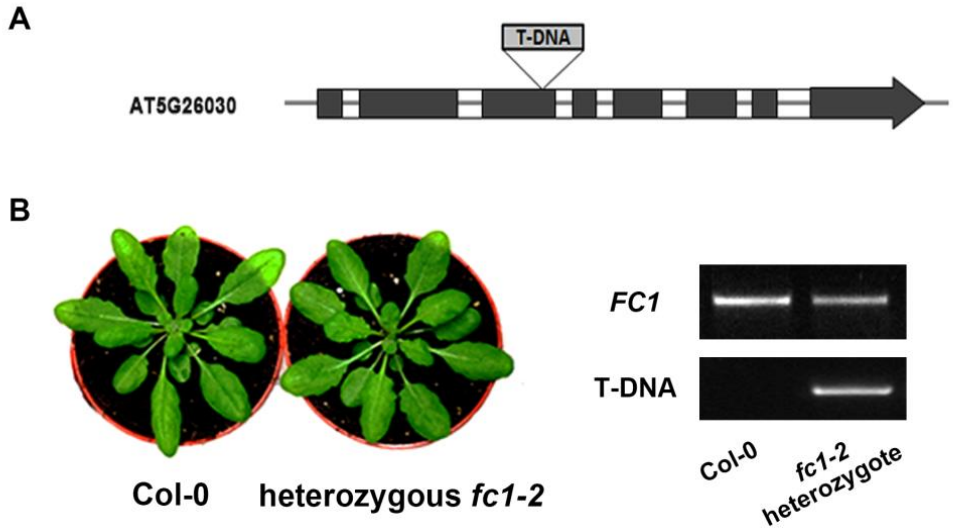

Figure 3. 37 Phenotype of heterozygous *fc1-2* plants.
(A) The scheme of T-DNA insertion of the *FC1* (AT5G26030) loci. Introns (white boxes), exons (black boxes) are indicated. (B) Pictures of 5-week-old heterozygous *fc1-2* seedling and comparable wild type (left panel). Genotyping analyses of the plants from left panel (right panel).

To verify these primary findings, siliques of both heterozygous *fc1-2* and wild-type plants were dissected at different developmental stages and examined under the light microscope. Up to 7 days after pollination (DAP), mutant and wild-type seeds displayed the same growth showing no visible differences in siliques development. At 16 DAP, seeds with different pigmentation could be distinguished. During continuous ripening of seeds, the white seeds converted into dark brown and shrunken seeds, while normal developing seeds matured at 22 DAP (Figure 3.38).

As the first visible distinction among the seeds was observed at 16 DAP, the number of abnormal seeds in *fc1-2* heterozygote siliques were counted. The segregation revealed 52 either white or shrunken seeds among in total 192 seeds indicating 27% of abnormal seeds relative to a mixture of heterozygous mutant and homozygous wild-type seeds. This ratio supports the hypothesis that a defective FC1 expression during seed development may cause a lethal phenotype.

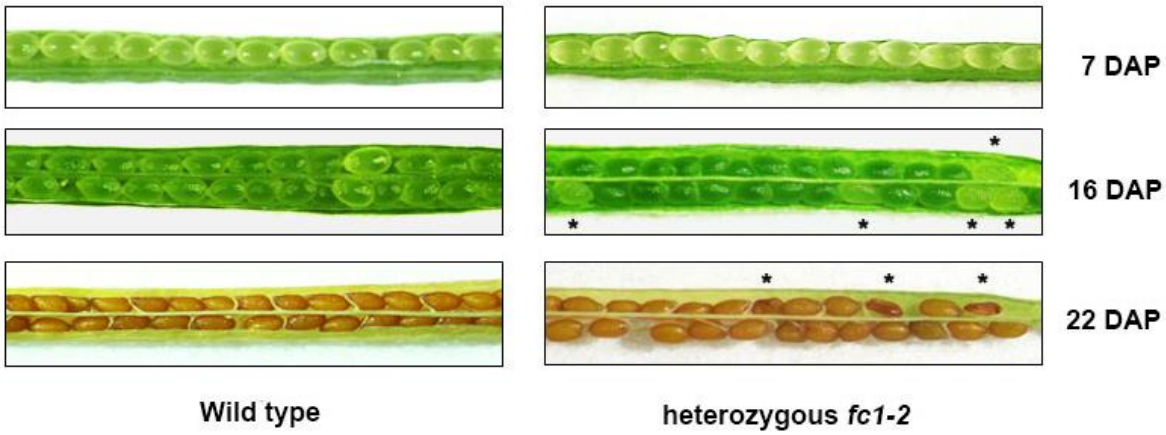

Figure 3. 38 Examination of heterozygous *fc1-2* and wild-type siliques under light microscopy.

Siliques from wild-type and heterozygous *fc1-2* plants at 7 DAP, 16 DAP and 22 DAP were observed under light microscope. At 16 DAP a population of mutant seeds was observed in *fc1-2* heterozygote silique, then the white seeds turn shrunken and abnormal brown at 22 DAP compared to wild-type seeds. Mutant seeds are indicated with asterisks.

In Arabidopsis, two development phases compose of embryogenesis, i.e. morphogenesis and maturation. During morphogenesis phase, the basic body plan of the seedling is established, whereas the embryo undergoes cell expansion and accumulates storage macromolecules for subsequent germination during maturation (Park and Harada, 2008). To further assess at which experimental stage the mutant embryogenesis is perturbed, the embryo developmental processes in wild-type and *fc1/fc1* seeds were examined by differential interference contrast microscopy (DIC). During the early developmental stages, up to the heart stage, no significant morphological differences were observed between wild-type and mutant embryos (Figure 3.39 A-C and F-H). However, at 10 DAP, when the majority of embryos continued the maturation towards mid-torpedo stage, some embryos showed delayed development (mid-torpedo versus early-torpedo) in heterozygous *fc1-2* siliques (Figure 3.39 I and D). At the end of embryo development, the wild-type-like embryos reached the mature green stage at 14 DAP with the cotyledons entirely filled the seed sacs, whereas mutant embryos were ultimately arrested in the premature stages and did not reach the mature green stage (Figure 3.39J and L). From this observation, it can be concluded that the aborted embryos display the *fc1/fc1* phenotype. In the mutant seeds, either the embryos are arrested or its development will be delayed after mid-torpedo stage. This reveals that FC1 plays an important role in embryogenesis, particularly during maturation, which function cannot be compensated by *FC2* expression in wild type.

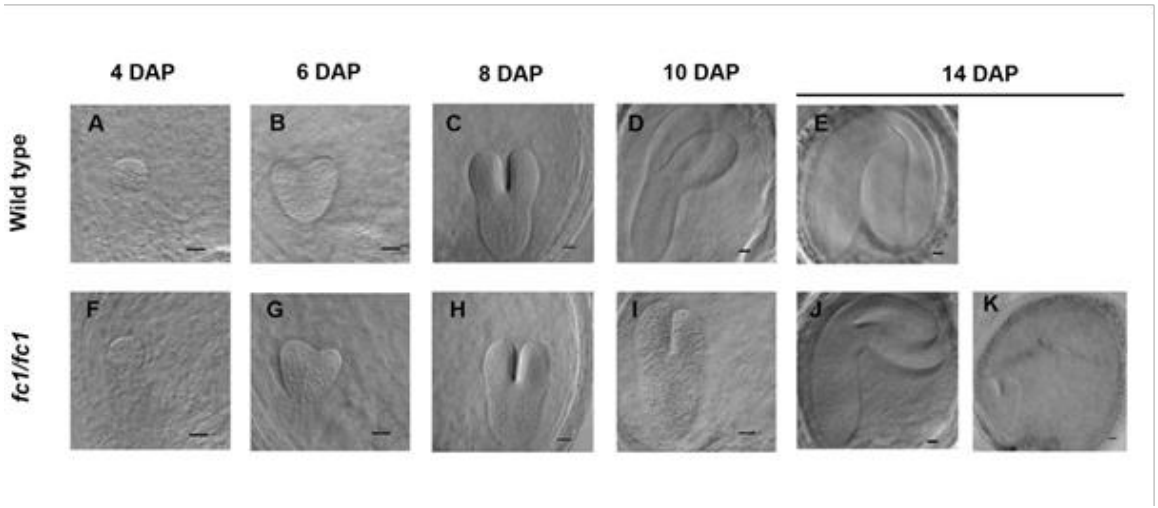

Figure 3. 39 Homozygous *fc1/fc1* embryo development is arrested in seeds of heterozygous *fc1-2* plants.

Embryogenesis in wild-type and homozygous *fc1* seeds was monitored by differential interference contrast microscopy. (A-E) Embryos from the globular to the mature green stage in wild-type ovules: (A) globular stage (at 4 DAP); (B) heart stage (at 6 DAP); (C) early-torpedo stage (at 8 DAP); (D) mid-torpedo stage (at 10 DAP); (E) mature green stage (at 14 DAP). (F-H) Embryos in *fc1-2* ovules developed normally from the globular to the early-torpedo stage. (I) Delayed development of homozygous *fc1-2* embryos relative to wild-type embryos (D) was observed at 10 DAP. (J-K) Delayed embryo development at 14 DAP, when putatively homozygous *fc1-2* embryos are stalled in the early and late torpedo stage while wild-type embryos reached the mature green stage of bend cotyledons (E). Bars = 20μm.

Apart from the observation of aberrant development of *fc1/fc1* embryos, among heterozygous *fc1-2* progenies, two abnormal sizes of seeds could be observed in addition to wild-type seeds, which likely correlates with the perturbations during embryogenesis (Figure 3.40A). Successfully dissected embryos from type #1 dry seeds indicated much smaller growth size compared to wild type (Figure 3.40B). Derived from the phenotypes, the smallest seeds (type #2) are speculated to be the malfunctioning mutant seeds aborted at the torpedo stage, while seeds with an intermediate size (type #1) between wild-type and type #2 seeds may be characterized by a postponed embryo development, which will be terminated at the final cotyledon stage. When grown both defective seeds on MS media with 1% sugar, a few of the type #2 seeds occasionally germinated but died after several days, while the more severely impaired seeds did not germinate on sugar-containing MS plates (Figure 3.40C). These observations were in agreement with the previous report on germination of homozygous *fc1-2* seeds (Espinas et al., 2016). By genotyping, knockout of *fc1* could be confirmed for the occasionally germinated type #1 seedlings, while the wild-type-like seeds resulted in seedlings carrying FC1 alle including both wild type and heterozygous *fc1-2*. Thus, it can be concluded that a *fc1* null mutation results in both type #1 and type #2 seeds, which is attributable to the two possible perturbations of embryo development respectively.

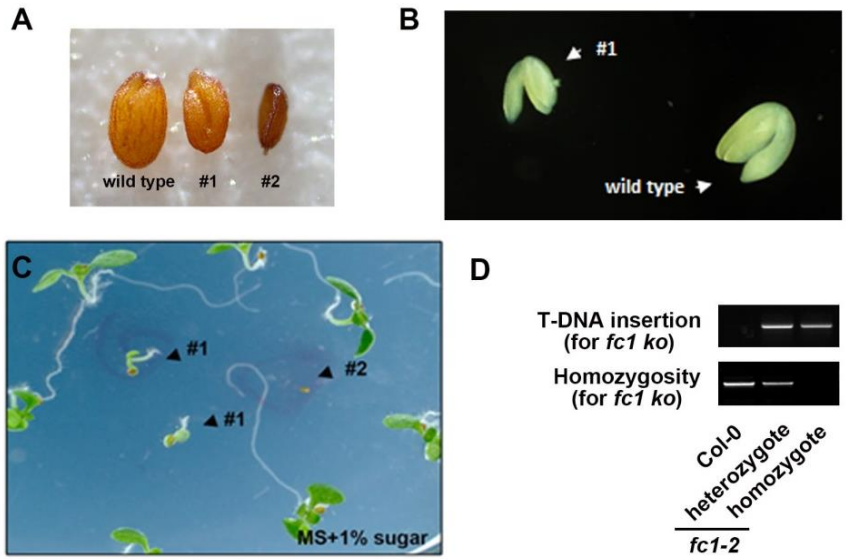

Figure 3. 40 Examination of heterozygous *fc1-2* progenies by light microscopy.
(A) Mature dry seeds of *fc1-2* heterozygous plants. At the end of seed maturation, siliques contained in addition to wild-type seeds two abnormally sized seeds which are designated type #1 and #2. (B) Embryos dissected from dry seeds. Type #1 seeds contain smaller embryos than wild-type seeds. (C) Germination of seeds from a heterozygous *fc1-2* plant on MS medium supplemented with 1% sucrose. Apart from normally developing seedlings, seedlings exhibiting developmental arrest and non-germinating seeds (tentatively identified as type #1 and #2, respectively) were observed. These mutant seeds are marked by arrowheads. (D) Genotyping analyses of progenies of heterozygous *fc1-2* plants germinated on MS plates with sugar.

3.3.2 *FC1* is expressed at different embryo developmental stages, with higher transcript accumulation compared to *FC2*.

In order to characterize the function of FC in Arabidopsis, particularly during embryogenesis, transgenic lines carrying a *GUS* reporter gene fused to *FC1* promoter sequence (pFC1::GUS) was generated by employing a 1670 bp genomic sequence upstream of Arabidopsis FC1 translation start site. With three individual *pFC1::GUS* lines, the expression pattern of *FC1* in different organs and developmental stages was detected (Figure 3.41A-E). As a result, GUS activity was detectable in leaves, in roots, and in flower organs. Additionally, *FC1* was also expressed through all the embryo developmental stages, such as globular stage, torpedo stage, bent-cotyledon and mature green stage (Figure 3.41F-I).

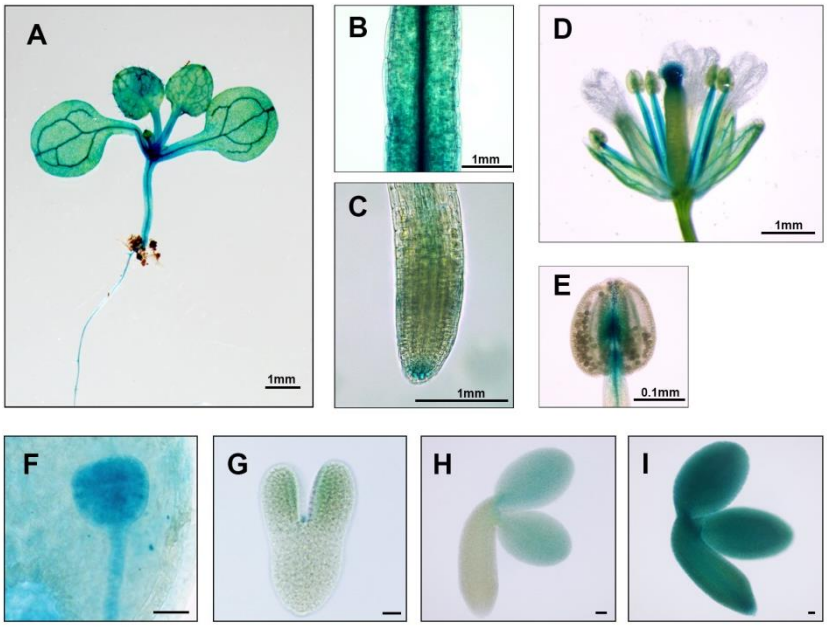

Figure 3. 41 Expression patterns of FC1 gene at different stages and in various organs.

(A-E) Expression pattern of *pFC1::GUS* in different plant organs: (A) seedling; (B) stem; (C) root; (D) flower; (E) anther. (F-I) Expression pattern of *pFC1::GUS* in embryos at different developmental stages: (F) globular stage; (G) torpedo stage; (H) bent cotyledon stage; (I) mature green stage. Scale bars are indicated, and bars= 20 μm in F-I.

Besides *FC1*, expression of *pFC2::GUS* was also monitored during embryo development, such as late-torpedo and mature green stages (Figure 3.42). Unequivocal evidence for *pFC2::GUS* expression prior to these stages could not be obtained, as the reporter was highly expressed in the seed coat during early embryo development (Figure 3.42D).

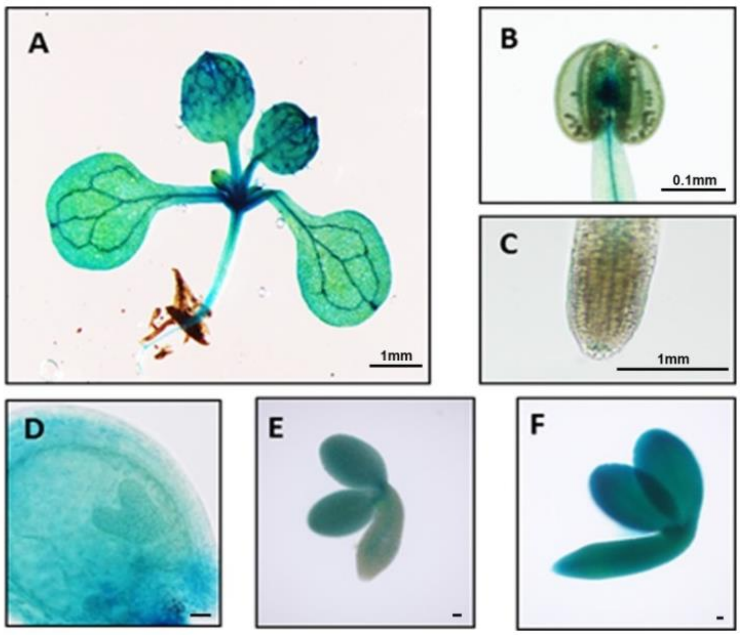

Figure 3. 42 Histochemical analysis of *pFC2::GUS* expression at different developmental stages.

Expression pattern of *pFC2::GUS* in different plant organs: (A) seedling; (B) anther; (C) root; (D-F) embryos. Expression of *pFC2::GUS* is also detected during embryo development, such as in the late torpedo (E) and mature green stage with bent-cotyledons (F). As *pFC2::GUS* is also expressed in the seed coat during early seed developmental stages (shown for heart stage in D), unequivocal assessment of *FC2* expression levels during early stages of embryogenesis is not possible. Scale bars are indicated, and bars = 20 μm in D-F.

Furthermore, to better quantify the relative expression of the two *FC* genes, accumulation of both transcripts in embryos, flowers, roots and leaf tissues was determined by qRT-PCR analysis (Figure 3.43). The result indicated *FC2* showed obvious higher expression in leaves compared to other tissues, and *FC1* transcript accumulated at similar levels in roots and leaves. The data is in accord with the previous assumption that *FC2* plays the dominant FC activity in leaves while *FC1* serves the main heme pool in root (Singh et al., 2002; Nagai et al., 2007; Scharfenberg et al., 2015). Additionally, the expression of the two *FC* genes at different embryo developmental stages was investigated. By applying RNA from embryos at early- and late-torpedo stages, as well as mature green stage, both *FC* transcripts were assessed. The results suggested a comparable accumulation of *FC1* mRNA in embryos compared to root and leaf tissues, while its expression remarkably increased at mature green stage, which is the final stage of embryo development. In contrast, the *FC2* transcript, which predominates in the leaf tissues, showed much lower accumulation at both torpedo stages as well as mature green stage. The varied expression profiles of the two *FC* genes suggested that *FC1* may play the major role in serving the heme pool for embryo development.

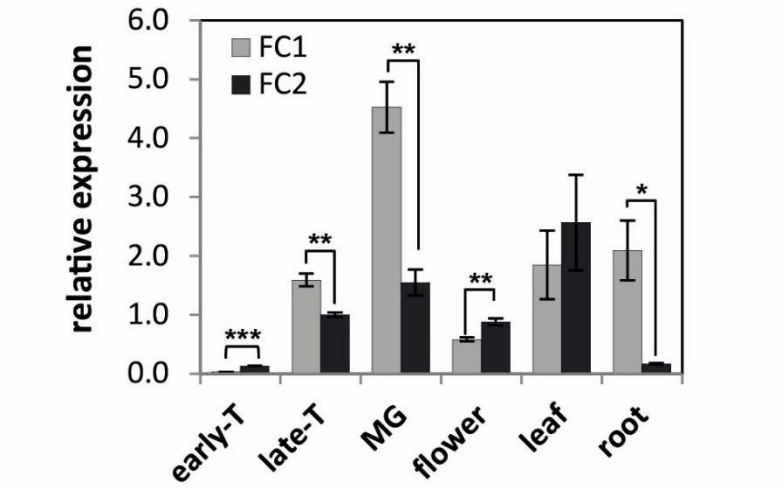

Figure 3. 43 qRT-PCR analysis of *FC1* and *FC2* transcript accumulation in different organs.

Embryo RNA samples were extracted at the early-torpedo (early-T), late-torpedo (late-T) and mature green (MG) stages. Expression data were normalized relative to *ACTIN2* (AT3G18780). Error bars indicate standard deviations. Asterisks represent significant difference; * P value < 0.05, ** P value < 0.01, *** P value < 0.001.

3.3.3 Expression of *FC1* under its native promoter can rescue the embryo lethality of *fc1-2*.

To obtain further indications for the essential *FC1* function during embryogenesis and to demonstrate the malfunction in embryos as results of the loss of *FC1*, a complementation approach of the *fc1* null mutant was performed. The *fc1-2* heterozygous mutants were transformed by *Agrobacterium tumefaciens* which contain a gene construct consisting of a genomic *FC1* sequence with its own promoter (pFC1FC1, *pFC1::FC1*). Genotyping analysis identified the complemented lines pFC1FC1 (*fc1/fc1)*. Their progenies contained no wild type but only *fc1* mutants with the expression of transgenic *pFC1::FC1*.

The *fc1* seedlings expressing *pFC1::FC1* showed a wild-type-like phenotype (Figure 3.44). Their siliques did not contain abnormal albino seeds, which were frequently observed in siliques of *fc1-2* heterozygous plants (Figure 3.35). As homozygous *fc1-2* plants were not viable, it could be proposed that the defective embryonic phenotype was rescued by *FC1* expression under its native promoter. This proposal was subsequently testified by examining the siliques of pFC1FC1 (*fc1/fc1)* plants, as they did not contain abnormal pale green or shrivelled seeds in comparison to heterozygous *fc1-2* siliques.

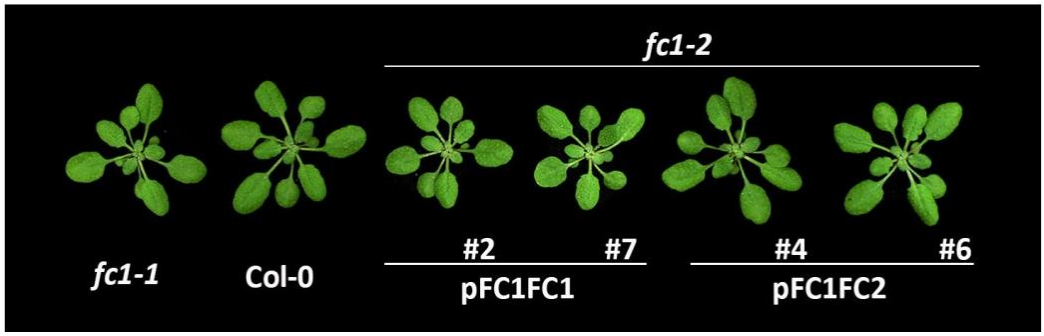

Figure 3. 44 Expression of *FC1* or *FC2* under control of the *FC1* promoter rescues the embryo-lethal phenotype of *fc1-2*.
4-week-old homozygous pFC1FC1 (*fc1/fc1*) and pFC1FC2 (*fc1/fc1*) mutants as well as wild-type Arabidopsis plants were grown under SD condition.

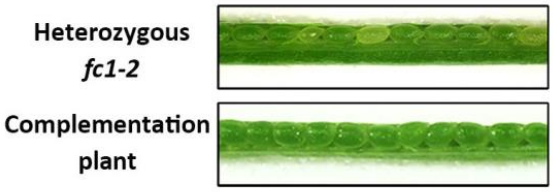

Figure 3. 45 Examination of siliques of *fc1-2* heterozygous and complemented plants.
Siliques from heterozygous *fc1-2* and complemented plants at 16 DAP were examined under light microscope.

3.3.4 *FC2* expression can compensate for the functional loss of *FC1* when driven by a *FC1* promoter.

The two FC isoforms in Arabidopsis are distinguished by the diverse expression profiles as well as their structural variations (Chow et al., 1998; Scharfenberg et al., 2015). To figure out whether FC2 expression can substitute the function loss of *FC1* in Arabidopsis, two different *FC2* expression constructs have been introduced into the *fc1-2* heterozygous mutant background. In both constructs, the full *FC2* genomic sequence was fused to either its original promoter (pFC2FC2, *pFC2::FC2*) or a 1670bp-long *FC1* promoter (pFC1FC2, *pFC1::FC2*). As a result, 2 complementation lines were identified from 8 individual pFC1FC2 transformants and used for further studies (Figure 3.44). In contrast, no successful complementation of the *fc1* null mutants could be obtained among 56 analyzed pFC2FC2 transformants. The results indicated that the FC2 expression contributes to rescue the *fc1-2* mutants, only when the transcription is driven by the *FC1* promoter. In addition, complementation of *fc1-2* was also attempted with a *FC1* gene construct driven by the *FC2* promoter (pFC2FC1, *pFC2::FC1*). 21 pFC2FC1 transformants were obtained in the heterozygous *fc1-2* mutant background in the T1 generation. Six transgenic pFC2FC1 T1 plants were selected for analysis of T2 generation. Twenty-four T2 progenies from each line were harvested for genotyping. The results revealed none of the progenies was in a

fc1 null mutant background indicating that complementation of *fc1-2* mutant was failed by *pFC2::FC1* expression.

The successful complementation of pFC1FC2 (*fc1/fc1)* has been firstly confirmed by genotyping analysis using specific primer pairs for T-DNA insertion of *fc1-2* and the intact *FC1* gene (Figure 3.46). By applying the two FC antibodies, the absence of FC1 protein, as well as increased FC2 expression, were confirmed in the pFC1FC2 (*fc1/fc1)* seedlings.

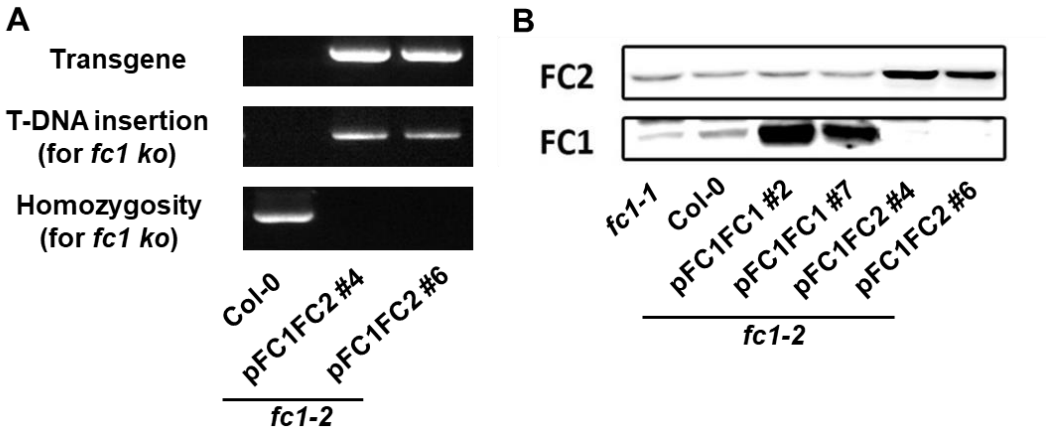

Figure 3. 46 Genetic and western blot analysis of *fc1-2* complemented lines and wild-type plants.

(A) Genomic DNA was extracted from pFC1FC2 (*fc1/fc1*) #4 and #6 plants as well as comparable wild type seedlings. Genotyping PCR was performed by applying primer pairs indicated in Appendix 1. (B) Total proteins were isolated from 3-week-old complemented *fc1-2* and *fc1-1* mutants, as well as Col-0 plants. α-FC1 and α-FC2 antisera were used for immunoblot analysis.

Under standard growth conditions, pFC1FC2 (*fc1/fc1)* complementation lines grew wild-type like. As FC (FC1 and FC2) catalyzes heme formation in TBS pathway, the steady-state levels of TBS intermediates and end products were determined in both pFC1FC1 (*fc1/fc1)* and pFC1FC2 (*fc1/fc1)* plants via HPLC analysis (Figure 3.47 and Figure 3.48). The 2 representative pFC1FC2 (*fc1/fc1)* lines accumulated wild-type level of MgProto, chlorophyll and heme, which could also be observed in the pFC1FC1 (*fc1/fc1)* complemented plants. However, the *fc1-1* mutants accumulated less heme despite of the wild-type-like chlorophyll accumulation. These results argue for the complete complementation of *fc1-2* by both FC1 and FC2 expression under the *FC1* promoter under standard growth conditions.

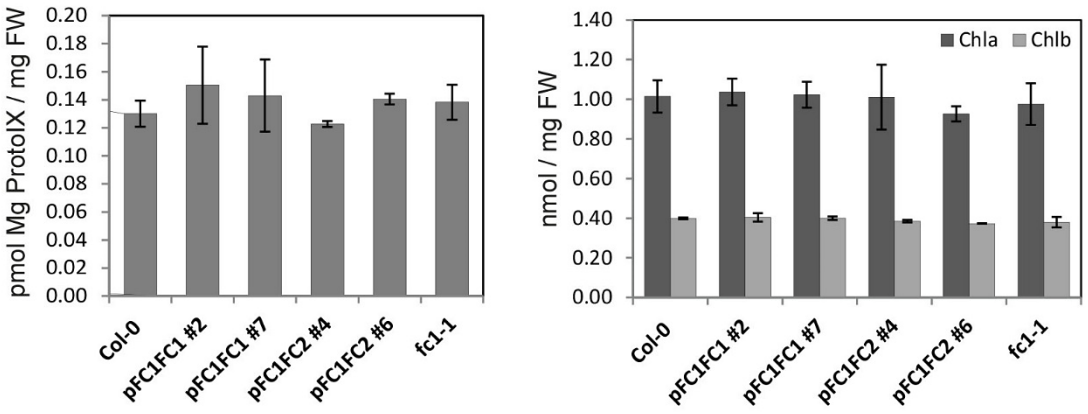

Figure 3. 47 Determination of MgProto and chlorophyll contents in wild type and *fc1-2* complemented plants.

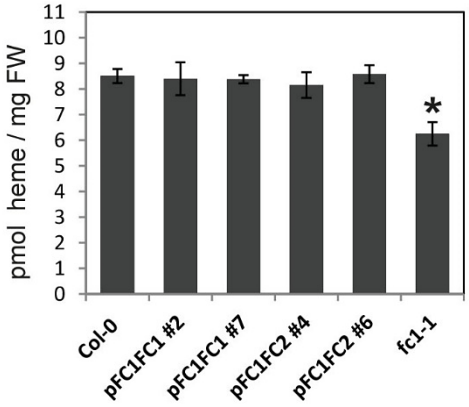

Figure 3. 48 Heme contents in the complemented *fc1-2* mutants.
Accumulation of intermediates (MgProto) and end-products (chlorophyll and heme) of TBS in complemented and control seedlings. For HPLC analyses, leaves from 3-week-old *fc1-1*, *fc2-1* complemented seedlings as well as wild type were used. Error bars indicate standard deviations (n≥3). Asterisks represent significant difference; * P value < 0.05.

In addition, transcripts and protein levels of TBS enzymes as well as LHCPs, were investigated in the pFC1FC1 (*fc1/fc1)* and pFC1FC2 (*fc1/fc1)* complemented lines in comparison to the control seedlings. By qRT-PCR analysis with specific primers, knockout of *FC1* was again verified in the pFC1FC2 (*fc1/fc1)* plants (Figure 3.49). The increased *FC2* transcripts were in correlation with the accumulated protein amounts (Figure 3.46). qRT-PCR analysis of most TBS enzymes revealed no detectable alterations, except for transcripts of *CHLI* and *PORA*, which exhibited slight but significant changes in both complemented lines. This result indicated that modifications of FC expression may affect the expression of genes involved in chlorophyll biosynthesis.

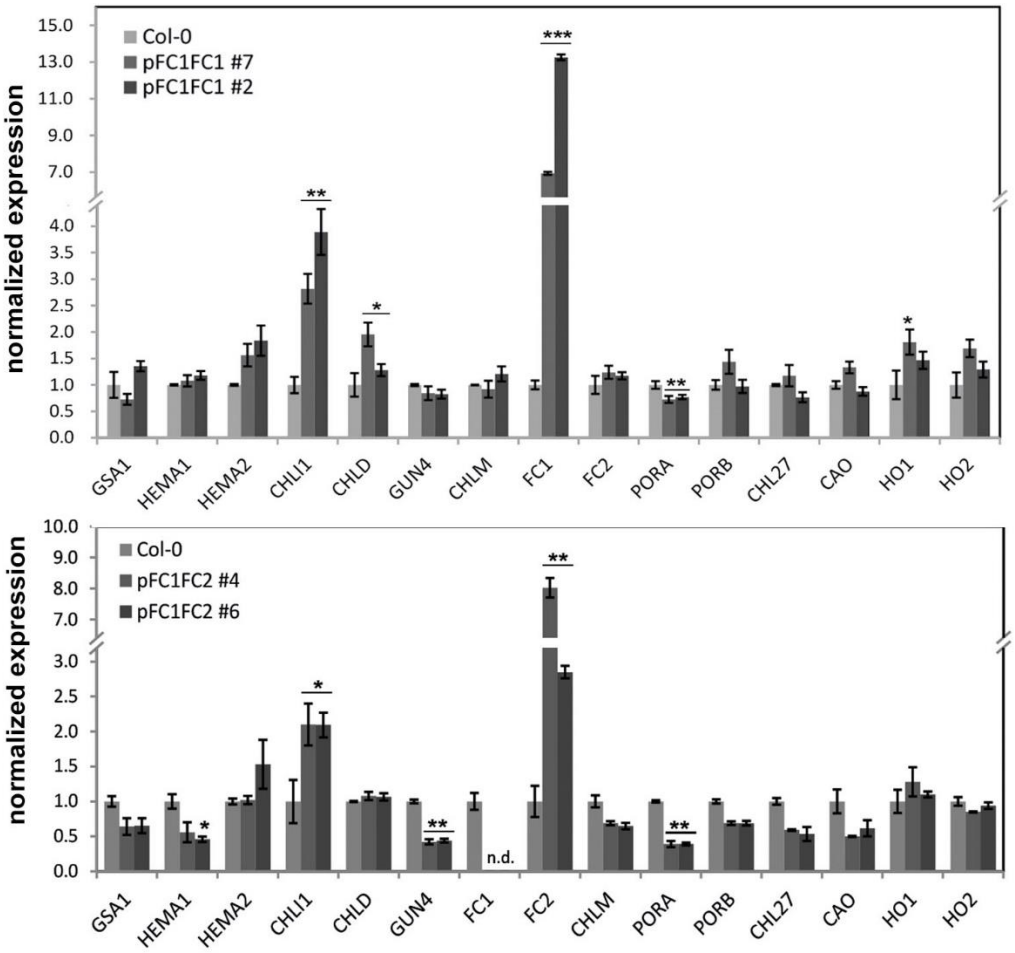

Figure 3. 49 qRT-PCR analysis of genes encoding enzymes involved in tetrapyrrole biosynthesis.

RNA samples were extracted from leaves of 3-week-old pFC1FC1 (*fc1/fc1*), pFC1FC2 (*fc1/fc1*) and wild-type plants. *FC1/FC2: ferrochelatases 1* and *2*, *GSA1: glutamate-1-semialdehyde aminotransferase*; *HEMA1*/*HEMA2*: encoding glutamyl-tRNA reductase; *CHLI1*: encoding Mg chelatase subunit I; *CHLD*: Mg chelatase subunit D; *GUN4*: *Genomes uncoupled 4*; *CHLM*: Mg-protoporphyrin IX methyltransferase; *PORA/PORB*: protochlorophyllide oxidoreductases A and B; *CHL27*: encoding Mg-protoporphyrin IX-monomethylester cyclase; *CAO*: *Chlorophyll a oxygenase*; *HO1/HO2*: *Heme oxygenases 1* and *2*. Error bars indicate standard deviations (n≥3). Asterisks represent significant difference; * P value < 0.05, * *P value < 0.01, *** P value < 0.005.

However, the slightly modified expression of TBS genes did not alter the protein accumulation, as TBS proteins examined in both pFC1FC1 (*fc1/fc1)* and pFC1FC2 (*fc1/fc1)* complemented lines displayed identical accumulation compared to wild type. In addition, LHC proteins in both complemented lines also showed wild-type amounts in consistence with the unchanged chlorophyll contents.

Elevated FC protein contents have the potential to modulate the synthesis of heme. As heme availability is expected to have a regulatory impact on the rate-limiting step in ALA synthesis, ALA synthesis rates of both *fc1-2* complemented lines as well as *fc1-1* mutants

were determined by an *in vitro* assay. However, no alterations in the ALA synthesis rate were observed in 5-week-old *fc1-1* mutants as well as the *fc1-2* complemented plants (Figure 3.50B).

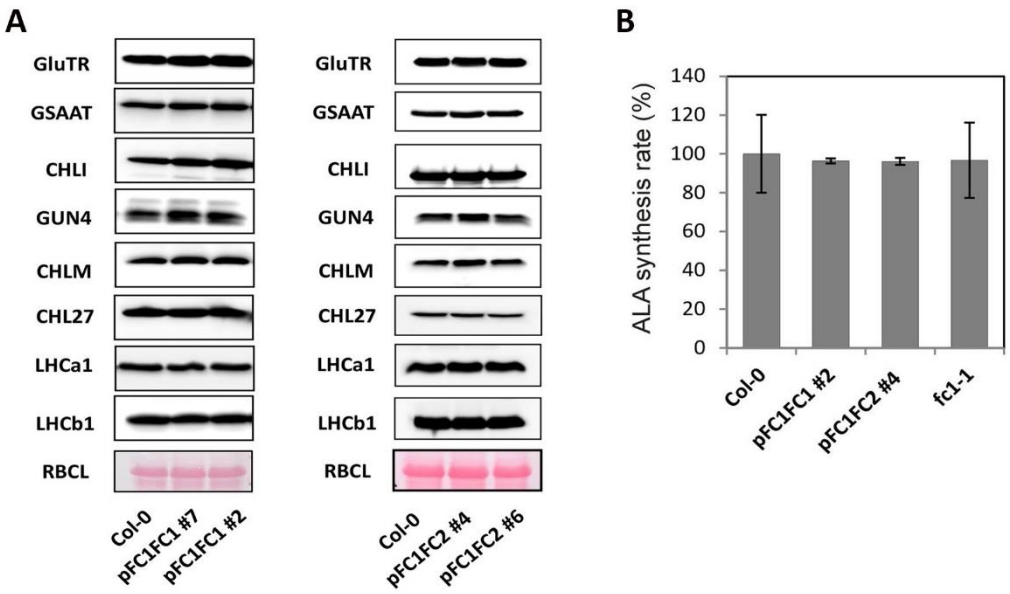

Figure 3. 50 Accumulation of TBS proteins and ALA synthesis rates in *fc1-2* complemented plants.

(A) Accumulation of proteins involved in the TBS pathway as well as light harvesting. Protein samples were extracted from leaves of 3-week-old pFC1FC1 (*fc1/fc1*), pFC1FC2 (*fc1/fc1*) complemented seedlings and wild-type plants. GluTR: Glutamyl-tRNA reductase; GSAAT*:* glutamate-1-semialdehyde aminotransferase; CHLI: Mg chelatase subunit I; GUN4: genomes uncoupled 4; CHLM: Mg-protoporphyrin IX methyltransferase; CHL27: Mg-protoporphyrin IX-monomethylester cyclase; LHCa1/LHCb1: light-harvesting chlorophyll-binding proteins a1 and b1; RBCL: ribulose 1,5-bisphosphate carboxylase oxygenase, large subunit. (B) Rates of ALA synthesis rates in complemented and wild-type seedlings. Error bars represent standard deviations (n≥3).

In addition, the FC activity for the pFC1FC2 (*fc1/fc1)* lines was also determined to assess FC2 function under the *FC1* promoter (Figure 3.51). By providing adequate amount of the substrate Proto, FC protein in plastid extracts is able to catalyze the insertion of ferrous iron or zinc into Proto. Both zinc and ferrous iron are competitive substrates for FC (Camadro and Labbe, 1982; Abraham et al., 1986; Camadro and Labbe, 1988). However, an *in vitro* activity assay with ferrous iron is technically complex, as it requires an absolutely anaerobic condition to maintain ferrous iron in the reduced state. Therefore, in this study, zinc was applied in cooperation with endogenous Proto. The production of zinc-protophophyrinIX (ZnProto) reflects the ability of FC to utilize Proto to yield protoheme. In the kinetic assay, samples from 5 different time points were collected. Within a 20min-reaction, the ZnProto amount displayed a linear accumulation, indicating a feasible assay system (Figure 3.51A). The results also revealed an increased FC activity in both pFC1FC2 (*fc1/fc1*) #4 and #6 lines, with 2,2-fold and 1,3-fold higher ZnProto production than wild-

type control (Figure 3.51B). This increase is in accord with the elevated FC2 protein amounts (Figure 3.46B).

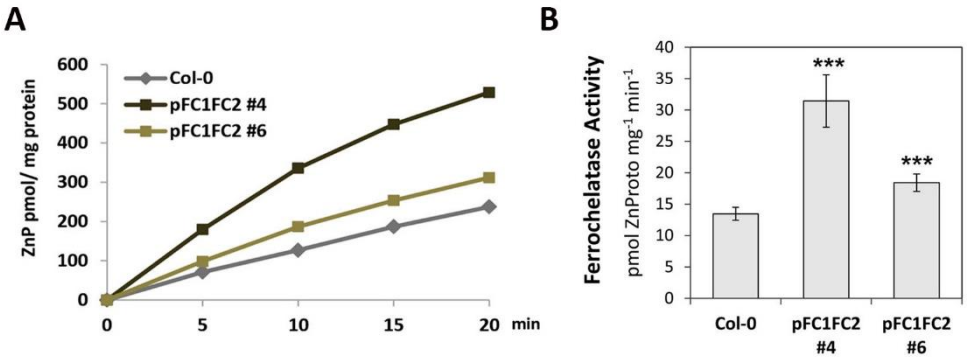

Figure 3. 51 *In vitro* FC activity assay of pFC1FC2 (*fc1/fc1*) plants.
In vitro FC activity from plastid extracts of the two pFC1FC2 (*fc1/fc1*) lines in comparison to wild type. Error bars indicate standard deviations (n>3). Asterisks represent significant differences; *** P value < 0.001.

3.3.5 Lack of FC1 does not impair formation of photosynthetic complexes

It is known that, besides chlorophyll, other pigments and cofactors, heme plays important roles in the assembly of photosynthetic complexes, in photosynthetic electron transport and probably in photoprotection (Nelson and Ben-Shem, 2004; Baniulis et al., 2008; Wei et al., 2016). Cytb559, an essential component of the PSII core complex, is a heme-bridged heterodimeric protein (its α and β subunits are encoded by *PsbE* and *PsbF*). Each subunit of Cytb559 provides a histidine ligand for non-covalently bound heme (Chu and Chiu, 2015). Functional loss of either subunit of Cytb559 leads to destabilization of PSII (Pakrasi et al., 1988; Morais et al., 1998; Swiatek et al., 2003; Suorsa et al., 2004). Moreover, site-directed mutagenesis of the axial heme ligands of Cytb559 revealed that lack of proper coordination of heme destabilizes the PSII reaction center proteins D1 and D2 (Pakrasi et al., 1991).

Arabidopsis FC1-YFP and FC2-YFP overexpression plants were reported to exhibit reductions of chlorophyll accumulation (Woodson et al., 2011). Previous characterization of *fc* mutants also pointed out reduced chlorophyll and carotenoid contents in *fc2* (*fc2-1* and *fc2-2*), but not in *fc1-1* seedlings (Scharfenberg et al., 2015; Espinas et al., 2016). Consistent with these results, the photosynthetic efficiency of PSII in both *fc2* knockdown and knockout mutants are significantly diminished, while a *fc1* knockdown (*fc1-1*) mutant with 30% of wild-type *FC1* transcript maintains wild-type pigment content as well as photosynthetic efficiency (Scharfenberg et al., 2015).

Analysis of the pFC1FC1 (*fc1/fc1*) and pFC1FC2 (*fc1/fc1*) complemented lines also revealed higher accumulation of FC1 or FC2 protein contents compared to control

seedlings (Figure 3.37), although the transgenic lines displayed eventually wild-type heme and chlorophyll accumulation (Figure 3.47 and 3.48).

To examine whether the enhanced FC protein levels or a lack of FC1 compromises the efficiency and assembly of the photosynthetic machineries, the successfully complemented plants (pFC1FC1 and pFC1FC2) were analyzed with respect to their photosynthetic parameters and plastidic membrane-bound protein complexes (Figure 3.52). Thylakoids of 4-week-old wild type, pFC1FC1 (*fc1*/*fc1*) and pFC1FC2 (*fc1*/*fc1*) complemented plants were extracted and solubilized with 1% DDM for 10min. The resolved protein samples were separated by a 4.5-12.5% gradient BN-PAGE gel. The migration of thylakoid complexes in the pFC1FC1 and pFC1FC2 lines revealed wild-type accumulation of PSI and PSII protein complexes, including the supercomplexes as well as the low-molecular-weight protein complexes, such as the CP43-less complex, PSII monomer and PSII dimer (Figure 3.52A). As PSI monomer/ PSII dimer and cytochrome b6f/ PSII monomer comigrate and could not be separated under the BN-PAGE condition employed, key proteins of PSII complexes and cytochrome b6f were analyzed by immunoblotting. The results confirmed the wild-type level of cytochrome b6f and PSII complexes in both *fc1-2* complemented lines, as D1 and PsbE (two subunits of the PSII core complex), as well as cytochrome f (a subunit of cytochrome b6f) displayed an identical accumulation compared to control seedlings (Figure 3.52B). Additionally, the relative quantum yield of chlorophyll fluorescence was determined by Pulse Amplitude Modulation (PAM) measurement. Both pFC1FC1 (*fc1*/*fc1*) and pFC1FC2 (*fc1*/*fc1*) complemented lines exhibited identical Fv/Fm values in consistence with the unchanged accumulation and assembly of photosynthetic complexes (Figure 3.52C).

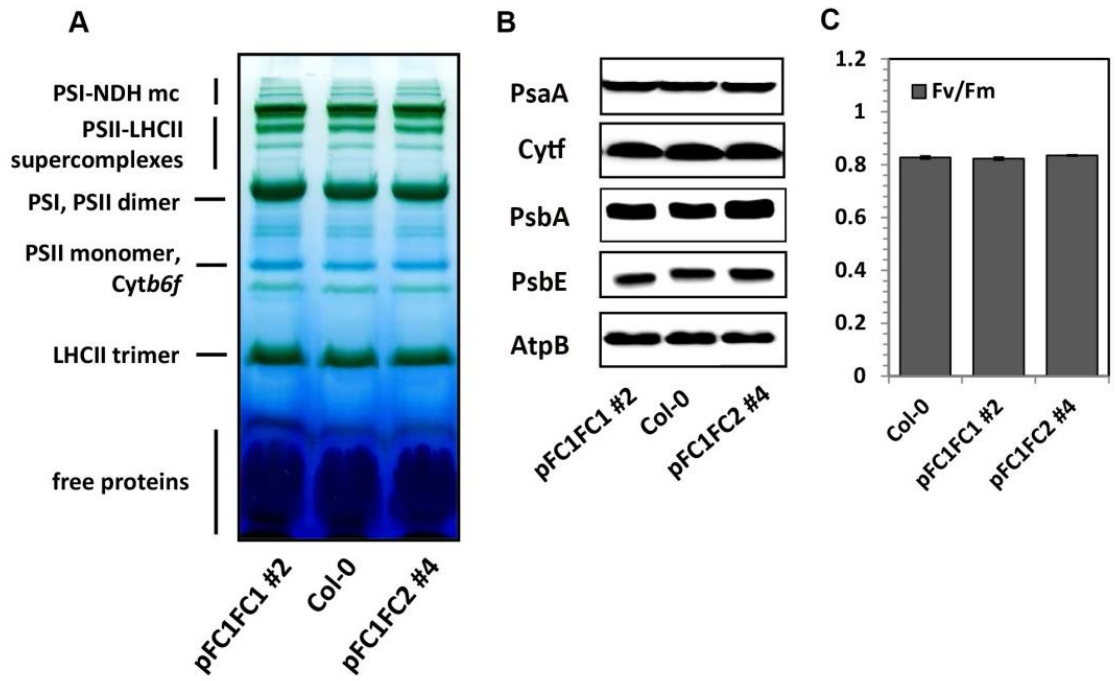

Figure 3. 52 Photosynthetic parameters in the complemented seedlings are restored to normal.

(A) BN-PAGE analysis of photosynthetic complexes in thylakoid membranes isolated from wild-type and pFC1FC1 *(fc1/fc1*), pFC1FC2 (*fc1/fc1*) leaves. (B) Western blot analysis of photosynthesis proteins from wild-type and pFC1FC1 (*fc1/fc1*), pFC1FC2 (*fc1/fc1*) plants. PsaA; main subunit of PSI; Cytf: Cytochrom f, heme-binding protein from cytochrome b6f complex, PsbA: also designated as D1, subunit of PSII core complex, PsbE: a heme-binding protein, β subunit of cytochrome b559, main component of PSII core complex; AtpB: β subunit of ATP synthase. (C) Quantified Fv/Fm values measured with FluroCam 700MF. Error bars represent standard deviations (n≥3).

Based on all the analyses above, it can be concluded that under normal growth conditions, the complete complementation of seedlings in the *fc1-2* background by *FC1* and *FC2* expression under the *FC1* promoter is verified by the analysis of the photosynthesis machineries. Neither accumulation of FC proteins nor a lack of FC1 affects the accumulation and assembly of photosynthetic complexes. Moreover, the transgenic FC2 activity can apparently cater for the needs of the heme-dependent proteins normally supplied by FC1 and thus provides an adequate amount of heme.

3.3.6 FC2 could not substitute FC1 function under salt stress.

According to the previous studies, FC1 has been proposed to play a significant role in stress resistance in Arabidopsis, as its expression is induced by sucrose, wounding, viral infection and oxidative stress (Smith et al., 1994; Chow et al., 1998; Singh et al., 2002; Nagai et al., 2007). Recent studies from Zhao et al. (2017) and Song et al. (2017) both indicated FC1 affects ions uptake in Arabidopsis roots by regulating gene expression (Zhao

et al., 2017; Song et al., 2017). As the two FC are plastid-located proteins, the function of both isoforms in leaf tissues under stress conditions remains unknown.

3.3.6.1 pFC1FC2 (*fc1/fc1*) exhibit early-senescence phenotype under salt stress.

In this study, salinity stress, one of the most common stress conditions, was applied to the *fc1-2* complemented lines as well as FC1 overexpression plants to characterize the functional differences of both FCs in stress tolerance. Detached rosette leaves from 3-week-old 35SFC1-YFP (*p35S::FC1-YFP*), pFC1FC2 (*fc1/fc1*) and wild-type seedlings were incubated in 3mM MES (pH5.8) with or without 250mM/450mM NaCl. As a result, after 72h incubation of the detached mutant and wild-type leaves in the control (mock) solution, both pFC1FC2 (*fc1/fc1*) and 35SFC1-YFP leaves showed no differences compared to wild type. Moreover, incubation of detached leaves in the mock solution did not affect the chlorophyll accumulation but with a similar increase of anthocyanin contents in leaf veins. However, pFC1FC2 (*fc1/fc1*) leaves, compared to both wild-type and 35SFC1-YFP, exhibited an early-senescence phenotype under both 250mM and 450mM NaCl treatments. Especially, after 24h incubation in 450mM NaCl solution, the pFC1FC2 (*fc1/fc1*) showed already pale-green leaves, which turned entirely pale after 72h while both Col-0 and 35SFC1-YFP leaves maintained green pigments in most of the leaf area (Figure 3.53).

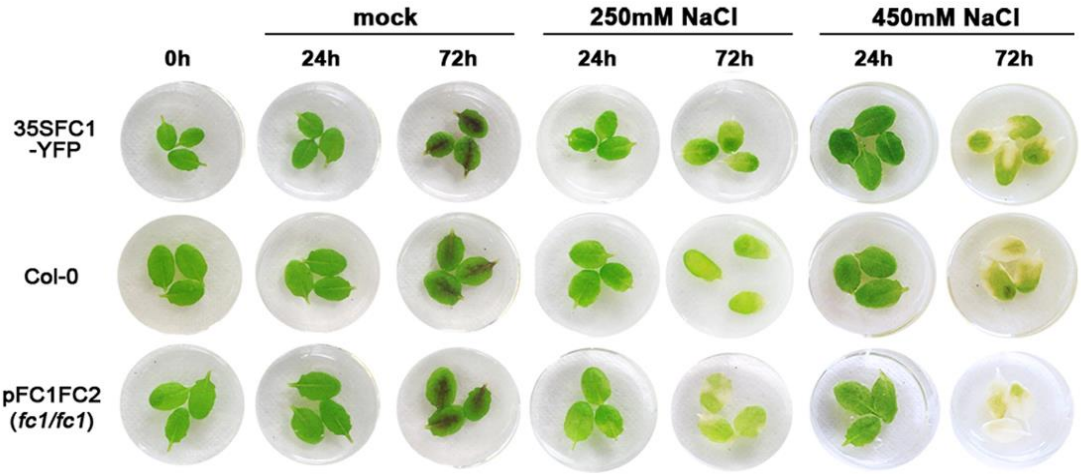

Figure 3. 53 Phenotypic characterization of detached rosette leaves under salt stress.

To verify all the microscopic phenotypes mentioned above, chlorophyll contents were determined in the control and salt-treated leaves. Consistent with the visible phenotypes, under both 250mM and 450mM NaCl treatments, pFC1FC2 (*fc1/fc1*) leaves displayed drastically accelerated chlorophyll degradation in comparison to wild type and 35SFC1-YFP, indicating an early-senescence phenotype (Figure 3.54A). However, 35SFC1-YFP leaves showed less chlorophyll reduction under 450mM NaCl treatment compared to wild type. In addition to the changes in the chlorophyll accumulation, heme contents in the control and salt-treated samples were also measured via HPLC analysis. Interestingly, in comparison to Col-0, a strong reduction of heme was observed in both 250mM and

450mM NaCl treated pFC1FC2 (*fc1/fc1*) leaves, which was in correlation of the severely reduced chlorophyll contents (Figure 3.54A).

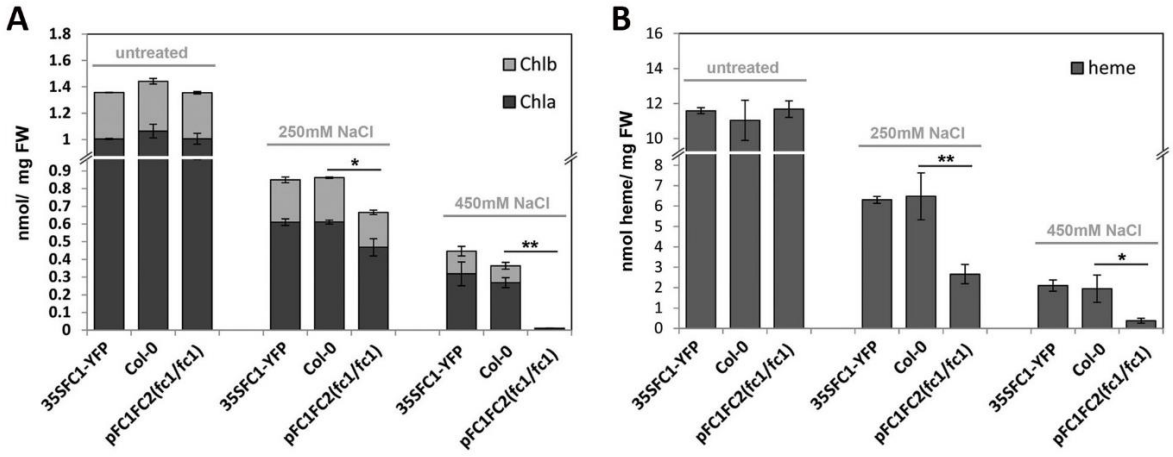

Figure 3. 54 Determination of chlorophyll and heme contents in control and salt-treated leaves.

Measurement of chlorophyll (A) and heme (B) contents in detached leaves from Figure 3.54, after 72h incubation in mock solutions with 250mM/450mM NaCl. Error bars indicate SD (n=3). Asterisk represents significant difference; * P value < 0.05, ** P value < 0.01.

Cell membrane integrity is one of the most important criteria for cell viability. Under stress conditions, electrolyte leakage accompanies plant response to stress. To further verify the visible phenotypical changes observed above, the ion leakage ratios of leaves treated with control and salt solutions were determined (Figure 55A). The rosette leaves from 3-week-old pFC1FC2 (*fc1/fc1*), 35SFC1-YFP and wild-type seedlings were incubated in mock and 250mM NaCl solutions for 24h. The detached leaves were then incubated in 0.4mM mannitol solution for 3h before the leakage conductance was recorded with WTW LF318 conductivity meter. The full conductivity was determined after 10min incubation at 100°C.

As a result, rosette leaves treated with mock solution showed barely an effect on membrane integrity. Under salt treatment, the ion leakage rates of pFC1FC2 (*fc1/fc1*) leaves were significantly higher compared to wild type, whereas 35SFC1-YFP leaves displayed lower ion leakage rates when treated with salt.

In addition, to determine the reactive oxygen species (ROS) accumulation, superoxide (O_2^-) was detected in the mock and salt-treated leaves by NBT solution (Figure 55B). As control, leaves of 35SFC1-YFP, pFC1FC2 (*fc1/fc1*) and Col-0 plants treated with mock solution showed equal minimal NBT staining indicating low superoxide levels. After salt treatment, wild-type leaves displayed much more accumulation of superoxide radicals, while FC1 overexpression leaves were barely more stained compared to the mock condition.

However, the salt-treated pFC1FC2 (*fc1/fc1*) leaves exhibited strong NBT staining overall in the leaf tissues indicating high accumulation of superoxide radicals.

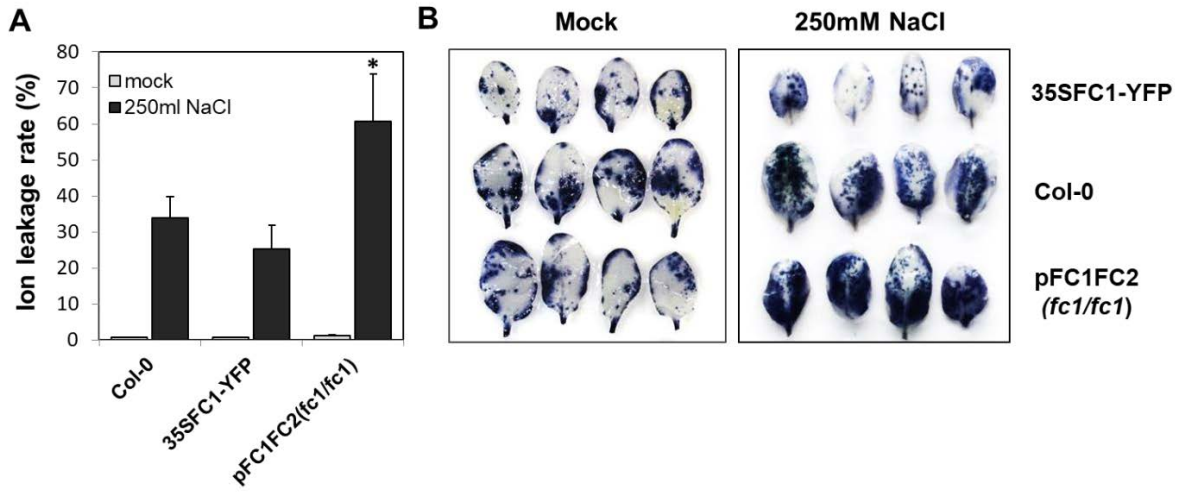

Figure 3. 55 Ion leakage rates and ROS accumulation of detached leaves after 24h control and salt treatment.

(A) Ion leakage rates were determined from detached leaves after 24h incubation in mock or 250mM NaCl solutions. Error bars represent SD (n≥3). Asterisk represents significant difference; * P value < 0.05. (B) Visualized detection of ROS accumulation by detecting Superoxide accumulation with NBT staining solution. Leaf samples were treated with mock or 250mM NaCl for 24 hours before staining.

Moreover, contents of FC and the proteins of photosynthesis machinery were examined by western blot, to assess the integrity of chloroplasts. Heme-binding proteins, e.g. Cybf and PsbE, and other photosynthetic proteins, such as LHCb1 and AtpB predominantly retained in 35SFC1-YFP leaves treated with salt. However, these proteins accumulated much less in pFC1FC2 (*fc1/fc1*) leaves after the treatment, suggesting more affected chloroplasts compared to wild type and 35SFC1-YFP lines.

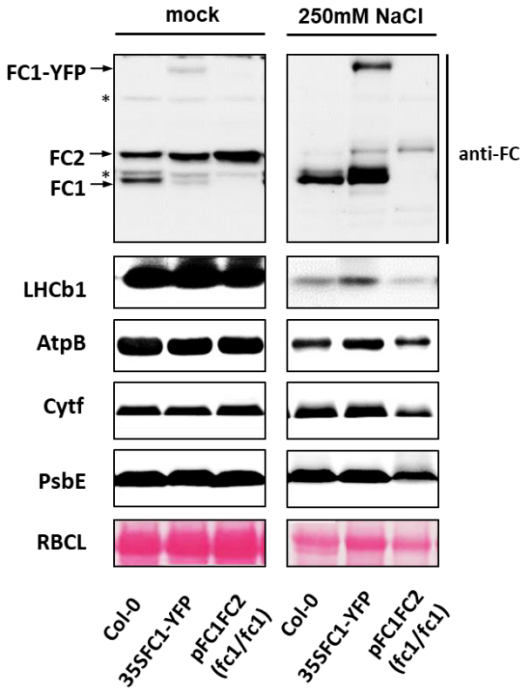

Figure 3. 56 Western blot analysis of the FC variants and photosynthetic proteins in control and salt-treated leaves.

Protein samples were extracted from detached leaves after 72h incubation in the mock and 250mM NaCl solutions. LHCb1: Light-harvesting protein b1; AtpB: β subunit of ATP synthase Cytf: Cytochrome f, heme-binding protein from cytochrome b6f complex PsbE: a heme-binding protein, β subunit of cytochrome b559, main component of PSII core complex. Non-specific immune-reacting bands were indicated with asterisks.

To verify the modified stress tolerance phenotypes of the detached leaves, germination tests were performed on MS agar plates. The sterilized pFC1FC2 (*fc1/fc1*), 35SFC1-YFP and wild-type seeds were germinated on the 2MS media plates containing 0mM, 75mM, 100mM and 150mM NaCl. After 6 days growth under SD condition, the germination ratios were recorded. As a result, both pFC1FC2 (*fc1/fc1*) and 35SFC1-YFP seeds showed identical germination ratios compared to wild type under control condition (Figure 3.57). However, as the concentration of NaCl increases, 35SFC1-YFP seeds displayed significantly higher germination ratios compared to wild type, while pFC1FC2 (*fc1/fc1*) exhibited much lower survival rates which is in consistence with the stress-sensitive phenotype of the detached leaves.

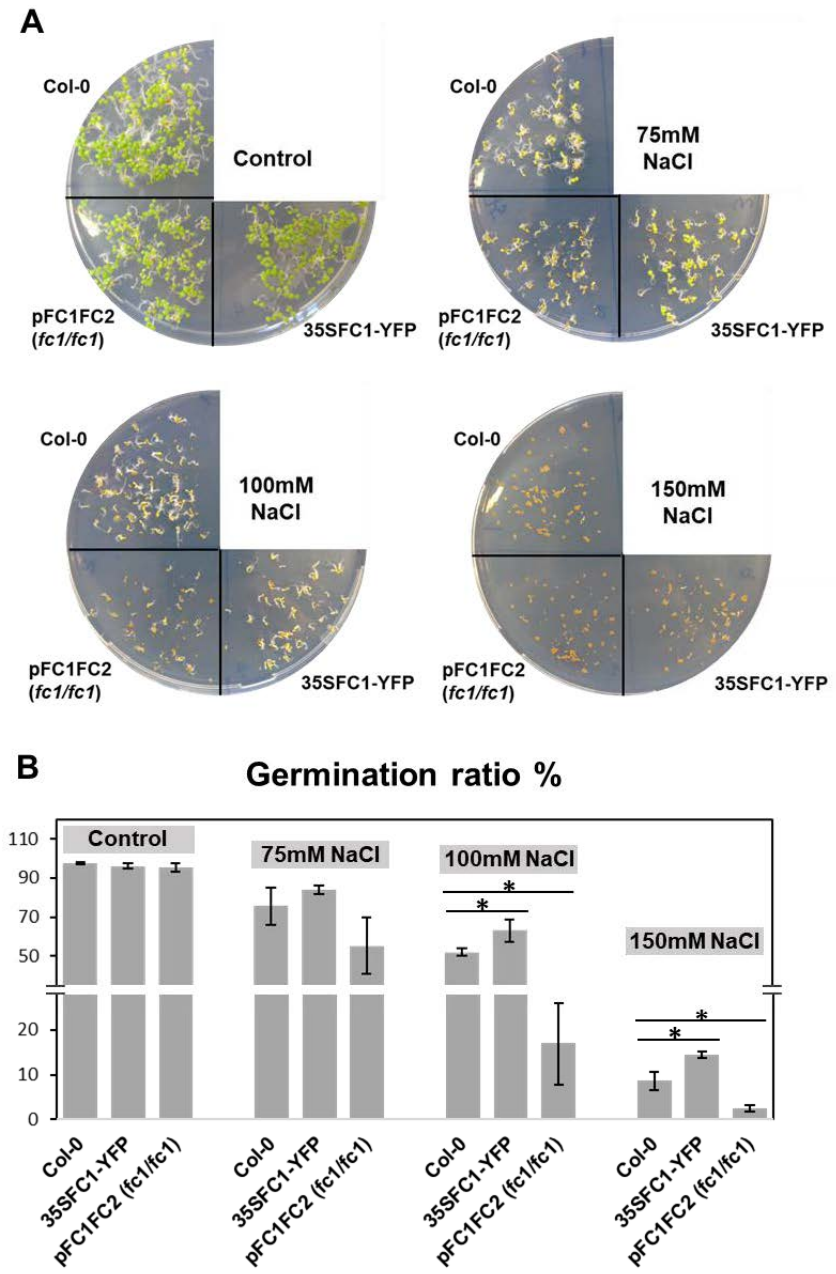

Figure 3. 57 Seeds germination of pFC1FC2 (*fc1/fc1*), 35SFC1-YFP and Col-0 under salt stress.

(A) Phenotypes of pFC1FC2 (*fc1/fc1*), 35SFC1-YFP and wild-type seeds germinated on 2MS plates containing 0mM, 75mM, 100mM and 150mM NaCl. Sterilized seeds were plated on MS medium with 2% sucrose, grown for 6 days under SD condition with 100μE light intensity. (B) Quantification of germination ratios of pFC1FC2 (*fc1/fc1*), 35SFC1-YFP and wild-type seeds on 2MS plates with or without NaCl. Error bars represent SD (n≥3). Asterisk represents significant difference; * P value < 0.05.

3.3.6.2 FC1-producing heme represses *CCEs* expression under salt stress.

To reveal the mechanism for the accelerated chlorophyll degradation of pFC1FC2 (*fc1/fc1*) in comparison to wild type under salt stress, expression of key genes encoding Chlorophyll

Catabolic Enzymes (CCEs) were analyzed in control and salt-treated leaves. Expression of representative *CCE* genes, i.e. *NYC1* (*NON-YELLOW COLORING 1*, encoding Chlorophyll b Reductase), *SGR* (*STAY-GREEN1*), *PAO* (*PHEOPHORBIDE a OXYGENASE*) and *PPH* (*PHEOPHYTIN PHEOPHORBIDE HYDROLASE*) were dramatically stimulated in wild-type leaves after 24h salt treatment. In comparison to wild type, the transcripts in pFC1FC2 (*fc1/fc1*) leaves were drastically up-regulated. This could explain the accelerated chlorophyll degradation. In contrast, the 35SFC1-YFP line showed significantly lower accumulation of *CCEs* transcripts compared to wild type, contributing to its slower chlorophyll breakdown. However, *NOL* (*NYC1-like*) and *HCAR* (*7-HYDROXYMETHYL-CHLOROPHYLL a REDUCTASE*), encoding enzymes catalyzing the conversion of chlorophyll b to chlorophyll a, showed not up-regulation but decreased expression under salt treatment in all three lines in agreement with the previous studies.

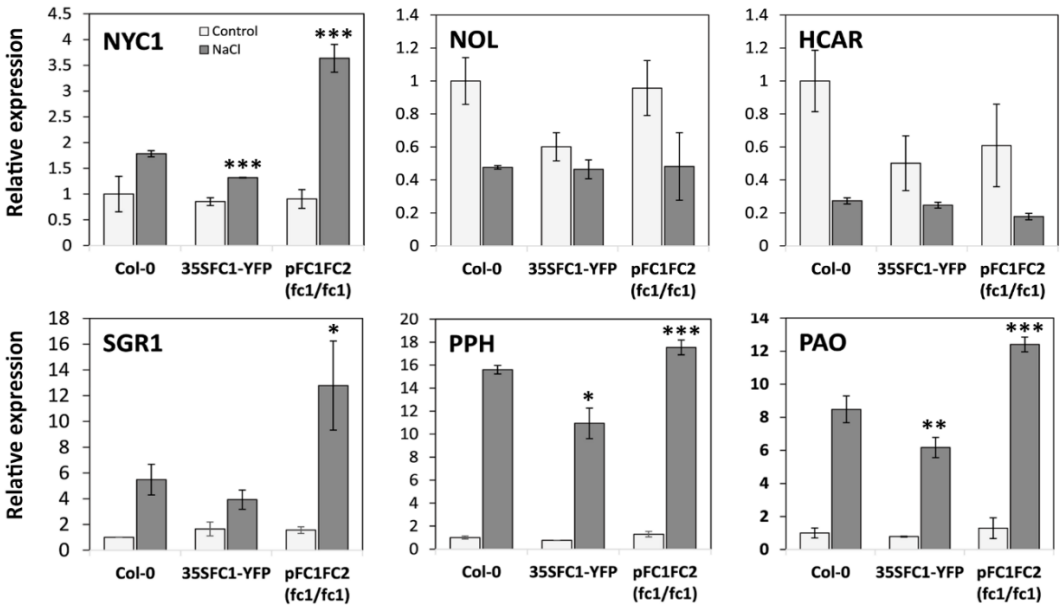

Figure 3. 58 FC1-producing heme represses expression of *CCEs* (*Chlorophyll Catabolic Enzymes*) genes under salt stress, contributing to stress defense.

Altered mRNA accumulation of genes involved in chlorophyll degradation in pFC1FC2 (*fc1/fc1*), 35SFC1-YFP and wild-type leaves. RNA samples were extracted from detached leaves treated with or without 250mM NaCl for 24h. RT-qPCR results were obtained by normalizing to transcript levels of *GAPDH*. The expression level of wild type with mock treatment was set to 1. Error bars indicate standard deviations (n=3). Asterisk represents significant difference; * P value < 0.05, ** P value < 0.01, *** P value < 0.001.

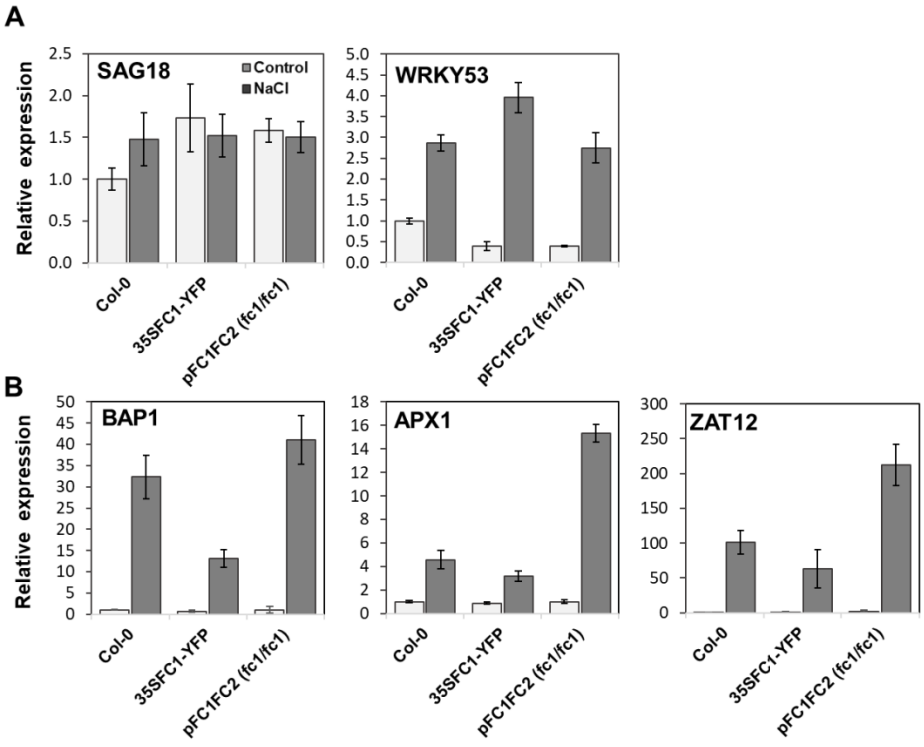

Figure 3. 59 RNA accumulation of senescence and ROS responsive genes in control and salt-treated leaves.

(A) RNA expression of typical senescence-associated genes in pFC1FC2 (*fc1/fc1*), 35SFC1-YFP and wild-type leaves. Leaf samples were treated with mock or 250mM NaCl for 24h. RT-qPCR results were obtained by normalizing to transcript levels of *GAPDH*. The expression level of wild type with mock treatment was set to 1. Error bars represent standard deviations (n=3). (B) Transcripts analyses of various ROS related genes in mock and salt-treated leaves. Representative marker genes were chosen according to (Baruah et al., 2009). *BAP1*: *BON association protein 1*, $^1O_2$-responsive gene; *APX1*: *Ascorbate Peroxidase 1*, H_2O_2-responsive gene; *ZAT12*: *AT5G59820*, a zinc finger protein, general oxidative stress responsive gene.

To examine the mechanism for the modified stress tolerance further, expression profiles of marker genes involved in stress response, stress protection and senescence were investigated (Figure 3.59). *SAG18* (*senescence-associated gene 18*) and *WRKY53* are implicated to be indicative for senescence (Miller et al., 1999; Miao and Zentgraf, 2007; Zentgraf et al., 2010). *APX1* (*Ascorbate Peroxidase 1*) *and BAP1* (*BON association protein 1*) are representatives for H_2O_2 and $^1O_2$-responsive genes, respectively. *ZAT12* (*AT5G59820*), encodes a zinc finger protein which transcript is inducible upon general oxidative stress (Karpinski et al., 1997; Davletova et al., 2005; Yang et al., 2007). *SAG18* expression showed no alterations under salt treatment in both mutants and wild-type plants, while all other genes accumulated under salt treatment compared to the control condition. Under salt treatment, pFC1FC2 (*fc1/fc1)* seedlings accumulated more transcripts of the ROS-inducible *BAP1*, *ZAT12* and *APX1* genes, which revealed the severe oxidative stress occurring in the cells. This was in agreement with the stress-sensitive phenotype.

To verify the regulatory impact of FC1- produced heme on *CCEs* expression, *NYC1*, *SGR1*, *PPH* and *PAO* transcript accumulation provoked by salt stress were analyzed in pFC1FC2 (*fc1/fc1*), 35SFC1-YFP and wild-type leaves. RNA samples were harvested from the salt-treated leaves at time point 0h, 3h and 6h. As a result, senescence triggered by salt stress occured rapidly within 3h incubation in salt solutions. After a 3h incubation, the expression of *SGR1* and *NYC1* was two-folds higher in the pFC1FC2 (*fc1/fc1*) leaves than wild type, and transcript levels of *PPH* and *PAO* also showed elevated accumulation in pFC1FC2 (*fc1/fc1*) compared to the wild-type control. Meanwhile, 35SFC1-YFP displayed either a similar increase or less accumulation of these *CCEs* in comparison to wild type. After a 6h treatment, wild-type leaves alleviated the increase of *SGR1*, *PPH* and *PAO* transcripts, which expression was repressed in 35SFC1-YFP samples. However, pFC1FC2 (*fc1/fc1*) leaves maintained a drastic stimulation of the four *CCEs*. Taken all together, it can be concluded that salt-triggered induction of *CCEs* expression, is attenuated upon *FC1* expression.

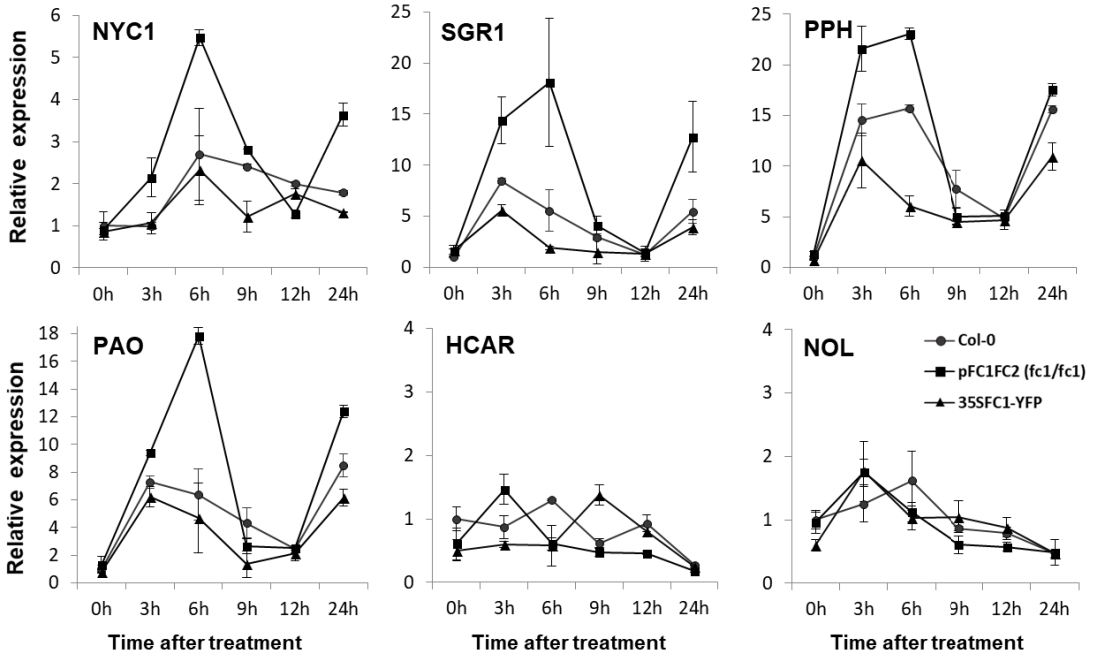

Figure 3. 60 Induction of chlorophyll catabolic genes in pFC1FC2 (*fc1/fc1*) and FC1 overexpression lines under salt stress

Leaf samples were harvested after 0, 3, 6, 9. 12 and 24 hours treatment with 250mM NaCl. Error bars indicate standard deviations, n=3.

3.3.6.3 Both elevated promoter activity and transcript stability of Arabidopsis *FC1* contribute to its essential function under salt stress.

To investigate the reason for the failed complementation of pFC1FC2 (*fc1/fc1*) under salt stress, both FC protein contents in the control and salt-treated leaves were determined (Figure 3.56). As a result, FC1 protein showed much higher accumulation in the salt-treated leaves compared to control in all the three lines, whereas FC2 in both wild-type

and pFC1FC2 (*fc1/fc1*) leaves revealed a dramatically reduced content, which resembled the drop of photosynthetic proteins after salt treatment. To figure out whether the varying stabilities resulted from a control of transcription or posttranscription processes, a qPCR was performed to compare the accumulation of both FC transcripts in pFC1FC2 (*fc1/fc1*) and wild-type leaves within 12h incubation with salt solutions. The quantification results suggested that wild-type *FC1* highly and continuously accumulated after the treatment, while *FC2* barely showed stimulation by salt stress (Figure 3.61). These results verified the stress-inducible activity of *FC1* promoter presented in previous study (Singh et al., 2002). Although driven by the same promoter, the *FC2* transcript levels in pFC1FC2 (*fc1/fc1*) leaves were significantly lowered after transient stimulation. A shorter half-life of *FC2* mRNA in comparison to *FC1* is proposed to be responsible for the alleviated FC2 protein content as well as reduced heme accumulation under salt stress treatment, which eventually led to the failure of complementation of *FC1* deficiency.

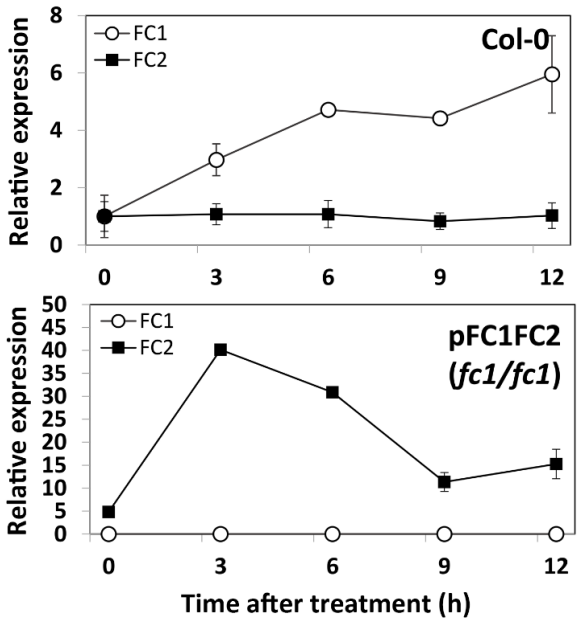

Figure 3. 61 *FC2* transcript in pFC1FC2 (*fc1/fc1*) plants is not stable under salt stress.
Changes of FC1 and FC2 transcripts in pFC1FC2 (fc1/fc1) and wild-type leaves provoked by salt stress were analyzed by qRT-PCR. Relative expression levels were normalized to the expression of reference gene GADPH.

4. Conclusion and discussion

Heme, as a requisite biomolecule in all living cells, mainly serves as a cofactor for numerous fundamental biological processes. In all eukaryotes and most prokaryotes, heme is synthesized via the conserved Tetrapyrrole biosynthesis pathway. Once Proto is formed, ferrochelatase (FC) is able to insert ferrous iron into the tetrapyrrole ring to yield protoheme. In contrast to mammalian, yeast and bacterial FCs, plant cells utilize always two FC isoforms. In Arabidopsis, the two FC homologues are distinguished by their diverse expression profiles and subcellular allocations, despite of the highly conserved amino acid sequences (Figure 4.1). Preliminary characterization of Arabidopsis *fc* mutants as well as overexpressing plants has shed light on the potential functional distributions of the two isoforms (Chow et al., 1998; Singh et al., 2002; Woodson et al., 2011; Scharfenberg et al., 2015; Hey et al., 2016). However, the genuine functions of the two FC isoforms in different biological processes and developmental stages remain largely unknown. In addition, the reason that the two isoforms could play diverse function roles and their ability to substitute each others function await elucidation.

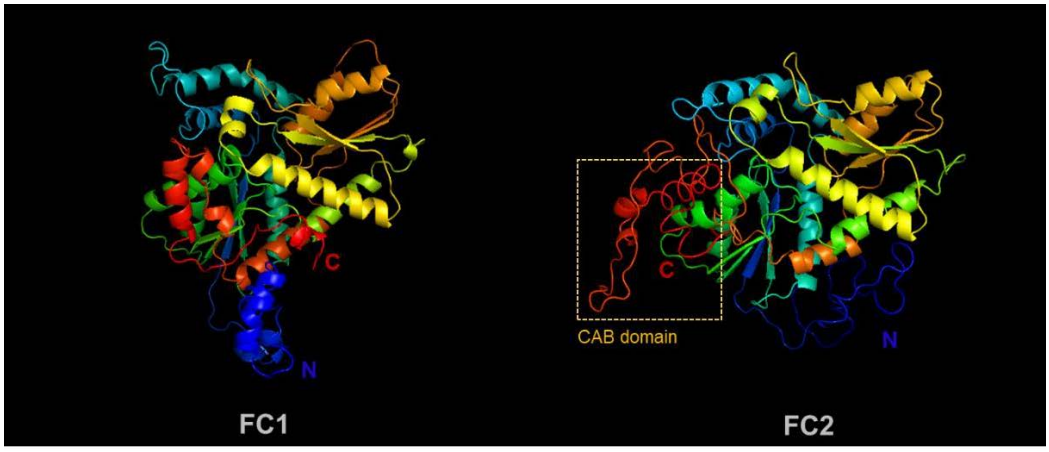

Figure 4. 1 Structures of Arabidopsis FC isoforms.
Visualization of the 3D structures were performed by Pymol and represented in the form of ribbons. The amino-acid sequences of N-terminus and C-terminus were indicated in blue and red, respectively. CAB domain: chlorophyll a/b- binding domain.

To explore the distinct functions of the two FC isoforms, in this study, multiple Arabidopsis *fc* mutants have been re-analyzed and complementation approaches have been conducted with a *fc1* or *fc2* null mutant. Through the characterization of the newly generated complementation lines, FC overexpressing plants as well as a series of defective mutants in context with ALA synthesis, the presented study was able to uncover the essential function of FC1 in embryo development as well as plant defense and emphasize the importance of FC2 presence for ALA synthesis regulation and photosynthetic complexes assembly. In addition, the thesis also illustrated to which extent FC1 (FC2) can substitute FC2 (FC1) function in all these biological processes. The possibilities and

limitations in the functional substitution of one FC isoform for the other, also contribute to a better understanding of differences between the two FCs, in respects of subcellular localization, structural differences and varying stabilities of mRNA.

4.1 Arabidopsis FC1 function in seedling development

4.1.1 FC1-produced heme is critical for embryo maturation.

Arabidopsis embryogenesis consists of two main phases, morphogenesis and maturation. During morphogenesis, the basic body plan of the plant is established, whereas during maturation, the embryo undergoes cell expansion and accumulates storage macromolecules (Park and Harada, 2008). In this study, the embryo lethality phenotype and development-dependent defects of homozygous *fc1-2* mutants were identified (Figure 3.39). Examination of heterozygous *fc1-2* siliques revealed two size classes of seeds in addition to wild-type-like progenies. Further dissection of Col-0 and heterozygous *fc1-2* seeds throughout embryo development stages pointed out that homozygous *fc2-1* seeds undergo perturbed maturation in comparison with the wild-type control. The *fc1/fc1* mutant seeds are either arrested or its development will be postponed after mid-torpedo stage, which emphasizes an essential role of FC1 in Arabidopsis embryogenesis, particularly during maturation.

In accord with the phenotype, expression profiles of *FC1* and *FC2* during embryogenesis suggested that *FC1* is always higher expressed throughout the maturation phase of embryogenesis than *FC2*. A complementation approach of *fc1-2* by expressing *FC* isoforms under a *FC1* or *FC2* promoter indicated that loss of *FC1* expression during embryo development is neither complemented by the wild-type *FC*2 nor by additional expression of a transgenic *pFC2FC2* gene construct in the *fc1-2* mutant background.

Heme serves as a cofactor in electron transport chains and in enzymes involved in oxygen metabolism (Layer et al., 2010). During its maturation, the embryo becomes photosynthetically active to provide oxygen for seed respiration (Borisjuk and Rolletschek, 2009). Therefore, the heme produced by FC1 during embryogenesis may be specifically incorporated into hemoproteins necessary for oxygen homeostasis, as well as photosynthetic and respiratory cytochromes required for energy transduction. The FC1-produced heme, during embryo development, might also contribute to the regulation of gene expression for seeds maturation. Several nuclear transcription factors have been found to be hemoproteins, although no such heme-requiring factors have yet been described in plants (Kobayashi and Masuda, 2016). Of more direct relevance to the presented study is the arrest of embryo development at the globular stage reported for a homozygous null mutation of the *AtHEMN1* gene (Pratibha et al., 2017). This gene encodes an oxygen-independent coproporphyrinogen oxidase, which intervenes in tetrapyrrole biosynthesis two steps upstream of the reaction catalyzed by FC. The Arabidopsis genome also contains two *HEMF* genes that encode oxygen-dependent coproporphyrinogen oxidases. The *athemn1* and *fc1-2* phenotypes both suggest that specific genes of

tetrapyrrole synthesis are essential for embryo development, while other isoenzymes are required for later stages of plant development.

4.1.2 FC1 produces heme for signal transduction.

Besides acting as a prosthetic group for hemoproteins, FC1-produced heme has been demonstrated to play a significant role in signaling transduction. It has recently been shown in Arabidopsis that overexpression of *FC1* de-represses *PhANG*s expression when biogenic control of chloroplasts is impaired by treatment with NF, indicating a function for heme in retrograde signal transduction to regulate nuclear gene expression (Woodson et al., 2011). Biogenic control via retrograde signaling from chloroplast to nucleus is known to occur during early stages of chloroplast development, which is distinct from an operational control circuit that functions in adult seedlings (Pogson et al., 2008; Kleine and Leister, 2016). Thus, whether FC1-produced heme also functions in signaling transduction in mature chloroplasts, does FC1 also react to abiotic stresses and what is FC1 genuine function during signaling processes, all these questions need to be elucidated.

In the presented study, abiotic stress treatments have been applied to the pFC1FC2 (*fc1/fc1*) complementation lines, 35SFC1 overexpression plants as well as wild type. The results revealed modified senescence in the mutant lines under salt stress in comparison to the wild-type control. When exposed to salt stress, the 35SFC1 overexpression plants displayed relative slower chlorophyll degradation, while the pFC1FC2 (*fc1/fc1*) mutants exhibited accelerated chlorophyll breakdown compared to wild type. Transcriptional analysis of genes encoding chlorophyll catabolic enzymes (CCEs) suggested that in wild-type Arabidopsis, FC1-produced heme may negatively regulate *CCE*s expression, contributing to plant defense against salt stress.

Consistent with the previous study under NF treatment, the presented study also observed FC1 function in regulating gene expression under abiotic stress conditions. In addition, the novel gene targets were shown to be key *CCE*s, such as *NYC1*, *SGR1*, *PPH* and *PAO*. Besides these target genes suggested in this study, FC1-producing heme also contribute to the expression control of genes involved the GSH-dependent phytochelatin synthetic pathway as well as genes associated with Na^+ exclusion (Song et al., 2017; Zhao et al., 2017). FC1-produced heme has been long time suggested as a retrograde signal (Kwast et al., 1998; von Gromoff et al., 2008; Woodson et al., 2011). However, it is still unclear in which manner could this specific heme pool mediate the communication between plastids and nucleus. The study of heme trafficking can provide a clue to this question. Although heme biosynthesis and degradation pathways have been well characterized, nevertheless, the mechanism of heme trafficking and incorporation into apoproteins remains poorly understood in plants. It is known that in mammalian cells, mitochondrial FC forms complexes with the ATP-binding cassette (ABC) transporters to accomplish the transport of heme on membranes (Khan and Quigley, 2011; Yuan et al., 2013). In plant cells, the process of heme transfer from plastids to other subcellular compartments remains unknown. A few of putative heme binding proteins (HBPs) have been identified in the

cytosol and plastids (Lee et al., 2012). The cytosolic Arabidopsis HBP1 and HBP2 have been proposed as tetrapyrrole carriers in the cytosol, as they can bind porphyrins including heme (Takahashi et al., 2008). The plastid-localized HBP5 also showed heme binding ability and a physical interaction with HO1 (Lee et al., 2012). Additionally, the Golgi-localized tryptophan-rich sensory protein (TSPO) was suggested to be a heme-binding protein and a potential scavenger of porphyrin via an autophagy-dependent degradation (Vanhee et al., 2011). All these studies suggested the existence of a specific heme trafficking pathway in plant cells. In the future, more investigations are needed to obtain a comprehensive understanding of heme transport in plant cells.

4.2 FC2 ability to substitute FC1 function in Arabidopsis

4.2.1 In Arabidopsis, FC2 can fully substitute FC1 function under standard growth conditions.

The two isoforms of ferrochelatase, FC1 and FC2, are assumed to act in the synthesis of two different heme pools. Their functional differences were proposed to be attributed to dissimilarities in the expression of their genes, as well as differences in their protein sequences (Chow et al., 1998; Nagai et al., 2007; Woodson et al., 2011). The presented work attempted to complement *fc1-2*, which has an embryonic lethal phenotype. Complementation with *pFC1::FC1* was successful and allowed the mutant phenotype to be definitively attributed to the loss of FC1 function. Interestingly, *fc1-2* was also complemented by *FC2* expressed from the *FC1* promoter (Figure 3.44). The resulting pFC1FC2 (*fc1/fc1*) plants grew normally and accumulated wild-type levels of heme and chlorophyll (Figure 3.47 and Figure 3.48), as expected for complete complementation. In contrast, both *pFC2::FC2* and *pFC2::FC1* gene constructs failed to rescue *fc1-2*. These results suggest that the inability of *pFC2*-driven constructs to rescue *fc1-2* is due to an inadequate promoter activity during embryogenesis.

Comparison of *FC1* and *FC2* mRNA levels in wild-type embryos from maturation stages revealed that *FC1* transcripts are more abundant than *FC2* mRNA, in comparison with other organs (Figure 3.43). Thus, it can be concluded that the *FC1* promoter is more active during embryogenesis, which in turn implies that FC1 is the predominant FC isoform present during embryo maturation. The successful complementation of the *fc1-2* mutant by *pFC1::FC2* demonstrates that precise regulation of *FC* expression in time and space during embryogenesis is a prerequisite for proper embryo development. Only expression under control of the *FC1* promoter apparently enables FC2 to synthesize sufficient heme for the needs of embryo maturation. Whether *pFC1::FC2* might also rescue an *fc1/fc2* double mutant, i.e. complement the heme restrictions caused by the loss of FC2 function in photosynthetically active tissues, remains an intriguing question.

That FC2 can fully compensate the lack of *FC1* has an impact on the subcellular localization of the two isoforms. As FC2 can functionally substitute for FC1 during embryogenesis and subsequently during germination as well as in the adult stage, it can be concluded that

both FC isoforms are either located in the same cellular compartment(s) or that FC2 is translocated into plastids where it synthesizes heme which is subsequently allocated to all subcellular compartments. Even if dual-targeting of FC1 occurs in Arabidopsis, the presence of a mitochondrial fraction of FC does not seem to be essential, as the present findings indicate that export of heme from plastids can provide enough for all compartments in the pFC1FC2 (*fc1/fc1*) seedlings.

In contrast to other eukaryotic species, plant cells possess 2 types of endosymbiotic organelles: mitochondria and chloroplasts. In plants, the majority of the organelle proteins is encoded in nuclear, synthesized in the cytosol as precursor proteins carrying a N-terminal transit peptide, which determines the specific translocation. The precursor proteins are then guided by cytosolic chaperones to the target organelle and imported mainly via a classic translocase system on the membranes of mitochondria (TIM/TOM) and plastids (TIC/TOC) (Langner et al., 2014; Murcha et al., 2014; Paila et al., 2015). Generally, as a result, the precursor proteins are specifically targeted to a single organelle. However, in some rare cases, certain proteins are dual-targeted to both subcellular compartments. With the presence of dual-targeted proteins, a number of activity events could be carried out parallel in both mitochondria and chloroplasts. This allows the inter-organelle communication of mitochondria and plastids, as the two organelles may share and coordinate the distribution of the dual-targeted enzymes.

To achieve dual-targeting ability, there exist two mechanisms: alternative transcriptional or translational initiation or splicing and ambiguous targeting signals (Peeters and Small, 2001; Carrie et al., 2009; Carrie and Small, 2013; Ge et al., 2014; Sharma et al., 2018). As a key enzyme catalyzing the formation of Proto in the TBS pathway, spinach PPO II is targeted to both mitochondria and chloroplasts by alternative use of the two in-frame initiation codons (Watanabe et al., 2001). Tobacco PPO II also showed exclusive mitochondria localization (Lermontova et al. 1997). Recent reports have cast doubt on the heme synthesis pathway in Arabidopsis mitochondria (Lister et al., 2001; Woodson et al., 2011). To figure that out, attempts to search for potential alternative initiation codons of Arabidopsis PPO II were made in this study. Two additional methionines upstream from the putative start codon were found and used to transcribe a *PPO II* genomic sequence followed by a *Green Fluorescence Protein* (*GFP*) tag. Transient expression in tobacco leaves revealed that the two alternate initiation codons led to the same chloroplast-localization of PPO II, as the native PPO II (Supplemental data, Figure S1). This indicates that different from the spinach protein, Arabidopsis PPO II is unlikely to show dual-targeting via alternative transcriptional initiation.

Nevertheless, studies on the recently characterized *ATHEMN1*-encoded coproporphyrinogen oxidase have shown that this protein is translocated into mitochondria (Pratibha et al., 2017). The two isoforms of maize oxygen-dependent coproporphyrinogen oxidase are also targeted either to plastids or mitochondria (Williams et al., 2006). More recently, the research from our group demonstrated FC activity, supported by immunological evidence for FC, in the mitochondria of tobacco

plants (Hey et al., 2016). However, when the mitochondrial extracts of pFC1FC2 (*fc1/fc1*) and wild-type Arabidopsis were applied to immunoblot analysis by employing the newly generated α-FC antibodies (raised against Arabidopsis FC1/FC2 protein), no specific immune-reacting band representing mitochondria-FC could be detected (Supplemental data, Figure S2). As no hard data currently indicate that FC1 is translocated into Arabidopsis mitochondria, it cannot be excluded that in Arabidopsis seedlings both FC isoforms are localized in plastids, and that heme is exported to all non-plastid compartments, while the oxygen-independent coproporphyrinogen oxidase HEMN1 (Pratibha et al., 2017) supplies the embryo's needs for heme in mitochondria through another heme-synthesizing branch of tetrapyrrole biosynthesis. At present, whether heme synthesis and allocations are differently organized at different developmental stages in tobacco, maize and Arabidopsis remain undecided.

4.2.2 Under salt stress FC1-produced heme represses *CCEs* expression, which function could not be compensated by FC2.

Although under standard growth conditions, *FC2* expression driven by *FC1* promoter may contribute to a full complementation of *fc1-2*, *FC2* however failed to compensate *FC1* function under salt stress. The presented findings further uncovered the FC1 function in retrograde signaling in mature chloroplasts, by regulating the expression of chlorophyll breakdown genes under salt stress. In addition, by analysis of the pFC1FC2 (*fc1/fc1*) seedlings, it can be concluded that the significant role of FC1 in stress response could not be compensated by *FC2* expression, most likely due to their different mRNA stabilities. These results revealed that Arabidopsis FC1 serves a specific heme pool for stress tolerance in comparison to FC2 (Figure 4.2).

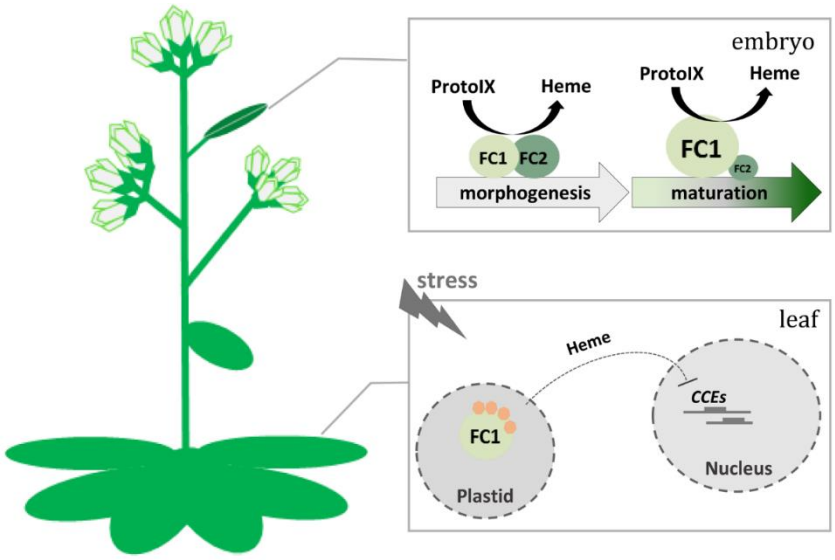

Figure 4. 2 Model for the functional distribution of FC1 and FC2 in embryos and leaves.

In Arabidopsis both FCs are present in embryo and leaf tissue. During embryogenesis, particularly the maturation phase, FC1 is the predominant FC which supplies the heme required to complete embryo maturation, while FC2 mainly produces heme in photosynthetically active leaves. Under stress conditions, FC1 synthesizes heme in plastids, which generates a retrograde signal suppressing *CCEs* gene expression in the nucleus and slows down leaf senescence contributing to plant defense.

4.3 FC2 function in chloroplast biogenesis

4.3.1 FC2 plays a regulatory role in ALA formation via the interaction with a POR-FLU-GluTR complex.

For a long time, heme has been proposed as a feedback inhibitor of ALA formation by direct binding to GluTR. Bacterial GluTR proteins form dimers and bind to heme *in vitro* (Huang and Castelfranco, 1989; Castelfranco and Zeng, 1991; Vothknecht et al., 1996; Jones and Elliott, 2010; de Armas-Ricard et al., 2011). Enzymatic activity of GluTR in green algae, *Chlorella vulgaris*, was cut down to 50% by adding protoheme (Weinstein and Beale, 1985). Different from bacteria, algae, yeast, as well as mammal cells, always two isoforms of FC exist in higher plants. This evolutionary specificity, however, turns plant TBS into a much more complex regulatory pathway, as the two FC isoforms serve different heme pools and display distinctive function roles.

In plant cells, a modified expression of either FC isoform resulted in varying impacts on heme and chlorophyll production. Previous characterization of Arabidopsis *fc* mutants repeatedly emphasized the specific reduction of chlorophyll contents and photosynthetic parameters in *fc2* mutants (*fc2-1* and *fc2-2*) in comparison with the *fc1* deficient seedlings (*fc1-1*) (Papenbrock et al., 2001; Woodson et al., 2011; Scharfenberg et al., 2015; Espinas

et al., 2016; Hey et al., 2016). Phenotypic analysis of 35SFC2 transgenic lines in this study, also revealed pale-green leaves, which was attributed to a highly elevated *FC2* expression (Figure 3.16 and Figure 3.24).

Enhanced ALA synthesis activity was obtained when *FC2* expression was down-regulated in tobacco (Papenbrock et al., 2001) and Arabidopsis (this study, Figure 3.18), whereas FC2 overexpression resulted in significantly reduced ALA synthesis rates and chlorophyll intermediates accumulation (this study, Figure 3.18 and Figure 3.21). However, neither a defective nor over-accumulated *FC1* expression affects ALA synthesis rate in tobacco (Hey et al., 2016). This could be also observed in Arabidopsis *fc1-1* mutant lines (Figure 3.50). Why does FC2, but not FC1 expression affect ALA formation and chlorophyll production? And how does FC2 achieve this function in comparison to the type-I FC isoform? Both are intriguing questions need to be answered.

To address these issues, *fc2-2* mutants expressing *pFC2::FC2* (designated as pFC2FC2) and *pFC2::FC1* (designated as pFC2FC1) were generated and analyzed in comparison with the *fc2* mutants. When grown under SD condition, the pFC2FC1 construct could partially compensate *FC2* deficiency, exhibiting necrotic leaves of pFC2FC1 (*fc2/fc2*) seedlings (Figure 3.2). A pFC2FC2 construct was able to fully complement *fc2-2*, as pFC2FC2 (*fc2/fc2*) seedlings revealed wild-type-like growth. Under CL condition, both pFC2FC2 (*fc2/fc2*) and pFC2FC1 (*fc2/fc2*) plants accumulated wild-type-level of chlorophyll and heme contents, displaying a full compensation of FC2 functional loss. Analyses of TBS intermediates and proteins suggested a distinctive destabilization of PORB protein in the SD-grown pFC2FC1 (*fc2/fc2*) seedlings (Figure 3.9). Meanwhile, both SD and CL-grown pFC2FC1 (*fc2/fc2*) plants accumulated two times more Pchlide contents than wild type during dark incubation. The same increase of Pchlide accumulation can be also observed in the *fc2-2* mutants (Figure 3.7). Both *in vivo* and *in vitro* analyses verified a direct interaction between PORB and FC2 (Figure 3.11 – Figure 3.13). In addition, sub-localization on thylakoid membranes and BiFC analysis suggest that FC2 is in association with a POR-FLU-GluTR complex (Figure 3.14). Subsequent characterization of *porb*, *flu*, *fc2* defective mutants and FC2 overexpressing plants in comparison with wild type, revealed that in darkness, Arabidopsis seedlings undergo inhibition of ALA synthesis which leads to a repressed heme synthesis in comparison to the light-exposed plants. However, a defective assembly of FC2-PORB-FLU complex led to perturbed inhibition of ALA synthesis, resulted in an identical heme accumulation in the light- and dark-treated seedlings (Figure 3.22 and Figure 3.27).

Results from the presented study uncovered the distinct interaction between PORB and FC2, in comparison to FC1. This specific interaction establishes a crosstalk of heme and chlorophyll biosynthesis branches. The fact that FC2 is in association with the POR-FLU-GluTR complex reveals the mechanism of action of FC2 on ALA formation and subsequent chlorophyll synthesis (Figure 4.3). That is, under the light, the dimeric GSAAT interacts with the V-shaped GluTR dimer to yield ALA. This enzymatic reaction occurs predominantly in the stroma fraction, while a minor amount of GluTR is attached to the

thylakoid membranes through interaction with GBP (Czarnecki et al., 2011; Apitz et al., 2016; Schmied et al., 2018). Chloroplasts undergo active heme and chlorophyll production for efficient photosynthesis, via both FC isoforms as well as MgCH activity. In darkness, the light-dependent protochlorophyllide oxidoreductase becomes inactive, results in the accumulation of Pchlide. However, the presence of PORB protein remains critical, for a proper assembly of the Pchlide-POR-FLU-GluTR complex, which inhibits ALA synthesis activity during the night phase. Through a direct interaction with PORB, FC2 is able to stabilize PORB protein, as well as the Pchlide-POR-FLU-GluTR complex which enables the inhibition of GluTR activity by FLU via protein-protein interactions. Through this shared inhibitory regulation, both heme and chlorophyll synthesis are able to control their production via attenuating the synthetic flow of the common precursor, ALA.

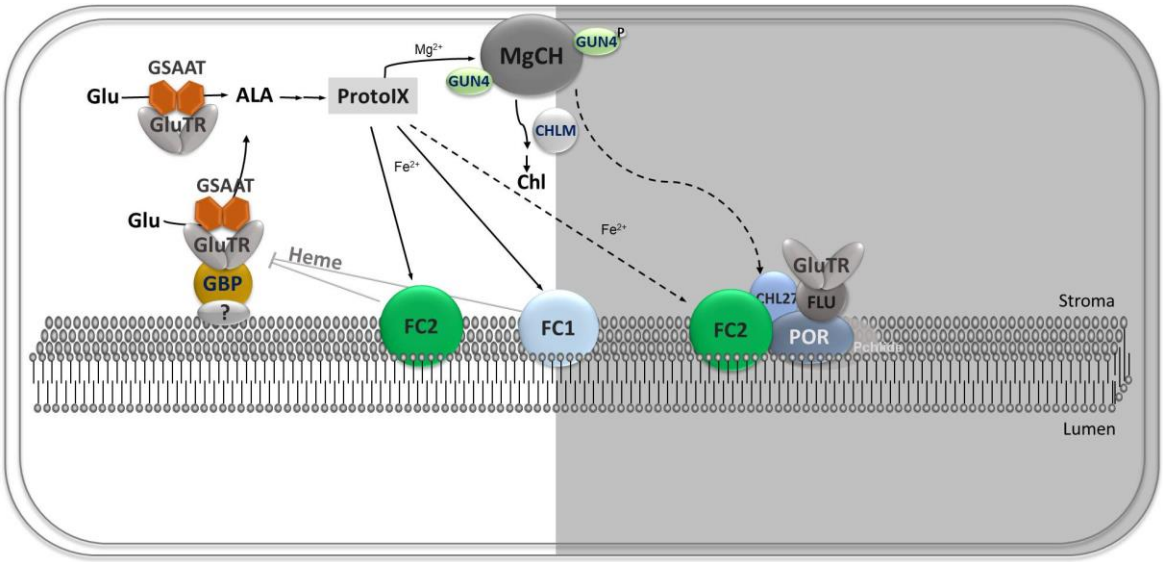

Figure 4. 3 Hypothetical working model for ALA synthesis regulation in Arabidopsis chloroplasts.

During daytime, chloroplasts undergo efficient ALA formation via an interaction between GSAAT and GluTR. The dimeric GSAAT binds to the V-shaped GluTR dimers, mainly in stroma, while a minor portion of GluTR is attached to the thylakoid membranes through the interaction with GBP. Due to light exposure, GUN4 stimulates MgCH activity on envelope membranes, leading to chlorophyll production. Meanwhile, both FC isoforms catalyze the insertion of ferrous iron into ProtoIX to yield heme. In the dark, FC2 interacts with and stabilizes PORB protein. As activity of the light-dependent protochlorophyllide oxidoreductase is abolished in darkness, Pchlide accumulates and contributes to a POR-CHL27-FLU complex. Due to the formation of this regulatory complex, FLU turns into its active form to inhibit GluTR activity through unknown mechanism. Repression of ALA formation attenuates the synthesis of both heme and chlorophyll in the dark, in order to coordinate the accumulation of both components for proper photosynthetic activities, as well as avoid phototoxicity after subsequent light exposure.

In chloroplasts, both heme and chlorophyll contribute to the accurate assembly of photosynthetic machineries. A PSII core is composed of D1, D2, chlorophyll binding

proteins CP43 and CP47, as well as a heme-binding subunit, Cytb559 (Nixon et al., 2010; Komenda et al., 2012; Nickelsen and Rengstl, 2013; Nelson and Junge, 2015). The two subunits of Cytb559, PsbE and PsbF, each provides a His-ligand to coordinate heme. A disruption of proper heme-binding in Cytb559 severely abolishes the stability of PSII core (Pakrasi et al., 1988; Pakrasi et al., 1991; Morais et al., 2001; Hung et al., 2007; Hung et al., 2010; Chu and Chiu, 2015). Defects or over-accumulation of either heme or chlorophyll may result in destabilized photosynthetic machineries. Thus, it is crucial for plant cells to maintain precise production of both components for their apoproteins involved in photosynthesis processes, as an over-accumulation of TBS end-products causes either phototoxicity. By applying the proposed regulatory mechanism (Figure 4.3) in plastids, the synthesis of heme and chlorophyll molecules are tightly regulated and balanced to maintain a homeostatic TBS pathway.

By analyzing cyanobacteria *fc* mutants with different deletions in the C-terminus of Synechocystis FC (SynFC) sequences, Sobotka et al. (2008 and 2011) was able to specify the functions of different domains in SynFC. SynFC, as a homologue of the type II-FC in plant cells, has a putative chlorophyll a/b binding domain (CAB) as well as a proline-rich linker sequence (designated as region II), which connects the CAB domain to the FC catalytic core. It has been demonstrated that the CAB domain is not required for FC activity but is essential for dimerization of SynFC. Moreover, an absence of CAB domain led to highly elevated ALA synthesis rates as well as accumulation of chlorophyll precursors (Sobotka et al., 2008; Sobotka et al., 2011). Therefore, it was proposed that the CAB domain may enable SynFC to serve a regulatory function on chlorophyll biosynthesis independently from its enzymatic activity. The presented working model of FC2 function on ALA synthesis regulation is consistent with the characterization of cyanobacteria *fc* mutants and, furthermore, uncovers the mechanism of FC action on TBS regulation. In the future, a full set of experiments conducted in this study can be performed in cyanobacteria to testify the hypothetical working model. Moreover, a defective *FC2* expression in tobacco resembled the phenotypes of Arabidopsis *fc2* mutants (Papenbrock et al., 2001). This indicates the type-II FC-dependent regulation on ALA synthesis might be widely distributed and highly conserved in cyanobacteria and higher plants.

Besides the current studies of regulations on TBS pathway, there exists still a plenty of open questions on the tightly regulated ALA synthesis. For instance, why does FLU inhibit GluTR activity only with the presence of a Pchlide-POR-CHL27-FLU complex? By which way does FLU inhibit the activity of GluTR? Both FC2 (this study) and heme (Weinstein and Beale, 1985; Vothknecht et al., 1996) have been suggested to regulate ALA synthesis activity. Do both regulations take place independently, or in a coordinated manner? Although current reviews repeatedly claim heme as a feedback inhibitor by directly binding to GluTR. However, no solid experimental evidence could show over-accumulated heme gives a consequence to a decreased ALA synthesis capacity in plant cells. The hypothesis that heme, as an end-product of the TBS pathway, directly binds to the rate-limiting enzyme to regulate its synthesis might be too simplified. Thus, more efforts should be made to reveal the detailed mechanism of action of heme on ALA formation. As

so many factors contribute to the control of GluTR activity and some of them even share the binding motifs of GluTR (for instance, GBP and cpSRP43 both bind the HBD domain of GluTR), do these regulations occur parallel in an independent way or some of them may coordinate with each other? And given that condition, how does the coordination take place? Additionally, besides the control of ALA formation, what else regulatory factors could also modify the synthetic flow of TBS pathway? All these questions need to be further elucidated.

4.3.2 The presence of FC2 is critical for the assembly of photosynthetic complexes.

Previous characterization of Arabidopsis *fc2* mutants has pointed out the defective assembly of PSII-LHCII supercomplexes in the *fc2* mutants, in addition to multiple decreased photosynthetic parameters (Espinas et al., 2016). The dominant photosynthetic machineries in *fc2-2* mutants revealed relatively higher accumulation of LHC proteins to the reaction center proteins. The authors explained the modified assembly with a perturbed overall heme production in the mutant lines (Espinas et al., 2016).

In this study, by applying BN-PAGE, the assembly of photosynthetic complexes in *fc2* mutants and FC2 overexpression lines was examined. The results verified the significant role of *FC2* expression in PSII-LHCII supercomplexes assembly. However, this crucial function of FC2 is likely to be independent from the overall heme accumulation in chloroplasts, as the three FC2 overexpressing plants (35SFC2, 35SFC2-CFP and FusB) exhibited same effects on the TBS pathway but different assembly of the PSII supercomplexes. The modified C-terminus of FC2 in the 35SFC2-CFP and FusB constructs suggested that the C-terminal extension, particularly the CAB domain, is a prerequisite for FC2 function in the assembly processes. There might be two possibilities for FC2 function in the assembly of the supercomplexes. On one hand, FC2 may interact with assembly factors for PSII supercomplexes, for instance, Psb28/ THF1 (Wang et al., 2004; Keren et al., 2005; Huang et al., 2013) or MET1 (Bhuiyan et al., 2015). Or FC2 itself acts as an auxiliary factor contributing to PSII-LHCII supercomplexes assembly, as the distinct CAB domain implies the potential of FC2 to bind chlorophyll molecules. On the other hand, so far, hemoproteins have already been characterized as factors involved in multiple photosynthetic processes (i.e. cytochromes) (Pakrasi et al., 1991; Morais et al., 2001; Baniulis et al., 2008). Due to the highly hydrophobic C-terminus, the sub-localization of FC2 may differ from FC1 on thylakoid membranes. The CAB domain might enable the type-II FC to be localized in the hydrophobic grana stacks ensuring FC2 to serve the heme pool for the assembly activities of PSII supercomplexes.

In plants, the most abundant peripheral antennae are the intrinsic chlorophyll a/b-binding light-harvesting complexes, encoded by a gene family of at least 10 *cab* genes (Hernandez-Prieto et al., 2011). Besides genes coding for light-harvesting proteins (LHCPs), the multi-gene family also includes gene sequences encoding light-harvesting like (LIL) proteins. Instead of absorbing light energy, LIL proteins are proposed to play function roles in photoprotection (Klimmek et al., 2006). In plants, the large LIL family consists of proteins

containing four membrane spanning helices (such as PsbS) (Li et al., 2000), three transmembrane α-helices (early light induced proteins, ELIPs) (Adamska and Kloppstech, 1991), two α-helices (stress enhanced proteins, SEPs) (Andersson et al., 2003), as well as proteins possessing one single membrane span (one helix protein, OHPs) (Garczarek et al., 2003; Hey and Grimm, 2018). Recent experiments have demonstrated the chlorophyll-binding ability of LIL proteins *in vitro* (Mork-Jansson et al., 2015; Staleva et al., 2015; Hey and Grimm, 2018; Mork-Jansson and Eichacker, 2018; Shukla et al., 2018). In cyanobacteria, the homologues of plant OHPs are designated as HliPs (high-light induced proteins) or SCPs (small CAB-like proteins), which are thought to be the evolutionary ancestors of eukaryotic CAB proteins (Garczarek et al., 2003). Thus, functional characterization of Hlips may shed light on the general function of CAB domain-containing proteins. Five coding sequences have been identified for HliPs in the cyanobacterium *Synechecystis* sp.PCC 6803. Four of them (*hlipA-D*) encode proteins of around 6kDa, while the fifth encodes the C-terminal extension of SynFC. The essential function of Hlips in stabilizing chlorophyll binding proteins has been well documented (Xu et al., 2002, 2004; Vavilin et al., 2005; Vavilin et al., 2007). Besides, a deletion of all Hlips in a PSI-less mutant led to decreased chlorophyll contents and oxidative stress, while Hlips deficiency in a wild-type or a PSII-deficient mutant background did not show visible effect (Funk and Vermaas, 1999; Xu et al., 2004; Vavilin et al., 2007). Thus it was proposed that Hlips probably serve as stabilizers of chlorophyll freed during assembly or repair of PSII. In addition, HliC and HliD were reported to function in the regulation of chlorophyll synthesis (Xu et al., 2002). It was speculated that the two Hlips contribute to regulating chlorophyll synthesis as a function of chlorophyll availability. Chlorophyll binding of HliC and HliD may be a signal of sufficient chlorophyll production in cells. When inadequate chlorophyll is produced for the binding of HliC and HliD, the TBS pathway may be activated.

Taken all together, the previous studies of CAB domain favored the hypothetical working model from this study (Figure 4.4). That is, Arabidopsis FC2, similar to its homologues in cyanobacteria, plays a significant role in serial photosynthetic activities from the prerequisite chlorophyll biosynthesis to the assembly of PSII-LHCII supercomplexes, in addition to heme production. These functions may not be compensated by FC1 due to the lack of CAB domain.

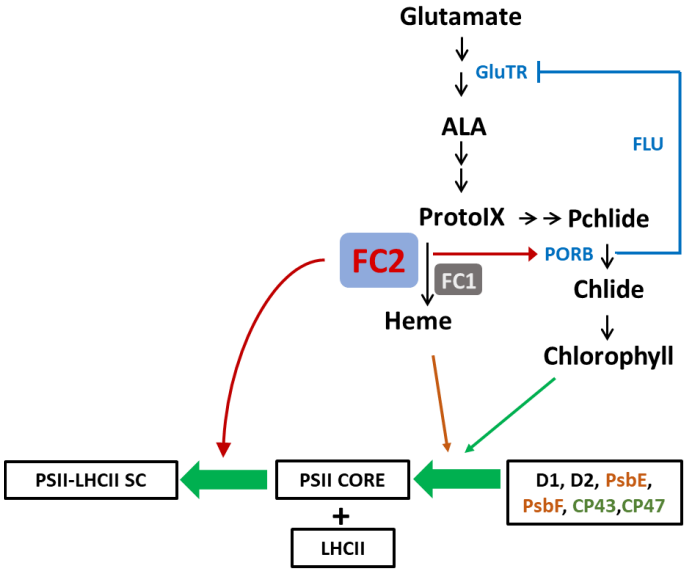

Figure 4. 4 The mechanism of action of FC2 on photosynthesis regulation.
In chloroplasts, both FC1 and FC2 isoforms catalyze the insertion of ferrous iron into Proto to yield heme. As the prerequisite step for photosynthesis, chlorophyll synthesis is regulated by FC2 expression via the assembly of POR-FLU-GluTR complex. Once synthesized, both heme and chlorophyll contribute to the assembly of PSII core complex. However, subsequent assembly of PSII-LHCII supercomplexes requires the presence of FC2 but not FC1.PSII-LHCII SC: PSII-LHCII supercomplexes. Among the subunits of PSII core, heme and chlorophyll-binding proteins were indicated in yellow and green respectively.

4.4 FC1 ability to compensate functional loss of FC2

4.4.1 FC1 could fully replace FC2 activity with a *pFC2*-driven expression.

In addition to the diverse expression profiles of both *FC* genes in different Arabidopsis organisms, *FC1* and *FC2* were also classified into different gene clusters based on their expression in terms of endogenous rhythm (Matsumoto et al., 2004). *FC1* expression was grouped into cluster 3, which genes show a constitutive expression pattern independently from any diurnal or circadian rhythm. *FC2* exhibits a light-inducible expression, was classified into cluster 2 representing TBS genes expressed in a diurnal-rhythm-dependent manner.

In the presented study, the *fc2* null mutants were complemented by *FC1* or *FC2* expression driven by a *FC2* native promoter. Growth under CL condition revealed a full complementation of FC2 deficiency by the expression of either FC isoform (Figure 3.5). Regardless of the critical regulatory function of FC2 under day-night conditions, the results indicated that *FC1*, when expressed under the *pFC2* promoter, is able to produce sufficient FC activity to fulfill the heme demand for all cellular processes in Arabidopsis. It seems that the two FC isoforms utilize the same Proto pool. Moreover, FC1 could also serve the regular "FC2-heme pool" under light exposure, which implied that heme

produced by FC1 could also be utilized for all photosynthesis processes, while the *FC2* promoter enables it to make the predominant FC activity in chloroplasts during daytime.

4.4.2 *FC1* expression is not able to substitute FC2 regulatory roles in TBS pathway and photosynthetic assembly.

Although the *pFC2*-driven *FC1* expression was able to fully compensate the functional loss of FC2 under constant light exposure, the necrotic leaves and retarded growth of pFC2FC1 (*fc2/fc2*) seedlings under light-dark condition indicated functional differences of both FC isoforms, in addition to their varying promoter activities. The presented study has pointed out the essential functions of FC2 in chlorophyll biosynthesis and PSII-LHCII supercomplexes assembly. These functions, however, could not be substituted by *FC1* expression, even under a *pFC2* promoter. Results from this study implied that the CAB domain contributes to FC2 an important role in the assembly of PSII supercomplexes, while it remains unknown which characteristics distinguish FC2 from FC1 to regulate chlorophyll synthesis or, in other words, to interact with PORB in plastids. It could be possible that the CAB domain is responsible for the interaction between FC2 and PORB, but whether it is attributable to a direct binding of the CAB domain to PORB, or the distinct sub-localization of FC2 defined by the hydrophobic motif, remains an open question.

For that, sub-localizations of both FC isoforms in different membrane fractions need to be analyzed. Intact wild-type chloroplasts could be extracted and purified via a Percoll gradient. The membrane pellet can be fractionated into envelope and thylakoid membranes through a discontinuous sucrose gradient. Although current reviews favored an exclusive thylakoid sub-localization for plastidal FC, as its activity was shown to be detectable only on thylakoid but not envelope membrane in pea chloroplasts (Matringe et al., 1994), one cannot exclude the existence of an envelope-FC fraction, since an *in vitro* import of cucumber FC precursors showed a small portion of mature FC proteins in envelope fractions (Suzuki et al., 2002). To further sub-fractionate thylakoids, detergents such as digitonin and Triton X-100 will be used. Subsequent ultracentrifugation allows the separation of grana core, grana margins and stroma lamellae. This part of work is already in process to obtain a hint for the spatial functional distributions of the two FC isoforms in chloroplast sub-compartments.

Additionally, the responsible domains for the interaction between FC2 and PORB need to be elucidated. So far, the results from this study proposed a significant role of CAB domain in the regulation of TBS pathway. A truncated FC2 fragment without the CAB domain has been amplified and inserted into certain plasmids which will be used for yeast two hybrid screening and BiFC experiments.

4.5 What defines the functional differences between FC1 and FC2?

Protein isoforms are proteins that share similarities in amino acids sequences, usually play similar biological functions within cells. Protein variants could be products from either one single gene or multiple gene copies. Through alternative RNA splicing or using variable promoters of the same gene sequence, two or more allozymes could be produced. Besides, isoforms could also be encoded by different genetic loci, which usually arise through gene duplication and divergence (Berg et al., 2006). These isozymes catalyze the same chemical reaction, but often display altered kinetic parameters. The existence of isozymes allows the fine-tuning of metabolism to meet the particular needs in certain tissues or at diverse developmental stages.

The two genes, *FC1* and *FC2*, encode FC isoforms in plants. The basis for the requirement for two FCs in plants awaits elucidation. The disparate expression profiles of the two *FC* genes point to distinct roles of the two isoforms in different organs and developmental stages (Smith et al., 1994; Chow et al., 1998; Singh et al., 2002; Nagai et al., 2007). This study concluded that, in Arabidopsis, either FC can supply sufficient heme to complete embryo morphogenesis. Only when the embryo becomes photosynthetically active and begins to accumulate pigments and nutrients for subsequent germination, is the *FC1* promoter required to ensure that enough FC is produced to provide the level of heme synthesis necessary for embryo maturation.

During chloroplast biogenesis, heme and chlorophyll synthesis share the conserved TBS pathway from ALA formation to the production of Proto. Under normal growth conditions, either FC protein is able to synthesize adequate heme for leaf cells to accomplish all the cellular processes under light exposure. Only the light inducible promoter of *FC2* defines it as the predominant FC in photosynthetic tissues. The complementation studies of *fc2* null mutants illustrated that *FC1* expression driven by the *pFC2* promoter can partially rescue *fc2* mutants, indicating the *FC2* promoter is apparently not the only factor responsible for the predominance of FC2 in leaves. The interaction between PORB and FC2, but not between PORB and FC1, reveals that FC2 plays a specific regulatory role in ALA synthesis, as well as in the TBS pathway. In terms of that, the alignment of both FC protein sequences suggested a distinct CAB domain in FC2, which may contribute to this distinct function of FC2 in leaf tissues.

In this study, by taking advantage of all sets of *fc1* (*fc2*) mutants and complemented plants, it could be concluded that a lack of FC1-produced heme does not alter the photosynthetic complexes, while FC2 deficiency causes compromised photosynthetic parameters as well as complexes assembly. These results are in agreement with the previous studies demonstrating that FC2 supplies the vast bulk of heme in photosynthetic tissues. Additionally, the characterization of multiple FC2 overexpressing (35SFC2, 35SFC2-CFPand FusB) plants revealed the significance of FC2 presence, particularly CAB domain of FC2, on regulation of PSII-LHCII complexes assembly. The type-I FC isoform failed to substitute this regulatory role probably due to the lack of the CAB domain.

Although both promoter activity and the specific CAB domain define FC2 as the predominant FC isoform during chloroplast development, plants require FC1-produced heme to cope with abiotic stress. When exposed to stress, FC1-produced heme negatively regulates the expression of *CCE*s to suppress chlorophyll degradation and leaf senescence, contributing to plant defense. However, FC2 is not able to fulfill this function role, due to the low promoter activity and transcript stability under stress conditions. Global transcriptome analyses regarding stress response have been performed in yeast (Romero-Santacreu et al., 2009), plants (Kreps et al., 2002; Kurihara et al., 2009) and human cells (Fan et al., 2002). The steady-state of mRNA abundancy under stress reveals the mRNA destabilization at both transcriptional and posttranscriptional level (Kawa and Testerink, 2017). According to the current data, there may exist a posttranscriptional regulation of *FC2* transcript in Arabidopsis under stress treatment, as it might be transcribed and temporarily accumulated under *FC1* promoter. But by which transcription factor, and what mRNA trait of *FC2* contributes to this specific regulation need to be elucidated.

References

1. Abraham NG, Camadro JM, Hoffstein ST, Levere RD (1986) Effects of iron deficiency and chronic iron overloading on mitochondrial heme biosynthetic enzymes in rat liver. Biochim Biophys Acta 870: 339-349
2. Adamska I, Kloppstech K (1991) Evidence for an association of the early light-inducible protein (ELIP) of pea with photosystem II. Plant Mol Biol 16: 209-223
3. Adhikari ND, Froehlich JE, Strand DD, Buck SM, Kramer DM, Larkin RM (2011) GUN4-porphyrin complexes bind the ChlH/GUN5 subunit of Mg-Chelatase and promote chlorophyll biosynthesis in Arabidopsis. Plant Cell 23: 1449-1467
4. Alawady A, Reski R, Yaronskaya E, Grimm B (2005) Cloning and expression of the tobacco CHLM sequence encoding Mg protoporphyrin IX methyltransferase and its interaction with Mg chelatase. Plant Mol Biol 57: 679-691
5. Alfonso-Prieto M, Biarnes X, Vidossich P, Rovira C (2009) The molecular mechanism of the catalase reaction. J Am Chem Soc 131: 11751-11761
6. Alfonso-Prieto M, Vidossich P, Rovira C (2012) The reaction mechanisms of heme catalases: an atomistic view by ab initio molecular dynamics. Arch Biochem Biophys 525: 121-130
7. Andersson U, Heddad M, Adamska I (2003) Light stress-induced one-helix protein of the chlorophyll a/b-binding family associated with photosystem I. Plant Physiol 132: 811-820
8. Ang LH, Chattopadhyay S, Wei N, Oyama T, Okada K, Batschauer A, Deng XW (1998) Molecular interaction between COP1 and HY5 defines a regulatory switch for light control of Arabidopsis development. Mol Cell 1: 213-222
9. Anzaldi LL, Skaar EP (2010) Overcoming the heme paradox: heme toxicity and tolerance in bacterial pathogens. Infect Immun 78: 4977-4989
10. Apchelimov AA, Soldatova OP, Ezhova TA, Grimm B, Shestakov SV (2007) The analysis of the ChlI 1 and ChlI 2 genes using acifluorfen-resistant mutant of Arabidopsis thaliana. Planta 225: 935-943
11. Apel K (1981) The protochlorophyllide holochrome of barley (Hordeum vulgare L.). Phytochrome-induced decrease of translatable mRNA coding for the NADPH: protochlorophyllide oxidoreductase. Eur J Biochem 120: 89-93
12. Apitz J, Nishimura K, Schmied J, Wolf A, Hedtke B, van Wijk KJ, Grimm B (2016) Posttranslational Control of ALA Synthesis Includes GluTR Degradation by Clp Protease and Stabilization by GluTR-Binding Protein. Plant Physiol 170: 2040-2051
13. Apitz J, Schmied J, Lehmann MJ, Hedtke B, Grimm B (2014) GluTR2 complements a hema1 mutant lacking glutamyl-tRNA reductase 1, but is differently regulated at the post-translational level. Plant Cell Physiol 55: 645-657

14. Armstrong GA, Runge S, Frick G, Sperling U, Apel K (1995) Identification of NADPH:protochlorophyllide oxidoreductases A and B: a branched pathway for light-dependent chlorophyll biosynthesis in Arabidopsis thaliana. Plant Physiol 108: 1505-1517

15. Baniulis D, Yamashita E, Zhang H, Hasan SS, Cramer WA (2008) Structure-function of the cytochrome b6f complex. Photochem Photobiol 84: 1349-1358

16. Bansal N, Kanwar SS (2013) Peroxidase(s) in environment protection. ScientificWorldJournal 2013: 714639

17. Baruah A, Simkova K, Apel K, Laloi C (2009) Arabidopsis mutants reveal multiple singlet oxygen signaling pathways involved in stress response and development. Plant Mol Biol 70: 547-563

18. Benli M, Schulz R, Apel K (1991) Effect of light on the NADPH-protochlorophyllide oxidoreductase of Arabidopsis thaliana. Plant Mol Biol 16: 615-625

19. Berg JM, Tymoczko JL, Stryer L (2006) Biochemistry. W.H. Freeman, New York

20. Bhuiyan NH, Friso G, Poliakov A, Ponnala L, van Wijk KJ (2015) MET1 is a thylakoid-associated TPR protein involved in photosystem II supercomplex formation and repair in Arabidopsis. Plant Cell 27: 262-285

21. Block MA, Tewari AK, Albrieux C, Marechal E, Joyard J (2002) The plant S-adenosyl-L-methionine:Mg-protoporphyrin IX methyltransferase is located in both envelope and thylakoid chloroplast membranes. Eur J Biochem 269: 240-248

22. Bollivar DW, Jiang ZY, Bauer CE, Beale SI (1994) Heterologous expression of the bchM gene product from Rhodobacter capsulatus and demonstration that it encodes S-adenosyl-L-methionine:Mg-protoporphyrin IX methyltransferase. J Bacteriol 176: 5290-5296

23. Bollivar DW, Suzuki JY, Beatty JT, Dobrowolski JM, Bauer CE (1994) Directed mutational analysis of bacteriochlorophyll a biosynthesis in Rhodobacter capsulatus. J Mol Biol 237: 622-640

24. Borisjuk L, Rolletschek H (2009) The oxygen status of the developing seed. New Phytol 182: 17-30

25. Bowman SE, Bren KL (2008) The chemistry and biochemistry of heme c: functional bases for covalent attachment. Nat Prod Rep 25: 1118-1130

26. Burke DH, Alberti M, Hearst JE (1993) bchFNBH bacteriochlorophyll synthesis genes of Rhodobacter capsulatus and identification of the third subunit of light-independent protochlorophyllide reductase in bacteria and plants. J Bacteriol 175: 2414-2422

27. Burmester T, Hankeln T (2014) Function and evolution of vertebrate globins. Acta Physiol (Oxf) 211: 501-514

28. Camadro JM, Labbe P (1982) Kinetic studies of ferrochelatase in yeast. Zinc or iron as competing substrates. Biochim Biophys Acta 707: 280-288

29. Camadro JM, Labbe P (1988) Purification and properties of ferrochelatase from the yeast Saccharomyces cerevisiae. Evidence for a precursor form of the protein. J Biol Chem 263: 11675-11682

30. Carrie C, Giraud E, Whelan J (2009) Protein transport in organelles: Dual targeting of proteins to mitochondria and chloroplasts. FEBS J 276: 1187-1195

31. Carrie C, Small I (2013) A reevaluation of dual-targeting of proteins to mitochondria and chloroplasts. Biochim Biophys Acta 1833: 253-259

32. Castelfranco PA, Zeng X (1991) Regulation of 5-Aminolevulinic Acid Synthesis in Developing Chloroplasts : IV. An Endogenous Inhibitor from the Thylakoid Membranes. Plant Physiol 97: 1-6

33. Castillon A, Shen H, Huq E (2007) Phytochrome Interacting Factors: central players in phytochrome-mediated light signaling networks. Trends Plant Sci 12: 514-521

34. Choquet Y, Rahire M, Girard-Bascou J, Erickson J, Rochaix JD (1992) A chloroplast gene is required for the light-independent accumulation of chlorophyll in Chlamydomonas reinhardtii. EMBO J 11: 1697-1704

35. Chow KS, Singh DP, Roper JM, Smith AG (1997) A single precursor protein for ferrochelatase-I from Arabidopsis is imported in vitro into both chloroplasts and mitochondria. J Biol Chem 272: 27565-27571

36. Chow KS, Singh DP, Walker AR, Smith AG (1998) Two different genes encode ferrochelatase in Arabidopsis: mapping, expression and subcellular targeting of the precursor proteins. Plant J 15: 531-541

37. Chu HA, Chiu YF (2015) The Roles of Cytochrome b 559 in Assembly and Photoprotection of Photosystem II Revealed by Site-Directed Mutagenesis Studies. Front Plant Sci 6: 1261

38. Czarnecki O, Grimm B (2012) Post-translational control of tetrapyrrole biosynthesis in plants, algae, and cyanobacteria. J Exp Bot 63: 1675-1687

39. Czarnecki O, Grimm B (2013) New insights in the topology of the biosynthesis of 5-aminolevulinic acid. Plant Signal Behav 8: e23124

40. Czarnecki O, Hedtke B, Melzer M, Rothbart M, Richter A, Schroter Y, Pfannschmidt T, Grimm B (2011) An Arabidopsis GluTR binding protein mediates spatial separation of 5-aminolevulinic acid synthesis in chloroplasts. Plant Cell 23: 4476-4491

41. Dahlin C, Sundqvist C, Timko MP (1995) The in vitro assembly of the NADPH-protochlorophyllide oxidoreductase in pea chloroplasts. Plant Mol Biol 29: 317-330

42. Daudi A, O'Brien JA (2012) Detection of Hydrogen Peroxide by DAB Staining in Arabidopsis Leaves. Bio Protoc 2

43. Davison PA, Schubert HL, Reid JD, Iorg CD, Heroux A, Hill CP, Hunter CN (2005) Structural and biochemical characterization of Gun4 suggests a mechanism for its role in chlorophyll biosynthesis. Biochemistry 44: 7603-7612

44. Davletova S, Schlauch K, Coutu J, Mittler R (2005) The zinc-finger protein Zat12 plays a central role in reactive oxygen and abiotic stress signaling in Arabidopsis. Plant Physiol 139: 847-856

45. de Armas-Ricard M, Levican G, Katz A, Moser J, Jahn D, Orellana O (2011) Cellular levels of heme affect the activity of dimeric glutamyl-tRNA reductase. Biochem Biophys Res Commun 405: 134-139

46. Delker C, Sonntag L, James GV, Janitza P, Ibanez C, Ziermann H, Peterson T, Denk K, Mull S, Ziegler J, Davis SJ, Schneeberger K, Quint M (2014) The DET1-COP1-HY5 pathway constitutes a multipurpose signaling module regulating plant photomorphogenesis and thermomorphogenesis. Cell Rep 9: 1983-1989

47. Espinas NA, Kobayashi K, Sato Y, Mochizuki N, Takahashi K, Tanaka R, Masuda T (2016) Allocation of Heme Is Differentially Regulated by Ferrochelatase Isoforms in Arabidopsis Cells. Front Plant Sci 7: 1326

48. Fan J, Yang X, Wang W, Wood WH, 3rd, Becker KG, Gorospe M (2002) Global analysis of stress-regulated mRNA turnover by using cDNA arrays. Proc Natl Acad Sci U S A 99: 10611-10616

49. Fang Y, Zhao S, Zhang F, Zhao A, Zhang W, Zhang M, Liu L (2016) The Arabidopsis glutamyl-tRNA reductase (GluTR) forms a ternary complex with FLU and GluTR-binding protein. Sci Rep 6: 19756

50. Ferreira GC, Andrew TL, Karr SW, Dailey HA (1988) Organization of the terminal two enzymes of the heme biosynthetic pathway. Orientation of protoporphyrinogen oxidase and evidence for a membrane complex. J Biol Chem 263: 3835-3839

51. Fluhr R, Harel E, Klein S, Meller E (1975) Control of delta-Aminolevulinic Acid and Chlorophyll Accumulation in Greening Maize Leaves upon Light-Dark Transitions. Plant Physiol 56: 497-501

52. Fodje MN, Hansson A, Hansson M, Olsen JG, Gough S, Willows RD, Al-Karadaghi S (2001) Interplay between an AAA module and an integrin I domain may regulate the function of magnesium chelatase. J Mol Biol 311: 111-122

53. Ford MJ, Kasemir H (1980) Correlation between 5-aminolaevulinate accumulation and protochlorophyll photoconversion. Planta 150: 206-210

54. Forreiter C, van Cleve B, Schmidt A, Apel K (1991) Evidence for a general light-dependent negative control of NADPH-protochlorophyllide oxidoreductase in angiosperms. Planta 183: 126-132

55. Franck F, Sperling U, Frick G, Pochert B, van Cleve B, Apel K, Armstrong GA (2000) Regulation of etioplast pigment-protein complexes, inner membrane architecture, and protochlorophyllide a chemical heterogeneity by light-dependent NADPH:protochlorophyllide oxidoreductases A and B. Plant Physiol 124: 1678-1696

56. Frick G, Su Q, Apel K, Armstrong GA (2003) An Arabidopsis porB porC double mutant lacking light-dependent NADPH:protochlorophyllide oxidoreductases B and C is highly chlorophyll-deficient and developmentally arrested. Plant J 35: 141-153

57. Frustaci JM, O'Brian MR (1992) Characterization of a Bradyrhizobium japonicum ferrochelatase mutant and isolation of the hemH gene. J Bacteriol 174: 4223-4229

58. Fujita Y (1996) Protochlorophyllide reduction: a key step in the greening of plants. Plant Cell Physiol 37: 411-421

59. Fujita Y, Bauer CE (2000) Reconstitution of light-independent protochlorophyllide reductase from purified bchl and BchN-BchB subunits. In vitro confirmation of nitrogenase-like features of a bacteriochlorophyll biosynthesis enzyme. J Biol Chem 275: 23583-23588

60. Fujita Y, Matsumoto H, Takahashi Y, Matsubara H (1993) Identification of a nifDK-like gene (ORF467) involved in the biosynthesis of chlorophyll in the cyanobacterium Plectonema boryanum. Plant Cell Physiol 34: 305-314

61. Fujita Y, Takagi H, Hase T (1996) Identification of the chlB gene and the gene product essential for the light-independent chlorophyll biosynthesis in the cyanobacterium Plectonema boryanum. Plant Cell Physiol 37: 313-323

62. Fujita Y, Takagi H, Hase T (1998) Cloning of the gene encoding a protochlorophyllide reductase: the physiological significance of the co-existence of light-dependent and -independent protochlorophyllide reduction systems in the cyanobacterium Plectonema boryanum. Plant Cell Physiol 39: 177-185

63. Funk C, Vermaas W (1999) A cyanobacterial gene family coding for single-helix proteins resembling part of the light-harvesting proteins from higher plants. Biochemistry 38: 9397-9404

64. Fusada N, Masuda T, Kuroda H, Shiraishi T, Shimada H, Ohta H, Takamiya K (2000) NADPH-protochlorophyllide oxidoreductase in cucumber is encoded by a single gene and its expression is transcriptionally enhanced by illumination. Photosynth Res 64: 147-154

65. Garczarek L, Poupon A, Partensky F (2003) Origin and evolution of transmembrane Chl-binding proteins: hydrophobic cluster analysis suggests a common one-helix ancestor for prokaryotic (Pcb) and eukaryotic (LHC) antenna protein superfamilies. FEMS Microbiol Lett 222: 59-68

66. Ge C, Spanning E, Glaser E, Wieslander A (2014) Import determinants of organelle-specific and dual targeting peptides of mitochondria and chloroplasts in Arabidopsis thaliana. Mol Plant 7: 121-136

67. Gibson KD, Neuberger A, Tait GH (1963) Studies on the Biosynthesis of Porphyrin and Bacteriochlorophyll by Rhodopseudomonas Spheroides. 4. S-Adenosylmethioninemagnesium Protoporphyrin Methyltransferase. Biochem J 88: 325-334

68. Gibson LC, Hunter CN (1994) The bacteriochlorophyll biosynthesis gene, bchM, of Rhodobacter sphaeroides encodes S-adenosyl-L-methionine: Mg protoporphyrin IX methyltransferase. FEBS Lett 352: 127-130

69. Gibson LC, Jensen PE, Hunter CN (1999) Magnesium chelatase from Rhodobacter sphaeroides: initial characterization of the enzyme using purified subunits and evidence for a BchI-BchD complex. Biochem J 337 (Pt 2): 243-251

70. Gietz RD, Schiestl RH (2007) Large-scale high-efficiency yeast transformation using the LiAc/SS carrier DNA/PEG method. Nat Protoc 2: 38-41

71. Girvan HM, Munro AW (2013) Heme sensor proteins. J Biol Chem 288: 13194-13203

72. Gorchein A (1972) Magnesium protoporphyrin chelatase activity in Rhodopseudomonas spheroides. Studies with whole cells. Biochem J 127: 97-106

73. Goslings D, Meskauskiene R, Kim C, Lee KP, Nater M, Apel K (2004) Concurrent interactions of heme and FLU with Glu tRNA reductase (HEMA1), the target of metabolic feedback inhibition of tetrapyrrole biosynthesis, in dark- and light-grown Arabidopsis plants. Plant J 40: 957-967

74. Hansson M, Hederstedt L (1992) Cloning and characterization of the Bacillus subtilis hemEHY gene cluster, which encodes protoheme IX biosynthetic enzymes. J Bacteriol 174: 8081-8093

75. Hansson M, Kannangara CG (1997) ATPases and phosphate exchange activities in magnesium chelatase subunits of Rhodobacter sphaeroides. Proc Natl Acad Sci U S A 94: 13351-13356

76. Hansson M, von Wachenfeldt C (1993) Heme b (protoheme IX) is a precursor of heme a and heme d in Bacillus subtilis. FEMS Microbiol Lett 107: 121-125

77. Hardison RC (2012) Evolution of hemoglobin and its genes. Cold Spring Harb Perspect Med 2: a011627

78. Hauser I, Dehesh K, Apel K (1984) The proteolytic degradation in vitro of the NADPH-protochlorophyllide oxidoreductase of barley (Hordeum vulgare L.). Arch Biochem Biophys 228: 577-586

79. Hederstedt L (2012) Heme A biosynthesis. Biochim Biophys Acta 1817: 920-927

80. Hernandez-Prieto MA, Tibiletti T, Abasova L, Kirilovsky D, Vass I, Funk C (2011) The small CAB-like proteins of the cyanobacterium Synechocystis sp. PCC 6803: their involvement in chlorophyll biogenesis for Photosystem II. Biochim Biophys Acta 1807: 1143-1151

81. Hey D, Grimm B (2018) Requirement of ONE-HELIX PROTEIN 1 (OHP1) in early Arabidopsis seedling development and under high light intensity. Plant Signal Behav: 1-3

82. Hey D, Ortega-Rodes P, Fan T, Schnurrer F, Brings L, Hedtke B, Grimm B (2016) Transgenic Tobacco Lines Expressing Sense or Antisense FERROCHELATASE 1 RNA

Show Modified Ferrochelatase Activity in Roots and Provide Experimental Evidence for Dual Localization of Ferrochelatase 1. Plant Cell Physiol 57: 2576-2585

83. Hey D, Rothbart M, Herbst J, Wang P, Muller J, Wittmann D, Gruhl K, Grimm B (2017) LIL3, a Light-Harvesting Complex Protein, Links Terpenoid and Tetrapyrrole Biosynthesis in Arabidopsis thaliana. Plant Physiol 174: 1037-1050
84. Hinchigeri SB, Hundle B, Richards WR (1997) Demonstration that the BchH protein of Rhodobacter capsulatus activates S-adenosyl-L-methionine:magnesium protoporphyrin IX methyltransferase. FEBS Lett 407: 337-342
85. Holm M, Ma LG, Qu LJ, Deng XW (2002) Two interacting bZIP proteins are direct targets of COP1-mediated control of light-dependent gene expression in Arabidopsis. Genes Dev 16: 1247-1259
86. Holtorf H, Reinbothe S, Reinbothe C, Bereza B, Apel K (1995) Two routes of chlorophyllide synthesis that are differentially regulated by light in barley (Hordeum vulgare L.). Proc Natl Acad Sci U S A 92: 3254-3258
87. Hon T, Hach A, Lee HC, Cheng T, Zhang L (2000) Functional analysis of heme regulatory elements of the transcriptional activator Hap1. Biochem Biophys Res Commun 273: 584-591
88. Hon T, Hach A, Tamalis D, Zhu Y, Zhang L (1999) The yeast heme-responsive transcriptional activator Hap1 is a preexisting dimer in the absence of heme. J Biol Chem 274: 22770-22774
89. Hou S, Reynolds MF, Horrigan FT, Heinemann SH, Hoshi T (2006) Reversible binding of heme to proteins in cellular signal transduction. Acc Chem Res 39: 918-924
90. Huang L, Castelfranco PA (1989) Regulation of 5-aminolevulinic Acid synthesis in developing chloroplasts : I. Effect of light/dark treatments in vivo and in organello. Plant Physiol 90: 996-1002
91. Huang W, Chen Q, Zhu Y, Hu F, Zhang L, Ma Z, He Z, Huang J (2013) Arabidopsis thylakoid formation 1 is a critical regulator for dynamics of PSII-LHCII complexes in leaf senescence and excess light. Mol Plant 6: 1673-1691
92. Huang YS, Li HM (2009) Arabidopsis CHLI2 can substitute for CHLI1. Plant Physiol 150: 636-645
93. Hung CH, Huang JY, Chiu YF, Chu HA (2007) Site-directed mutagenesis on the heme axial-ligands of cytochrome b559 in photosystem II by using cyanobacteria Synechocystis PCC 6803. Biochim Biophys Acta 1767: 686-693
94. Hung CH, Hwang HJ, Chen YH, Chiu YF, Ke SC, Burnap RL, Chu HA (2010) Spectroscopic and functional characterizations of cyanobacterium Synechocystis PCC 6803 mutants on and near the heme axial ligand of cytochrome b559 in photosystem II. J Biol Chem 285: 5653-5663

95. Huq E, Al-Sady B, Hudson M, Kim C, Apel K, Quail PH (2004) Phytochrome-interacting factor 1 is a critical bHLH regulator of chlorophyll biosynthesis. Science 305: 1937-1941

96. Ishijima S, Uchibori A, Takagi H, Maki R, Ohnishi M (2003) Light-induced increase in free Mg2+ concentration in spinach chloroplasts: measurement of free Mg2+ by using a fluorescent probe and necessity of stromal alkalinization. Arch Biochem Biophys 412: 126-132

97. Jarvi S, Suorsa M, Paakkarinen V, Aro EM (2011) Optimized native gel systems for separation of thylakoid protein complexes: novel super- and mega-complexes. Biochem J 439: 207-214

98. Jensen PE, Gibson LC, Hunter CN (1999) ATPase activity associated with the magnesium-protoporphyrin IX chelatase enzyme of Synechocystis PCC6803: evidence for ATP hydrolysis during Mg2+ insertion, and the MgATP-dependent interaction of the ChlI and ChlD subunits. Biochem J 339 (Pt 1): 127-134

99. Jones AM, Elliott T (2010) A purified mutant HemA protein from Salmonella enterica serovar Typhimurium lacks bound heme and is defective for heme-mediated regulation in vivo. FEMS Microbiol Lett 307: 41-47

100. Jones P (2001) Roles of water in heme peroxidase and catalase mechanisms. J Biol Chem 276: 13791-13796

101. Jung HS, Okegawa Y, Shih PM, Kellogg E, Abdel-Ghany SE, Pilon M, Sjolander K, Shikanai T, Niyogi KK (2010) Arabidopsis thaliana PGR7 encodes a conserved chloroplast protein that is necessary for efficient photosynthetic electron transport. PLoS One 5: e11688

102. Kang K, Lee K, Park S, Lee S, Kim Y, Back K (2010) Overexpression of Rice Ferrochelatase I and II Leads to Increased Susceptibility to Oxyfluorfen Herbicide in Transgenic Rice. Journal of Plant Biology 53: 291-296

103. Kanjo N, Nakahigashi K, Oeda K, Inokuchi H (2001) Isolation and characterization of a cDNA from soybean and its homolog from Escherichia coli, which both complement the light sensitivity of Escherichia coli hemH mutant strain VS101. Genes Genet Syst 76: 327-334

104. Karpinski S, Escobar C, Karpinska B, Creissen G, Mullineaux PM (1997) Photosynthetic electron transport regulates the expression of cytosolic ascorbate peroxidase genes in Arabidopsis during excess light stress. Plant Cell 9: 627-640

105. Kauss D, Bischof S, Steiner S, Apel K, Meskauskiene R (2012) FLU, a negative feedback regulator of tetrapyrrole biosynthesis, is physically linked to the final steps of the Mg(++)-branch of this pathway. FEBS Lett 586: 211-216

106. Kawa D, Testerink C (2017) Regulation of mRNA decay in plant responses to salt and osmotic stress. Cell Mol Life Sci 74: 1165-1176

107. Keren N, Ohkawa H, Welsh EA, Liberton M, Pakrasi HB (2005) Psb29, a conserved 22-kD protein, functions in the biogenesis of Photosystem II complexes in Synechocystis and Arabidopsis. Plant Cell 17: 2768-2781

108. Khan AA, Quigley JG (2011) Control of intracellular heme levels: heme transporters and heme oxygenases. Biochim Biophys Acta 1813: 668-682

109. Kikuchi G, Yoshida T, Noguchi M (2005) Heme oxygenase and heme degradation. Biochem Biophys Res Commun 338: 558-567

110. Kim J, Kimber MS, Nishimura K, Friso G, Schultz L, Ponnala L, van Wijk KJ (2015) Structures, Functions, and Interactions of ClpT1 and ClpT2 in the Clp Protease System of Arabidopsis Chloroplasts. Plant Cell 27: 1477-1496

111. Kirkman HN, Gaetani GF (1984) Catalase: a tetrameric enzyme with four tightly bound molecules of NADPH. Proc Natl Acad Sci U S A 81: 4343-4347

112. Kitamuro T, Takahashi K, Ogawa K, Udono-Fujimori R, Takeda K, Furuyama K, Nakayama M, Sun J, Fujita H, Hida W, Hattori T, Shirato K, Igarashi K, Shibahara S (2003) Bach1 functions as a hypoxia-inducible repressor for the heme oxygenase-1 gene in human cells. J Biol Chem 278: 9125-9133

113. Kleine T, Leister D (2016) Retrograde signaling: Organelles go networking. Biochim Biophys Acta 1857: 1313-1325

114. Klimmek F, Sjodin A, Noutsos C, Leister D, Jansson S (2006) Abundantly and rarely expressed Lhc protein genes exhibit distinct regulation patterns in plants. Plant Physiol 140: 793-804

115. Kobayashi K, Masuda T (2016) Transcriptional Regulation of Tetrapyrrole Biosynthesis in Arabidopsis thaliana. Front Plant Sci 7: 1811

116. Kobayashi K, Obayashi T, Masuda T (2012) Role of the G-box element in regulation of chlorophyll biosynthesis in Arabidopsis roots. Plant Signal Behav 7: 922-926

117. Koch M, Breithaupt C, Kiefersauer R, Freigang J, Huber R, Messerschmidt A (2004) Crystal structure of protoporphyrinogen IX oxidase: a key enzyme in haem and chlorophyll biosynthesis. EMBO J 23: 1720-1728

118. Komenda J, Sobotka R, Nixon PJ (2012) Assembling and maintaining the Photosystem II complex in chloroplasts and cyanobacteria. Curr Opin Plant Biol 15: 245-251

119. Koncz C, Mayerhofer R, Koncz-Kalman Z, Nawrath C, Reiss B, Redei GP, Schell J (1990) Isolation of a gene encoding a novel chloroplast protein by T-DNA tagging in Arabidopsis thaliana. EMBO J 9: 1337-1346

120. Koreny L, Obornik M, Lukes J (2013) Make it, take it, or leave it: heme metabolism of parasites. PLoS Pathog 9: e1003088

121. Koreny L, Sobotka R, Kovarova J, Gnipova A, Flegontov P, Horvath A, Obornik M, Ayala FJ, Lukes J (2012) Aerobic kinetoplastid flagellate Phytomonas does not require heme for viability. Proc Natl Acad Sci U S A 109: 3808-3813

122. Kreps JA, Wu Y, Chang HS, Zhu T, Wang X, Harper JF (2002) Transcriptome changes for Arabidopsis in response to salt, osmotic, and cold stress. Plant Physiol 130: 2129-2141

123. Kruse E, Mock HP, Grimm B (1997) Isolation and characterisation of tobacco (Nicotiana tabacum) cDNA clones encoding proteins involved in magnesium chelation into protoporphyrin IX. Plant Mol Biol 35: 1053-1056

124. Kurihara Y, Kaminuma E, Matsui A, Kawashima M, Tanaka M, Morosawa T, Ishida J, Mochizuki Y, Shinozaki K, Toyoda T, Seki M (2009) Transcriptome analyses revealed diverse expression changes in ago1 and hyl1 Arabidopsis mutants. Plant Cell Physiol 50: 1715-1720

125. Kwast KE, Burke PV, Poyton RO (1998) Oxygen sensing and the transcriptional regulation of oxygen-responsive genes in yeast. J Exp Biol 201: 1177-1195

126. Labbe-Bois R (1990) The ferrochelatase from Saccharomyces cerevisiae. Sequence, disruption, and expression of its structural gene HEM15. J Biol Chem 265: 7278-7283

127. Lan C, Lee HC, Tang S, Zhang L (2004) A novel mode of chaperone action: heme activation of Hap1 by enhanced association of Hsp90 with the repressed Hsp70-Hap1 complex. J Biol Chem 279: 27607-27612

128. Langner U, Baudisch B, Klosgen RB (2014) Organelle import of proteins with dual targeting properties into mitochondria and chloroplasts takes place by the general import pathways. Plant Signal Behav 9: e29301

129. Larkin RM, Alonso JM, Ecker JR, Chory J (2003) GUN4, a regulator of chlorophyll synthesis and intracellular signaling. Science 299: 902-906

130. Layer G, Reichelt J, Jahn D, Heinz DW (2010) Structure and function of enzymes in heme biosynthesis. Protein Sci 19: 1137-1161

131. Lee HJ, Mochizuki N, Masuda T, Buckhout TJ (2012) Disrupting the bimolecular binding of the haem-binding protein 5 (AtHBP5) to haem oxygenase 1 (HY1) leads to oxidative stress in Arabidopsis. J Exp Bot 63: 5967-5978

132. Lee J, He K, Stolc V, Lee H, Figueroa P, Gao Y, Tongprasit W, Zhao H, Lee I, Deng XW (2007) Analysis of transcription factor HY5 genomic binding sites revealed its hierarchical role in light regulation of development. Plant Cell 19: 731-749

133. Lee KP, Kim C, Lee DW, Apel K (2003) TIGRINA d, required for regulating the biosynthesis of tetrapyrroles in barley, is an ortholog of the FLU gene of Arabidopsis thaliana. FEBS Lett 553: 119-124

134. Leivar P, Tepperman JM, Monte E, Calderon RH, Liu TL, Quail PH (2009) Definition of early transcriptional circuitry involved in light-induced reversal of PIF-imposed repression of photomorphogenesis in young Arabidopsis seedlings. Plant Cell 21: 3535-3553

135. Lermontova I, Kruse E, Mock HP, Grimm B (1997) Cloning and characterization of a plastidal and a mitochondrial isoform of tobacco protoporphyrinogen IX oxidase. Proc Natl Acad Sci U S A 94: 8895-8900

136. Li D, Stuehr DJ, Yeh SR, Rousseau DL (2004) Heme distortion modulated by ligand-protein interactions in inducible nitric-oxide synthase. J Biol Chem 279: 26489-26499

137. Li XP, Bjorkman O, Shih C, Grossman AR, Rosenquist M, Jansson S, Niyogi KK (2000) A pigment-binding protein essential for regulation of photosynthetic light harvesting. Nature 403: 391-395

138. Lister R, Chew O, Rudhe C, Lee MN, Whelan J (2001) Arabidopsis thaliana ferrochelatase-I and -II are not imported into Arabidopsis mitochondria. FEBS Lett 506: 291-295

139. Liu X, Chen CY, Wang KC, Luo M, Tai R, Yuan L, Zhao M, Yang S, Tian G, Cui Y, Hsieh HL, Wu K (2013) PHYTOCHROME INTERACTING FACTOR3 associates with the histone deacetylase HDA15 in repression of chlorophyll biosynthesis and photosynthesis in etiolated Arabidopsis seedlings. Plant Cell 25: 1258-1273

140. Masoumi A, Heinemann IU, Rohde M, Koch M, Jahn M, Jahn D (2008) Complex formation between protoporphyrinogen IX oxidase and ferrochelatase during haem biosynthesis in Thermosynechococcus elongatus. Microbiology 154: 3707-3714

141. Masuda S, Ikeda R, Masuda T, Hashimoto H, Tsuchiya T, Kojima H, Nomata J, Fujita Y, Mimuro M, Ohta H, Takamiya K (2009) Prolamellar bodies formed by cyanobacterial protochlorophyllide oxidoreductase in Arabidopsis. Plant J 58: 952-960

142. Masuda T, Fusada N, Oosawa N, Takamatsu K, Yamamoto YY, Ohto M, Nakamura K, Goto K, Shibata D, Shirano Y, Hayashi H, Kato T, Tabata S, Shimada H, Ohta H, Takamiya K (2003) Functional analysis of isoforms of NADPH: protochlorophyllide oxidoreductase (POR), PORB and PORC, in Arabidopsis thaliana. Plant Cell Physiol 44: 963-974

143. Masuda T, Fusada N, Shiraishi T, Kuroda H, Awai K, Shimada H, Ohta H, Takamiya K (2002) Identification of two differentially regulated isoforms of protochlorophyllide oxidoreductase (POR) from tobacco revealed a wide variety of light- and development-dependent regulations of POR gene expression among angiosperms. Photosynth Res 74: 165-172

144. Masuda T, Takamiya K (2004) Novel Insights into the Enzymology, Regulation and Physiological Functions of Light-dependent Protochlorophyllide Oxidoreductase in Angiosperms. Photosynth Res 81: 1-29

145. Matringe M, Camadro JM, Joyard J, Douce R (1994) Localization of ferrochelatase activity within mature pea chloroplasts. J Biol Chem 269: 15010-15015

146. Matsumoto F, Obayashi T, Sasaki-Sekimoto Y, Ohta H, Takamiya K, Masuda T (2004) Gene expression profiling of the tetrapyrrole metabolic pathway in Arabidopsis with a mini-array system. Plant Physiol 135: 2379-2391

147. Mense SM, Zhang L (2006) Heme: a versatile signaling molecule controlling the activities of diverse regulators ranging from transcription factors to MAP kinases. Cell Res 16: 681-692

148. Meskauskiene R, Apel K (2002) Interaction of FLU, a negative regulator of tetrapyrrole biosynthesis, with the glutamyl-tRNA reductase requires the tetratricopeptide repeat domain of FLU. FEBS Lett 532: 27-30

149. Meskauskiene R, Nater M, Goslings D, Kessler F, op den Camp R, Apel K (2001) FLU: a negative regulator of chlorophyll biosynthesis in Arabidopsis thaliana. Proc Natl Acad Sci U S A 98: 12826-12831

150. Miao Y, Zentgraf U (2007) The antagonist function of Arabidopsis WRKY53 and ESR/ESP in leaf senescence is modulated by the jasmonic and salicylic acid equilibrium. Plant Cell 19: 819-830

151. Miller JD, Arteca RN, Pell EJ (1999) Senescence-associated gene expression during ozone-induced leaf senescence in Arabidopsis. Plant Physiol 120: 1015-1024

152. Miyamoto K, Kanaya S, Morikawa K, Inokuchi H (1994) Overproduction, purification, and characterization of ferrochelatase from Escherichia coli. J Biochem 115: 545-551

153. Miyamoto K, Nakahigashi K, Nishimura K, Inokuchi H (1991) Isolation and characterization of visible light-sensitive mutants of Escherichia coli K12. J Mol Biol 219: 393-398

154. Miyamoto K, Tanaka R, Teramoto H, Masuda T, Tsuji H, Inokuchi H (1994) Nucleotide sequences of cDNA clones encoding ferrochelatase from barley and cucumber. Plant Physiol 105: 769-770

155. Monte E, Tepperman JM, Al-Sady B, Kaczorowski KA, Alonso JM, Ecker JR, Li X, Zhang Y, Quail PH (2004) The phytochrome-interacting transcription factor, PIF3, acts early, selectively, and positively in light-induced chloroplast development. Proc Natl Acad Sci U S A 101: 16091-16098

156. Morais F, Barber J, Nixon PJ (1998) The chloroplast-encoded alpha subunit of cytochrome b-559 is required for assembly of the photosystem two complex in both the light and the dark in Chlamydomonas reinhardtii. J Biol Chem 273: 29315-29320

157. Morais F, Kuhn K, Stewart DH, Barber J, Brudvig GW, Nixon PJ (2001) Photosynthetic water oxidation in cytochrome b(559) mutants containing a disrupted heme-binding pocket. J Biol Chem 276: 31986-31993

158. Mork-Jansson AE, Eichacker LA (2018) Characterization of chlorophyll binding to LIL3. PLoS One 13: e0192228

159. Mork-Jansson AE, Gargano D, Kmiec K, Furnes C, Shevela D, Eichacker LA (2015) Lil3 dimerization and chlorophyll binding in Arabidopsis thaliana. FEBS Lett 589: 3064-3070

160. Moseley J, Quinn J, Eriksson M, Merchant S (2000) The Crd1 gene encodes a putative di-iron enzyme required for photosystem I accumulation in copper deficiency and hypoxia in Chlamydomonas reinhardtii. EMBO J 19: 2139-2151

161. Moseley JL, Page MD, Alder NP, Eriksson M, Quinn J, Soto F, Theg SM, Hippler M, Merchant S (2002) Reciprocal expression of two candidate di-iron enzymes affecting photosystem I and light-harvesting complex accumulation. Plant Cell 14: 673-688

162. Mosinger E, Batschauer A, Schafer E, Apel K (1985) Phytochrome control of in vitro transcription of specific genes in isolated nuclei from barley (Hordeum vulgare). Eur J Biochem 147: 137-142

163. Moulin M, Smith AG (2005) Regulation of tetrapyrrole biosynthesis in higher plants. Biochem Soc Trans 33: 737-742

164. Muramoto T, Kohchi T, Yokota A, Hwang I, Goodman HM (1999) The Arabidopsis photomorphogenic mutant hy1 is deficient in phytochrome chromophore biosynthesis as a result of a mutation in a plastid heme oxygenase. Plant Cell 11: 335-348

165. Murcha MW, Wang Y, Narsai R, Whelan J (2014) The plant mitochondrial protein import apparatus - the differences make it interesting. Biochim Biophys Acta 1840: 1233-1245

166. Nagai S, Koide M, Takahashi S, Kikuta A, Aono M, Sasaki-Sekimoto Y, Ohta H, Takamiya K, Masuda T (2007) Induction of isoforms of tetrapyrrole biosynthetic enzymes, AtHEMA2 and AtFC1, under stress conditions and their physiological functions in Arabidopsis. Plant Physiol 144: 1039-1051

167. Nakabayashi K, Ito M, Kiyosue T, Shinozaki K, Watanabe A (1999) Identification of clp genes expressed in senescing Arabidopsis leaves. Plant Cell Physiol 40: 504-514

168. Nakahashi Y, Taketani S, Okuda M, Inoue K, Tokunaga R (1990) Molecular cloning and sequence analysis of cDNA encoding human ferrochelatase. Biochem Biophys Res Commun 173: 748-755

169. Nelson N, Ben-Shem A (2004) The complex architecture of oxygenic photosynthesis. Nat Rev Mol Cell Biol 5: 971-982

170. Nelson N, Junge W (2015) Structure and energy transfer in photosystems of oxygenic photosynthesis. Annu Rev Biochem 84: 659-683

171. Nickelsen J, Rengstl B (2013) Photosystem II assembly: from cyanobacteria to plants. Annu Rev Plant Biol 64: 609-635

172. Nielsen OF (1974) Macromolecular physiology of plastids. XII. Tigrina mutants in barley: genetic, spectroscopic and structural characterization. Hereditas 76: 269-304

173. Nishimura K, Apitz J, Friso G, Kim J, Ponnala L, Grimm B, van Wijk KJ (2015) Discovery of a Unique Clp Component, ClpF, in Chloroplasts: A Proposed Binary ClpF-ClpS1

Adaptor Complex Functions in Substrate Recognition and Delivery. Plant Cell 27: 2677-2691

174. Nishimura K, Asakura Y, Friso G, Kim J, Oh SH, Rutschow H, Ponnala L, van Wijk KJ (2013) ClpS1 is a conserved substrate selector for the chloroplast Clp protease system in Arabidopsis. Plant Cell 25: 2276-2301

175. Nishimura K, van Wijk KJ (2015) Organization, function and substrates of the essential Clp protease system in plastids. Biochim Biophys Acta 1847: 915-930

176. Nixon PJ, Michoux F, Yu J, Boehm M, Komenda J (2010) Recent advances in understanding the assembly and repair of photosystem II. Ann Bot 106: 1-16

177. Ogawa K, Sun J, Taketani S, Nakajima O, Nishitani C, Sassa S, Hayashi N, Yamamoto M, Shibahara S, Fujita H, Igarashi K (2001) Heme mediates derepression of Maf recognition element through direct binding to transcription repressor Bach1. EMBO J 20: 2835-2843

178. Oosawa N, Masuda T, Awai K, Fusada N, Shimada H, Ohta H, Takamiya K (2000) Identification and light-induced expression of a novel gene of NADPH-protochlorophyllide oxidoreductase isoform in Arabidopsis thaliana. FEBS Lett 474: 133-136

179. Paddock TN, Mason ME, Lima DF, Armstrong GA (2010) Arabidopsis protochlorophyllide oxidoreductase A (PORA) restores bulk chlorophyll synthesis and normal development to a porB porC double mutant. Plant Mol Biol 72: 445-457

180. Paila YD, Richardson LGL, Schnell DJ (2015) New insights into the mechanism of chloroplast protein import and its integration with protein quality control, organelle biogenesis and development. J Mol Biol 427: 1038-1060

181. Pakrasi HB, De Ciechi P, Whitmarsh J (1991) Site directed mutagenesis of the heme axial ligands of cytochrome b559 affects the stability of the photosystem II complex. EMBO J 10: 1619-1627

182. Pakrasi HB, Williams JG, Arntzen CJ (1988) Targeted mutagenesis of the psbE and psbF genes blocks photosynthetic electron transport: evidence for a functional role of cytochrome b559 in photosystem II. EMBO J 7: 325-332

183. Panek H, O'Brian MR (2002) A whole genome view of prokaryotic haem biosynthesis. Microbiology 148: 2273-2282

184. Papenbrock J, Mishra S, Mock HP, Kruse E, Schmidt EK, Petersmann A, Braun HP, Grimm B (2001) Impaired expression of the plastidic ferrochelatase by antisense RNA synthesis leads to a necrotic phenotype of transformed tobacco plants. Plant J 28: 41-50

185. Park S, Harada JJ (2008) Arabidopsis embryogenesis. Methods Mol Biol 427: 3-16

186. Parks BM, Quail PH (1991) Phytochrome-Deficient hy1 and hy2 Long Hypocotyl Mutants of Arabidopsis Are Defective in Phytochrome Chromophore Biosynthesis. Plant Cell 3: 1177-1186

187. Peeters N, Small I (2001) Dual targeting to mitochondria and chloroplasts. Biochim Biophys Acta 1541: 54-63

188. Petersen BL, Kannangara CG, Henningsen KW (1999) Distribution of ATPase and ATP-to-ADP phosphate exchange activities in magnesium chelatase subunits of Chlorobium vibrioforme and Synechocystis PCC6803. Arch Microbiol 171: 146-150

189. Pierce EJ, Rey ME (2013) Assessing Global Transcriptome Changes in Response to South African Cassava Mosaic Virus [ZA-99] Infection in Susceptible Arabidopsis thaliana. PLoS One 8: e67534

190. Pogson BJ, Woo NS, Forster B, Small ID (2008) Plastid signalling to the nucleus and beyond. Trends Plant Sci 13: 602-609

191. Ponka P, Sheftel AD, English AM, Scott Bohle D, Garcia-Santos D (2017) Do Mammalian Cells Really Need to Export and Import Heme? Trends Biochem Sci 42: 395-406

192. Pontier D, Albrieux C, Joyard J, Lagrange T, Block MA (2007) Knock-out of the magnesium protoporphyrin IX methyltransferase gene in Arabidopsis. Effects on chloroplast development and on chloroplast-to-nucleus signaling. J Biol Chem 282: 2297-2304

193. Pratibha P, Singh SK, Srinivasan R, Bhat SR, Sreenivasulu Y (2017) Gametophyte Development Needs Mitochondrial Coproporphyrinogen III Oxidase Function. Plant Physiol 174: 258-275

194. Puustinen A, Wikstrom M (1991) The heme groups of cytochrome o from Escherichia coli. Proc Natl Acad Sci U S A 88: 6122-6126

195. Quail PH (2000) Phytochrome-interacting factors. Semin Cell Dev Biol 11: 457-466

196. Radmer RJ, Bogorad L (1967) (Minus) S-adenosyl-L-methionine-magnesium protoporphyrin methyltransferase, an enzyme in the biosynthetic pathway of chlorophyll in Zea mays. Plant Physiol 42: 463-465

197. Rao AU, Carta LK, Lesuisse E, Hamza I (2005) Lack of heme synthesis in a free-living eukaryote. Proc Natl Acad Sci U S A 102: 4270-4275

198. Richter A, Peter E, Pors Y, Lorenzen S, Grimm B, Czarnecki O (2010) Rapid dark repression of 5-aminolevulinic acid synthesis in green barley leaves. Plant Cell Physiol 51: 670-681

199. Richter AS, Peter E, Rothbart M, Schlicke H, Toivola J, Rintamaki E, Grimm B (2013) Posttranslational influence of NADPH-dependent thioredoxin reductase C on enzymes in tetrapyrrole synthesis. Plant Physiol 162: 63-73

200. Richter AS, Wang P, Grimm B (2016) Arabidopsis Mg-Protoporphyrin IX Methyltransferase Activity and Redox Regulation Depend on Conserved Cysteines. Plant Cell Physiol 57: 519-527

201. Rissler HM, Collakova E, DellaPenna D, Whelan J, Pogson BJ (2002) Chlorophyll biosynthesis. Expression of a second chl I gene of magnesium chelatase in Arabidopsis supports only limited chlorophyll synthesis. Plant Physiol 128: 770-779

202. Rodgers KR, Lukat-Rodgers GS (2005) Insights into heme-based O2 sensing from structure-function relationships in the FixL proteins. J Inorg Biochem 99: 963-977

203. Rodriguez-Lopez JN, Lowe DJ, Hernandez-Ruiz J, Hiner AN, Garcia-Canovas F, Thorneley RN (2001) Mechanism of reaction of hydrogen peroxide with horseradish peroxidase: identification of intermediates in the catalytic cycle. J Am Chem Soc 123: 11838-11847

204. Romero-Santacreu L, Moreno J, Perez-Ortin JE, Alepuz P (2009) Specific and global regulation of mRNA stability during osmotic stress in Saccharomyces cerevisiae. RNA 15: 1110-1120

205. Runge S, Sperling U, Frick G, Apel K, Armstrong GA (1996) Distinct roles for light-dependent NADPH:protochlorophyllide oxidoreductases (POR) A and B during greening in higher plants. Plant J 9: 513-523

206. Rzeznicka K, Walker CJ, Westergren T, Kannangara CG, von Wettstein D, Merchant S, Gough SP, Hansson M (2005) Xantha-l encodes a membrane subunit of the aerobic Mg-protoporphyrin IX monomethyl ester cyclase involved in chlorophyll biosynthesis. Proc Natl Acad Sci U S A 102: 5886-5891

207. Sah JF, Ito H, Kolli BK, Peterson DA, Sassa S, Chang KP (2002) Genetic rescue of Leishmania deficiency in porphyrin biosynthesis creates mutants suitable for analysis of cellular events in uroporphyria and for photodynamic therapy. J Biol Chem 277: 14902-14909

208. Saiki K, Mogi T, Anraku Y (1992) Heme O biosynthesis in Escherichia coli: the cyoE gene in the cytochrome bo operon encodes a protoheme IX farnesyltransferase. Biochem Biophys Res Commun 189: 1491-1497

209. Sawicki A, Willows RD (2010) BchJ and BchM interact in a 1 : 1 ratio with the magnesium chelatase BchH subunit of Rhodobacter capsulatus. FEBS J 277: 4709-4721

210. Scharfenberg M, Mittermayr L, E VONR-L, Schlicke H, Grimm B, Leister D, Kleine T (2015) Functional characterization of the two ferrochelatases in Arabidopsis thaliana. Plant Cell Environ 38: 280-298

211. Schmied J, Hou Z, Hedtke B, Grimm B (2018) Controlled partitioning of glutamyl-tRNA reductase in stroma- and membrane-associated fractions affects the synthesis of 5-amino levulinic acid. Plant Cell Physiol

212. Sharma M, Bennewitz B, Klosgen RB (2018) Rather rule than exception? How to evaluate the relevance of dual protein targeting to mitochondria and chloroplasts. Photosynth Res

213. Shimizu T, Huang D, Yan F, Stranava M, Bartosova M, Fojtikova V, Martinkova M (2015) Gaseous O2, NO, and CO in signal transduction: structure and function relationships of heme-based gas sensors and heme-redox sensors. Chem Rev 115: 6491-6533

214. Shin J, Kim K, Kang H, Zulfugarov IS, Bae G, Lee CH, Lee D, Choi G (2009) Phytochromes promote seedling light responses by inhibiting four negatively-acting phytochrome-interacting factors. Proc Natl Acad Sci U S A 106: 7660-7665

215. Shukla MK, Llansola-Portoles MJ, Tichy M, Pascal AA, Robert B, Sobotka R (2018) Binding of pigments to the cyanobacterial high-light-inducible protein HliC. Photosynth Res 137: 29-39

216. Sinclair J, Hamza I (2015) Lessons from bloodless worms: heme homeostasis in C. elegans. Biometals 28: 481-489

217. Sinclair PR, Gorman N, Jacobs JM (2001) Measurement of heme concentration. Curr Protoc Toxicol Chapter 8: Unit 8 3

218. Singh DP, Cornah JE, Hadingham S, Smith AG (2002) Expression analysis of the two ferrochelatase genes in Arabidopsis in different tissues and under stress conditions reveals their different roles in haem biosynthesis. Plant Mol Biol 50: 773-788

219. Sjogren LL, Stanne TM, Zheng B, Sutinen S, Clarke AK (2006) Structural and functional insights into the chloroplast ATP-dependent Clp protease in Arabidopsis. Plant Cell 18: 2635-2649

220. Smith AG, Santana MA, Wallace-Cook AD, Roper JM, Labbe-Bois R (1994) Isolation of a cDNA encoding chloroplast ferrochelatase from Arabidopsis thaliana by functional complementation of a yeast mutant. J Biol Chem 269: 13405-13413

221. Sobotka R, McLean S, Zuberova M, Hunter CN, Tichy M (2008) The C-terminal extension of ferrochelatase is critical for enzyme activity and for functioning of the tetrapyrrole pathway in Synechocystis strain PCC 6803. J Bacteriol 190: 2086-2095

222. Sobotka R, Tichy M, Wilde A, Hunter CN (2011) Functional assignments for the carboxyl-terminal domains of the ferrochelatase from Synechocystis PCC 6803: the CAB domain plays a regulatory role, and region II is essential for catalysis. Plant Physiol 155: 1735-1747

223. Soldatova O, Apchelimov A, Radukina N, Ezhova T, Shestakov S, Ziemann V, Hedtke B, Grimm B (2005) An Arabidopsis mutant that is resistant to the protoporphyrinogen oxidase inhibitor acifluorfen shows regulatory changes in tetrapyrrole biosynthesis. Mol Genet Genomics 273: 311-318

224. Song J, Feng SJ, Chen J, Zhao WT, Yang ZM (2017) A cadmium stress-responsive gene AtFC1 confers plant tolerance to cadmium toxicity. BMC Plant Biol 17: 187

225. Staleva H, Komenda J, Shukla MK, Slouf V, Kana R, Polivka T, Sobotka R (2015) Mechanism of photoprotection in the cyanobacterial ancestor of plant antenna proteins. Nat Chem Biol 11: 287-291

226. Stobart AK, Ameen-Bukhari I (1986) Photoreduction of protochlorophyllide and its relationship to delta-aminolaevulinic acid synthesis in the leaves of dark-grown barley (Hordeum vulgare) seedlings. Biochem J 236: 741-748

227. Stuehr DJ, Santolini J, Wang ZQ, Wei CC, Adak S (2004) Update on mechanism and catalytic regulation in the NO synthases. J Biol Chem 279: 36167-36170

228. Su Q, Frick G, Armstrong G, Apel K (2001) POR C of Arabidopsis thaliana: a third light- and NADPH-dependent protochlorophyllide oxidoreductase that is differentially regulated by light. Plant Mol Biol 47: 805-813

229. Sun J, Hoshino H, Takaku K, Nakajima O, Muto A, Suzuki H, Tashiro S, Takahashi S, Shibahara S, Alam J, Taketo MM, Yamamoto M, Igarashi K (2002) Hemoprotein Bach1 regulates enhancer availability of heme oxygenase-1 gene. EMBO J 21: 5216-5224

230. Suorsa M, Regel RE, Paakkarinen V, Battchikova N, Herrmann RG, Aro EM (2004) Protein assembly of photosystem II and accumulation of subcomplexes in the absence of low molecular mass subunits PsbL and PsbJ. Eur J Biochem 271: 96-107

231. Suzuki T, Masuda T, Singh DP, Tan FC, Tsuchiya T, Shimada H, Ohta H, Smith AG, Takamiya K (2002) Two types of ferrochelatase in photosynthetic and nonphotosynthetic tissues of cucumber: their difference in phylogeny, gene expression, and localization. J Biol Chem 277: 4731-4737

232. Swiatek M, Regel RE, Meurer J, Wanner G, Pakrasi HB, Ohad I, Herrmann RG (2003) Effects of selective inactivation of individual genes for low-molecular-mass subunits on the assembly of photosystem II, as revealed by chloroplast transformation: the psbEFLJoperon in Nicotiana tabacum. Mol Genet Genomics 268: 699-710

233. Takahashi S, Ogawa T, Inoue K, Masuda T (2008) Characterization of cytosolic tetrapyrrole-binding proteins in Arabidopsis thaliana. Photochem Photobiol Sci 7: 1216-1224

234. Taketani S, Nakahashi Y, Osumi T, Tokunaga R (1990) Molecular cloning, sequencing, and expression of mouse ferrochelatase. J Biol Chem 265: 19377-19380

235. Terry MJ, Kendrick RE (1999) Feedback inhibition of chlorophyll synthesis in the phytochrome chromophore-deficient aurea and yellow-green-2 mutants of tomato. Plant Physiol 119: 143-152

236. Toledo-Ortiz G, Johansson H, Lee KP, Bou-Torrent J, Stewart K, Steel G, Rodriguez-Concepcion M, Halliday KJ (2014) The HY5-PIF regulatory module coordinates light and temperature control of photosynthetic gene transcription. PLoS Genet 10: e1004416

237. Tottey S, Block MA, Allen M, Westergren T, Albrieux C, Scheller HV, Merchant S, Jensen PE (2003) Arabidopsis CHL27, located in both envelope and thylakoid membranes, is

required for the synthesis of protochlorophyllide. Proc Natl Acad Sci U S A 100: 16119-16124

238. Tsiftsoglou AS, Tsamadou AI, Papadopoulou LC (2006) Heme as key regulator of major mammalian cellular functions: Molecular, cellular, and pharmacological aspects. Pharmacology & Therapeutics 111: 327-345

239. van Lis R, Atteia A, Nogaj LA, Beale SI (2005) Subcellular localization and light-regulated expression of protoporphyrinogen IX oxidase and ferrochelatase in Chlamydomonas reinhardtii. Plant Physiol 139: 1946-1958

240. Vanhee C, Zapotoczny G, Masquelier D, Ghislain M, Batoko H (2011) The Arabidopsis multistress regulator TSPO is a heme binding membrane protein and a potential scavenger of porphyrins via an autophagy-dependent degradation mechanism. Plant Cell 23: 785-805

241. Vavilin D, Brune DC, Vermaas W (2005) 15N-labeling to determine chlorophyll synthesis and degradation in Synechocystis sp. PCC 6803 strains lacking one or both photosystems. Biochim Biophys Acta 1708: 91-101

242. Vavilin D, Yao D, Vermaas W (2007) Small Cab-like proteins retard degradation of photosystem II-associated chlorophyll in Synechocystis sp. PCC 6803: kinetic analysis of pigment labeling with 15N and 13C. J Biol Chem 282: 37660-37668

243. Vlasits J, Jakopitsch C, Schwanninger M, Holubar P, Obinger C (2007) Hydrogen peroxide oxidation by catalase-peroxidase follows a non-scrambling mechanism. FEBS Lett 581: 320-324

244. von Gromoff ED, Alawady A, Meinecke L, Grimm B, Beck CF (2008) Heme, a plastid-derived regulator of nuclear gene expression in Chlamydomonas. Plant Cell 20: 552-567

245. Vothknecht UC, Kannangara CG, von Wettstein D (1996) Expression of catalytically active barley glutamyl tRNAGlu reductase in Escherichia coli as a fusion protein with glutathione S-transferase. Proc Natl Acad Sci U S A 93: 9287-9291

246. Vothknecht UC, Kannangara CG, von Wettstein D (1998) Barley glutamyl tRNAGlu reductase: mutations affecting haem inhibition and enzyme activity. Phytochemistry 47: 513-519

247. Walker CJ, Weinstein JD (1994) The magnesium-insertion step of chlorophyll biosynthesis is a two-stage reaction. Biochem J 299 (Pt 1): 277-284

248. Wang P, Liang FC, Wittmann D, Siegel A, Shan SO, Grimm B (2018) Chloroplast SRP43 acts as a chaperone for glutamyl-tRNA reductase, the rate-limiting enzyme in tetrapyrrole biosynthesis. Proc Natl Acad Sci U S A

249. Wang Q, Sullivan RW, Kight A, Henry RL, Huang J, Jones AM, Korth KL (2004) Deletion of the chloroplast-localized Thylakoid formation1 gene product in Arabidopsis leads to deficient thylakoid formation and variegated leaves. Plant Physiol 136: 3594-3604

250. Wang Y, Zhang WZ, Song LF, Zou JJ, Su Z, Wu WH (2008) Transcriptome analyses show changes in gene expression to accompany pollen germination and tube growth in Arabidopsis. Plant Physiol 148: 1201-1211

251. Wang Z, Hong X, Hu K, Wang Y, Wang X, Du S, Li Y, Hu D, Cheng K, An B, Li Y (2017) Impaired Magnesium Protoporphyrin IX Methyltransferase (ChlM) Impedes Chlorophyll Synthesis and Plant Growth in Rice. Front Plant Sci 8: 1694

252. Warnatz HJ, Schmidt D, Manke T, Piccini I, Sultan M, Borodina T, Balzereit D, Wruck W, Soldatov A, Vingron M, Lehrach H, Yaspo ML (2011) The BTB and CNC homology 1 (BACH1) target genes are involved in the oxidative stress response and in control of the cell cycle. J Biol Chem 286: 23521-23532

253. Watanabe N, Che FS, Iwano M, Takayama S, Yoshida S, Isogai A (2001) Dual targeting of spinach protoporphyrinogen oxidase II to mitochondria and chloroplasts by alternative use of two in-frame initiation codons. J Biol Chem 276: 20474-20481

254. Watanabe S, Hanaoka M, Ohba Y, Ono T, Ohnuma M, Yoshikawa H, Taketani S, Tanaka K (2013) Mitochondrial localization of ferrochelatase in a red alga Cyanidioschyzon merolae. Plant Cell Physiol 54: 1289-1295

255. Wei X, Su X, Cao P, Liu X, Chang W, Li M, Zhang X, Liu Z (2016) Structure of spinach photosystem II-LHCII supercomplex at 3.2 A resolution. Nature 534: 69-74

256. Weinstein JD, Beale SI (1985) Enzymatic conversion of glutamate to delta-aminolevulinate in soluble extracts of the unicellular green alga, Chlorella vulgaris. Arch Biochem Biophys 237: 454-464

257. Welsch R, Zhou X, Yuan H, Alvarez D, Sun T, Schlossarek D, Yang Y, Shen G, Zhang H, Rodriguez-Concepcion M, Thannhauser TW, Li L (2018) Clp Protease and OR Directly Control the Proteostasis of Phytoene Synthase, the Crucial Enzyme for Carotenoid Biosynthesis in Arabidopsis. Mol Plant 11: 149-162

258. Wettstein DV, Kahn A, Nielsen OF, Gough S (1974) Genetic regulation of chlorophyll synthesis analyzed with mutants in barley. Science 184: 800-802

259. Williams P, Hardeman K, Fowler J, Rivin C (2006) Divergence of duplicated genes in maize: evolution of contrasting targeting information for enzymes in the porphyrin pathway. Plant J 45: 727-739

260. Willows RD, Gibson LC, Kanangara CG, Hunter CN, von Wettstein D (1996) Three separate proteins constitute the magnesium chelatase of Rhodobacter sphaeroides. Eur J Biochem 235: 438-443

261. Woodson JD, Joens MS, Sinson AB, Gilkerson J, Salome PA, Weigel D, Fitzpatrick JA, Chory J (2015) Ubiquitin facilitates a quality-control pathway that removes damaged chloroplasts. Science 350: 450-454

262. Woodson JD, Perez-Ruiz JM, Chory J (2011) Heme synthesis by plastid ferrochelatase I regulates nuclear gene expression in plants. Curr Biol 21: 897-903

263. Wu H, Ji Y, Du J, Kong D, Liang H, Ling HQ (2010) ClpC1, an ATP-dependent Clp protease in plastids, is involved in iron homeostasis in Arabidopsis leaves. Ann Bot 105: 823-833

264. Wu Q, Vermaas WF (1995) Light-dependent chlorophyll a biosynthesis upon chlL deletion in wild-type and photosystem I-less strains of the cyanobacterium Synechocystis sp. PCC 6803. Plant Mol Biol 29: 933-945

265. Xu H, Vavilin D, Funk C, Vermaas W (2002) Small Cab-like proteins regulating tetrapyrrole biosynthesis in the cyanobacterium Synechocystis sp. PCC 6803. Plant Mol Biol 49: 149-160

266. Xu H, Vavilin D, Funk C, Vermaas W (2004) Multiple deletions of small Cab-like proteins in the cyanobacterium Synechocystis sp. PCC 6803: consequences for pigment biosynthesis and accumulation. J Biol Chem 279: 27971-27979

267. Yamasaki C, Tashiro S, Nishito Y, Sueda T, Igarashi K (2005) Dynamic cytoplasmic anchoring of the transcription factor Bach1 by intracellular hyaluronic acid binding protein IHABP. J Biochem 137: 287-296

268. Yang H, Yang S, Li Y, Hua J (2007) The Arabidopsis BAP1 and BAP2 genes are general inhibitors of programmed cell death. Plant Physiol 145: 135-146

269. Yang ZM, Bauer CE (1990) Rhodobacter capsulatus genes involved in early steps of the bacteriochlorophyll biosynthetic pathway. J Bacteriol 172: 5001-5010

270. Yuan X, Fleming MD, Hamza I (2013) Heme transport and erythropoiesis. Curr Opin Chem Biol 17: 204-211

271. Zeller G, Henz SR, Widmer CK, Sachsenberg T, Ratsch G, Weigel D, Laubinger S (2009) Stress-induced changes in the Arabidopsis thaliana transcriptome analyzed using whole-genome tiling arrays. Plant J 58: 1068-1082

272. Zentgraf U, Laun T, Miao Y (2010) The complex regulation of WRKY53 during leaf senescence of Arabidopsis thaliana. Eur J Cell Biol 89: 133-137

273. Zhang L, Hach A (1999) Molecular mechanism of heme signaling in yeast: the transcriptional activator Hap1 serves as the key mediator. Cell Mol Life Sci 56: 415-426

274. Zhang M, Zhang F, Fang Y, Chen X, Chen Y, Zhang W, Dai HE, Lin R, Liu L (2015) The Non-canonical Tetratricopeptide Repeat (TPR) Domain of Fluorescent (FLU) Mediates Complex Formation with Glutamyl-tRNA Reductase. J Biol Chem 290: 17559-17565

275. Zhao A, Fang Y, Chen X, Zhao S, Dong W, Lin Y, Gong W, Liu L (2014) Crystal structure of Arabidopsis glutamyl-tRNA reductase in complex with its stimulator protein. Proc Natl Acad Sci U S A 111: 6630-6635

276. Zhao WT, Feng SJ, Li H, Faust F, Kleine T, Li LN, Yang ZM (2017) Salt stress-induced FERROCHELATASE 1 improves resistance to salt stress by limiting sodium accumulation in Arabidopsis thaliana. Sci Rep 7: 14737

277. Zheng B, MacDonald TM, Sutinen S, Hurry V, Clarke AK (2006) A nuclear-encoded ClpP subunit of the chloroplast ATP-dependent Clp protease is essential for early development in Arabidopsis thaliana. Planta 224: 1103-1115

278. Zsebo KM, Hearst JE (1984) Genetic-physical mapping of a photosynthetic gene cluster from R. capsulata. Cell 37: 937-947

Supplemental data

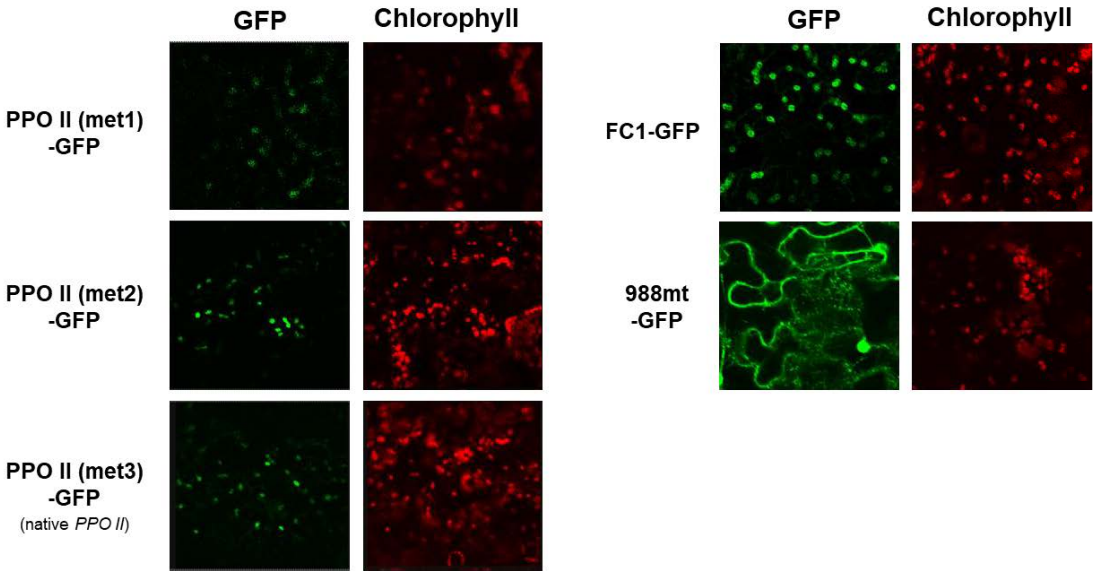

Figure S 1: Subcellular localization of PPOII proteins transcribed with different initiation codons.

Arabidopsis PPOII was transcribed with different initiation codons and transiently expressed in leaf epidermal cells of *Nicotiana benthamiana* plants. Green fluorescence indicates GFP, red fluorescence displays chloroplast autofluorescence. The GFP-tagged FC1 was used as a reference for chloroplast localization, while 988mt-GFP sequence (encodes the first 29 amino acids of *Saccharomyces cerevisiae* cytochrome c oxidase IV) was expressed as a maker for mitochondria localized proteins.

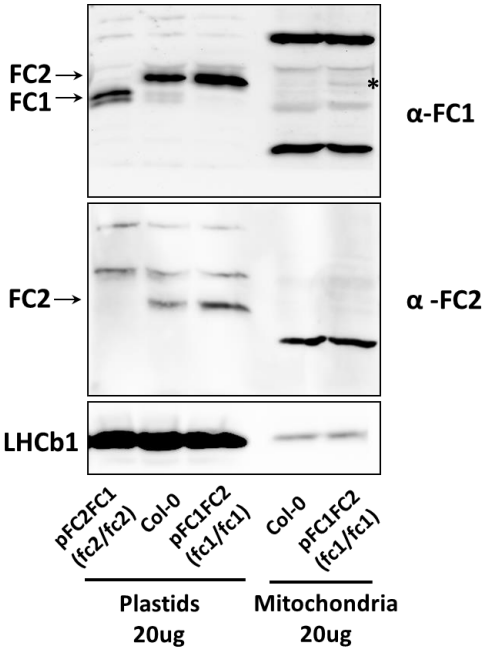

Figure S 2 Western blot analysis of FC proteins in chloroplasts and mitochondria of Arabidopsis.

Chloroplasts and mitochondria were extracted from pFC1FC2 (*fc1/fc1*), pFC2FC1 (*fc2/fc2*) and wild-type seedlings. Plants were grown under SD condition with 100μE light intensity. The resolved proteins were separated by a 10% SDS-PAGE gel. α-FC1, α-FC2 and α-LHCb1 antibodies were applied for immunoblotting analysis. An α-FC1 recognizes FC1 and FC2 in Arabidopsis, while α-FC2 antibody specifically recognize FC2 protein. An α-LHCb1 antibody was used to reveal a contamination of plastids in the mitochondria extracts and confirm that equal amount of plastid proteins has been loaded. The asterisk indicates a FC2 band in pFC1FC2 (*fc1/fc1*) mitochondria. This might be due to a contamination of plastids during the extraction of mitochondria, as a small amount of LHCb1 was present in the mitochondria extracts.

Acknowledgement

I would like to express my great appreciation to Prof. Dr. Bernhard Grimm, who kindly offered me the chance to do my PhD research in the Plant Physiology Institute. Thanks for his valuable and constructive suggestions during the planning and development of this study. I have gained a lot from his wisdom. That includes not only the right way to develop scientific ideas but also the attitudes towards research and plenty of supervision skills.

I am particularly grateful for the help from Prof. Dr. Christian Schmitz-Linneweber and Prof. Dr. Mats Hansson. Many thanks to them for reviewing my dissertation. I also thank my committee members, Prof. Dr. Kerstin Kaufmann and Dr. Christina Kühn, for their willingness to assess my PhD work and offer their valuable suggestions and comments.

Many thanks to all the lovely colleagues. Sincerely, I have enjoyed myself a lot when we shared the ups and downs in the research as well as daily life. Thanks to Lena Roling and Anna Meier. From the time we fought together to "crack" ferrochelatse 1, I have learned the way to do good supervision and cooperation. Lena has also been a very nice and helpful colleague since she stayed in the Plant Physiology Institute for PhD study.

I want to specially thank Dr. Boris Hedtke. He has been doing an excellent job to help Prof. Grimm organize the lab issues, in order to provide the best working condition for everyone. Boris also helped me a lot when I started my research with ferrochelatase 1. Dear Kersten and Magdalena have been so caring and nice. They never hesitate to offer me a hand when I need help.

I extend my sincere thanks to Dr. Peng Wang, Zhiwei Hou, Josephine Herbst, Daniel Wittmann, Patrick Schall, Shuiling Ji, Daniel Hey and every group member who helped me a lot in many aspects. Thanks to my very good friends Dr. Qianqian Ming and Dr. Juan Zhang for being there and support me. I also want to address my appreciation to the China Scholarship Council for the financial support of my study.

Finally, I would like to express my sincere thanks and love to my husband Jun Xu, my parents and parents-in-law. They have been so supportive, I could not manage any of this without them. Thanks to all the people around, they make me so happy with my daily life.

Curriculum vitae

CV removed for online publication.

Publications

Metabolism, Structure and Function of Plant Tetrapyrroles (**co-author**, *Advances in Botanical Research-volume 90*, book to be published in 2019)

Fan T, Roling L, Meiers A, Brings L, Ortega-Rodes P, Hedtke B, Grimm B (2018) Complementation studies of the Arabidopsis fc1 mutant substantiate essential functions of ferrochelatase 1 during embryogenesis and salt stress. *Plant Cell Environ* (doi: 10.1111/pce.13448)

Hey D, Ortega-Rodes P, **Fan T**, Schnurrer F, Brings L, Hedtke B, Grimm B (2016) Transgenic Tobacco Lines Expressing Sense or Antisense FERROCHELATASE 1 RNA Show Modified Ferrochelatase Activity in Roots and Provide Experimental Evidence for Dual Localization of Ferrochelatase 1. *Plant Cell Physiol* 57: 2576-2585

Luo T, Luo S, Araujo WL, Schlicke H, Rothbart M, Yu J, **Fan T**, Fernie AR, Grimm B, Luo M (2013) Virus-induced gene silencing of pea CHLI and CHLD affects tetrapyrrole biosynthesis, chloroplast development and the primary metabolic network. *Plant Physiol Biochem* 65: 17-26

Xu J, Xiong W, Cao B, Yan T, Luo T, **Fan T**, Luo M (2013) Molecular characterization and functional analysis of "fruit-weight 2.2-like" gene family in rice. *Planta* 238: 643-655

Luo T, **Fan T**, Liu Y, Rothbart M, Yu J, Zhou S, Grimm B, Luo M (2012) Thioredoxin redox regulates ATPase activity of magnesium chelatase CHLI subunit and modulates redox-mediated signaling in tetrapyrrole biosynthesis and homeostasis of reactive oxygen species in pea plants. *Plant Physiol* 159: 118-130

Manuscript in preparation

Fan T, Grimm B Ferrochelatase 2 contributes to the GluTR inactivation complex to control appropriate heme and chlorophyll synthesis.

Selbständigkeitserklärung

Hiermit erkläre ich, die Dissertation selbstständig und nur unter Verwendung der angegebenen Hilfen und Hilfsmittel angefertigt zu haben. Ich habe mich anderwärts nicht um einen Doktorgrad beworben und besitze keinen entsprechenden Doktorgrad. Ich erkläre, dass ich die Dissertation oder Teile davon nicht bereits bei einer anderen wissenschaftlichen Einrichtung eingereicht habe und dass sie dort weder angenommen noch abgelehnt wurde.

Tingting Fan

Berlin, December 2018